IOWA STATE UNIVERSITY
Digital Repository

Graduate Theses and Dissertations

Iowa State University Capstones, Theses and Dissertations

2009

Engineering behavior of small-scale foundation piers constructed from alternative materials

Maxim Mikhaylovich Prokudin
Iowa State University

Follow this and additional works at: https://lib.dr.iastate.edu/etd

 Part of the Civil and Environmental Engineering Commons

Recommended Citation
Prokudin, Maxim Mikhaylovich, "Engineering behavior of small-scale foundation piers constructed from alternative materials" (2009). *Graduate Theses and Dissertations*. 10990.
https://lib.dr.iastate.edu/etd/10990

This Thesis is brought to you for free and open access by the Iowa State University Capstones, Theses and Dissertations at Iowa State University Digital Repository. It has been accepted for inclusion in Graduate Theses and Dissertations by an authorized administrator of Iowa State University Digital Repository. For more information, please contact digirep@iastate.edu.

www.manaraa.com

Engineering behavior of small-scale foundation piers constructed from alternative materials

by

Maxim Mikhaylovich Prokudin

A thesis submitted to the graduate faculty

in partial fulfillment of the requirements for the degree of

MASTER OF SCIENCE

Major: Civil Engineering (Geotechnical Engineering)

Program of Study Committee:
David J. White, Major Professor
Charles Jahren
Terry Wipf

Iowa State University

Ames, Iowa

2009

Copyright © Maxim Mikhaylovich Prokudin, 2009. All rights reserved.

www.manaraa.com

To
The memory of my mother

www.manaraa.com

TABLE OF CONTENTS

LIST OF FIGURES vi

LIST OF TABLES x

LIST OF EQUATIONS xii

LIST OF SYMBOLS xiii

ABSTRACT xv

CHAPTER 1: INTRODUCTION 1

- Industry Problem 1
- Technical Problem 1
- Research Goals 2
- Research Objectives 2
- Forecasting 3

CHAPTER 2: BACKGROUND 5

- Full-Scale Aggregate Pier Foundation Element Features 5
  - Overview 5
  - Materials 8
  - Upper and Lower Zone 10
  - Other Technologies 12
  - Bearing Capacity 13
  - Group Efficiency 17
  - Case Studies 17
  - Case 1 – Bucher et al., 2008 18
  - Case 2 – White et al., 2007 20
  - Case 3 – Wissmann et al., 2007 22
- Model Scale Testing 24
  - Case Studies 27
  - Case 1 – Black et al., 2007b 27
  - Case 2 – Fang and Yin, 2007 29
  - Case 3 – Black et al., 2007a 31
  - Case 4 – Sivakumar et al., 2004 33
  - Case 5 – Bachus and Barksdale, 1984 35
  - Case 6 – Balaam et al., 1977 36
  - Case 7 – Hughes and Withers, 1974 37

www.manaraa.com

CHAPTER 3: RESEARCH METHODOLOGY 39

Load Frame 39
Test Bed Characterization Methods 44
Test Bed Compaction 44
Particle Size Distribution 47
DCP Test 47
CBR from DCP 49
Nuclear Density Gauge 51
Shelby Tube Sample 52
Unconfined Compression Triaxial Test 54
Data Collection and Sensors 58
Pier Construction Approach 61
Cavity Preparation 61
Ramming Device 62
Beveled Tamper Heads 64
Cement Mixes 65
Load-Settlement DAQ Approach 66
Loading Mechanism 66
DAQ Data Collection 68
Group and Individual Pier Layout 69

CHAPTER 4: MATERIALS 74

Loess Material 74
Pier Composition Materials 78
Scaled Aggregate Piers – AASHTO No. 57 79
Scaled Aggregate Piers – Manufactured Sand 82
Grout Piers - Type 1 83
Grout Piers - Type K 84
Grout Piers - NS7 86
Loess Piers – Fibers 87
Other Piers - Sand 89

CHAPTER 5: TEST RESULTS AND ANALYSIS 90

Single Aggregate Piers Compacted via Different Shape Tamper Heads 90
Stress-Settlement 90
Single Piers of Various Composition 93
Stress-Settlement 93
Bearing Capacity 106
Groups of Piers 111
Aggregate Piers - Stress-Settlement 111
Aggregate Piers - Group Efficiency 119
Aggregate Piers - Group Bearing Capacity 121
C(I) + C(K) - Stress-Settlement 123

www.manaraa.com

C(I) + C(K) – Group Efficiency 131
C(I) + C(K) – Group Bearing Capacity 132

CHAPTER 6: DISCUSSION.....133

Aggregate Piers Compacted via Different Shape Tamper Heads.....133
Stress-Settlement.....133
Single Piers of Various Mixes 136
Stress-Settlement.....136
Bearing Capacity.....141
Groups of Piers 143
Aggregate Piers - Stress-Settlement.....143
Aggregate Piers – Bearing capacity.....145
Aggregate Piers - Group Efficiency.....145
C(I) + C(K) - Stress-Settlement 146
C(I) + C(K) – Bearing Capacity 148
C(I) + C(K) - Group Efficiency 149
Aggregate Piers vs. C(I) + C(K) - Load-settlement.....150
Aggregate Piers vs. C(I) + C(K) - Group Efficiency.....153

CHAPTER 7: SUMMARY AND CONCLUSIONS.....154

Aggregate Piers.....154
Tamper Heads 154
Partial Grouting.....154
Bearing Capacity.....155
Materials 156
Loess-Cement 156
Admixtures.....156
Single Piers 157
Bulging.....157
Plunging 157
Groups of Piers 158
Group of Aggregate Piers 158
Group of C(I) + C(K) Piers.....158
Group of Aggregate Piers versus C(I) + C(K) Piers.....159

CHAPTER 8: FUTURE RESEARCH.....160

REFERENCES 161

APPENDIX.....169

ACKNOWLEDGEMENTS.....191

www.manaraa.com

LIST OF FIGURES

Figure 1: Concept of aggregate pier floating foundation (reproduced per Kwong et.al, 2002) 6
Figure 2: Simplified aggregate pier installation procedure (reproduced per Fox et al., 2004).....7
Figure 3: (a) Bulging of aggregate pier elements and (b) shearing below tips of aggregate pier elements (reproduced per Wissmann, 1999).....8
Figure 4: Friction angle for AASHTO No. 57 and No. 21A limestone aggregate (reproduced per Fox et al., 1998, Jian and Park, 2007 and White and Suleiman, 2004) 9
Figure 5: Schematic drawing of aggregate pier Upper and Lower Zones (reproduced per Kwong et al., 2002).....11
Figure 6: Aggregate pier tell-tale instrumentation (reproduced per White et al., 2007) 12
Figure 7: Schematic of group of three footing instrumentation (reproduced per Bucher et al., 2008) 18
Figure 8: Modulus and footing load test results (reproduced per Bucher et al., 2008) 19
Figure 9: Measured load-settlement curves for single pier (reproduced per White et al., 2007) ..21
Figure 10: Measured load-settlement curves for group of four pier footing (reproduced per White et al., 2007).....21
Figure 11: Subsurface profile at Utah site – group of five piers (a) top view and (b) profile view (reproduced per Wissmann et al., 2007) 22
Figure 12: Utah modulus test for single pier and group of five (reproduced per Wissmann et al, 2007) 23
Figure 13: Column arrangement for (a) single pier and (b) group of three piers (reproduced per Black et al., 2007b) 28
Figure 14: Treated ground model consisting of preconsolidated untreated soft clay and a cement mixed soil column at the center in a cylinder mold (Fang and Yin, 2007) 29
Figure 15: Testing box (Black et al., 2007a) 31
Figure 16: (a) Excavated bridge reinforcement and (b) column enclosed in tabular wire mesh (reproduced per Black et al., 2007a).....32
Figure 17: (a) Enerpac hydraulic jack in operation, (b) Enerpac hydraulic jack applied to stacked sensors, (c) Enerpac hydraulic jack mounted on load bearing frame 40
Figure 18: Load frame (a) schematic drawing and (b) as-built photo 41
Figure 19: Load frame schematic drawing (isometric).....42
Figure 20: Test bed preparation (a) excavation, (b) finished after compaction, (c) placement of single piers and (d) testing of single piers 44
Figure 21: Compaction tools (a) vibratory plate compactor, (b) hand tamper 46
Figure 22: DCP equipment (a) in operation in test bed (b) schematic drawing 48
Figure 23: Nuclear density gauge device in use in test bed.....51
Figure 24: (a) Shelby tube inserted in matrix soil, (b) Shelby tube sample being extruded, (c) 72 mm x 140 mm sample trimmed, and (d) sample weighted and measured.....53
Figure 25: 72 mm x 140 mm sample (a) placed in unconfined compression triaxial chamber, (b) and (c) samples after failure 54
Figure 26: Load cell and LVDT sensor set-up (a) test set-up, (b) in use.....58
Figure 27: DAQ data logger 59
Figure 28: Honeywell pancake load cell.....59
Figure 29: Micro Epsilon LDR-CA50 LVDT 60

www.manaraa.com

Figure 30: (a) Humboldt displacement transducer, (b) tell-tale plate, (c) cavity in the soil with tell-tale plate inserted, and (d) complete set-up of sensors 61
Figure 31: DeWall hammer drill 62
Figure 32: (a) Pier installation process reproduced per Fox et al., 2004 and (b) through (f) depicted in the test bed while constructing small-scale piers 63
Figure 33: Beveled tamper heads (a) cone, (b) truncated cone, (c) flat and (d) wedge 64
Figure 34: Truncated cone beveled tamper head schematic drawing 64
Figure 35: Cementitious pier installation process 65
Figure 36: 28 day compressive strength test 66
Figure 37: (a) 305 mm pier prior to testing and (b) after plunging failure 67
Figure 38: (a) 610 mm pier prior to testing and (b) after bulging failure 67
Figure 39: DAQ sample (a) displacement output raw data and (b) load output raw data 68
Figure 40: Test bed single isolated pier layout (top view) 70
Figure 41: Test bed single isolated pier layout (top view) 71
Figure 42: Test bed group pier layout for (a) single pier and unit cell, (b) group of two and four piers, and (c) group of five and six piers (profiles views) 72
Figure 43: Test bed group pier schematic layout (top view) 73
Figure 44: Test bed group pier photographic layout (top view) 73
Figure 45: Standard Proctor compaction curve 75
Figure 46: Particle size distribution for loess, full and $1/10^{th}$ scale AASHTO No. 57, and sand materials 76
Figure 47: (a) Direct shear machine and (b) scaled aggregate sample after shearing 81
Figure 48: Direct shear (a) test results, failure envelope and (b) plotted friction angle for crushed limestone aggregate 82
Figure 49: Cement type I compound 84
Figure 50: $1/10^{th}$ scaled aggregate pier material mixed with cement type I 84
Figure 51: Cement type K compound 85
Figure 52: Volumetric changes of type I and type K cements (reproduced per Mehta and Monteiro, 2006). 85
Figure 53: NS7 admixture compound 86
Figure 53: Expansive C(I) + C(K) + NS7 and C(I) + NS7 mixtures (a), (b), (c) shown within the cavity in matrix soil and (d) placed in cylinders for curing and 28 day strength evaluation 87
Figure 55: 19 mm polypropylene fibers 88
Figure 56: Loess + C(I) + fiber mix during sample preparation 88
Figure 57: Stress-settlement test results for matrix soil used for placement of piers compacted via different shape tamper heads 91
Figure 58: Stress-settlement test results (a) for 305 mm and (b) for 610 mm long piers compacted using cone, truncated cone, flat and wedge tamper heads 92
Figure 59: Stress-settlement test results for matrix soil used for placement of single piers of various composition 93
Figure 60: Stress-settlement test results (a) for 305 mm long aggregate piers and (b) for 610 mm long aggregate piers 94
Figure 61: Stress-settlement test results (a) for 305 mm and (b) for 610 mm long aggregate piers with cemented bulb 95

www.manaraa.com

Figure 62: Stress-settlement test results (a) for 305 mm and (b) for 610 mm long aggregate piers with cemented top 100 mm. 96
Figure 63: Stress-settlement test results (a) for 305 mm and (b) for 610 mm long piers composed of loess and fibers 97
Figure 64: Stress-settlement test results (a) for 305 mm and (b) for 610 mm long piers composed of loess and cement....98
Figure 65: Stress-settlement test results (a) for 305 mm and (b) for 610 mm long piers composed of loess, cement and fibers....99
Figure 66: Stress-settlement test results (a) for 305 mm and (b) for 610 mm long piers composed of cement type I and K....100
Figure 67: Stress-settlement test results (a) for 305 mm and (b) for 610 mm long piers composed of cement type I, K and NS7 101
Figure 68: Stress-settlement test results (a) for 305 mm and (b) for 610 mm long piers composed of cement type I and NS7 102
Figure 69: Stress-settlement test results (a) for 305 mm and (b) for 610 mm long piers composed of sand....103
Figure 70: Overall stress-settlement test results for all (a) 305 mm and (b) 610 mm long single piers of various composition 104
Figure 71: Calculated design versus actual bearing capacity values for single piers of various composition (bar chart)....109
Figure 72: Calculated design versus actual bearing capacity for single piers of various composition (scatter chart)....110
Figure 73: Stress-settlement test results for matrix soil used for placement of aggregate pier groups....111
Figure 74: Stress-settlement test results (a) for 305 mm and (b) for 610 mm long single aggregate piers 112
Figure 75: Stress-settlement test results (a) for 305 mm and (b) for 610 mm long aggregate piers unit cell....113
Figure 76: Stress-settlement test results(a) for 305 mm and (b) for 610 mm long groups of two aggregate piers 114
Figure 77: Stress-settlement test results (a) for 305 mm and (b) for 610 mm long groups of four aggregate piers....115
Figure 78: Stress-settlement test results (a) for 305 mm and (b) for 610 mm long groups of five aggregate piers....116
Figure 79: Stress-settlement test results (a) for 305 mm and (b) for 610 mm long groups of six aggregate piers....117
Figure 80: Overall stress-settlement test results for all (a) 305 mm and (b) 610 mm long aggregate piers 118
Figure 81: Bearing capacity values compared between laboratory and field tested footings (single pier, group of four and group of five footings)....122
Figure 81: Stress-settlement test results for matrix soil used for placement of C(I) + C(K) groups of piers....124
Figure 83: Stress-settlement test results for 305 mm and (610 mm group of four was not tested due to technical difficulties) 124
Figure 82: Stress-settlement test results (a) for 305 mm and (b) for 610 mm long single C(I)

www.manaraa.com

+ C(K) piers 125
Figure 83: Stress-settlement test results (a) for 305 mm and (b) for 610 mm long C(I) + C(K) unit cell piers.....126
Figure 84: Stress-settlement test results (a) for 305 mm and (b) for 610 mm long group of two C(I) + C(K) piers.....127
Figure 86: Stress-settlement test results (a) for 305 mm and (b) for 610 mm long group of five C(I) + C(K) piers 128
Figure 87: Stress-settlement test results (a) for 305 mm and (b) for 610 mm long group of six C(I) + C(K) piers.....129
Figure 88: Overall stress-settlement test results for all (a) for 305 mm and (b) for 610 mm long C(I) + C(K) groups of piers 130
Figure 90: Stiffness comparison at 10mm of settlement for aggregate piers compacted via cone and truncated cone heads.....136
Figure 91: Stiffness ratio comparison between C(I) + C(K) composition piers and aggregate piers.....152
Figure 92: DCPI for single piers compacted via cone, truncated cone, and flat heads 171
Figure 93: DCPI for single piers compacted via wedge head.....172
Figure 94: DCPI for single aggregate piers: aggregate pier, aggregate pier w/cem. bulb and aggregate pier w/cem. top 0.1m.....173
Figure 95: DCPI for single loess piers: loess+fibers, loess+cement, loess+cement+fibers 174
Figure 96: DCPI for single cement piers: C(I) + C(K), C(I) + C(K) + NS7, C(I) + NS7 175
Figure 97: DCPI for single sand piers.....176
Figure 98: DCPI for group aggregate piers: unit cell, single pier, group of 2.....177
Figure 99: DCPI for group aggregate piers: group of 4, group of 5, group of 6 178
Figure 100: DCPI for group C(I) + C(K) piers: unit cell, single pier, group of 2 179
Figure 101: DCPI for group C(I) + C(K) piers: group of 4, group of 5, group of 6.....180
Figure 102: CBR for single piers compacted via cone, truncated cone, and flat heads.....181
Figure 103: CBR for single piers compacted via wedge head.....182
Figure 104: CBR for single aggregate piers: aggregate pier, aggregate pier w/cem. bulb and aggregate pier w/cem. top 0.1m.....183
Figure 105: CBR for single loess piers: loess+fibers, loess+cement, loess+cement+fibers.....184
Figure 106: CBR for single cement piers: C(I) + C(K), C(I) + C(K) + NS7, C(I) + NS7.....185
Figure 107: CBR for single sand piers.....186
Figure 108: CBR for group aggregate piers: unit cell, single pier, group of 2 187
Figure 109: CBR for group aggregate piers: group of 4, group of 5, group of 6.....188
Figure 110: CBR for group C(I) + C(K) piers: unit cell, single pier, group of 2 189
Figure 111: DCPI for group C(I) + C(K) piers: group of 4, group of 5, group of 6.....190

www.manaraa.com

LIST OF TABLES

Table 1: Stiffness modulus for small and large scale aggregate piers 24
Table 2: Case studies 1-3 for reduced scale columns 25
Table 3: Case studies 4-6 for reduced scale columns 26
Table 4: Case 7 for reduced scale columns.....27
Table 4: DCPI and CBR average values for matrix soil of single piers compacted via different beveled heads 49
Table 6: DCPI and CBR average values for matrix soil of various mix single piers 50
Table 7: DCPI and CBR average values for matrix soil of group aggregate piers.....50
Table 8: DCPI and CBR average values for matrix soil of group cement type I and K composition piers.....50
Table 9: UC loess sample γ_{dry} and w% for single piers compacted via various beveled heads.....55
Table 10: Top UC loess sample C_u for single piers compacted via various beveled heads 55
Table 11: Top nuclear density gauge loess γ_{dry} and w% for single piers mixes 55
Table 12: Top and bottom UC loess sample γ_{dry} and w% for single pier mixes.....56
Table 13: Top and bottom UC loess sample C_u for single pier mixes.....56
Table 14: Top and bottom UC loess sample γ_{dry} and w% for group of aggregate piers 56
Table 15: Top and bottom UC loess sample C_u for group of aggregate piers 57
Table 16: Top and bottom UC loess sample γ_{dry} and w% for group C(I) + C(K) piers.....57
Table 17: Top and bottom UC loess sample C_u for group C(I) + C(K) piers.....57
Table 18: Average C_u, w% and γ_{dry} for 305 mm and 610 mm loess samples.....77
Table 18: Pier mix proportions, compressive strengths, and pier construction details.....78
Table 20: Full-scale and $1/10^{th}$ scale aggregate pier dimensions.....79
Table 21: $1/10^{th}$ scale aggregate pier mix proportions.....80
Table 22: Direct shear test initial density and void ratio of scaled aggregate pier material 81
Table 23: Stress and stiffness comparison measurements for simulated aggregate piers constructed via different shape tamper heads 91
Table 24: Stress, stiffness and deflection comparison measurements for load test results for single piers of various mixes.....105
Table 25: Ultimate bearing capacity due to bulging failure for single piers 107
Table 26: Ultimate bearing capacity due to plunging failure for single piers 108
Table 27: Stress, stiffness and deflection comparison measurements for aggregate pier group load test results and group efficiency in comparison to a single pier 119
Table 28: Stress, stiffness and deflection comparison measurements for aggregate pier group load test results and group efficiency in comparison to a unit cell pier.....120
Table 29: Group efficiency comparison measurements for small and full-scale aggregate piers.....121
Table 30: Stiffness modulus for small and full-scale aggregate piers 121
Table 31: Measured ultimate bearing capacity 122
Table 32: Stress, stiffness and deflection comparison measurements for C(I) + C(K) group load test results.....131
Table 33: Group efficiency comparison measurements for small and full-scale piles 132
Table 34: Ultimate bearing capacity for a single pier within C(I) + C(K) group 132

www.manaraa.com

Table 35: Comparison measurements for single aggregate piers at different testing stages compacted via cone and truncated cone beveled heads 135
Table 36: Stiffness ratio calculations for single piers of various composition 140
Table 37: Stress concentration calculations for groups of aggregate piers 144
Table 38: Stress concentration calculations for groups of C(I) + C(K) 147
Table 39: Stiffness comparison at 2 mm displacement between groups of aggregate piers and C(I)+C(K) 150
Table 40: Stiffness comparison at 5 mm displacement between groups of aggregate piers and C(I)+C(K) 151
Table 41: Stiffness comparison at 10 mm displacement between groups of aggregate piers and C(I)+C(K) 151

www.manaraa.com

LIST OF EQUATIONS

Equation 1: Ultimate bearing capacity due to bulging....13
Equation 2: Limiting radial stress....14
Equation 3: Limiting radial stress (simplified)....14
Equation 4: Effective stress....14
Equation 5: Ultimate bearing capacity due to plunging....14
Equation 6: Bearing capacity due to shaft friction....15
Equation 7: Average unit friction....15
Equation 8: Bearing capacity due to tip resistance....15
Equation 9: Bearing capacity on the unreinforced matrix soil for circular footings....16
Equation 10: Total ultimate load on a footing....16
Equation 11: Load resistance provided by the piers....16
Equation 12: Load resistance provided by the matrix soil....17
Equation 13: Stress imposed on piers....17
Equation 14: Stress imposed on matrix soil....17
Equation 15: Group efficiency....17
Equation 16: Group efficiency....17
Equation 17: CBR and DCPI correlation....49
Equation 18: Stiffness modulus....106
Equation 19: Top of the pier tell-tale deflection ratio....106
Equation 20: Stiffness ratio for cone and truncated cone compacted aggregate piers....135
Equation 21: Stiffness ratio for pier supported versus unreinforced footing....139

www.manaraa.com

LIST OF SYMBOLS

Symbol	Description	Units
σ_{I+K}	Stress Imposed on Top of Pier composed of cement Type I and K	kPa
$\sigma_{aggregate\ pier}$	Stress Imposed on Top of Aggregate Pier	kPa
μ	Poisson's Ratio of Matrix Soil	-
A_g	Cross-sectional Area of Piers	m^2
A_m	Cross-sectional Area of Matrix Soil	m^2
C_u	Undrained Shear Strength	kPa
$C_{u\ bot}$	Undrained Shear Strength for Matrix Soil below 305mm zone	kg/m^3
$C_{u\ top}$	Undrained Shear Strength for Top 305mm Portion of Matrix Soil	kg/m^3
d_{10}	Effective Size	mm
d_{60}	Diameter corresponding to 60% Finer	mm
d_f	Depth of the Bottom of the Footing below Adjacent Grade	mm
$d_{nominal}$	Nominal Diameter of Cavity for Pier Placement	mm
d_{shaft}	Diameter of Bulged pier Shaft	mm
$d_{steel\ cap}$	Diameter of the Footing Cap placed on Unreinforced Soil	mm
E	Undrained Modulus of Matrix Soil	kPa
f_s	Average Unit Friction	kg/m^2
H_{shaft}	Pier Shaft Length	mm
k	Stiffness Modulus	kPa/m
$Load_{isolated\ pier}$	Load Imposed on a Single Isolated Pier	kN
$Load_{pier\ group}$	Total Load Imposed on a Group of Piers	kN
N_c	Bearing Capacity Depth Factor	-
n_{pier}	Stiffness ratio	-
N_{piers}	Number of Piers within a Group	-
N_q	Bearing Capacity Shape Factor	-
N_γ	Bearing Capacity Inclination Factor	-
q	Average Bearing Pressure	kPa
Q_g	Load Resistance provided by the Piers	kN
q_g	Stress imposed on the Piers	kPa
Q_m	Load Resistance provided by the Matrix Soil	kN
q_m	Stress imposed on the Matrix Soil	kPa
q_{shaft}	Ultimate Bearing Capacity due to Shaft Resistance	kPa
q_{tip}	Ultimate Bearing Capacity due to Tip Resistance	kPa
$q_{ult\ aggregate\ pier}$	Ultimate Bearing Capacity	kPa
R_a	Ratio of the Area Coverage of the Pier Elements	-
R_s	Ratio of Pier to Soil Stiffness Values	-
w%	Moisture Content	%
w_{bot}	Moisture Content for Matrix Soil below 305mm zone	kg/m^3
w_{top}	Moisture Content for Top 305mm Portion of Matrix Soil	kg/m^3
$\gamma_{dry\ bot}$	Dry Unit Weight for Matrix Soil below 305mm zone	kg/m^3

www.manaraa.com

Symbol	Description	Units
$\gamma_{dry\ loess}$	Dry Unit Weight of Matrix Soil	kg/m
$\gamma_{dry\ top}$	Dry Unit Weight for Top 305mm Portion of Matrix Soil	kg/m
γ_{wet}	Wet Unit Weight of Matrix Soil	kg/m
$\delta_{tell\text{-}tale}$	Deflection at the Bottom on the Pier	mm
δ_{top}	Deflection at the Top of the Pier	mm
ρ_{dry}	Dry Density	kg/m
σ	Stress at Top of the Pier	kPa
σ_{cone}	Stress Imposed at the Top of the Pier constructed via Cone Head	kPa
$\sigma'_{r.lim}$	Limiting Radial Stress	kPa
$\sigma'_{r.o}$	Total Radial Stress after Installation of Aggregate Pier	kPa
$\sigma_{truncated\ cone}$	Stress Imposed at the Top of the Pier constructed via Truncated Cone	kPa
σ'_{v}	Vertical Effective Stress	kPa
$\sigma'_{v\ avg}$	Effective Vertical Force at the Midpoint of Pier Shaft Length	kPa
φ	Friction Angle	degr
$\varphi_{p\ loess}$	Friction Angle of Loess Matrix Soil Material	degr
$\varphi_{p\ aggregate\ pier}$	Friction Angle of Rammed Aggregate Material	degr

www.manaraa.com

ABSTRACT

Testing small-scale prototype pier foundations to evaluate engineering behavior is an alternative to full-scale testing that facilitates testing of several piers and pier groups at relatively low cost. In this study, various pier systems and pier groups at one tenth scale were subjected to static vertical loading under controlled conditions to evaluate stiffness, bearing capacity, and group efficiency. Pier length, material properties and methods of installation were evaluated.

Pier length to diameter ratios varied between four and eight. A unique soil pit with dimensions of 2.1 m in width, 1.5 m in length and 2.0 m in depth was designed to carry out this research. The test pit was filled with moisture conditioned and compacted Western Iowa loess. A special load test frame was designed and fabricated to provide up to 25,000 kg vertical reaction force for load testing. A load cell and displacement instrumentation was setup to capture the load test data.

Alternative materials to conventional cement concrete were studied. The pier materials evaluated in this study included compacted aggregate, cement stabilized silt, cementitious grouts, and fiber reinforced silt.

Key findings from this study demonstrated that (1) the construction method influences the behavior of aggregate piers, (2) the composition of the pier has a significant impact on the stiffness, (3) group efficiencies were found to be a function of pier length and pier material, (4) in comparison to full-scale testing the scaled piers were found to produce a stiffer response with load-settlement and bearing capacities to be similar.

Further, although full-scale test results were not available for all pier materials, the small-scale testing provided a means for comparing results between pier systems. Finally, duplicate pier tests for a given length and material were found to be repeatable.

www.manaraa.com

CHAPTER 1: INTRODUCTION

Industry Problem

Variation in subsurface soil conditions provides site specific foundation design considerations for every job. This variability however also creates opportunities to identify and utilize more efficient foundation systems that are optimized for the site and loading conditions. Traditionally, deep steel piles, reinforced concrete piers, or shallow spread footings are the primary foundations used to support structures. However, there are often site conditions where these two extremes (i.e. deep vs. shallow) are not necessarily an optimum solution. Therefore, intermediate foundations are being increasingly studied. One such system is Geopier® Rammed Aggregate Piers (RAPs).

When developing a foundation or footing support for a structure, the ability to utilize available resources and materials in the most efficient manner is becoming increasingly important. As a result a more sustainable and better engineered design can be utilized while maintaining the design guidelines and load requirements.

In the past century, the alternative of performing research on scaled model systems has gained popularity and has proven to be successful as long as all the physical properties of the full-scale system are recreated. The following research will present the approach of evaluating intermediate foundation support systems by investigating alternative methods of construction and testing different foundation materials.

Technical Problem

There are many foundation systems currently available in the industry ranging from deep piling to horizontal soil stabilization, dynamic compaction, and group improvement with intermediate pier systems. However, regardless of the system being utilized, the critical technical concerns include the settlement and bearing capacity provided by the system.

www.manaraa.com

While different structures can tolerate different amount of total or differential settlement, the goal for every geotechnical project is to minimize the amount of settlement that the footing and, consequently, the structure would undergo. Some of the established approaches of estimating design settlement are utilized by approximating foundation element as an elastic spring, and using cavity expansion theory.

The design bearing capacity is typically calculated by using Terzaghi's bearing capacity theory. Also some of the established methods of calculating settlement are represented by work of Meyerhof, Bowles, and Schmertmann.

Research Goals

The goals of this project were to (1) develop an effective test pit and loading system to evaluate pier elements subjected to vertical load, (2) evaluate the engineering behavior of scaled pier elements at length to diameter ratios varying between four and eight, and (3) identify similitude and scaling limitations of analyzed $1/10^{th}$ scale piers and make comparisons to full-scale tests.

The research was to be performed on scaled aggregate piers, cementitious grout columns, sand piers and other composition mixes constructed within the Western Iowa loess matrix soil. The testing was to be carried out to evaluate settlement, bearing capacity and group efficiency parameters.

Research Objectives

To accomplish the goals of this research, the investigation of different foundation systems was to be performed and the findings are to be presented by:

www.manaraa.com

- applying different installation methods, where some of the piers are to be compacted through ramming aggregate with various tamper heads, other grout piers are to be cast in place and some partial grouting is to be performed,
- varying shaft length, where short 305 mm and long 610 mm elements are to be constructed,
- altering pier composition, such as aggregate, grout, loess, or through addition of admixture components, such as fibers and expansive cement grouts,
- varying the number of piers within a group, where groups of two, four, five and six piers are to be constructed.

Research Benefit and Significance

Results from this study will be used to develop full-scale test plans for alternative foundation systems. The industry will benefit from this research by understanding how various tamper heads contribute to stiffening of aggregate piers, possibly using other composition systems that are more economical and efficient, utilizing admixture components in order to enhance performance of the piers and selecting appropriate length of the foundation support elements to balance the amount of material used with the load-displacement requirements.

Overall, the foundation support industry can benefit from this research by utilizing the outlined construction and design techniques in different geotechnical applications. The outcomes of this research can encourage industrial companies to develop new ideas by investing into research through small-scale modeling, and possibly prompt to perform additional testing to confirm the findings obtained in this investigation.

Forecasting

The Background chapter introduces characteristics associated with full-scale aggregate piers, as well as, historical studies performed on scaled piers and columns by different researchers, supplemented with case histories.

www.manaraa.com

The Research Methodology chapter presents a summary of tests and methods used to construct the pier load frame system, prepare the test bed matrix soil, construct scaled aggregate piers and grouted piers, as well as, procedures developed for pier testing and data collection.

The Materials chapter describes the more detailed information on composition and characterization of matrix loess soil and pier elements.

The Test Results chapter includes a summary of load-settlement results summarized in tables, as well as, bearing capacity and group efficiency parameters calculated and tabulated from the collected data.

The Discussion of Results chapter provides the analysis of the results, tabulated in the previous chapter, and supplements outcomes of the study with observations and conclusions.

Finally, the last chapter outlines major conclusions associated with the performed study.

www.manaraa.com

CHAPTER 2: BACKGROUND

This chapter presents the background information on the full-scale Geopier® Rammed Aggregate Pier (RAP) intermediate foundations, as well as, small-scale model tests performed by different researchers over the past several decades. Several supplemental case studies are summarized with a brief description of the testing apparatus, soil conditions and major conclusions outlined for each case.

Full-Scale Aggregate Pier Foundation Element Features

Overview

The concept of reinforcing and stabilizing in-situ soils with structural elements of higher stiffness has been known for many thousands of years dating back to the ancient Mesopotamian temples and Egyptian pyramids, reinforced with boulders placed in excavated soil cavities (Construction of the Great Pyramids, 2002). Since then, the concepts and ideas of reinforcing in-situ soils have been advanced and modernized. Many of the techniques are now well established in the industry and proven to be reliable in a variety of applications. However, as more civil engineering projects require exploration of highly organic, peaty and high moisture content soils, the development of new methods of reinforcing poor soils is encouraged.

While many of the currently available foundation technologies have been well developed and adopted in practice, many of them provide limited application and high cost when used in poor soil conditions. As an alternative, in 1989 the RAP intermediate foundation technology was developed and patented by Geopier Foundation Company™ (GFC). The idea of ramming aggregate in even sized lifts has rapidly established itself to be successful in reinforcing soil and has proven to be an innovative, cost saving and suitable foundation system for many projects, where other conventional methods can be cost prohibitive (Figure 1).

www.manaraa.com

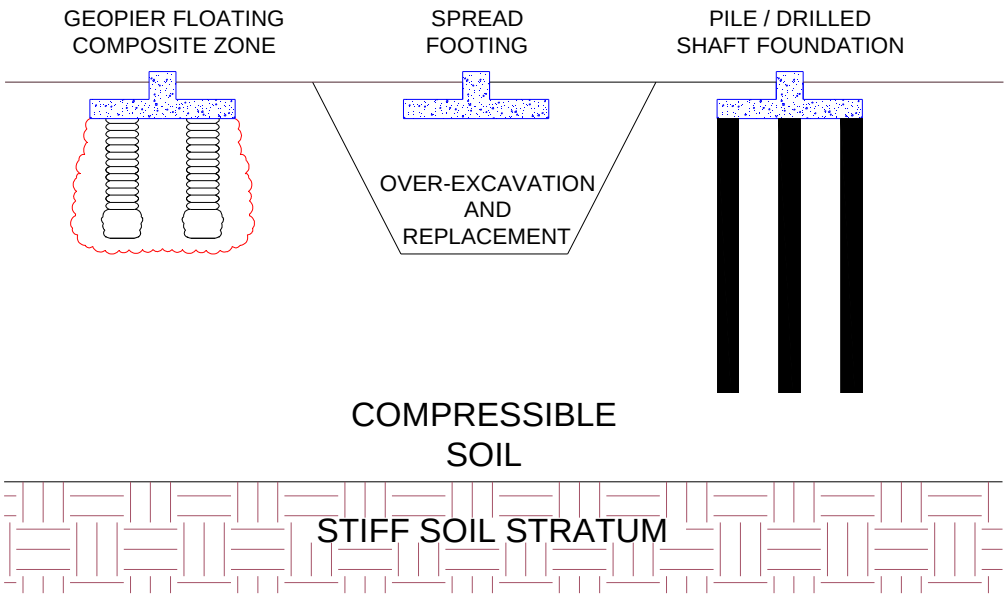

Figure 1: Concept of aggregate pier floating foundation (reproduced per Kwong et.al, 2002)

A successful application of aggregate pier technology in particular is attributed to the relatively simple process of ramming aggregate in a 760 mm diameter hole at 300 mm compacted thickness lifts. A key feature of the aggregate pier success is lateral confinement that is developed between matrix soil and rammed material. Construction of the first lift, also known as the bottom bulb, is typically done by ramming open graded base coarse stone, while the rest of the shaft is built with well graded base coarse stone. A simplified model of full-scale aggregate pier construction process can be found in Figure 2.

The typical stiffness improvement provided to the unreinforced soil by an aggregate pier element has been measured between 8 and 35 (Wissmann et al., 1999). Another important parameter that contributes towards the degree of soil improvement is the stiffness of the pier which is dependent on the interlock between the rammed aggregate particles. Friction angle is related to the level of aggregate interlock and resistance to internal shear failure of the pier and has been evaluated to be in the range of 49 and 52 degrees (Fox et al, 1998).

www.manaraa.com

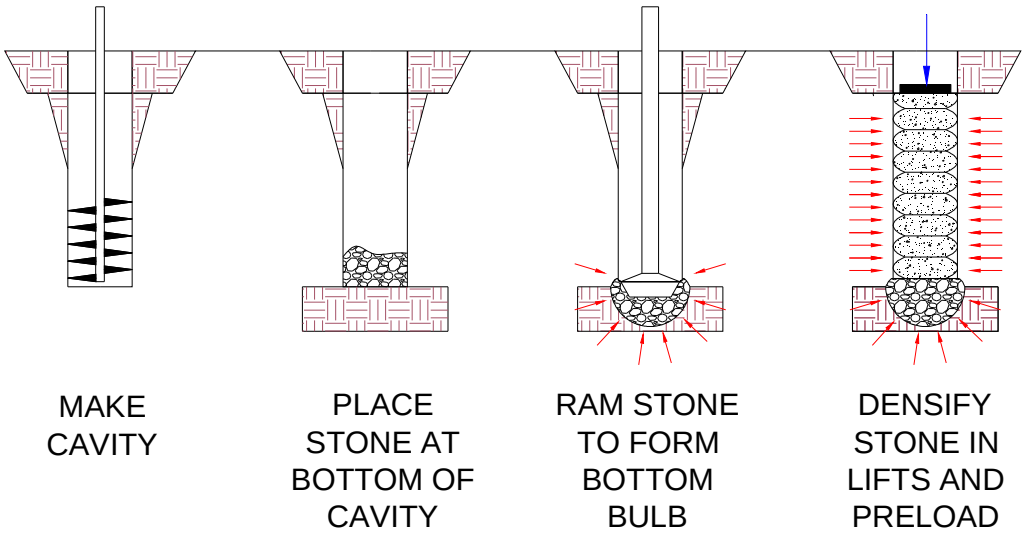

Figure 2: Simplified aggregate pier installation procedure (reproduced per Fox et al., 2004)

Uncemented aggregate piers typically deform by bulging or tip movement. Bulging deformation typically develops in longer piers or where the bulb is supported by a stiffer layer of soil. Pier bulging is supplemented with lateral displacement in the adjacent matrix soil, which is typically observed to occur within the top portion of the pier (Wissmann, 1999). The lateral confinement provided by the matrix soil controls the amount of soil lateral displacement and has been proven to correlate with the amount of settlement that the aggregate pier undergos (Handy, 2001).

However, the mechanism of aggregate pier punching failure can also be developed when stresses at the pier bottom are high. As the length of the aggregate pier decreases, the pier tends to act more as a solid structural element and undergo less internal deformation. Therefore, shorter length aggregate piers are less vulnerable to settle through process of bulging and more inclined to undergo shearing deformation at the tip of the aggregate pier element by process of plunging (White and Suleiman, 2004). Additional to the failure at the tip, aggregate pier skin friction is mobilized on the interface of pier shaft (White and Suleiman, 2004). However, unlike other types of supporting systems (for example piles), aggregate pier construction is not limited by the presence of a better layer of firm soil at a pier tip. The additional amount of confinement at the tip of the aggregate pier is first

www.manaraa.com

provided by the bulb and then supplemented by a stiffer layer of soil, if available. Figure 3 provides a schematic drawing of the plunging and bulging types of failure.

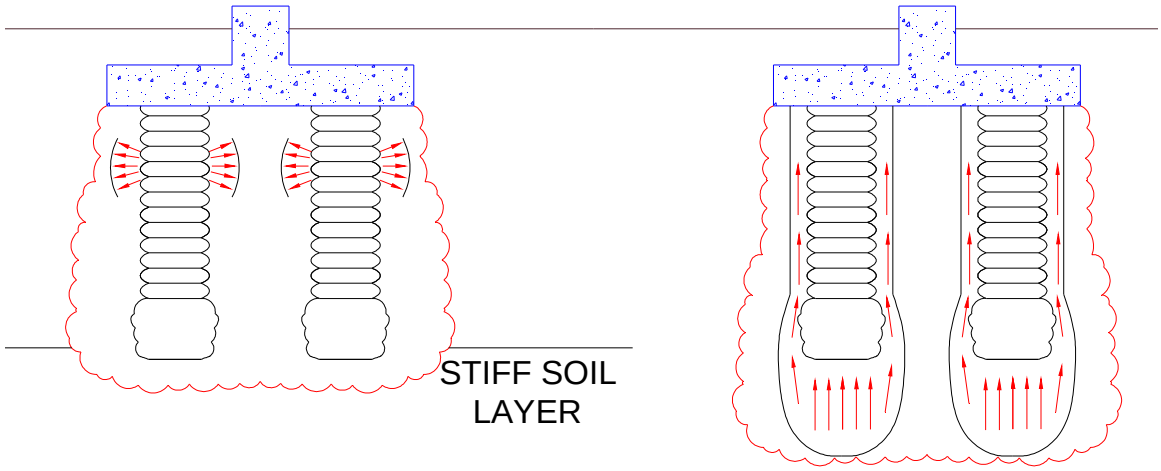

(a) **(b)**

Figure 3: (a) Bulging of aggregate pier elements and (b) shearing below tips of aggregate pier elements (reproduced per Wissmann, 1999)

Materials

Typically, when designing an aggregate pier element, the materials involved in the design are separated into two main categories: the constituent material of the aggregate pier itself and the matrix soil where the aggregate pier is being installed.

Aggregate pier elements are usually built using recycled concrete or well graded crushed stone. Use of AASHTO No.57 stone or AASHTO No.21A base coarse stone is common, where the former is typically used below the water table. The friction angle for a full-scale pier constructed with AASHTO No.57 stone was estimated at 48 degrees, where for No.21A aggregate the angle of friction was found to be 52 degrees (Fox et al., 1998). More recent studies have shown the friction angle to range between 44 and 56 degrees (Jian and Park, 2007).

www.manaraa.com

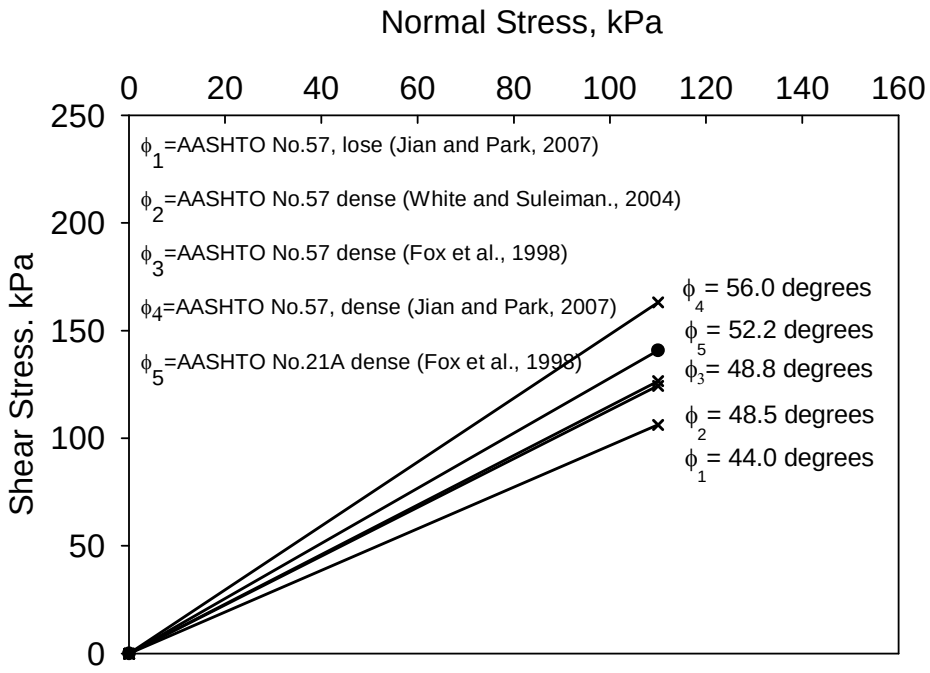

Figure 4: Friction angle for AASHTO No. 57 and No. 21A limestone aggregate (reproduced per Fox et al., 1998, Jian and Park, 2007 and White and Suleiman, 2004)

Another unique feature of aggregate pier is associated with the potential of the aggregate to gain strength with time. While concrete or cementitious grout composition piles and columns undergo strength gain with time due to curing, the intermediate foundation elements feature a process of strengthening through dissipation of pore water pressure in matrix soil (Lechner and Hanagan, 2009). As the pore water pressure of matrix soil is at its peak immediately after completion of the pier, the process of dissipation of pore water pressure over time leads to an increase in pier modulus (FitzPatrick et al., 2003). However, the dissipation of pore water pressure is highly dependent on the permeability of the matrix soil, as well as, moisture content, presence of drainage and overall level of soil consolidation.

Another material involved in the design of aggregate pier foundation systems is represented by the matrix soil. The most favorable soil conditions for aggregate pier applications are peat, weak soils and expansive clays. The peat type soils are typically associated with high moisture content and feature high compressibility. Using aggregate pier elements in peat soils has proven successful, while many other conventional methods have been cost prohibitive in reinforcing peat.

www.manaraa.com

Another good application of aggregate pier elements is within landfills, debris, weak top soils and waste filled sites. A good illustration of aggregate piers being applied in unknown deposits is represented by construction of the Ice House at the municipal landfill in Hackensack, New Jersey (GFC Newsletter, 2000). Other weak soils such as soft clays, soft silts and lose sands are also very applicable for the aggregate pier foundation systems. In some cases the level of stiffness improvement has been found to be up to 5 times (Fox and Cowell, 1998) and 8 and 35 times (Wissmann et al., 1999).

Finally, expansive clays can also be reinforced by aggregate pier elements, where providing uplift resistance is a common application. However, the piers that are constructed to control uplift are highly dependent on proper construction practices. Careful design and construction practices have shown high levels of improvement in the footing bearing capacity (Wissmann et al., 2001a).

Upper and Lower Zone

Another unique feature associated with aggregate pier type elements is the separation of the settlement zones into Upper and Lower Zones. Upper Zone is located within the matrix soil reinforced by the pier, while Lower Zone is found below the aggregate pier element (Figure 5). The Upper Zone settlement calculations are performed using stiffness of the pier and the matrix soil parameters, while the calculations for the settlement in the Lower Zone are based on conventional settlement methods (White and Suleiman, 2004).

As previously discussed, pier bulging is typically found within the top portion of the aggregate pier or within the Upper Zone, while settlement in Lower Zone is based on soil compressibility below aggregate pier and induced pier stress. Therefore, it can be concluded that settlement of the pier within the Upper Zone is controlled by stiffness of the aggregate pier itself and stiffness of the matrix soil, while in Lower Zone the calculations are based on estimating modulus and bearing capacity of the soil. It is common to design the aggregate

www.manaraa.com

pier element for a maximum of 25 mm in total settlement and 12 mm in differential settlement (Kwong et al, 2002).

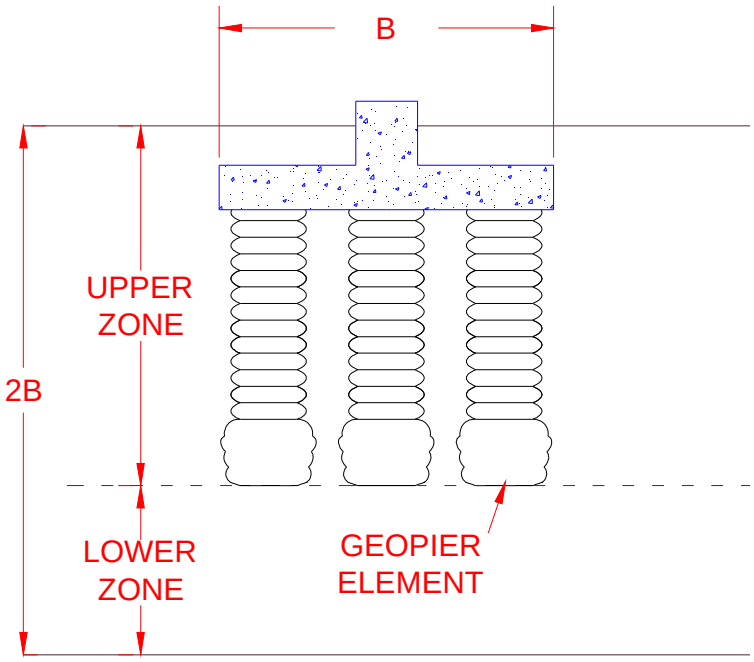

Figure 5: Schematic drawing of aggregate pier Upper and Lower Zones (reproduced per Kwong et al., 2002)

In the experimental environment, settlement within the Upper Zone is typically measured via displacement transducers that are used to record deflection of the footing under load. The Lower Zone settlement is typically verified via tell-tale plate installed at the bulb elevation level of the pier. Typically, the tell-tale plate is placed at the bottom of the cavity and connected with two rebars extended above the ground surface (Figure 6). The rebars are placed within the casing tubes to allow free movement. The movement is produced at the pier bulb and is reflected and recorded at the tips of the rods.

By evaluating relative movement of top and bottom of the pier, the amount of load dissipation from the top of the pier to the bottom bulb can be estimated, and the conclusion can be made regarding bulging or plunging mechanisms of failure. The process of pier bulging is normally associated with little to no movement at the pier tip, and process of pier plunging is associated with significant amount of movement at the tip of the pier. Acceptable

www.manaraa.com

amount of relative displacement at the pier bulb is normally considered not to exceed 20 percent of the top of the pier deflection (Fox and Cowell, 1998).

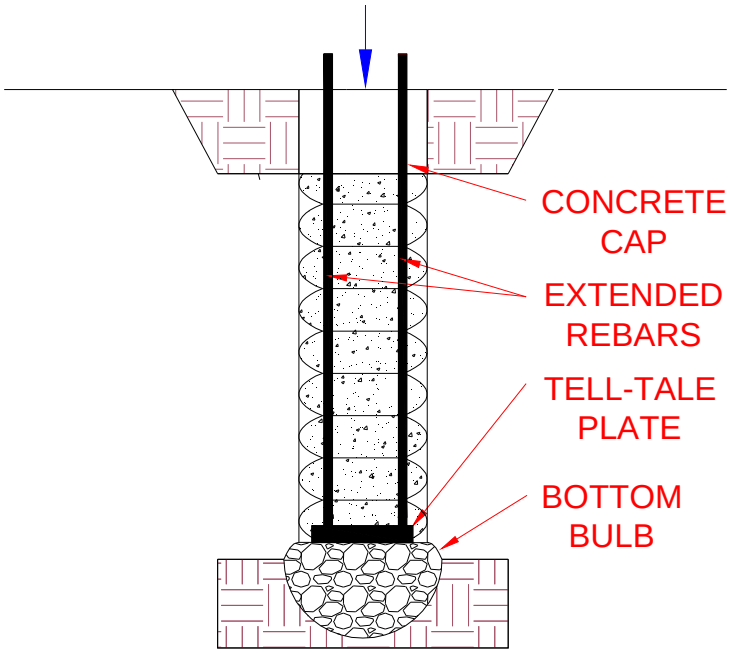

Figure 6: Aggregate pier tell-tale instrumentation (reproduced per White et al., 2007)

Other Technologies

While there are many soil reinforcement techniques available in the industry, the selection of a certain system for most civil engineering projects is primarily governed by the cost. Many conventional methods, such as overexcavation and replacement, can prove to be very expensive due to the extensive use of machinery and need for stock piling of the excavated material. Deep piling technology, on the other hand, requires extension of the foundation system to a stiffer soil layer, which in some cases is located at a great depth.

Construction of a mini storage building in Edina, MN is a good example, where deep overexcavation and replacement was required due to the presence of organic rich soils. The alternative at this site was to install piles reaching 18 m in shaft length. The aggregate pier intermediate foundations were selected over both alternatives due to considerable cost

www.manaraa.com

savings provided by the system (Allgood et al., 2003). Another example, where ability to reach bedrock was restricted, is the construction of an aboveground storage tank in Houston, TX (Wissmann et al., 2001b). By using aggregate pier intermediate foundations this particular project was finished 40 days ahead of schedule and yielded significant amount of cost savings.

Other types of soils such as silty and sandy soils are typically reinforced by a method of dynamic compaction. Being often successful in densifying soil, the dynamic compaction approach often introduces major vibrations to the ground surface and possible disturbance to the structures within a close vicinity of the project. The process of ramming aggregate pier aggregate produces a significantly reduced level of frequency vibration at 300 to 600 cycles per minute, thus, enabling construction of the pier at low level of noise and vibration (Fox and Cowell, 1998). A good representative example, where the reduction of vibration and noise level was of the essence, is outlined in the construction of the Baptist Memorial Hospital in Columbus, Mississippi (FitzPatrick and Wissmann, 2006). Installation of the aggregate piers provided acceptable level of noise and significantly reduced amount of vibration.

Bearing Capacity

When evaluating design bearing capacity of the bulging piers, the calculations are performed by incorporating limiting radial stress and using Rankine passive earth pressure theory (Wissmann, 1999). Having this approach only to be valid for piers placed in cohesive soils, Western Iowa loess was deemed to be suitable (98% fraction of silt and clay). Ultimate bearing capacity of bulging piers can, therefore, be estimated as following:

Equation 1: Ultimate bearing capacity due to bulging

$$q_{ult\ aggregate\ pier} = \sigma'_{r.lim} \tan^2(45 + \varphi_{p\ aggregate\ pier}/2) \qquad \textit{(Equation 1)}$$

Equations 1-7 were taken from Wissmann, 1999.

www.manaraa.com

$\sigma'_{r.lim}$ or limiting radial stress is an unknown and can be calculated from Equation 2.

Equation 2: Limiting radial stress

$$\sigma'_{r.lim} = \sigma'_{r.o} + C_u\,(1+In(E/(2C_u(1+\mu))))) \qquad \textit{(Equation 2)}$$

Limiting radial stress is evaluated from estimating the undrained shear strength, undrained modulus, Poisson's ratio of matrix soil, and total radial stress parameter. The limiting radial stress value is normally calculated for the soil conditions after pier installation and prior to load application. The undrained shear strength of the matrix soil parameter can be obtained from Triaxial Unconfined Compression laboratory tests. Assuming Poisson's ratio for the undrained condition to be 0.5 and the E/c ratio to be conservatively estimated at 200, the equation for $\sigma'_{r.lim}$ is simplified to:

Equation 3: Limiting radial stress (simplified)

$$\sigma'_{r.lim} = 2\sigma'_v + 5.2C_u \qquad \textit{(Equation 3)}$$

Finally, σ'_v or effective vertical stress parameter can be calculated at the elevation of the pier bulging. The dry unit weight of the matrix soil and the depth to the elevation of pier bulging are used to estimate the effective stress:

Equation 4: Effective stress

$$\sigma'_v = H_{bulging}\,\gamma_{dry\ loess} \qquad \textit{(Equation 4)}$$

In case with plunging mechanism of failure, the ultimate bearing capacity is calculated by knowing the shaft friction of the pier and the tip resistance:

Equation 5: Ultimate bearing capacity due to plunging

$$q_{ult} = q_{shaft} + q_{tip} \qquad \textit{(Equation 5)}$$

www.manaraa.com

The bearing capacity accredited to the fiction of the pier shaft can be estimated through Equation 6:

Equation 6: Bearing capacity due to shaft friction

$$q_{shaft} = 4f_s d_{shaft} H_{shaft} / d_{nominal}^2 \quad \textit{(Equation 6)}$$

The next parameter to be evaluated is f_s or average unit friction. The following formula was adopted for the purpose of estimating average unit friction:

Equation 7: Average unit friction

$$f_s = \sigma'_{v\,avg} \tan(\varphi_s) k_{p,s} = (d_f + H_{shaft}/2)\gamma \tan(\varphi_{p\,loess}) \tan^2(45 + \varphi_{p\,loess}/2) \quad \textit{(Equation 7)}$$

Footing depth, friction angle, and shaft length parameters had to be considered in order for the average unit friction to be calculated. Typically, the concrete footing of d_f thickness is poured on top of compacted piers. Friction angle of the matrix loess material can be assumed to be 30 degrees as per Lohnes and Kjartanson (2007). and σ'_v or the effective vertical stress parameter can be calculated in the same manner as for the bulging piers outlined in Equation 4. However the depth is taken not to the level where bulging is to occur but at a length of pier shaft.

The other component of the ultimate bearing capacity for plunging piers is attributed to the tip resistance (Terzaghi, 1943):

Equation 8: Bearing capacity due to tip resistance

$$q_{tip} = C_u N_c + 0.5 d_{shaft} \gamma_{dry\,loess} N_\gamma + \sigma'_v N_q \quad \textit{(Equation 8)}$$

A classic Terzaghi-Buisman approach is typically used and the dimensionless N_c, N_γ and N_q parameters can be found in table provided by Kumbhojkar, 1993 for a 30 degree angle of loess frictional resistance.

www.manaraa.com

Additionally, the ultimate bearing capacity of the unreinforced matrix soil can be calculated through Terzaghi's bearing capacity approach. The cohesion C_u of loess can be approximated as undrained shear strength estimated through laboratory triaxial testing. The bearing capacity formula can vary depending on the shape of the area of the footing. The following equation provides ultimate bearing capacity calculations for a circular shape footing (Terzaghi, 1943):

Equation 9: Bearing capacity on the unreinforced matrix soil for circular footings

$$q_u = 1.3C_u N_c + 0.3d_{footing}N_\gamma + \sigma'_v N_q \qquad \textit{(Equation 9)}$$

When performing bearing capacity calculations for a group of aggregate piers, a consideration must be given to piers and the matrix soil under the footing. Aggregate piers are typically approximated as stiff springs and the stiffness modulus parameters for soil and piers are taken into account.

Bearing capacity results for group of piers can be presented in form of ultimate bearing capacity or ultimate load. To find the total ultimate load Q, the separation is made into load carried by the pier (Q_g) and by matrix soil (Q_m). Resistance provided by aggregate pier element is found by using stress applied to the piers (q_g) and cumulative cross sectional area of the pier elements (A_g). Similar calculations are carried out with respect to the load imposed on matrix soil. Ratio of aggregate pier and matrix soil is outlined as R_s, and ratio of aggregate pier and soil cross-sectional areas is outlined as R_a. The following Equation 10 through Equation 14 are presented according with the procedure outlined in many aggregate pier publications or specifically found in Kwong et al., 2002:

Equation 10: Total ultimate load on a footing

$$Q = Q_g + Q_m = q_g A_g + q_m A_m \qquad \textit{(Equation 10)}$$

Equation 11: Load resistance provided by the piers

$$Q_g = q_g A_g \qquad \textit{(Equation 11)}$$

www.manaraa.com

Equation 12: Load resistance provided by the matrix soil

$Q_m = q_m A_m$ *(Equation 12)*

Equation 13: Stress imposed on piers

$q_g = qR_s / (R_s R_a - R_a + 1)$ *(Equation 13)*

Equation 14: Stress imposed on matrix soil

$q_m = q_g / R_s$ *(Equation 14)*

Group Efficiency

In order to evaluate performance of an individual pier within a group a group of piers, an efficiency parameter is often utilized. The formula that is used for group efficiency calculations is shown in Equation 15:

Equation 15: Group efficiency in terms of single pier

$Group\ Efficiency = Load_{pier\ group} / (Load_{isolated\ pier} \times N_{piers})$ *(Equation 15)*

To evaluate the group efficiency in terms of unit cell the Equation 16 can be used:

Equation 16: Group efficiency in terms of unit cell

$Group\ Efficiency = Load_{pier\ group} / (Load_{unit\ cell} \times N_{piers})$ *(Equation 16)*

Case Studies

The following case studies present valuable information related to construction and testing of full-scale individual and groups of aggregate piers. The case studies outline behavior of a single isolated pier, unit cell, and groups of three, four and five aggregate piers. Correlations between different foundation systems, group efficiency calculations, comparison of pier

www.manaraa.com

stiffness parameters and many other factors are outlined in the described projects, and are targeted to benefit the proposed small-scale pier research study.

Case 1 – Bucher et al., 2008 – Comparison of Load results and Performance of the RAP System in Undocumented Fill in Urban Areas (Chicago, Illinois)

Construction of a 13,000 m^2 retail store was proposed in the vicinity of Chicago, Illinois. The presence of contaminated soils at the proposed site created a need for a more economical solution than conventional overexcavation and replacement method. Therefore, reinforcing existing in-situ soils was proposed to be completed with aggregate piers.

Aggregate piers were constructed at 0.76 m in diameter and spaced at 3.5 m on center. The piers were extended to a depth varying between 2.1 m and 7.6 m. Recycled concrete was used to construct the piers, which enabled Leadership in Energy and Environmental Design (LEED) certification of the project. The instrumentation for this project included tell-tale plates, total stress cells, and aggregate pier load test frame. Unit cell and group of three pier footings were constructed for the purpose of modulus and load-settlement investigation (Figure 7). The goal of the pier testing was to perform full-scale field modulus tests and determine the load capacity and settlement of the individual and groups of aggregate piers.

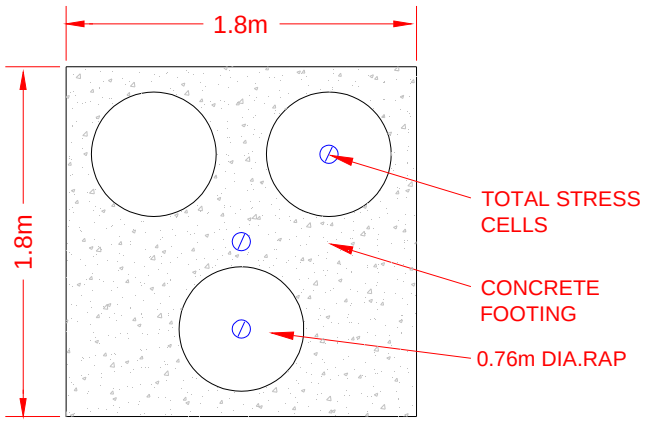

Figure 7: Schematic of group of three footing instrumentation (reproduced per Bucher et al., 2008)

www.manaraa.com

Soil conditions at the site were evaluated to consist of urban fill underlain by a 1.7m - 2.4 m layer of silt. Very soft to stiff clay and dense sand layers were found beneath the layer of silt. Urban fill featured cobbles and large diameter stones. Moisture content of the collected samples varied between 10 and 18 percent. Groundwater table was found to be located at approximate elevation depth of 5.5 m. The SPT (Standard Penetration Test) number of blows for the urban fill layer was found to range between 6 and 20, while the layer of silt was characterized by the N value ranging between 2 and 4. The SPT N values were found to range between 4 and 40 for the soft to stiff clay and dense sand layers.

The load test results have shown group efficiency to be equal to unity. Moreover, the total stress cell results obtained for the group of three pier footings showed a stiffness ratio on the order of 4 at low compression loads and stiffness ratio of 6 at high compression loads (Bucher et al., 2008). Load-settlement results are provided in Figure 8. It was noticed for the group of three footing to undergo a greater amount of settlement under lesser load than the unit cell, however no explanation to the anomaly was provided by the authors.

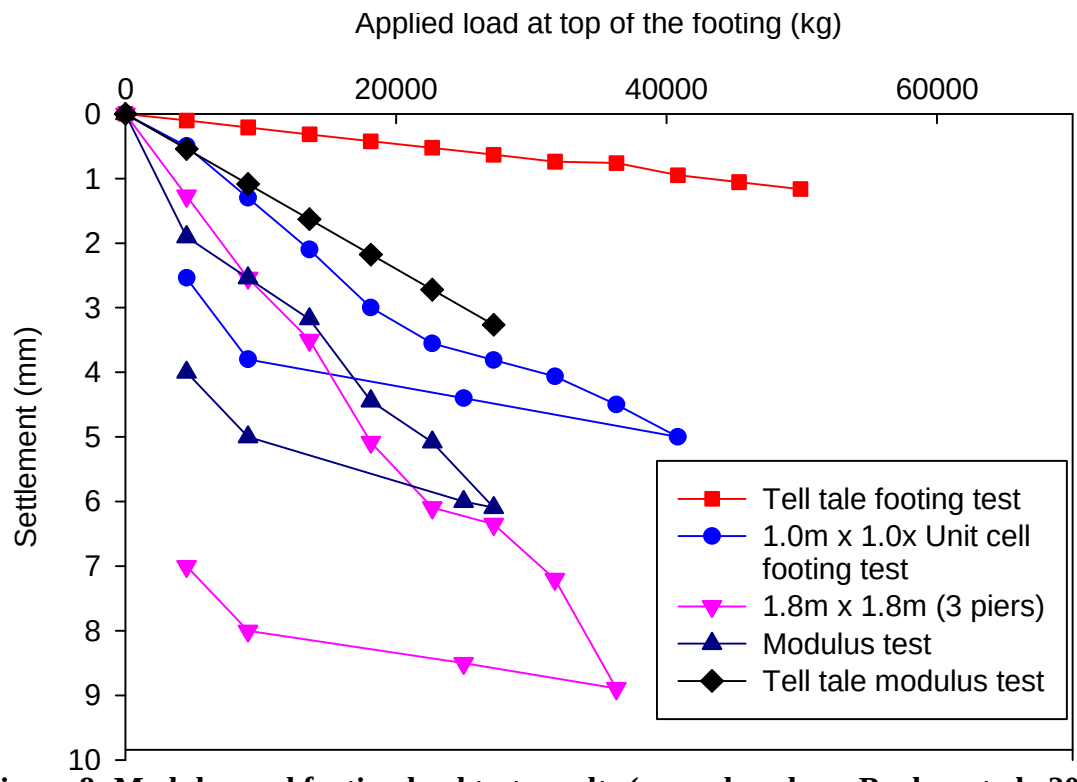

Figure 8: Modulus and footing load test results (reproduced per Bucher et al., 2008)

www.manaraa.com

Case 2 – White et al., 2007 – Box Culvert Foundation Reinforcement at IA Hwy 191 (Neola, IA)

The construction of the box culvert was proposed under a three span bridge on Iowa highway 191 near Neola, Iowa. Downdrag on the existing bridge foundation required remediation measures and, therefore, the construction of a culvert supported by aggregate pier elements was proposed.

Two groups of four aggregate piers were constructed at 0.76 m diameter and spaced at 1.07 m on center for the purpose of pier testing. Area replacement ratio, defined as the ratio of total cross-sectional area to the area of the piers, was estimated at 0.35 for the footing supported by a group of four piers. The constructed piers were extended to the depth of 2.8 m and 5.1 m. Three isolated aggregate piers were also installed and tested using the same installation specifications as for the group of four piers. Aggregate used for pier construction was described as crushed limestone (GP). Friction angle of the material was estimated at 47 degrees, cohesion at 4 kPa, d_{10} = 25 mm and 3 percent was found to pass No. 200 sieve. Soil was described as 13 m thick uniform soft alluvial clay overlain by a 1 m thick desiccated layer. Angle of drained friction was estimated to be 22 and 35 degrees for alluvial clay and desiccated layers, respectfully. Undrained shear strength was 30 kPa for the alluvial clay and 150 kPa for the desiccated layer. The alluvial clay was classified as CL with 98 percent fines and 11 percent clay. The moisture content of the soil near the surface was estimated at 42 percent, and 31 percent at a greater depth.

Instrumentation included total stress cells, tell-tale plates and inclinometers. The inclinometers were installed along the length of the pier shaft, and were used to monitor bulging in the pier when subjected to loading. A specially fabricated aggregate pier group load test frame and 100 ton hydraulic jacks were also used to perform the tests. The goal of the investigation was to perform data acquisition of the pier load and displacement, estimate group efficiency, calculate bearing capacity and stress concentration values for the individual and groups of four piers. Load-settlement results are provided in Figure 9 and Figure 10.

www.manaraa.com

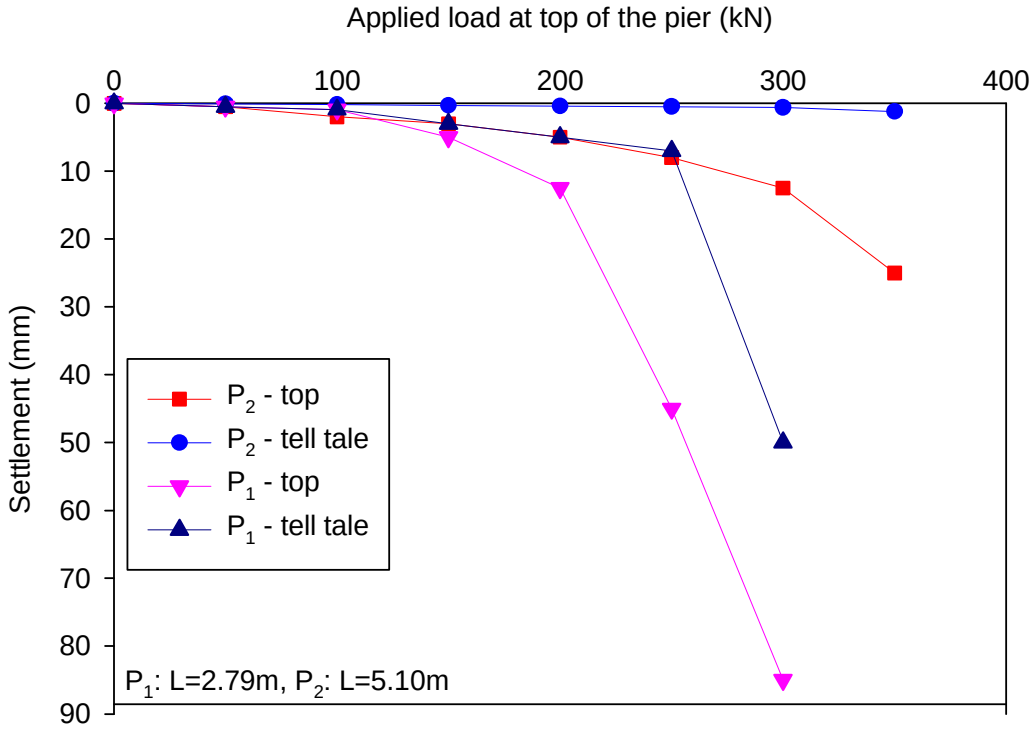

Figure 9: Measured load-settlement curves for single pier (reproduced per White et al., 2007)

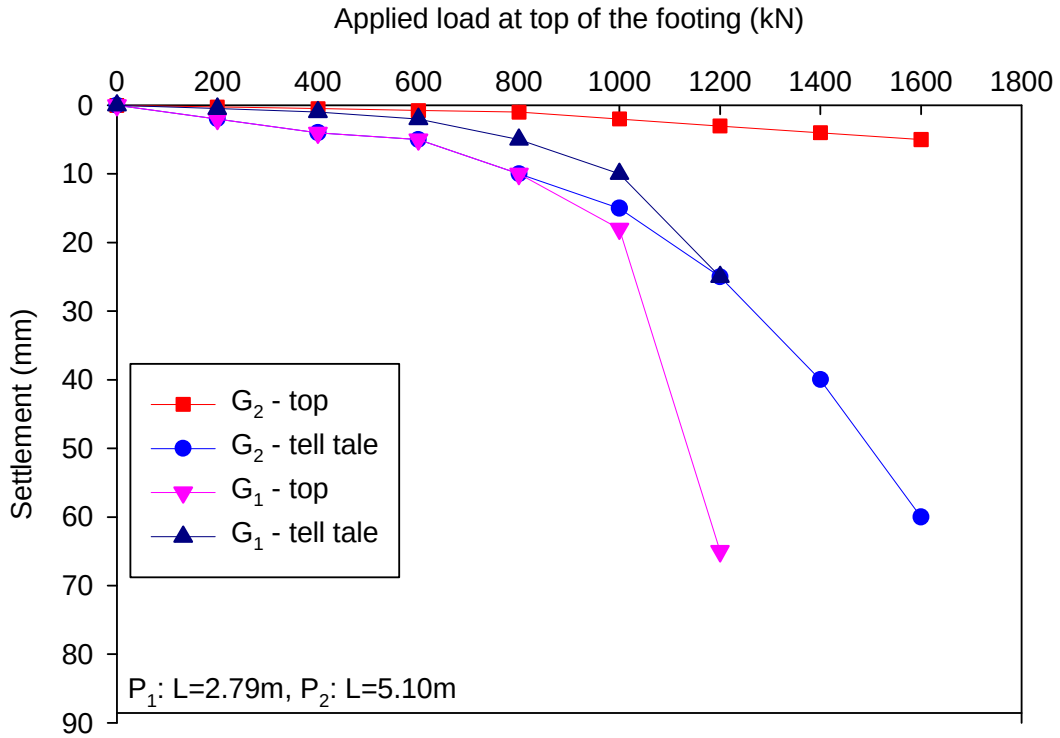

Figure 10: Measured load-settlement curves for group of four pier footing (reproduced per White et al., 2007)

www.manaraa.com

The major findings showed the group efficiency to be equal to 1.0 for group of four piers loaded under 150 kN, while at loads larger than 150 kN the efficiency rapidly increased to 4.7. Under high loads the piers were found to develop higher level of movement at the pier tip, while longer piers were confirmed to fail through the process of bulging. Stiffness of an individual pier was approximately of the same magnitude as the stiffness of the pier within a group.

Case 3 – Wissmann et al., 2007 – Load Test comparisons for Rammed Aggregate Piers and Pier Groups (Salt Lake City, Utah)

A new alignment of interstate I-15 was proposed in Salt Lake City, Utah. The aggregate pier soil reinforcement system was determined to be the most economical for the application and, therefore, was proposed to be used at the site.

Aggregate piers were to be constructed at 0.61 m in diameter and 2.4 m in length. Stiffness modulus tests were to be performed on individual piers, as well as, footings supported by a group of five piers. Well graded base coarse stone was used for the construction of the shaft portion of the aggregate pier, and open graded base coarse stone was used to build the bulb portion of the pier.

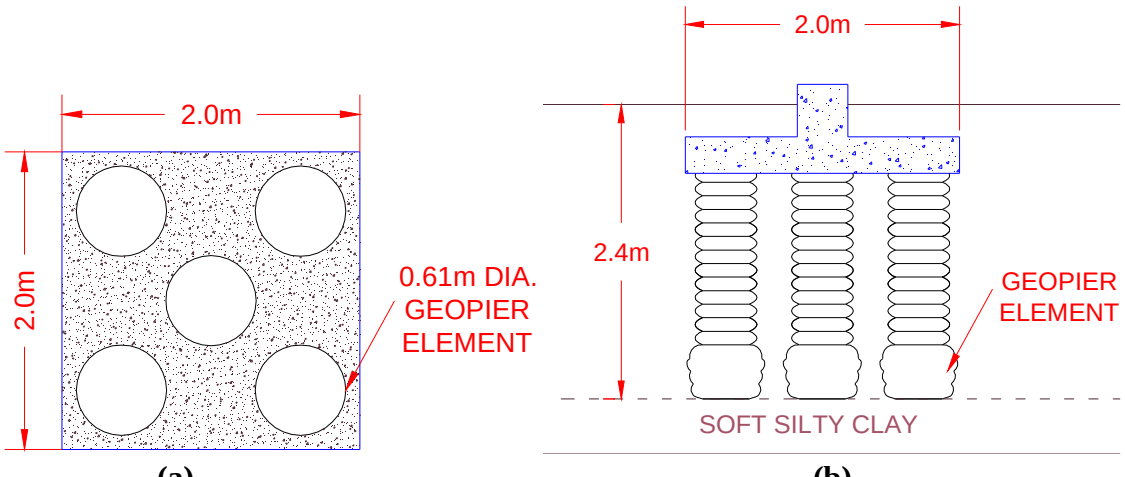

Figure 11: Subsurface profile at Utah site – group of five piers (a) top view and (b) profile view (reproduced per Wissmann et al., 2007)

www.manaraa.com

Site soil conditions were described as soft Lake Bonneville interbedded clay and silt deposits. The Cone Penetration Test (CPT) resistance was approximated at 1 MPa. The equipment used for testing of the piers included aggregate pier load test frame, tell-tale plates, stress cells, and displacement transducers. The investigation was primarily oriented towards modulus testing of single piers, groups of five piers and footings placed over the unreinforced matrix soil.

The major findings showed that the response of the individual pier closely follows the stress-settlement response of the pier within the group of five. At the 25 mm of settlement, the aggregate pier supported footing featured three times the bearing capacity of the footing supported by in-situ soil with no reinforcement. Obtained stress-settlement results can be found in Figure 12:

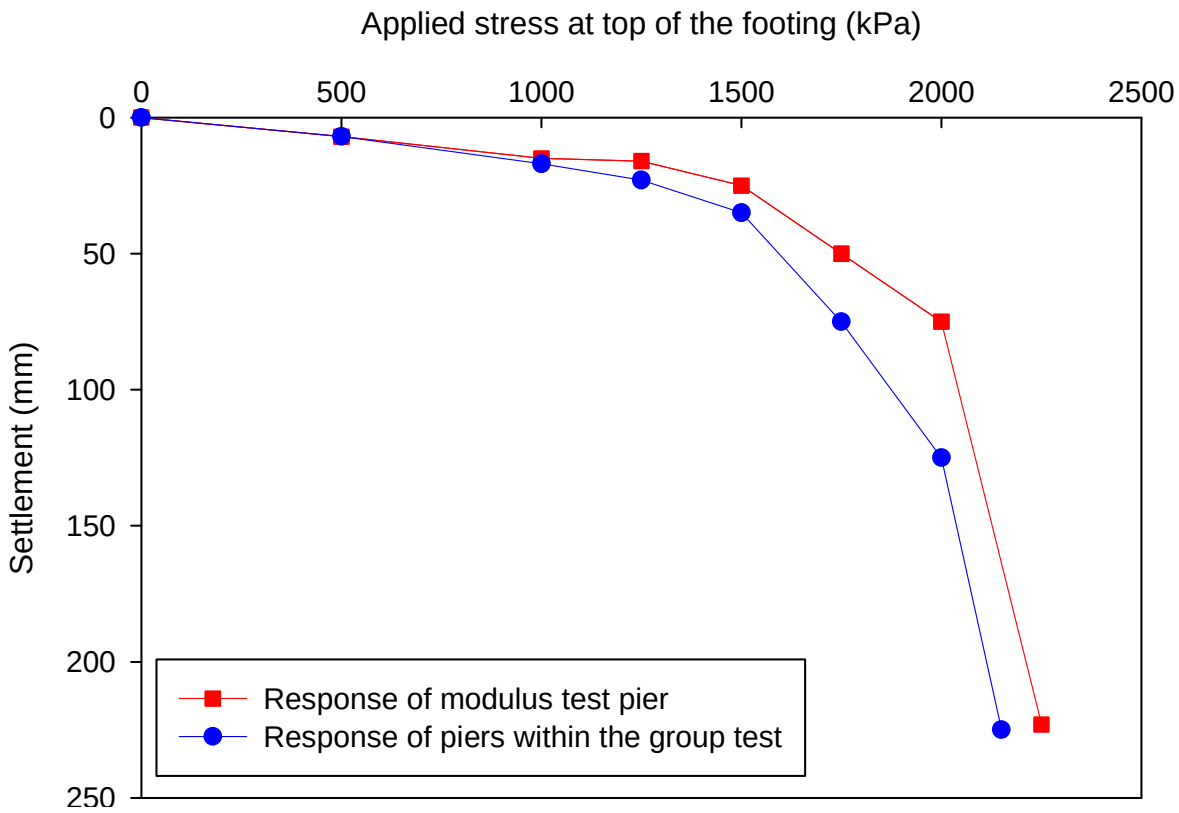

Figure 12: Utah modulus test for single pier and group of five (reproduced per Wissmann et al, 2007)

www.manaraa.com

Supplemental stiffness modulus parameters are summarized for the abovementioned different full-scale aggregate pier groups and can be found in Table 1.

Table 1: Stiffness modulus for small and large scale aggregate piers

	Stiffness Modulus (kPa/mm)		
Pier type	Full-Scale Aggregate Piers	Full-Scale Aggregate Piers	Full-Scale Aggregate Piers
Single Pier	80-35	220-170	
Unit Cell			
Group of 2			175-125
Group of 4	260-140		
Group of 5		430-260	
Group of 6			
Reference	White et al., 2007	Wissmann et al., 2007	Fox et al., 1998

Model Scale Testing

Seeing a great potential for intermediate foundation technology and having reviewed the essential properties of full-scale aggregate piers, the review of existing research performed on scaled foundation systems must be implemented. While there has been sufficient amount of research performed on scaled pile, column and compacted sand foundation systems, the following seven case are used to highlight some of the major findings in the area. The selected studies are summarized in Table 2, Table 3 and Table 5 where major outcomes, limitations and testing mechanisms are summarized:

www.manaraa.com

Table 2: Case studies 1-3 for reduced scale columns

Article #	Reference	Type of piers	Depth of pier installation	Soil material	Lab scale and apparatus	Significant findings, results and observations
1	Black et al., 2007b	Single and group of three sand vertical frozen granular columns	Single column - Ø32 mm, three - Ø20 mm each, H=120 mm and 200 mm H/D ~ 4-10	Soft Kaolin Clay, LL 70%, PL 36%, clay fraction 60%, σ_p 200 kPa	1/24-1/32 scale (if full-scale Ø0.76 m), columns placed in chamber Ø100 mm, H=200 mm	*Undrained soil condition: a column within the group of three performed better than the isolated column *Drained soil condition: the column in group of three performed to worse than the isolated single column. *Some effect of column buckling was identified.
2	Fang and Yin, 2007	Single Deep Cement Mixing (DCM) columns composed of ordinary Portland cement	Ø50 mm, H=100 mm and 200 mm H/D ~ 2-4	Hong Kong Marine Clay, LL 51%, PL 26%, G_s 2.58, w% 85%	1/15th scale (if full-scale Ø0.76 m), columns placed in chamber Ø300 mm, H=450 mm	*n was found to increase fast at the beginning of the loading, diminish with time & eventually approach a constant. *Column q_{ult} was evaluated at 1,100 kPa after 30 days of curing. Columns Q at 1,200 kPa in Hong Kong Marine Clay, i.e. effect of confining pressure. *At the unloading, the stress imposed on the matrix soil and the column was reduced proportionally. *Matrix soil PWP was high in early stages of loading and dissipated fast when reinforced with DCM columns.
3	Black et al., 2007a	Stone quarried basalt rock columns: (1) with tabular mesh, (2) with concrete plug within peat layer, (3) with internal bridge reinforcement	Ø75 mm, H=720 mm - tabular mesh and concrete plug, H=480 mm - bridging reinforcement H/D ~ 6-10	Peat layer sandwiched between two layers of Sand Peat: C_c 5.6, density 1,080kN/m^3, d_{10} 0.07, d_{60} 0.15	1/8th scale columns placed in box 1.75 m wide, H=2.0 m	*Q increased 50-75 % for short &150-260 % for long columns with mesh. *When excavated no splitting of mesh. *The column bulging found within top 300 mm portion of the column. *The bridge reinforcement performed well for Q & k_o of subbase reaction. *For concrete plug k of subgrade reaction found to be lower.

Legend:
G_s – specific gravity; e – void ratio; Ø – diameter; LL – liquid limit
PL – plastic limit; PI – plasticity index; H – length or depth; k_0 – initial stiffness
q_{ult} – compressive strength; C_u – cohesion; k – stiffness; d_{10} – effective size
w% - moisture content; C_c – compression index; d_{60} – Ø at 60% finer
σ_p – consolidation pressure; S_e – elastic settlement; PWP – pore water pressure

www.manaraa.com

Table 3: Case studies 4-6 for reduced scale columns

Article #	Reference	Type of piers	Depth of pier installation	Soil material	Lab scale and apparatus	Significant findings, results and observations
4	Sivakumar et al., 2004	Vibro-columns composed of (1) compacted moist sand & (2) frozen moist sand reinforced with geogrid	Ø32 mm frozen columns: H=120 & 200 mm single columns: H=80, 120, 160, & 200 mm H/D ~ 4-6	Soft Kaolin Clay - C_u 30 kPa, w% 105 %, σ_p 200 kPa, *e* 1.43	1/24th scale (if full-scale Ø0.76 m), columns placed in triaxial chamber Ø100 mm, H=200 mm	*****Low Q for wet compacted columns in soils with C_u < than 15 kPa. ***** Wet compacted columns found to have higher Q than frozen columns. *****The columns 5 times longer than Ø, did not contribute to the overall Q. * Geogrid improved Q by 70 %. *****Wet compacted column Q did not depend on column length, greater length frozen columns bore higher Q.
5	Bachus and Barksdale, 1984	Stone columns composed of uniformly gradated medium sand	Ø29 mm and Ø53 mm, H=305 mm H/D ~ 6-10	Soft Kaolin Clay - σ_p 45-60 kPa, LL 42 %, PI 15 %, clay 35 %	1/14-1/26 scale (if full-scale Ø0.76 m), columns were placed in test chamber Ø108 mm, H=305 mm	*****The groups of stone columns had Q 40 % > than the Q imposed on unreinforced soil. *A significant effect of time rate of loading was observed, where Q of a group of columns was 60 -70 % > when loaded at slower fashion. *****The C_u of unreinforced soil was found to be > than when reinforced with columns at 0.14 R_a ratio.
6	Balaam et al., 1977	Piles composed of granular material spaced in square and triangular patterns	No actual values were used, empirical approach was taken H/D ~ unknown	Drained cohesion of 0, drained angle of internal friction 40°, angle of dilatancy 20°, coefficient of effective horizontal stress 1.0	Scale unknown, empirical approach and finite element analysis used Ø=1.05spacing - triangular Ø=1.14spacing – square	*****For groups of piles in a rectangular pattern over a large area, spacing found important when reducing S_e. *****The spacing over Ø ratio has to be < than 5 to minimize the S_e of the pile groups when piles extended to full depth of soil layer. *****If the piles are only extended to the 1/4 distance of the full depth of soil layer, then even closer spacing does not significantly impact the reduction in S_e. *****It was found that as the column penetration was to increase from 50 % to 100 %, the k was found to increase proportionally by 50 percent.

Legend:

C_u – undrained shear strength	PWP – pore water pressure	Ø – diameter	PI – plasticity index
q_{ult} – compressive strength	c – cohesion	k_0 – initial stiffness	H – length or depth
w% - moisture content	C_c – compression index	k – stiffness	d_{10} – effective size
R_a – area replacement	σ_p – consolidation pressure	LL – liquid limit	d_{60} – Ø at 60% finer
S_e – elastic settlement	*e* – void ratio	PL – plastic limit	

www.manaraa.com

Table 4: Case 7 for reduced scale columns

Article #	Reference	Type of piers	Depth of pier installation	Soil material	Lab scale and apparatus	Significant findings, results and observations
7	Hughes and Withers, 1974	Stone columns were composed of Leighton Buzzard sand	Ø12.5mm and Ø38 mm, H=150 mm H/D ~ 4-12	Consolidated kaolin clay	1/10th scale, columns placed in consolidometer 225 mm wide and 160 mm long	*A significant amount of lateral stress found within the matrix soil at distance of 1.5 times the column Ø. *Ultimate column Q was governed by lateral reaction in bulging zone. *No movement was found at the distance of 4 times the column Ø. *Columns failed by bulging, degree of bulging was dependent on the *c* of matrix soil. *A lot of lateral of expansion found in the top portion of the columns.

Legend:

C_u – undrained shear strength	PWP – pore water pressure	Ø – diameter	PI – plasticity index
q_{ult} – compressive strength	c – cohesion	k_0 – initial stiffness	H – length or depth
w% - moisture content	C_c – compression index	k – stiffness	d_{10} – effective size
R_a – area replacement	σ_p – consolidation pressure	LL – liquid limit	d_{60} – Ø at 60% finer
S_e – elastic settlement	*e* – void ratio	PL – plastic limit	

Case Studies

Case 1 – Black et al., 2007b - Performance of Clay Samples Reinforced with Vertical Granular Columns (Queen's University of Belfast, United Kingdom)

This research study featured installation of single and groups of three vertical frozen granular columns in soft kaolin clay. The material was classified to have 60 percent clay fraction with liquid limit of 70 percent, and 36 percent plastic limit. Consolidation of clay was performed up to total pressure of 200 kPa. Sand material was characterized as medium sand with moisture content of 18 percent. Single columns were constructed at 32 mm in diameter, while the groups of three piers were built at 20 mm in diameter (Figure 13). Columns were placed to a depth of 120 mm and 200 mm.

The frozen columns were constructed in plastic Polyvinyl Chloride (PVC) tubes and placed into a premade soil cavity after the freezing and extraction of the column from the PVC tube. The columns were allowed to thaw out within the kaolin clay matrix soil prior to performing

www.manaraa.com

the load tests. A hydraulic device was used for the purpose of loading the columns, as well as, external transducers were utilized to measure the pore water pressure. Testing was performed within chamber of 100 mm in diameter and 200 mm in height (Figure 13). The tested columns and groups of columns were evaluated for load carrying capacity at drained and undrained soil conditions.

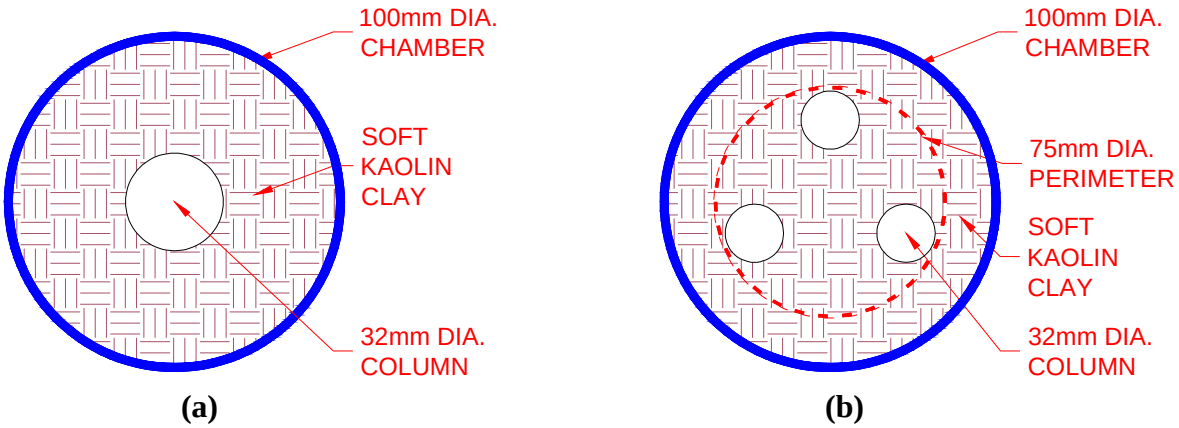

Figure 13: Column arrangement for (a) single pier and (b) group of three piers (reproduced per Black et al., 2007b)

The results of the study have shown the collapse of the column structure during the process of thawing. It was also found that the columns were more vulnerable to fail by shear and bulging prior to having the failure of the matrix soil at the tip due to excessive settlement.

In the undrained soil condition, a column within the group of three performed better than the isolated column. On other hand, at drained condition, the column in group of three performed to lesser extent than the isolated single column. Some effect of column buckling was also suspected, however more research is required to confirm the findings. The author also indicated that the full-scale testing would be required to confirm the findings.

The limitations that were encountered within this study were extended to inability to scale forces of gravity when replicating the full-scale model. The only way of scaling gravitational acceleration was through centrifuge modeling. Moreover, the ability to reproduce the “mini-vibrocat” method of column installation was economically inefficient and, therefore, was

www.manaraa.com

replaced with method of freezing columns and thawing within the matrix soil. Thus, the authors acknowledged radical difference between installation methods between the laboratory study and the field applications.

Case 2 – Fang and Yin, 2007 – Responses of Excess Pore Water Pressure in Soft Marine Clay around a Soil-Cement Column (Hong Kong Polytechnic University, Hong Kong)

This study was performed on soil-cement columns at Hong Kong Polytechnic University. The columns were built at 50 mm in diameter and at 100 mm and 200 mm shaft lengths. The construction of the columns was performed by a method of Deep Cement Mixing (DCM), where Portland cement concrete was used as a main component of the column composition mixture.

The soil where the columns were placed was classified as Hong Kong Marine Clay. Specific gravity of the material was experimentally identified at 2.58 with the moisture content value of 86 percent, liquid limit of 51 percent and plastic limit of 26 percent. Soil was consolidated to 90 percent level of consolidation for the period of twelve days prior to insertion of the columns. The placement and testing of the columns was performed within cylindrical steel mold of 300 mm in diameter and 450 mm in height (Figure 14).

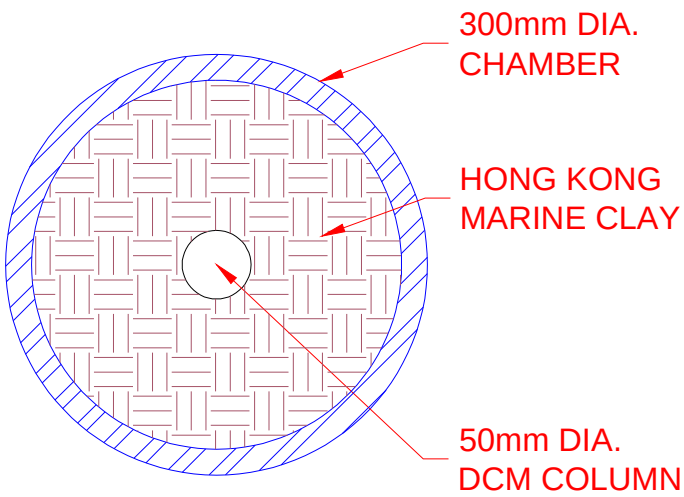

Figure 14: Treated ground model consisting of preconsolidated untreated soft clay and a cement mixed soil column at the center in a cylinder mold (Fang and Yin, 2007)

www.manaraa.com

The columns were composed of cement and clay, and were cured prior to insertion in premade cavities in the matrix soil. The gap between the DCM column and the matrix soil was filled with cement slurry. Once completed, the columns were subjected to evaluation of correlation between the load imposed on the column and pore water pressure generated within the matrix soil.

The equipment that was utilized included two linear velocity displacement transducers to measure the displacement of the loaded columns, as well as, earth pressure cells and pore pressure transducers which helped to collect necessary data to evaluate 90 percent of soil consolidation.

Stiffness ratio parameter was used in evaluation of the data. The parameter was defined as the ratio of total stress on the column to the total stress imposed on the untreated soil. The stiffness ratio was initially found to be rapidly increasing during initial loading. However the rate was consequently found to diminish and eventually to approach a constant value. When loaded in a triaxial chamber, the compressive strength of the columns was evaluated at 1,100 kPa after thirty days of curing period. When the columns were placed in Hong Kong Marine Clay soil, the compressive strength was evaluated at 1,200 kPa, therefore, supporting the concept of confining pressure contributing to the overall compressive strength of the pier. Moreover, as the unloading was performed, the stress imposed on the matrix soil and the column was reduced proportionally. Matrix soil pore water pressure was observed to be high in early stages of loading and was found to dissipate in a rapid rate along the soil-column boundary when reinforced with DCM columns.

It should be noted that the scaling of the testing apparatus, as well as, construction of the piers at the scaled level was completed at a single gravity and the corresponding stress level was low compared to the field conditions. These and other limitations were acknowledged by the authors and were necessary for the feasibility of the research study.

www.manaraa.com

Case 3 – Black et al., 2007a – Reinforced Stone Columns in Weak Deposits: Laboratory Model Study (Northern Ireland)

The research investigation was carried out on 1/8th scale stone columns in Northern Ireland. The columns were built at 75 mm in diameter and composed of quarried basalt rock crushed to 6 mm in diameter. The testing of the columns was performed in a chamber 1.75 m in width, 2.0 m in height. Soil was described as peat, obtained at Donganon Ireland (64 km from Belfast), placed between two layers of sand located at top and the bottom of the testing chamber (Figure 15). Peat was characterized to have density of 1,080 kN/m^3 and compression index of 5.6. Sand material was found to be uniformly graded with d_{10} = 0.07 mm and d_{60} = 0.15 mm.

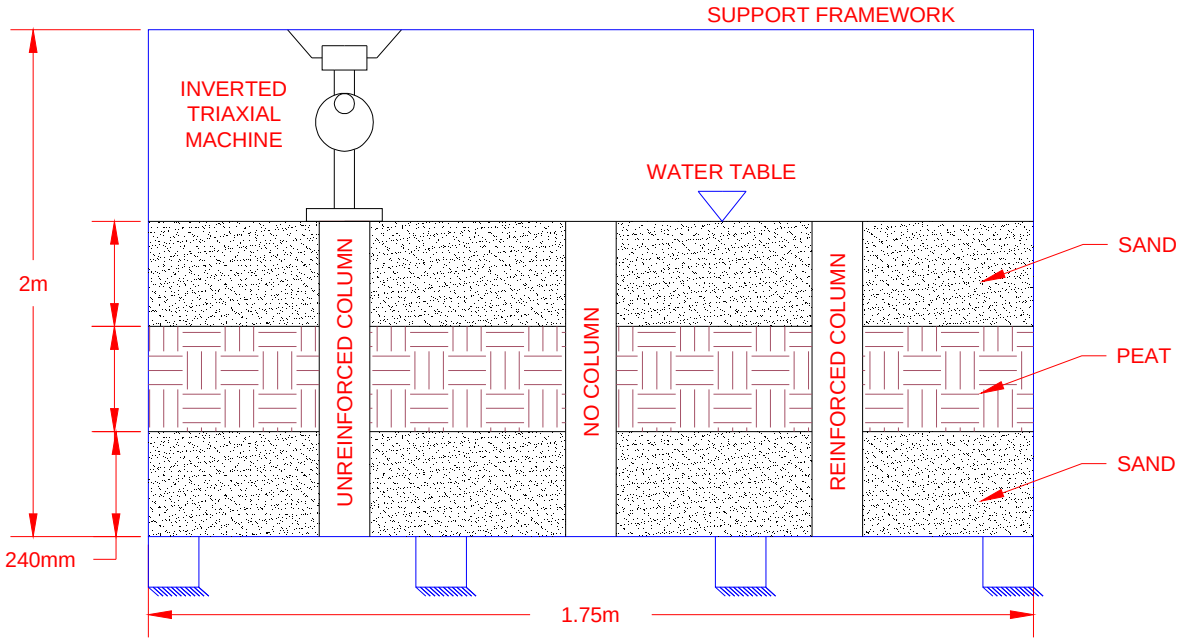

Figure 15: Testing box (Black et al., 2007a)

The compaction of the stone column basalt rock aggregate was performed in even size lifts within a premade soil cavity. The aggregate compaction tool consisted of a steel rod with tamper head attachment on one end and platform for striking the rod with a 5 kg mass, on the other. In order to avoid collapse of the cavity walls, the hollow tube was inserted in the

www.manaraa.com

cavity and incrementally lifted as the aggregate lifts were compacted. The compaction of the aggregate resulted in the average dry density of the compacted basalt rock to be 16.8 kN/m^3.

The design of the constructed columns was modified in three different ways - by wrapping column with a tabular mesh; using concrete plug composed of grout and injected in the column aggregate confined by the layer of peat; and by using metal internal bridging reinforcement rod installed along the column shaft and grouted at both ends (Figure 16a). The tabular mesh and concrete plug piers were built at 720 mm length (fully penetrated) and columns with bridging modification were of 280 mm or 540 mm length (partially penetrated). Figure 16b depicts a schematic drawing of tabular mesh application.

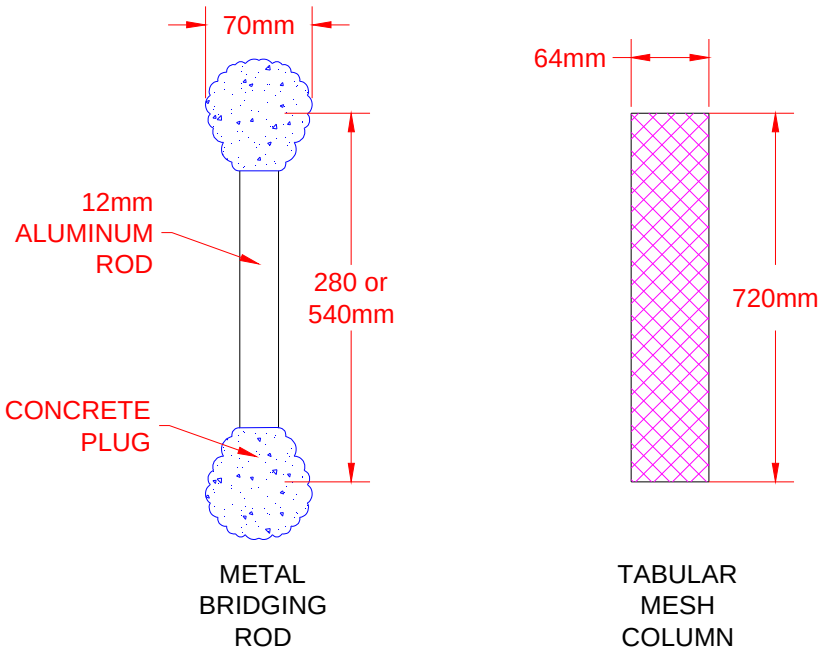

Figure 16: (a) Excavated bridge reinforcement and (b) column enclosed in tabular wire mesh (reproduced per Black et al., 2007a)

The mechanism of column loading was performed via a hydraulic jack suspended from a frame. Columns were evaluated for load carrying capacity and impact of design modifications on the overall bearing capacity results.

www.manaraa.com

The load carrying capacity was found to increase from 50 to 75 percent for partially penetrated columns and from 150 to 260 percent for fully penetrated columns when the mesh was utilized. The bulging effect of the column was noticed to be primarily within the top 300 mm portion of the column. Upon excavation no splitting of the mesh was observed. The bridge reinforcement was found to perform very well in terms of controlling load carrying capacity of the column and initial stiffness modulus of the subbase reaction.

In spite of the fact that the load transfer mechanism was the same for both the bridging reinforcement and the concrete plug, the modulus of the subgrade reaction was found to be lower for the concrete plug. Overall, the concluding remarks indicate potential for improvement of peat soil with different types of design modification methods (mesh, rod, etc.). The bridging rod reinforcing method was found to be especially effective, however full-scale tests were suggested to be carried out to supplement the findings.

The authors indicated a limited extent to which the tabular mesh could be constructed in the field conditions. Also bridging reinforcement techniques must be modified in order to be successfully implemented in the field.

Case 4 – Sivakumar et al., 2004 – Triaxial Tests on Model Sand Columns in Clay (Queen's University of Belfast, United Kingdom)

This research study was completed at Queen's University of Belfast, United Kingdom. The testing was performed on compacted moist sand vibro-columns and frozen columns of the same material. The sand material was categorized as uniformly graded fine crystal sand with d_{10} = 0.2 mm and d_{60} = 0.27 mm, mixed at 18 percent moisture content. The test soil was classified as kaolin soft clay mixed at 105 percent moisture content (1.5 times the liquid limit) and consolidated to 200 kPa vertical pressure. The undrained shear strength of the clay was evaluated at 30 kPa. The moist sand columns were built at 32 mm in diameter and 80, 120, 160, 200 mm in lengths, while the frozen columns were built at 120 mm and 200 mm lengths.

www.manaraa.com

Testing of the columns was performed within a triaxial chamber 100 mm in diameter and 200 mm in length. The process of reinforcing soil with columns was initiated by drilling cavities in the soil using an auger. Installation of vibro-columns composed of wet sand was performed in even thickness lifts by raising and dropping a rod 25 mm in diameter and 175 g in mass.

The frozen columns were prepared in a separate plastic tubes of the same diameter as the premade cavity. The samples were frozen within the tube and consequently inserted into the premade soil cavity. Frozen column samples were allowed to thaw prior to performing the load tests. A geogrid reinforcement technique was also utilized in frozen columns, where the compacted lifts were sandwiched with geogrid material in between. Columns were dyed with a different color to differentiate the boundary between the column and the surrounding matrix soil. Columns were subjected to uniform axial loading and the load carrying capacity was investigated.

The findings show that wet-compacted vibro-columns are not recommended in soils with undrained shear strength less than 15 kPa. The vibro-columns were also found to have higher load carrying capacity than frozen columns and by using geogrid reinforcement the load carrying capacity was improved by 70 percent. Vibro-columns were found to act as vertical drains, while the interface of the frozen column and clay was smeared, thus the skin friction was reduced and a higher rate of column settlement was noticed. Also, the columns, length of which was five times greater than the diameter, did not contribute to the overall load carrying capacity.

When performing foundation type tests the effect of boundary was encountered and, therefore, more testing was proposed by the authors. Also, while the wet-compacted column load carrying capacity did not depend on the length of the column, the frozen columns had a tendency to bear higher level of load with greater length.

www.manaraa.com

Case 5 – Bachus and Barksdale, 1984 – Vertical and Lateral Behavior of Model Stone Columns (Georgia Institute of Technology, Georgia)

The investigation was performed on model sand columns at the Georgia Institute of Technology. Two different size columns were tested at 29 mm and 53 mm diameters. Columns were constructed using sand material and placed in test chamber 108 mm in diameter, 305 mm in height, and with wall thickness of 16 mm. Uniformly graded medium sand was compacted in even size lifts in a pre-augered cavity using an air actuated hand held vibratory compactor.

Soft kaolin clay was used as the matrix soil where the columns were placed and tested. The soil was consolidated within the chamber to achieve 45 to 60 kPa undrained shear strength. The kaolin clay was described as uniform silty clay composed of 35 percent of clay and having liquid limit and plasticity index of 42 and 15 percent, respectfully. Once the construction was completed, single and groups of columns were tested for lateral response and load-settlement evaluation. Radiographic method was used to evaluate the lateral displacement of the column within the matrix soil. Lead markers were also used to investigate the shape of the columns after the columns were tested.

Area replacement ratio, defined as ratio of the diameter of the stone column to the diameter of the unit cell, was 0.4. It was found that the groups of stone columns had a tendency to support a load 40 percent greater than the load imposed on unreinforced soil of the same loading area. Moreover, a significant effect of time rate of loading was observed, where the load carrying capacity of a group of columns was 60 to 70 percent greater when the loading was performed in a slower fashion and slow dissipation of pore water pressure was allowed.

The area replacement ratio was found to be an important parameter when performing lateral load tests on the columns. The shear strength of the unreinforced kaolin clay soil was found to be higher than when the soil was reinforced with columns at 0.14 area replacement ratio.

www.manaraa.com

Moreover, the research performed on groups of model stone columns has shown the optimum spacing for 29 mm piers to be at 76 mm on center.

Overall, the authors concluded that the sand column reinforced soil system was complex and more testing was required to confirm the findings. Some of the findings were concluded to be inconsistent with the theoretical predictions and repeatable tests had to be performed to confirm the results.

Case 6 – Balaam et al., 1977 – Settlement Analysis of Soft Clays Reinforced with Granular Piles (University of Sydney, Australia)

The research was completed on single piles and groups of piles composed of granular material at the University of Sydney, Australia. The study was completed through empirical correlations and parameters assumed for the matrix soil and the piles. The finite element analysis and finite difference methods were used to make theoretical predictions of the pile behavior. The pile material was described as soil with no cohesion, internal friction angle of 40 degrees, and angle of dilatancy of 20 degrees. Piles were placed in drained soft clay with a drained angle of internal friction of 30 degrees and angle of dilatancy of 15 degrees.

Coefficient of effective horizontal stress was assumed to be 1.0 for both soil and the pile. The analysis of the data was performed in terms of diameter and length ratios and no actual numerical values were utilized in establishing empirical correlations. The study was mainly focused on improvement of soil behavior due to drainage provided by the pile and the stiffening effect of the pile.

Several different charts were developed where the diameter and height ratios were correlated with the settlement ratios. The findings have shown that when constructing groups of piles in a regular pattern over a large area, the spacing is of the great essence when trying to reduce the amount of settlement. The spacing over diameter ratio has to be less than five in order to minimize the settlement of the groups of piles, while the extent of the piles has to be to the

www.manaraa.com

full depth of the consolidated layer of the soil. If the piles are only extended to the quarter distance of the full depth of a soil layer, then an even closer spacing does not significantly impact the reduction in the amount of settlement for a certain group of piles. Also, it was found that as the column penetration was to increase from 50 to 100 percent, the modulus was found to increase proportionally by 50 percent.

Having performed the study at a theoretical or empirical level, the verification was needed through laboratory and field testing. The interaction between reinforcing sand column and soft soil was concluded to be extremely complex based on the parameters included in the correlations.

Case 7 – Hughes and Withers, 1974 – Reinforcing of Soft Cohesive Soils with Stone Columns (Cambridge, United Kingdom)

The study was performed on scaled stone columns at Cambridge in United Kingdom. The research involved placement of stone columns composed of Leighton Buzzard sand in kaolin clay. The columns were scaled to $1/10^{th}$ scale and, therefore, were built at 12.5 mm to 38 mm diameter and 150 mm length. The kaolin clay was one dimensionally consolidated and kept at a constant stress. For the purpose of consolidation of the clay material, the laboratory 225 mm by 160 mm consolidometer was used. Also, a scaled vibroflot was utilized to form a cavity in the soil. To measure displacement of a column in the soil, a radiograph of lead shot markers was used.

The investigation revealed a significant amount of displacement developed within the matrix soil at the distance of one and a half times the diameter of the column. The ultimate strength of the column was found to be governed by the lateral reaction in the bulging zone. At the same time, no movement was found at the distance of four times the diameter of the column below the surface. For columns deformed through bulging the degree of bulging was found to be dependent on the cohesion of the matrix soil. During the entire process of loading the

www.manaraa.com

lateral stress was found to continuously increase. A significant amount lateral of expansion was found in the top portion of the columns.

It was concluded that the stone columns could be successfully utilized to stiffen the matrix soil and thus could be used in improving the bearing capacity of the foundation. However, the columns were found to be not suitable for heavy loads due to inability to transmit loads to deeper layers of soil.

www.manaraa.com

CHAPTER 3: RESEARCH METHODOLOGY

Creating and developing a new concept requires a significantly greater amount of investigation at the development stage than by using the ideas that have been established, tested and have gained maturity through process of trial and error. The initial phase of a new development requires establishment of standards, procedures, guidelines, methodologies, as well as, testing equipment and data acquisition systems. This section will focus on the challenges that were overcome while developing a relatively new concept of scaled model pier testing in the laboratory environment. Feasibility of the study, constructability of the scaled system, applicability, and limitations of the obtained results were important in developing the methodology of this research. The main tasks and objectives were identified as follows:

- Design test pit load frame
- Identify test bed characterization methods
- Establish pier testing and construction approaches
- Develop load-settlement data collection approach

Load Frame

The process of pier testing had to be performed via a loading device capable of imposing pressure at the tops of the piers. In many field load test applications, a conventional steel load bearing frame or heavy piece of machinery such as dozer, semitrailer or a water tanker are utilized for the purpose of bearing support (Ping et.al., 2002). While having no capability to use the same approach in the lab due to the limited amount of space a different approach had to be developed.

The loading frame had to be designed, built and mounted against the interior walls of the test bed at the elevation of 60 cm above surface of the soil. MathCAD software was utilized for design iterations and for the purpose of creating a satisfactory design (1) capable of

www.manaraa.com

withholding the applied load, (2) physically adequate to fit within the confined space and (3) safe for continuous use and operation. Some of the engineering structural calculations that were performed included flange buckling, web yielding, and web buckling (AISC, 2007).

The design load capacity of the frame was estimated at 25,000 kg and several factors of safety were applied to the design as a precaution. The central W10x54 beam, as it can be seen from Figure 17c, was designed to transmit load applied to the pier via Enerpac hydraulic jack capable of producing pressure of up to 69,000 kPa (Figure 17a and b).

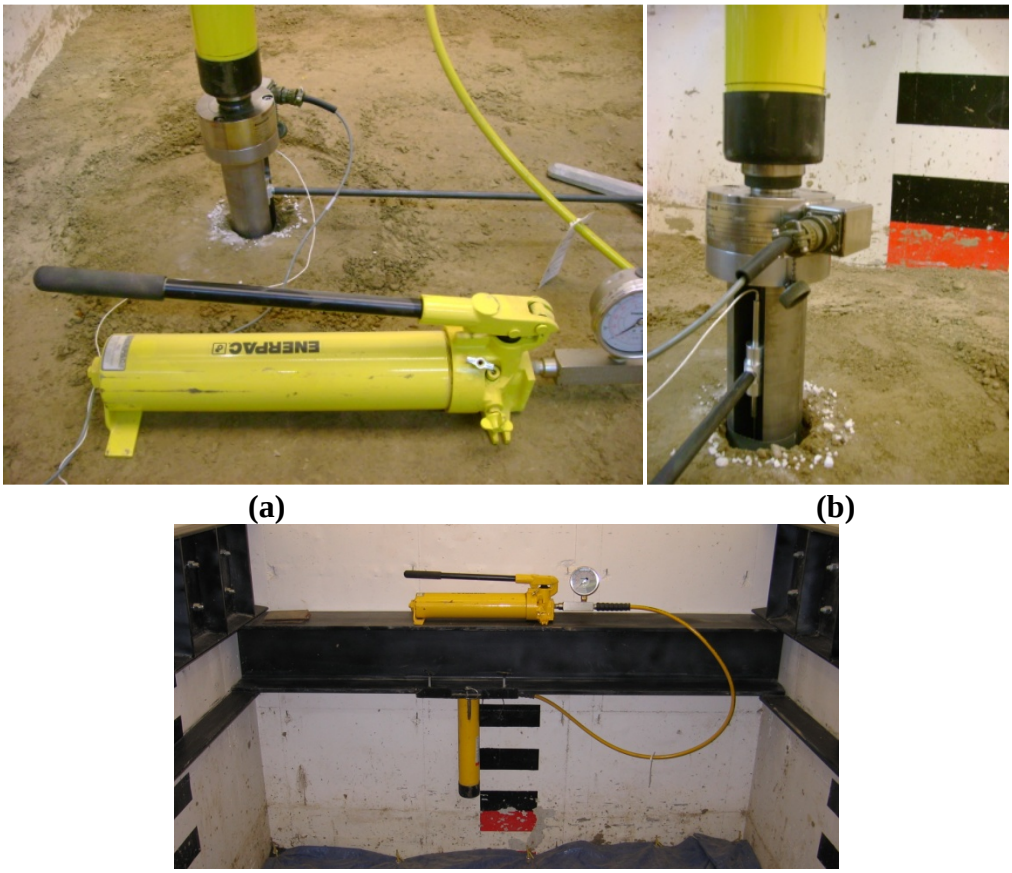

(a) **(b)**

(c)

Figure 17: (a) Enerpac hydraulic jack in operation, (b) Enerpac hydraulic jack applied to stacked sensors, (c) Enerpac hydraulic jack mounted on load bearing frame

The connection mechanism between the jack and the beam allowed for free movement of the jack along the length of the beam and, therefore, the entire width of the test bed. The beam

www.manaraa.com

itself was designed to be supported by two L6x4x05 steel angles and, therefore, allowed free movement in the direction of the length of the test bed (See Figure 18).

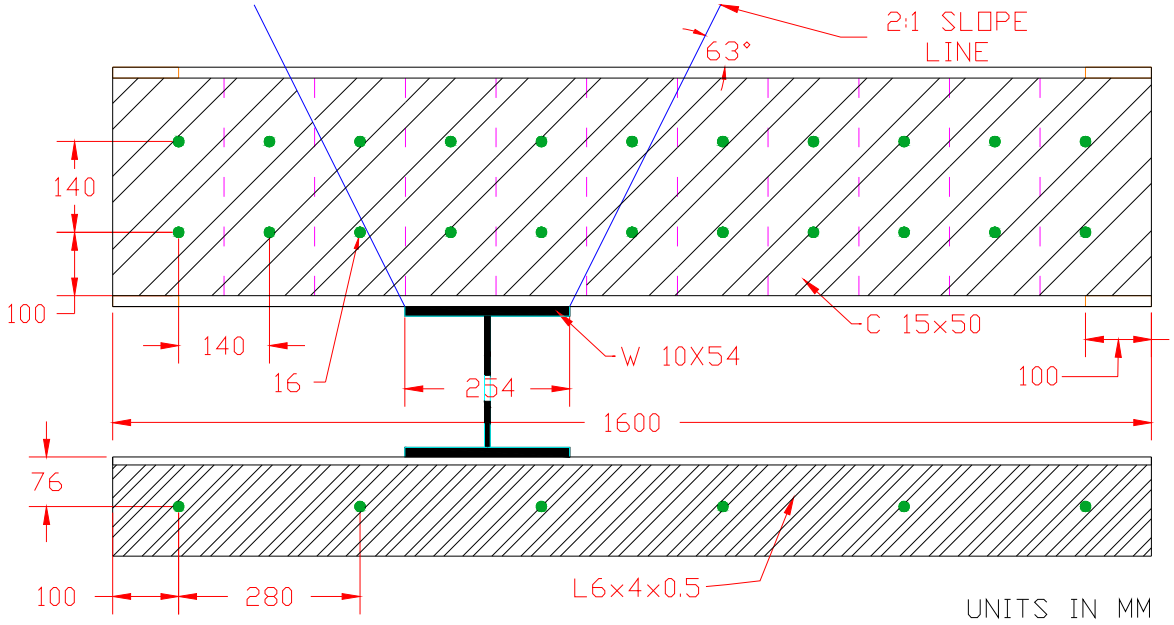

(a)

(b)

Figure 18: Load frame (a) schematic drawing and (b) as-built photo

www.manaraa.com

Thus, the design system allowed free movement in any X-Y horizontal direction and was capable of positioning the hydraulic jack in any desirable test bed location.

It is important to note that while at rest, the only vertical force within the system was the gravitational weight of the beam transmitted to the L-shape angles. However, during the pier testing, the load imposed by the hydraulic jack was directed upward and had to be counterbalanced by the structural elements big enough to withhold a much greater load. Therefore, a series of two C15x50 channels mounted on the walls directly above the beam were used to support the imposed load.

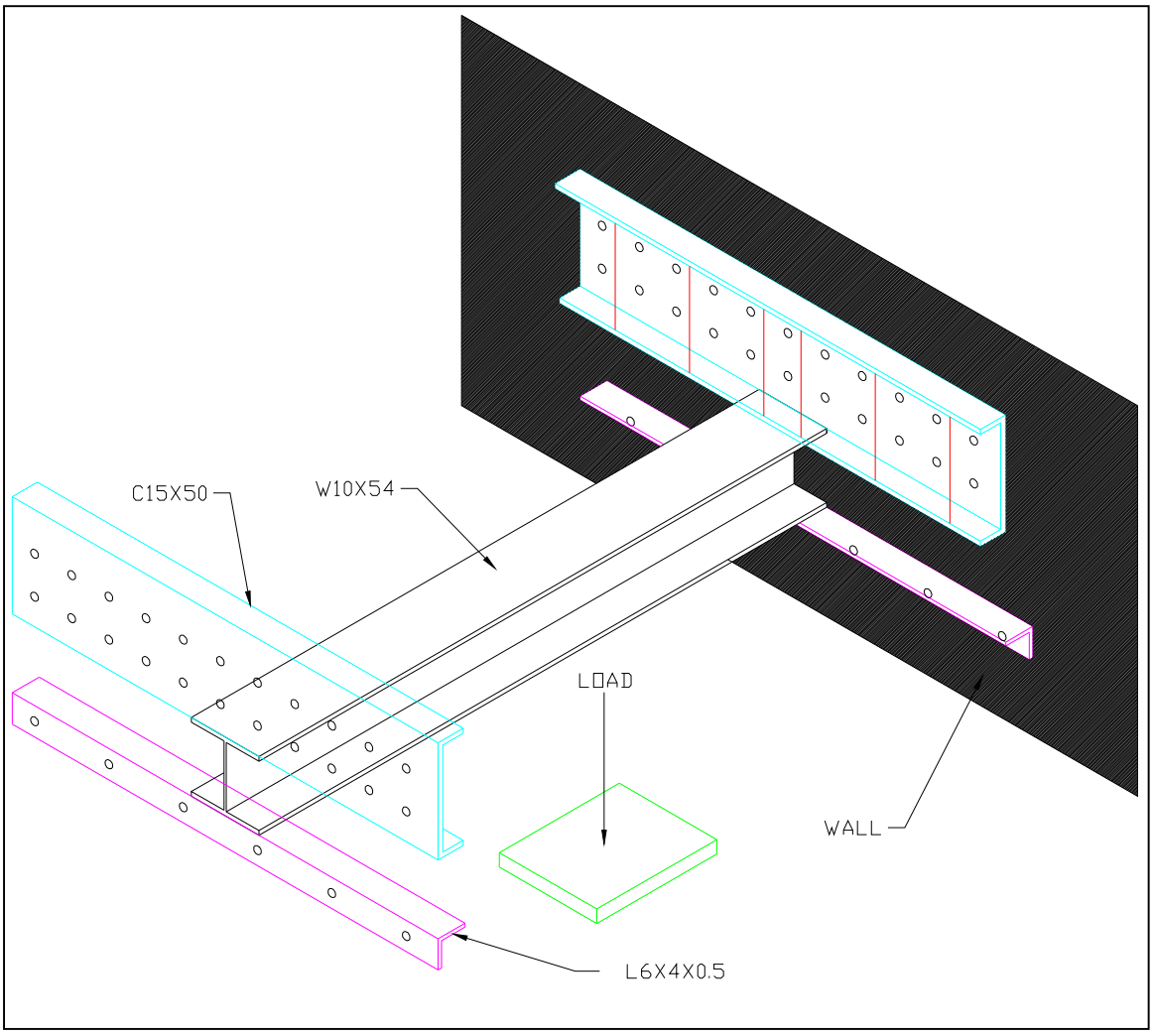

Figure 19: Load frame schematic drawing (isometric)

www.manaraa.com

While it is obvious that the channels were dimensionally larger than the angles, the number of anchor bolts supporting the channels was four times the number of anchors that the L-shape angles were supported with. A complete bearing frame design can be seen in Figure 19

Hilti® heavy duty expansion anchor bolts, 16 mm in diameter, were embedded to a depth of 150 mm in the concrete walls. The process of embedding anchors into the concrete walls was preceded by initially drilling cavities through the walls via the Hitachi hammer drill. The walls were internally reinforced with steel rebars and, therefore, the location of the rebars had to be identified and taken into account when spacing the bolts and locating the holes for the C-channels. As a result, a rebar stud finder device was successfully utilized and in the process of construction only 3 of all 56 anchor bolts met refusal due to presence of the reinforcement bar on the way and were not embedded to a full 150 mm depth.

Considering the flange of the W10x54 beam at 255 mm wide and the load distribution to be 2:1 at the interface between the flange of the beam and the flange of the C-channel, the total number of five anchors per every C-channel is thus engaged on each side of the beam at any point of load application. Therefore, every time the load is applied to the central beam, 10 anchors is holding the system in equilibrium, and load distribution is of 10 percent per each anchor. While the actual shear force imposed on each anchor bolt was estimated to be sufficiently lower than the design value of 76 kN per bolt force, the design of the entire system was calculated to be controlled by the pull-out force of 41 kN per bolt imposed on the anchors.

For this reason, the loading mechanism was not permitted to be utilized to its full design capacity if the control beam was positioned at the very edge of the C-channel, in other words, if the central beam is placed at the back or front of the test bed, where the zone of load distribution at 2:1 would capture a fewer number of anchors. As a result, the use of the entire frame load system was confined by 25,000 kg maximum load that could be applied, while the central beam is placed no closer than 100 mm away from the edge of the C-channel.

www.manaraa.com

Test Bed Characterization Methods

Test Bed Compaction

The elevator shaft located in the geotechnical laboratory at Iowa State University (ISU) was selected as a test bed for the purpose of placing and testing scaled piers. Western Iowa loess (loess) soil material was placed until the floor level elevation was reached. The testing had to be performed within a confined test bed space, dimensions of which are 2.1 m in width, 1.5 m in length and 2.0 m in depth.

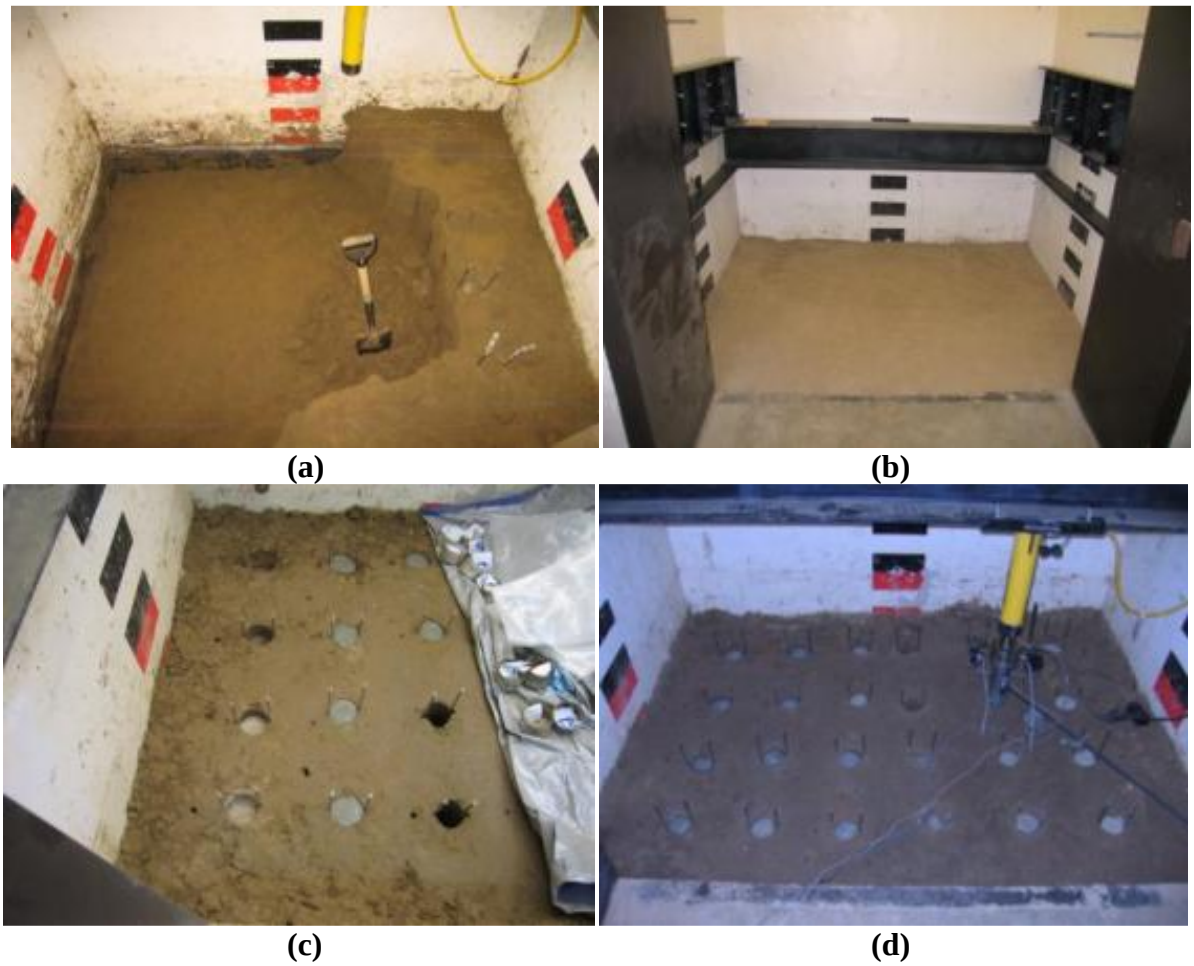

(a) **(b)**

(c) **(d)**

Figure 20: Test bed preparation (a) excavation, (b) finished after compaction, (c) placement of single piers and (d) testing of single piers

www.manaraa.com

To perform all the required testing and produce quality results, the test piers had to be spaced at a minimum radial distance to prevent interference, thus, the test bed had to be reconditioned multiple times to accommodate all the test piers (See Figure 20).

Every pier was built at 305 mm or 610 mm shaft lengths. Being able to fit a certain number of piers per each tests bed, every set of tested piers eventually had to be removed, and the surrounding matrix soil had to be prepared for the installation of the next set of piers. The process of test bed preparation included removal of the matrix soil, remolding of the large clods of the soil and placement and recompaction of the soil.

The excavation of the test bed material was performed to a depth of 610 mm, due to the length of the scaled piers being 305 mm for the short/floating piers or 610 mm for long piers. A stiff and well compacted layer of loess was expected to be prepared at the depth elevation of 610 mm, in the Lower Zone of 610 mm pier, for the purpose of having the bottom bulb of long piers to be placed against a stiff layer of soil. Shorter 305 mm piers were not confined by a stiffer layer of soil at the tip to simulate a floating foundation.

The test bed had to be reconditioned a total number of four times for the following piers to be installed:

- Single piers compacted via various shape beveled tamper heads (cone, truncated cone, flat and wedge).
- Single piers composed of various aggregate, cement and loess mixes
- Groups of aggregate piers and cement type I and K composition piers

Every test stage lasted approximately one month and, therefore, the top layer of soil at the surface was exposed to the room air temperature and, thus, was continuously subjected to air drying and losing moisture through evaporation. This was mitigated to some degree by covering the test pit with a tarp. Therefore, after performing excavation of the matrix soil it was important to moisture condition and thoroughly mix soil mass prior to placement and

www.manaraa.com

compaction back in place. However, knowing the collapsible nature of loess material, it was also important not to oversaturate the soil, which could have caused the collapse of cavity walls and restrict the ability to successfully construct the piers.

While keeping moisture content at a target level, the other control factor was unit weight (density) or level of soil compaction. To produce a desirable soil density two main compaction approaches were taken: vibratory plate compactor and hand tamper. Also, process of consolidation of soil under its own weight had a small contributor to the consolidation process.

As the matrix soil was excavated, moisturized and put back in even size lifts across the test bed area, the electrically powered vibratory plate compactor was used (See Figure 21a). Heavy 300 mm by 300 mm plate was vibrated in a simultaneous horizontal and vertical motion and provided a good compaction effort for the soil within the central area of the test bed.

(a)

(b)

Figure 21: Compaction tools (a) vibratory plate compactor, (b) hand tamper

www.manaraa.com

In the areas where access was limited (closer to the walls), the method of soil compaction was done by using a hand tamper (See Figure 21b). The hand tamper was equipped with a heavy steel tip 150 mm by 150 mm in size and was used to compact soil by pounding in a repetitive vertical motion. Also, due to small contribution of pore water pressure equilibrizaiton, a small level of compaction was induced via gravitational consolidation of soil under its own weight. The process lasted a period of three to four days.

Particle Size Distribution

Particle grain size distribution analysis for the loess was performed according with ASTM D422-63. However, since the test bed soil had to be removed and replaced multiple times, additional parameters like moisture content, density and undrained shear strength had to be evaluated. Moreover, test bed prepared for each phase of testing was used for placement of multiple number of piers and, therefore, the consistency and uniformity of the soil had to be ensured.

DCP Test

While many research investigations have utilized the assumption of uniform initial relative unit weight and initial void ratio throughout the entire test bed (Lim et.al., 2004), the soil parameters for this research were suspected to deviate throughout the entire test bed area and, therefore, were estimated for each pier placement location. Moreover, variation in soil conditions could have a significantly impact on pier modulus test results and, thus, jeopardizes findings and observations. To eliminate the uncertainty and access required information the first set of soil characterization tests was perfumed by using Dynamic Cone Penetrometer (DCP) equipment. The DCP device was used to evaluate the level of compaction and stiffness of the loess. The evaluation of soil stiffness using DCP test was performed according with ASTM D 6951-03.

www.manaraa.com

The image depicting DCP equipment in operation and schematic drawing can be found in Figure 22. The number of weight drops and depth of penetration were recorded whereas the obtained test penetration results were consequently converted into Penetration Index data (mm/blow).

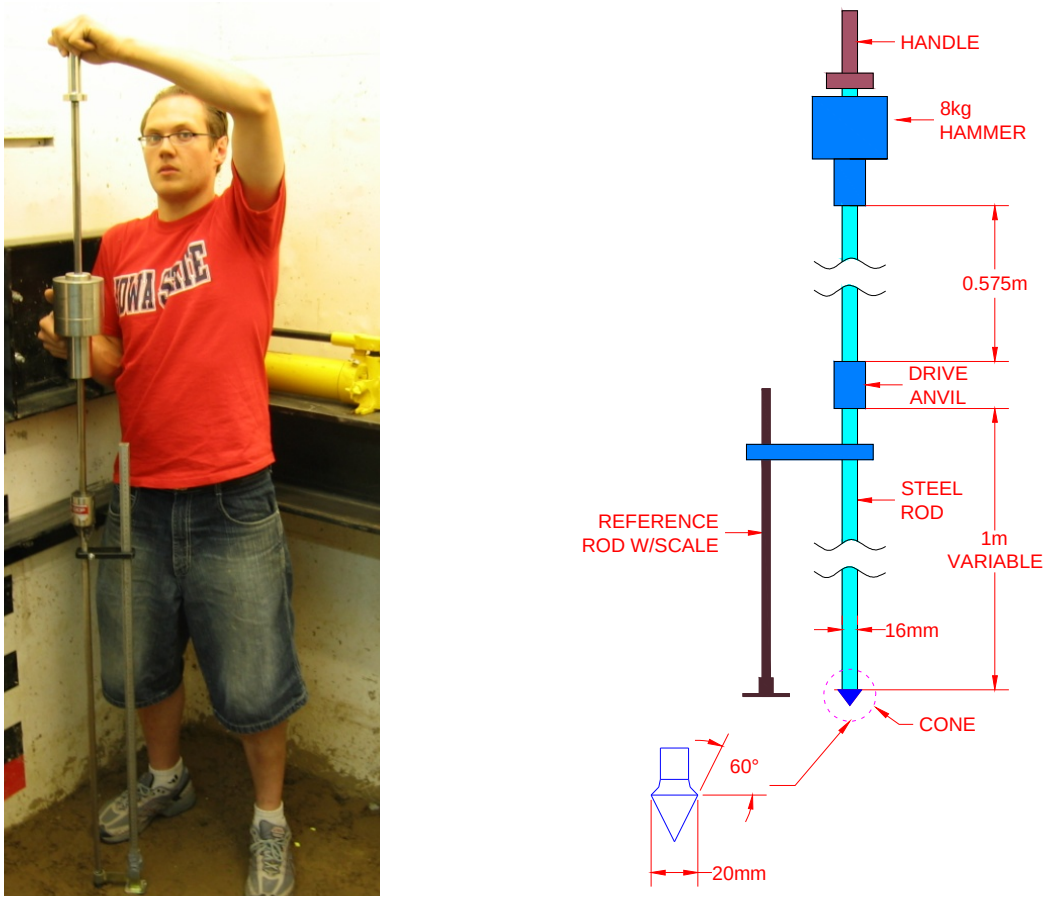

(a) **(b)**

Figure 22: DCP equipment (a) in operation in test bed (b) schematic drawing

Since the excavation of the test bed material was to be performed to the depth of 610 mm, the DCP level of penetration had to be extended to a depth of 610 mm as well. Occasionally the penetration depth was extended to the elevation of 700mm, however was concluded to be not sufficient to provide description to stiffer layer of soil beyond elevation of 610 mm. DCP profiles that were obtained for all stages of single and group of pier testing can also be found in Appendix.

www.manaraa.com

CBR from DCP

The California Bearing Ratio (CBR) test was another way of evaluating stiffness of the subgrade and uniformity of the in-situ soil. CBR is defined as the ratio of penetration resistance developed by a subgrade soil to penetration developed by a specimen of a standard base material (Burnham, 1993). CBR test is less cost efficient and more technically involved than DCP test, therefore, an empirical correlation between the DCP and CBR parameters was used. While, there are many correlations that have been established between PI, mm/blow and CBR, % in the past, the one that found the most application is US is shown in Equation 17 (Webster et al., 1992). ASTM D 6951-03 also provided means for converting DCP values to CBR, however this approach was not taken due to a more widespread practice of using Webster's equation.

Equation 17: CBR and DCPI correlation

$$CBR = 292 / (DCPI)^{1.12} \qquad \textit{(Equation 17)}$$

Table 5: DCPI and CBR average values for matrix soil of single piers compacted via different beveled heads

	Aggregate Pier Cone		Aggregate Pier Truncated Cone		Aggregate Pier Flat		Aggregate Pier Wedge		**AVERAGE**		**ST. DEV.**		**COV**	
Pier type	305 mm	610 mm	305 mm	610 mm	305 mm	610 mm	305 mm	610 mm	305 mm	610 mm	305 mm	610 mm	305 mm	610 mm
$DCP_{TOP<610mm}$ (mm/blow)	**34**	**26**	**34**	**65**	**34**	**61**	**97**	**97**	**49.8**	**62.3**	**31.5**	**29.0**	**63**	**47**
$DCP_{BOT>610mm}$ (mm/blow)	**27**	**27**	**27**	-	**27**	-	-	-	**27.0**	**27.0**	-	-	-	-
$CBR_{TOP<610mm}$ (%)	7.8	7.0	7.8	2.8	7.8	4.2	1.8	1.9	**6.3**	**4.0**	**3.0**	**2.2**	**48**	**56**
$CBR_{BOT>610mm}$ (%)	9.8	6.6	9.8	2.9	9.8	2.2	2.2	1.9	**7.9**	**3.4**	**3.8**	**2.2**	**48**	**64**

www.manaraa.com

The results of DCP and CBR tests performed on clay-like soils have proven to be valid within ten percent margin of error and the CBR values for clays are typically expected to range between 2 and 17 (Harrison, 1987). Western Iowa Loess was found to feature 98% silt and clay content, and therefore, the test bed CBR values were expected to be within the range specified by Harrison. All plotted CBR results can be seen in Appendix and are summarized in Table 7 through Table 8.

Table 6: DCPI and CBR average values for matrix soil of various mix single piers

	Aggregate Pier - truncated cone		Aggregate Pier - w/cem. Bulb		Aggregate Pier - w/cem. Top 0.1m		Loess + Fiber		Loess + Cement		Loess + Fiber + Cement		C (I) + C (K)		C (I) + C (K) + C (NS7)		C (I) + C (NS7)		Sand		**AVER-AGE**		**ST. DEV.**		**COV**	
Pier type	305 mm	610 mm	305 mm	610 mm	305 mm	610 mm	305 mm	610 mm	305 mm	610 mm	305 mm	610 mm	305 mm	610 mm	305 mm	610 mm	305 mm	610 mm	305 mm	610 mm	305 mm	610 mm	305 mm	610 mm	305 mm	610 mm
$DCP_{TOP<610mm}$ (mm/blow)	123	133	122	92	91	89	123	90	91	88	127	94	87	96	132	94	95	104	138	110	**112.9**	**99.0**	**19.5**	**13.8**	**17**	**14**
$CBR_{TOP<610mm}$ (%)	1.4	1.4	1.5	2.0	2.0	2.2	1.5	2.0	2.2	2.3	1.3	2.0	1.4	2.0	1.3	1.9	1.9	1.9	1.3	1.6	**1.6**	**1.9**	**0.3**	**0.3**	**21**	**14**

** Aggregate piers and loess mix piers were compacted using truncated cone beveled head*

** Cement mix piers were cast in place*

Table 7: DCPI and CBR average values for matrix soil of group aggregate piers

	Aggregate Pier Unit Cell		Aggregate Pier Single Pier		Aggregate Pier Group of 2		Aggregate Pier Group of 4		Aggregate Pier Group of 5		Aggregate Pier Group of 6		**AVERAGE**		**ST. DEV.**		**COV**	
Pier type	305 mm	610 mm	305 mm	610 mm	305 mm	610 mm	305 mm	610 mm	305 mm	610 mm	305 mm	610 mm	305 mm	610 mm	305 mm	610 mm	305 mm	610 mm
$DCP_{TOP<+610mm}$ (mm/blow)	102	100	134	162	143	111	83	96	102	127	88	85	**112.0**	**104.8**	**24.5**	**27.7**	**22**	**26**
$CBR_{TOP<610mm}$ (%)	2.0	1.9	1.5	2.0	1.9	1.9	2.4	2.1	1.7	1.6	2.3	3.0	**2.0**	**2.2**	**0.3**	**0.5**	**17**	**22**

** Aggregate piers and loess mix piers were compacted using cone beveled head*

** Cement mix piers were cast in place*

Table 8: DCPI and CBR average values for matrix soil of group cement type I and K

www.manaraa.com

composition piers

	C(I) + C(K) Unit Cell		C(I) + C(K) Single Pier		C(I) + C(K) Group of 2		C(I) + C(K) Group of 4		C(I) + C(K) Group of 5		C(I) + C(K) Group of 6		**AVERAGE**		**ST. DEV.**		**COV**	
Pier type	305 mm	610 mm	305 mm	610 mm	305 mm	610 mm	305 mm	610 mm	305 mm	610 mm	305 mm	610 mm	305 mm	610 mm	305 mm	610 mm	305 mm	610 mm
$DCP_{TOP<610mm}$ (mm/blow)	95	102	79	82	86	133	76	102	80	91	101	94	**86.2**	**100.7**	**9.9**	**17.5**	**11**	**17**
$CBR_{TOP<610mm}$ (%)	1.9	1.7	2.3	2.3	2.7	1.4	2.9	2.0	2.5	2.1	1.8	2.0	**2.4**	**1.9**	**0.4**	**0.3**	**19**	**17**

** Cement mix piers were cast in place*

Nuclear Density Gauge

While the impact of density and moisture content parameters on variation in stiffness of the soil is significant and can be detected through DCP and CBR tests, the effect of such parameters on the strength of the soil is very important as well (Burnham, 1993). Therefore, to characterize the properties of the test bed material to a greater degree, in addition to DCP and CBR tests, the nuclear density gauge device was used to obtain the supplemental moisture content and unit weight parameters. The nuclear gauge device in operation is depicted in Figure 23.

Figure 23: Nuclear density gauge device in use in test bed

www.manaraa.com

Nuclear gauge is portable, simple to use and very useful for quality control applications. However, the device possesses some limitation, where depth of penetration is only extended up to 150 mm and presence of organic matter and coarse particles may induce a discrepancy to the collected results (Randrup and Lichter, 2001). The loess material was deemed to be clean of any organic or coarse material and, therefore, the moisture content deviation of less than one percent was expected from the true water content value.

The test was carried out according with ASTM D7013-04 and the device was calibrated in the test bed prior to operation. Nuclear gauge device was used to obtain moisture content and density results for test bed prepared for single piers of various composition and can be found in Table 11. The test results have shown no particular influence of the concrete walls on the moisture content and density results.

Shelby Tube Sample

Being unable to utilize nuclear gauge device at depth greater than 150 mm, an additional method was utilized where a soil sample of 72 mm in diameter and 140 mm in height was extracted from each pier placement location via a Shelby tube and trimmed to the size (See Figure 24). The Shelby tube served the purpose of creating a cavity for installation of a $1/10^{th}$ scale pier and at the same time was used to obtain a soil sample subjected towards unit weight and moisture content evaluation.

While the concept of using the Shelby tube for the purpose of extracting a soil sample and performing volumetric and moisture content analysis is not new (Handy and Spangler, 2007), the application of the Shelby tube in a scaled pier research is a new idea introduced by this research study. Having the length of the Shelby tube to be 762 mm has made this method suitable for the long 610 mm and short 305 mm pier cavity applications. While having both the diameter of the scaled pier and diameter of the Shelby tube to coincide at 72 mm, the use of the Shelby tube was found to be even more feasible in this research.

www.manaraa.com

The process of using the Shelby tube in the test bed consisted of manually pushing the tube into the soil by means of lifting and dropping a heavy mass on the top of the tube. The extraction of the sample out of the tube was performed using a hydraulic press machine where a 70 mm diameter piston was used to push the sample out of the tube. After that the soil sample was placed between two steel mold casings designed to fit the 72 mm diameter sample and the casings were clamped around the sample. Finally, the ends of the sample were trimmed to the desired length of 140 mm and the sample preparation process was completed. Even though a small level of disturbance was caused during the pushing and extraction stages, the samples were treated with a great care and the best engineering practices were utilized as outlined in ASTM D2166-00.

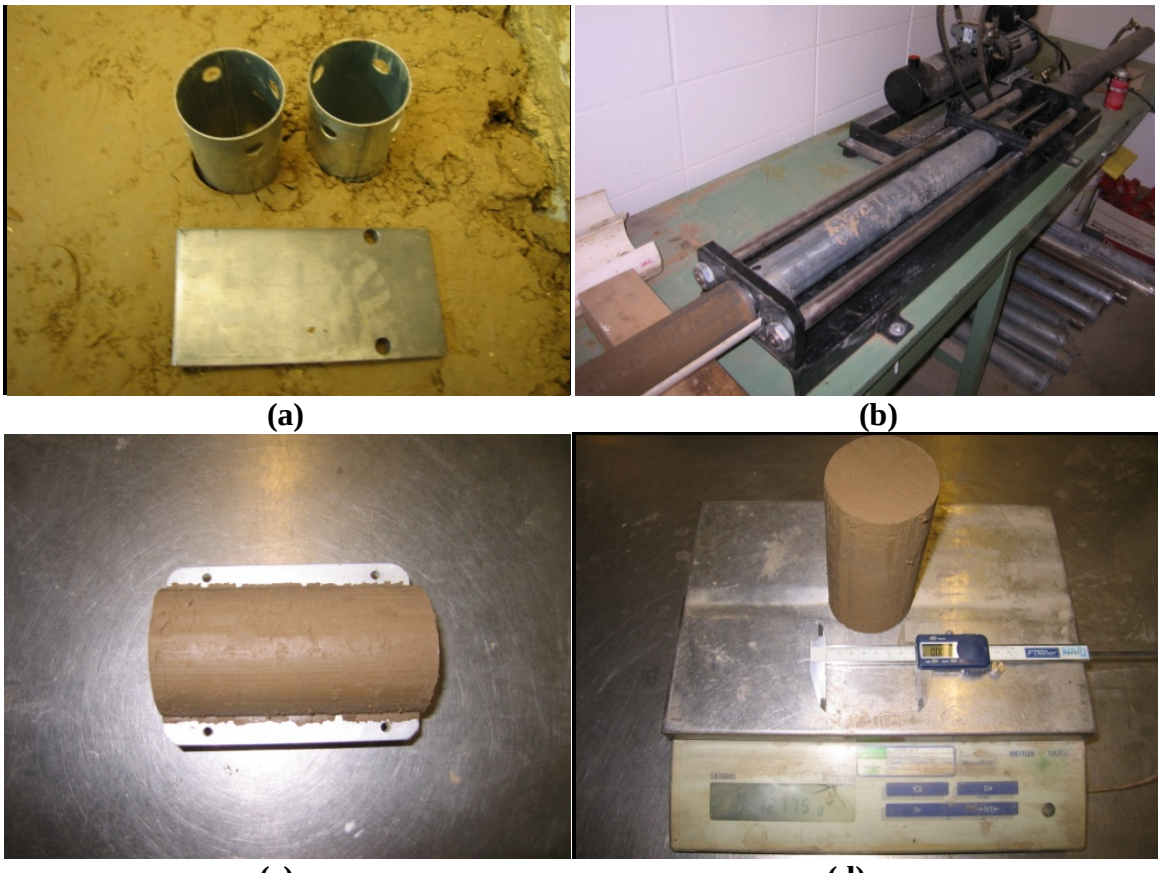

(a) **(b)**

(c) **(d)**

Figure 24: (a) Shelby tube inserted in matrix soil, (b) Shelby tube sample being extruded, (c) 72 mm x 140 mm sample trimmed, and (d) sample weighted and measured

www.manaraa.com

The entire process, as it can be seen from Figure 24, produced a relatively undisturbed sample of desired length and diameter, where the unit weight of the sample was estimated by weighing the sample and the sample dimensions were measured via calipers. Once the volumetric parameters were recorded, the sample was wrapped in a foil wrap and, thus, the moisture content of the sample was preserved. The test bed loess unit weight and moisture content results for all test stages are provided in Table 9, Table 12 and Table 14 and

Table 16

Unconfined Compression Triaxial Test

It is important to outline another benefit of having to obtain a sample of the specified length and diameter. By using the ELE International Triaxial Machine, the produced 72 mm by 140 mm sample was axially loaded and undrained shear strength values were evaluated (See Figure 25).

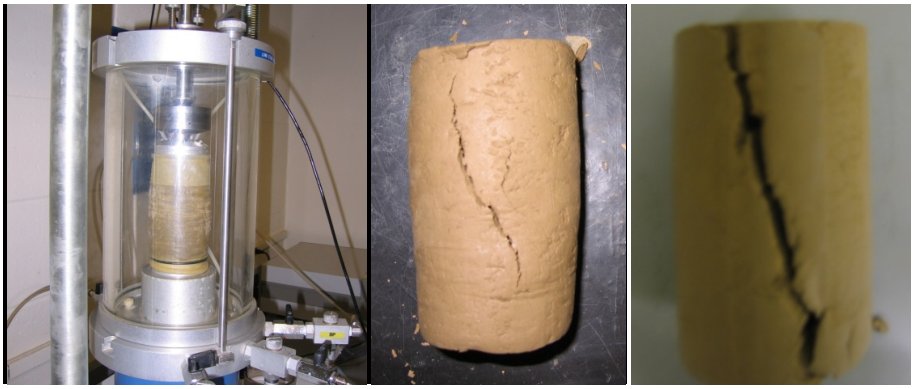

(a) (b) (c)

Figure 25: 72 mm x 140 mm sample (a) placed in unconfined compression triaxial chamber, (b) and (c) samples after failure

Having one UC test sample for every 305 mm pier and two UC samples for every 610 mm pier, the total number of 100 samples was tested. UC tests were performed according with ASTM D2166-00. Once the prepared samples were axially loaded to a point of failure and the load-displacement data was collected, the samples were further broken down and a small portion was collected for the moisture content evaluation. The moisture content testing of the

www.manaraa.com

sample was performed by utilizing a microwave oven, where the sample was incrementally dried until the weight of the sample was found to change by a margin of 0.02 g for every subsequent drying cycle.

The test bed loess undrained shear strength results for one 305 mm sample and two 610 mm samples for all testing stages are provided in Table 10, Table 13, Table 15 and Table 17.

Table 9: UC loess sample γ_{dry} and w% for single piers compacted via various beveled heads

	Aggregate Pier Beveled Heads	
Pier type	305 mm	610 mm
γ_{dry} (kg/m^3)	1456	N/A
w (%)	14.7	N/A

** Piers compacted various beveled head*

Table 10: Top UC loess sample C_u for single piers compacted via various beveled heads

	Aggregate Pier Beveled Heads	
Pier type	305 mm	610 mm
$C_{u\ top}$ kPa)	120	N/A
$C_{u\ bot}$ kPa)	-	N/A

** Piers compacted various beveled head*

Table 11: Top nuclear density gauge loess γ_{dry} and w% for single piers mixes

	Aggregate Pier - truncated Cone		Aggregate Pier w/cem. Bulb		Aggregate Pier w/cem. Top 0.1m		Loess + Fiber		Loess + Cement		Loess+ Fiber + Cement		C (I) + C (K)		C (I) + C (K) + C (NS7)		C (I) + C (NS7)		Sand		**AVERAGE**		**ST. DEV.**		**COV**	
Pier type	305 mm	610 mm	305 mm	610 mm	305 mm	610 mm	305 mm	610 mm	305 mm	610 mm	305 mm	610 mm	305 mm	610 mm	305 mm	610 mm	305 mm	610 mm	305 mm	610 mm	305 mm	610 mm	305 mm	610 mm	305 mm	610 mm
γ_{dry} (kg/m^3)	1588	1556	1448	1559	1597	1549	1527	1586	1588	1554	1517	1554	1559	1554	1512	1572	1564	1613	1464	1559	**1536**	**1566**	**52**	**20**	**3**	**1**
w (%)	20.2	23.4	23.8	22.3	22.1	23.6	21.8	23.2	22.3	22.5	21.6	21.0	22.1	22.8	24.6	23.0	22.4	20.6	23.4	22.1	**22.4**	**22.5**	**1**	**1**	**6**	**4**

** Aggregate piers and loess mix piers were compacted using truncated cone beveled head*

** Cement mix piers were cast in place*

www.manaraa.com

Table 12: Top and bottom UC loess sample γ_{dry} and w% for single pier mixes

	Aggregate Pier - Truncated Cone		Aggregate Pier w/cem. Bulb		Aggregate Pier w/cem. Top 0.1m		Loess + Fiber		Loess + Cement		Loess+ Fiber + Cement		C (I) + C (K)		C (I) + C (K) + C (NS7)		C (I) + C (NS7)		Sand		**AVERAGE**		**ST. DEV.**		**COV**	
Pier type	305 mm	610 mm	305 mm	610 mm	305 mm	610 mm	305 mm	610 mm	305 mm	610 mm	305 mm	610 mm	305 mm	610 mm	305 mm	610 mm	305 mm	610 mm	305 mm	610 mm	305 mm	610 mm	305 mm	610 mm	305 mm	610 mm
$\gamma_{dry\ top}$ (kg/m^3)	1601	1600	1567	1580	1627	1600	1579	1575	1626	1620	1571	1615	1610	1588	1597	1604	1566	1606	1561	1577	**1591**	**1597**	**25**	**16**	**2**	**1**
w_{top} (%)	23.7	24.4	25.0	24.7	22.3	23.2	24.8	25.1	24.4	25.3	24.8	23.2	23.0	24.3	25.2	24.1	23.9	23.9	24.9	24.3	**24.2**	**24.3**	**1**	**1**	**4**	**3**
$\gamma_{dry\ bot}$ (kg/m^3)	-	1602	-	1609	-	1587	-	1630	-	1632	-	N/A	-	1561	-	1604	-	1574	-	1600	-	**1600**	-	**23**	-	**1**
w_{bot} (%)	-	22.2	-	24.3	-	23.5	-	24.6	-	23.2	-	N/A	-	23.6	-	22.8	-	23.2	-	23.1	-	**23.4**	-	**1**	-	**3**

** Aggregate piers and loess mix piers were compacted using truncated cone beveled head*

Table 13: Top and bottom UC loess sample C_u for single pier mixes

	Aggregate Pier - truncated Cone		Aggregate Pier w/cem. Bulb		Aggregate Pier w/cem. Top 0.1m		Loess + Fiber		Loess + Cement		Loess+ Fiber + Cement		C (I) + C (K)		C (I) + C (K) + C (NS7)		C (I) + C (NS7)		Sand		**AVERAGE**		**ST. DEV.**		**COV**	
Pier type	305 mm	610 mm	305 mm	610 mm	305 mm	610 mm	305 mm	610 mm	305 mm	610 mm	305 mm	610 mm	305 mm	610 mm	305 mm	610 mm	305 mm	610 mm	305 mm	610 mm	305 mm	610 mm	305 mm	610 mm	305 mm	610 mm
$C_{u\ top}$ (kPa)	40	35	31	41	52	37	31	42	43	42	39	41	41	42	35	45	44	43	35	39	**39**	**41**	**6**	**3**	**17**	**7**
$C_{u\ bot}$ (kPa)	-	30	-	32	-	32	-	31	-	41	-	44	-	40	-	43	-	42	-	N/A	**-**	**37**	**-**	**6**	**-**	**16**

** Aggregate piers and loess mix piers were compacted using truncated cone beveled head*

.

Table 14: Top and bottom UC loess sample γ_{dry} and w% for group of aggregate piers

	Aggregate Pier Unit Cell		Aggregate Pier Single Pier		Aggregate Pier Group of 2		Aggregate Pier Group of 4		Aggregate Pier Group of 5		Aggregate Pier Group of 6		**AVERAGE**		**ST. DEV.**		**COV**	
Pier type	305 mm	610 mm	305 mm	610 mm	305 mm	610 mm	305 mm	610 mm	305 mm	610 mm	305 mm	610 mm	305 mm	610 mm	305 mm	610 mm	305 mm	610 mm
$\gamma_{dry\ top}$ (kg/m^3)	N/A	N/A	1602	N/A	1595	1623	1664	1583	1664	1621	1598	1592	**1615**	**1605**	**36**	**20**	**2**	**1**
w_{top} (%)	N/A	N/A	24.9	N/A	26.1	27.5	23.8	27.0	25.0	23.4	25.2	25.6	**25.0**	**25.9**	**1**	**2**	**3**	**7**
$\gamma_{dry\ bot}$ (kg/m^3)	-	1611	-	1599	-	1608	-	1656	-	1599	-	1640	-	**1626**	-	**24**	-	**1**
w_{bot} (%)	-	25.4	-	24.5	-	25.0	-	25.0	-	25.1	-	22.6	-	**24.6**	-	**1**	-	**4**

** Aggregate piers were compacted using cone beveled head*

www.manaraa.com

Table 15: Top and bottom UC loess sample C_u for group of aggregate piers

	Aggregate Pier Unit Cell		Aggregate Pier Single Pier		Aggregate Pier Group of 2		Aggregate Pier Group of 4		Aggregate Pier Group of 5		Aggregate Pier Group of 6		**AVERAGE**		**ST. DEV.**		**COV**	
Pier type	305 mm	610 mm	305 mm	610 mm	305 mm	610 mm	305 mm	610 mm	305 mm	610 mm	305 mm	610 mm	305 mm	610 mm	305 mm	610 mm	305 mm	610 mm
$C_{u\ top}$ (kPa)	N/A	N/A	26	N/A	28	29	56	32	N/A	25	41	29	**38**	**29**	**14**	**3**	**37**	**10**
$C_{u\ bot}$ (kPa)	-	39	-	N/A	-	32	-	36	-	32	-	34	-	**35**	-	**3**	-	**9**

** Aggregate piers were compacted using cone beveled head*

Table 16: Top and bottom UC loess sample γ_{dry} and w% for group C(I) + C(K) piers

	C(I) + C(K) Unit Cell		C(I) + C(K) Single Pier		C(I) + C(K) Group of 2		C(I) + C(K) Group of 4		C(I) + C(K) Group of 5		C(I) + C(K) Group of 6		**AVERAGE**		**ST. DEV.**		**COV**	
Pier type	305 mm	610 mm	305 mm	610 mm	305 mm	610 mm	305 mm	610 mm	305 mm	610 mm	305 mm	610 mm	305 mm	610 mm	305 mm	610 mm	305 mm	610 mm
$\gamma_{dry\ top}$ (kg/m^3)	1553	N/A	N/A	1589	1606	1525	1586	1660	1597	1570	1531	1465	**1575**	**1562**	**32**	**73**	**2**	**5**
w_{top} (%)	24.3	N/A	N/A	22.8	23.3	22.6	22.3	22.9	23.4	24.2	22.8	22.9	**23.2**	**23.1**	-	**1**	-	**3**
$\gamma_{dry\ bot}$ (kg/m^3)	-	1631	-	N/A	-	1590	-	1648	-	1556	-	1624	-	**1605**	-	**37**	-	**2**
w_{bot} (%)	-	24.5	-	N/A	-	24.5	-	24.4	-	24.1	-	25.6	-	**24.6**	-	**1**	-	**2**

** Piers were cast in place*

Table 17: Top and bottom UC loess sample C_u for group C(I) + C(K) piers

	C(I) + C(K) Unit Cell		C(I) + C(K) Single Pier		C(I) + C(K) Group of 2		C(I) + C(K) Group of 4		C(I) + C(K) Group of 5		C(I) + C(K) Group of 6		**AVERAGE**		**ST. DEV.**		**COV**	
Pier type	305 mm	610 mm	305 mm	610 mm	305 mm	610 mm	305 mm	610 mm	305 mm	610 mm	305 mm	610 mm	305 mm	610 mm	305 mm	610 mm	305 mm	610 mm
$C_{u\ top}$ (kPa)	47	39	N/A	N/A	43	N/A	34	30	32	20	32	16	**38**	**26**	**7**	**10**	**18**	**39**
$C_{u\ bot}$ (kPa)	-	47	-	39	-	39	-	43	-	36	-	40	-	**41**	-	**4**	-	**9**

** Piers were cast in place*

www.manaraa.com

Data Collection and Sensors

Having developed the pier loading and test bed preparation mechanisms of the pier, the next stage involved accommodation of load and deflection data collecting sensors. While the process of applying the piston of hydraulic jack directly to the top of the pier would have had no room left for implementation of data collecting sensors, the load application was, thus, developed through an indirect approach. The load applied from the hydraulic jack was, therefore, first transferred to the pancake load cell which in its turn was mounted on top of a hollow steel casing cylinder that in its turn contained a displacement transducer. The entire set-up of pier loading mechanism can be seen in Figure 26.

(a) **(b)**

Figure 26: Load cell and LVDT sensor set-up (a) test set-up, (b) in use

The following discussion presents detailed information on all the components of data acquisition system utilized in this research.

Data logger

The data collecting device was selected to be an IOtech DAQ 3000 Data Logger (See Figure 27). The data logger was equipped with analog and digital input and output ports, however the load cell and LVDT could only be connected in the analog mode. A series of signal amplifiers and power supplies were also utilized for the purpose of successfully amplifying

www.manaraa.com

signal and powering the sensors. The load and displacement data was collected via the data logger and the DAQView software was used as a viewer program. The analysis of the data was performed using SigmaPlot and Microsoft Excel Software.

Figure 27: DAQ data logger

Honeywell Load cell

The load cell served the purpose of accurately measuring the load applied to the tested pier (See Figure 28). The pancake shape load cell was purely for the compression measurements only and was equipped with a button sensor. The load was transferred between the load bearing frame and the load cell via hydraulic jack. The load cell capability was up to 9,000 kg. High measurement rate and great precision made this load cell suitable for the testing to be performed. Calibration was performed according to the manufacturer's specifications and the load measurements were manually verified to be accurate.

Figure 28: Honeywell pancake load cell

www.manaraa.com

Micro Epsilon displacement transducer

The Linear Variable Differential Transformer (LVDT) series LDR-CA50 purchased from MicroEpsilon was utilized for the testing in order for the top of the pier displacement to be measured (See Figure 29).

Figure 29: Micro Epsilon LDR-CA50 LVDT

The transducer itself consisted of a moveable plunger contained inside a metal housing. The housing was permanently fixed at a certain elevation and did not move during the experiment. The plunger, on the other hand, was free to move, where the relative distance was recorded between the tip of the plunger, fixed to the target, and the fixed elevation of the housing. The stroke length of the displacement sensor was 50 mm. This was a sufficient amount of stroke displacement for the prototype pier load testing since the amount of settlement anticipated to be captured was only on the order of 12 mm.

Humboldt displacement transducer

The Humboldt transducers were implemented in the test apparatus for the purpose of detecting tell-tale plate movement. The rods were connected to the tell-tale plate which placed at the bottom of the cavity and were extended above the ground surface and where they were placed against the tip of the displacement measuring transducer plungers (See Figure 30). The rods were placed in the housing tubes in order to allow free movement. A

www.manaraa.com

total of two transducers were used for the purpose of recording tell-tale deflection measurements on both sides of the pier being tested. Thus, by utilizing two sensors the possibility of the tell-tale plate to be tilted was taken into account. The measurements were manually recorded while the pier loading and DAQ data collection was taking place. The stroke length of the displacement transducer was limited to 25 mm. This was a sufficient amount of stroke displacement for the tell-tale movement to be recorded.

(a) (b) (c) (d)

Figure 30: (a) Humboldt displacement transducer, (b) tell-tale plate, (c) cavity in the soil with tell-tale plate inserted, and (d) complete set-up of sensors

Pier Construction Approach

Cavity Preparation

Two main construction approaches were used for the piers built in this research study. As it will be discussed in more detail in the Materials Section, the piers were constructed of loess, cement, limestone and graded manufactured sand. While the majority of the piers were built using a method of ramming material in even size lifts, some of the cement mixtures were cast in place.

For every pier placement location, once the Shelby tube was pushed and the cavity was created, the hole was vacuum cleaned to avoid having lose debris accumulation at the top of the pier. The next step in the pier installation procedure was delivering the tell-tale plate to the bottom of the hole. As it was shown in Figure 30, the approach was taken by forcing the

www.manaraa.com

plate down the cavity through manual vertical force being applied to the rods contained within the housing tubes.

Ramming Device

After creating a cavity, the procedure for aggregate pier installation was followed with delivering material down the cavity according to the design mix proportion chart (See Materials Section). The thickness of the first lift was to be twice the amount of a typical lift for a particular pier, thus, creating a bottom bulb at the tip of the pier. The compaction of the lifts was performed by ramming aggregate via a custom designed beveled heads attached to a hammer drill (See Figure 31 and Figure 32).

Figure 31: DeWall hammer drill

Being typically used for drilling or utilizing as a hammer vibratory machine, the application of the hammer drill in this research project was extended to compacting aggregate lifts. Capable of producing up to 4,300 beats per minute, 1,150 RPMs and of 60 Hz frequency (manufacturer's specifications), the drill was capable of producing vibration of a higher frequency than typically delivered in the field (300-600 cycles/minute).

Due to higher level of vibration a higher level of pier stiffening was to be expected. For repeatability purposes, however, the level of vibration was kept consistent for all the installed piers. Therefore, the same level of compaction was reproduced for all the piers and the ability to perform comparative analysis between scaled piers was not impacted. The stiffness modulus test results between small-scale piers were expected to deviate in a slight manner,

www.manaraa.com

while the field results were expected to be smaller due to having lower frequency of vibration.

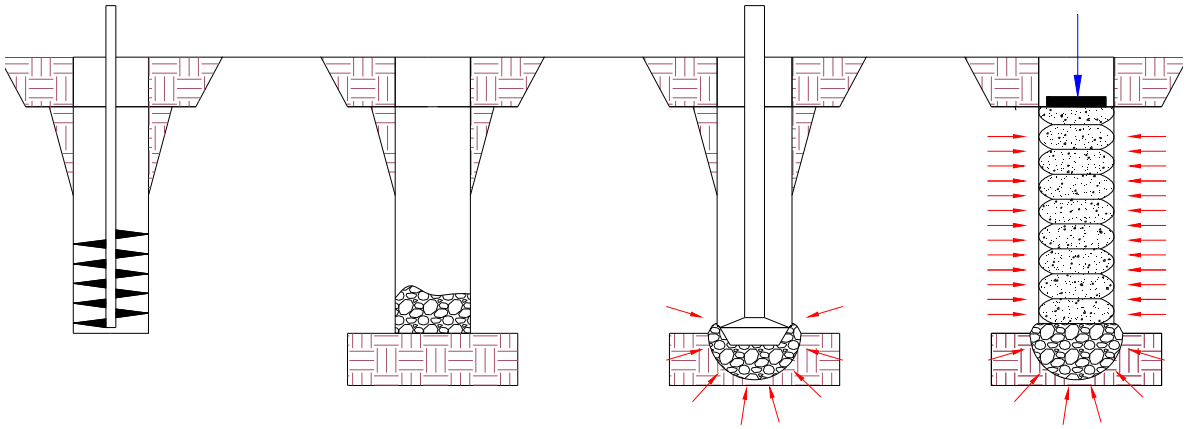

(a)

(b) **(c)** **(d)**

(e) **(f)**

Figure 32: (a) Pier installation process reproduced per Fox et al., 2004 and (b) through (f) depicted in the test bed while constructing small-scale piers

www.manaraa.com

Beveled Tamper Heads

The other aspect of the pier compaction was related to the application of different tamper heads. As it can be seen from Figure 33, various type and design beveled heads were built for the purpose of compacting scaled piers: cone, truncated cone, flat and wedge tamper heads.

(a) (b) (c) (d)

Figure 33: Beveled tamper heads (a) cone, (b) truncated cone, (c) flat and (d) wedge

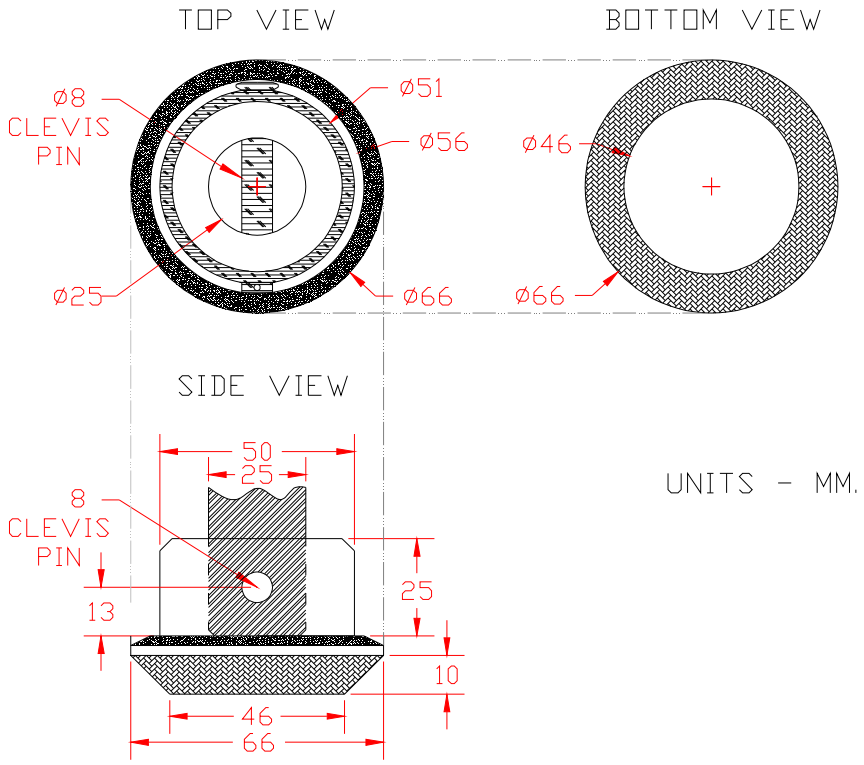

Figure 34: Truncated cone beveled tamper head schematic drawing

www.manaraa.com

Each being similar in design, except for the shape of the tamping surface, the cone, truncated cone and flat beveled heads were all 66 mm in diameter and were made out of ANSI 4140 hardened steel. While multiple design beveled heads were available for testing, the focus was made on utilizing the conventional aggregate pier truncated beveled head and cone shape heads for most applications in this research. The design drawing for the aggregate pier truncated head is provided in Figure 34.

A convenient process of attaching beveled heads to the steel rod was developed, where every beveled head was attached to the rod by means of a Cleves pin. Thus, having the hammer drill to be connected to the extended steel rod which in its turn was connected to the scaled size beveled head, made it possible to easily reproduce the aggregate pier compaction apparatus.

Cement Mixes

While most of the aggregate pier and loess pier mixes were compacted using the hammer drill in even size lifts, the cement mixes were simply delivered to the bottom of the cavity by pouring down the hole and allowing the mixture to cast in place. The mixtures were tamped with a steel rod to allow the entrapped air to be released.

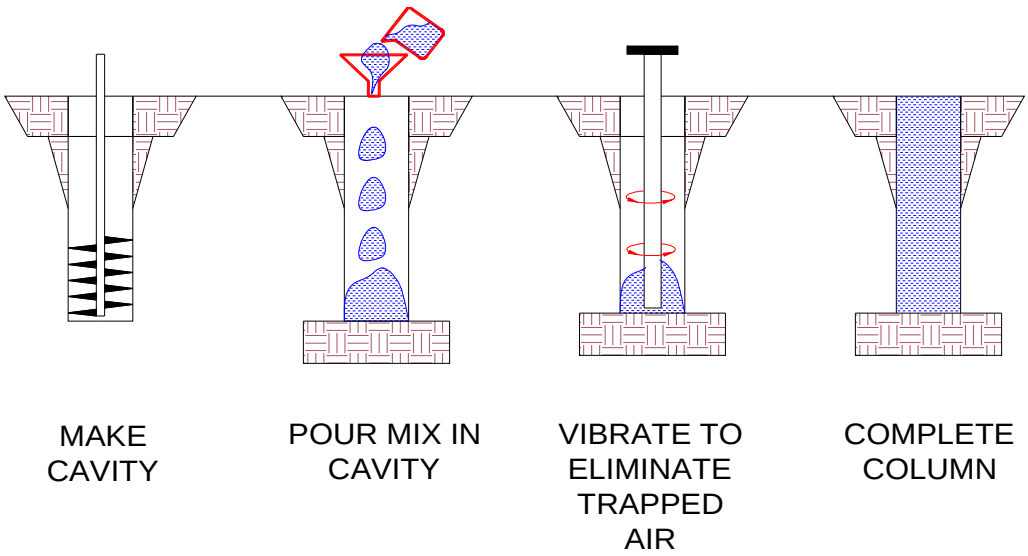

Figure 35: Cementitious pier installation process

www.manaraa.com

All, aggregate, cementitious and loess composition piers were allowed seven days for curing and the compressive strength of the cementitious composition mix materials was evaluated by preparing and testing total number of 30 concrete sample cylinders. Each sample was 76 mm in diameter and 152 mm in length. The testing samples were allowed to cure for 28 days and were axially loaded until failure in a compression machine (See Figure 36).

Figure 36: 28 day compressive strength test

Load-Settlement DAQ Approach

Loading Mechanism

As previously outlined, the strength of the pier is dependent on lateral pressure developed within matrix soil, and the shear strength within the pier element itself.

Depending on the amount of confinement provided by the matrix soil and length of the pier, the two main mechanisms of failure were plunging (305 mm piers) with tip resistance and skin friction being mobilized and by means of bulging (610 mm piers) where tip movement was limited. See Figure 37 and Figure 38 for schematic drawings representing the bulging and plunging failure modes.

www.manaraa.com

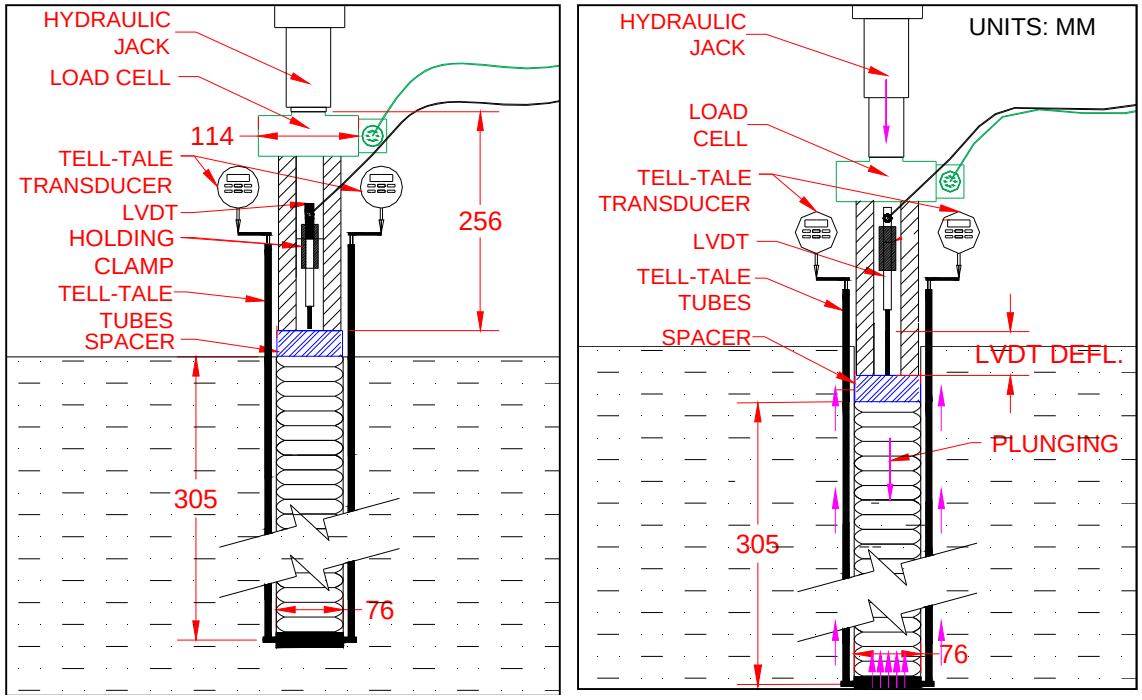

(a) **(b)**

Figure 37: (a) 305 mm pier prior to testing and (b) after plunging failure

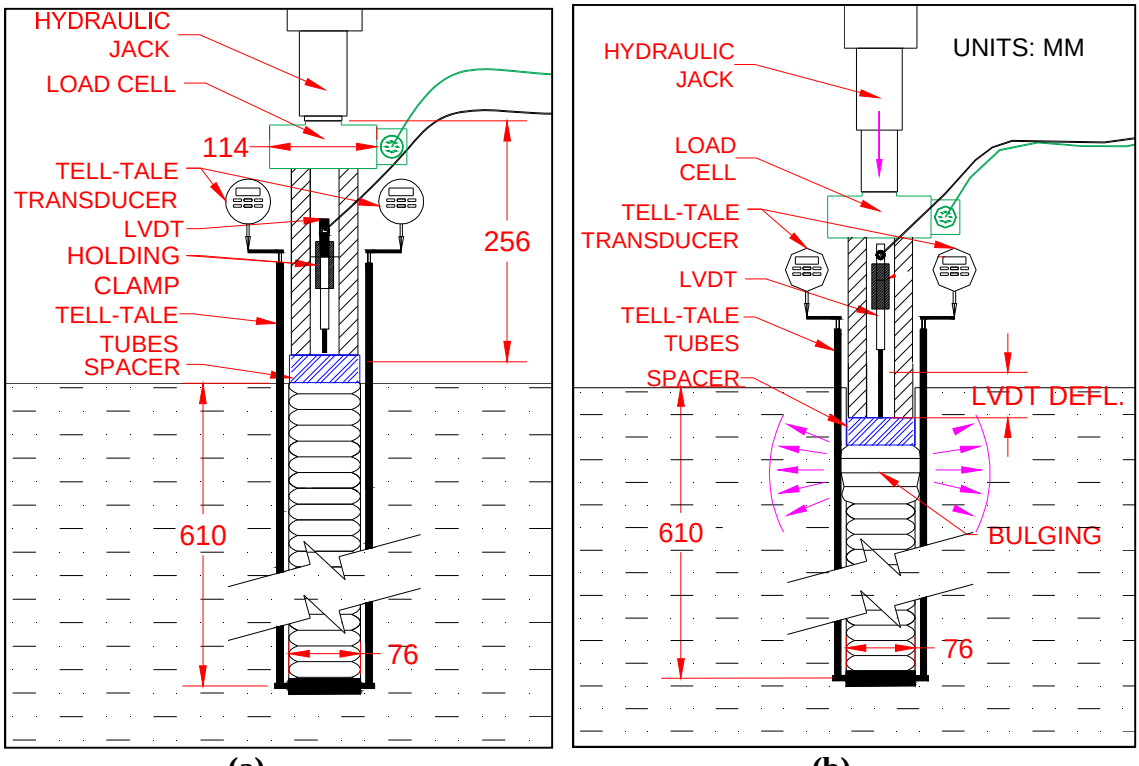

(a) **(b)**

Figure 38: (a) 610 mm pier prior to testing and (b) after bulging failure

www.manaraa.com

DAQ Data Collection

While performing loading on the pier or groups of piers, the top of the pier displacement as well as the axial load were recorded by the IOTech DAQ computer software. The tell-tale plate displacement data was collected manually. A sample of the data output file produced by DAQ software is depicted in Figure 39.

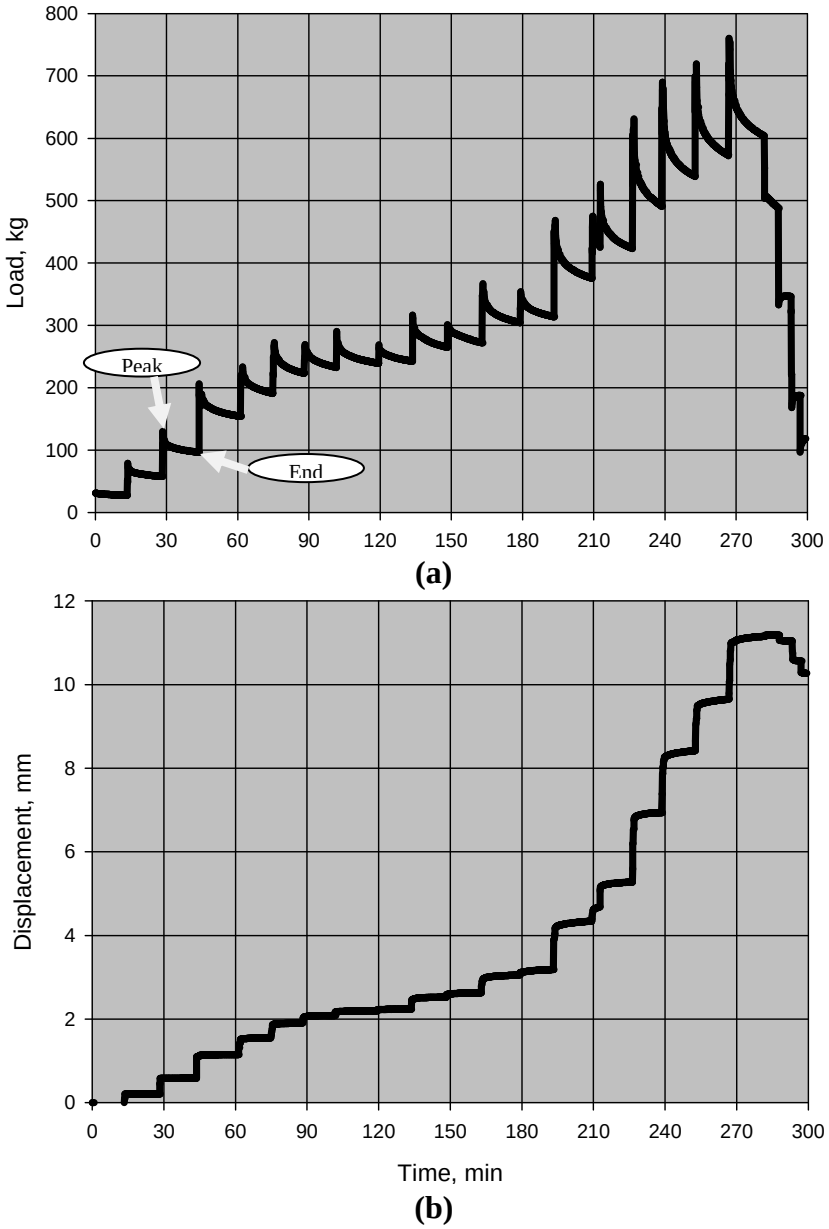

Figure 39: DAQ sample (a) displacement output raw data and (b) load output raw data

www.manaraa.com

The horizontal axis on both charts represents the time scale and is expressed in units of seconds. Therefore, from the data charts it can be observed that the loading was performed in incremental sequence. As the time-load chart shows, the duration of the load maintained at each load increment was limited to approximately 15 minutes. The reason behind applying the load for a certain time of duration is for the deflection measurement to reach the maximum magnitude while undergoing creep under load.

While the load would peak out at the initial phase of each load increment, the load would continue dropping in exponential fashion until an asymptote is reached. Therefore, a certain load was applied to the pier until the change in rate of deflection was less than 0.25 mm per hour or 0.0635 mm per each 15 minutes.

Maximum load applied to the aggregate piers was 150 percent of the maximum design stress (assumed at 70MPa), however the controlling parameter was the amount of settlement being produced. In some cases, the maximum stress imposed on the pier exceeded 150 percent to achieve the total 12 mm amount of displacement. For the purpose of generating stress-displacement plots the average value of peak and end loads was used for each interval.

Consequently, the incremental loading levels were different for different groups of piers, while the majority of aggregate piers were loaded at 9, 17, 33, 50, 67, 83, 100, 117, 133, 150 percent of maximum design stress (assumed at 70MPa). It is also important to note that the load on the aggregate piers at 117 percent level required special treatment, where longer load increment of 60 minutes was imposed. Therefore, the load was adjusted to the desired 117 percent for total number of four times. The unloading phase was also performed where load was reduced to the design stress levels of 100, 66, 33 percent of the design stress.

Group and Individual Pier Layout

The second stage of this research study, the individual piers of various length and composition were built. A total number of 20 piers were evenly spaced within the available

www.manaraa.com

space in the test bed (See Figure 40). Placing and testing individual piers within a short radial distance from the other piers was expected to develop lateral stresses in the matrix soil that could have had potential stress implications on the neighboring piers. However, having each individual pier to be within the same radial distance away from the other piers, the impact of soil developing additional lateral stresses was assumed to be equal for all piers located within the test bed.

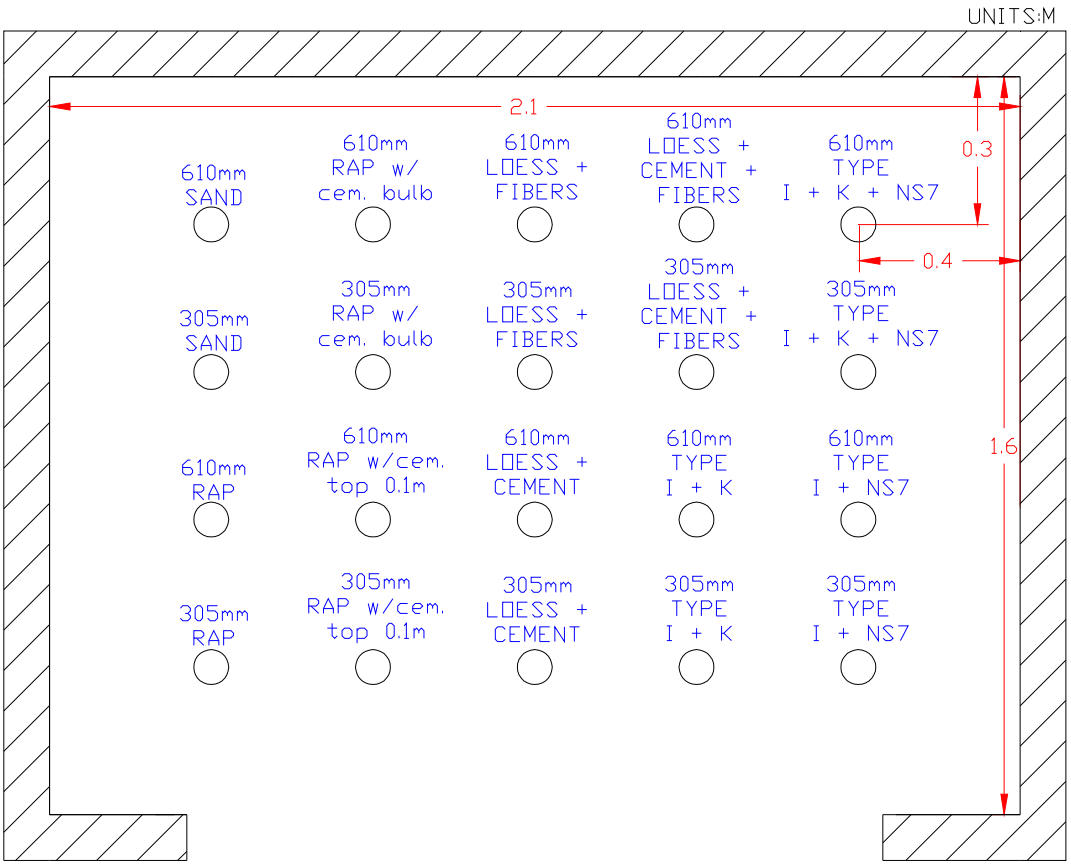

Figure 40: Test bed single isolated pier layout (top view)

Spacing piers at a radial distance of 230 mm was deemed to be sufficient to prevent interference (Lawton, 2000). Moreover, the research performed on groups of model stone columns has shown the optimum spacing for 29 mm piers to be at 76 mm on center, therefore, for the 76 mm piers used in this research the minimum spacing was estimated at 200 mm on center (Bachus and Barksdale, 1984).

www.manaraa.com

The testing and analysis of groups of piers was more complex. The groups of piers were expected to develop lateral stresses within the surrounding matrix soil as well as individual piers did, however to a greater extent due to an increased area of the footing loading. Little information is available in the literature regarding the extent of the influence and the spacing necessary for groups of piers within a confined test bed space, therefore, a conservative approach of spacing groups of piers was taken as outlined in Figure 43 and Figure 44. While having two mix variations of aggregate pier and cement type I and K composition groups of piers to be tested, the test bed preparation and pier placement locations were kept as identical as possible.

Figure 41: Test bed single isolated pier layout (top view)

www.manaraa.com

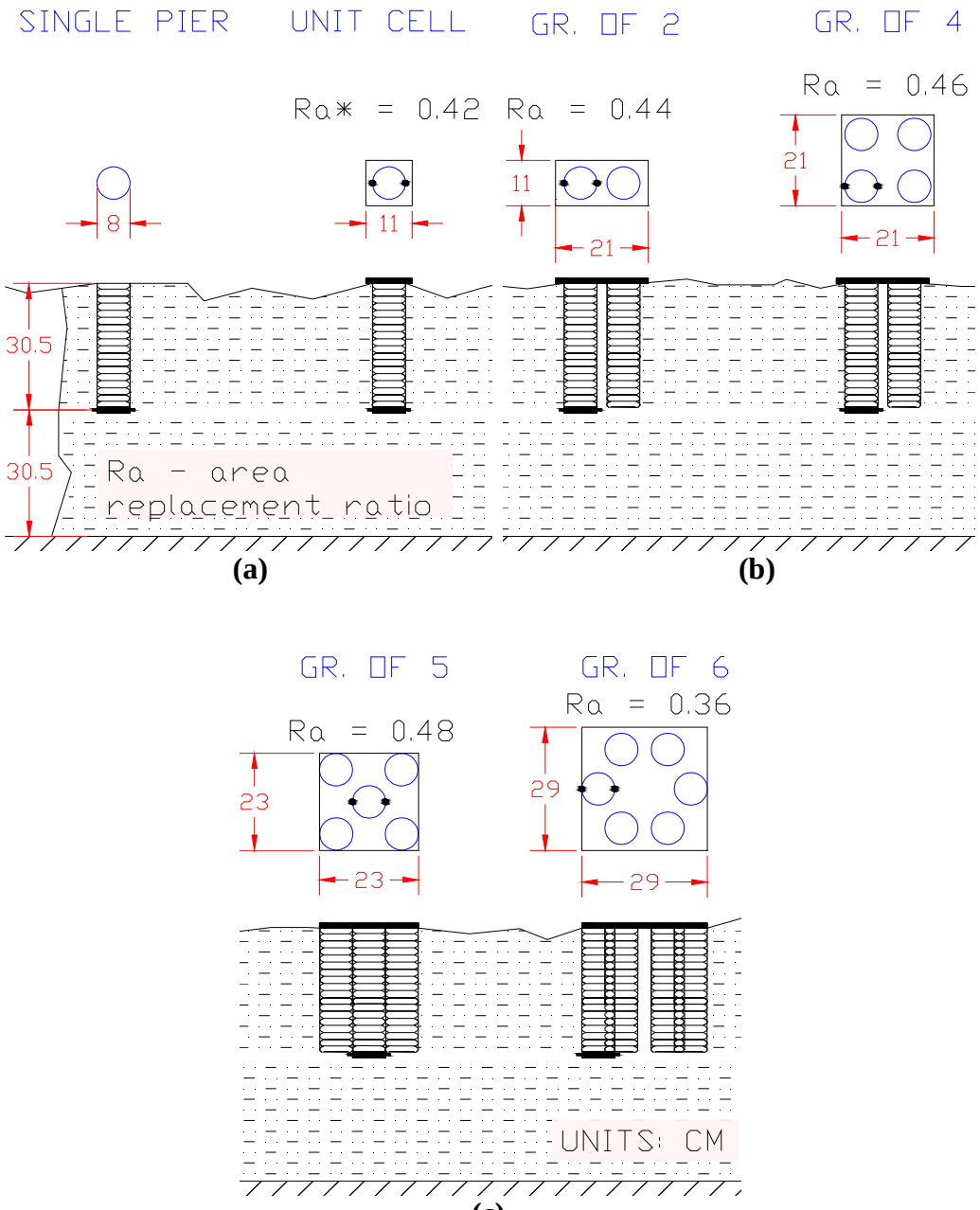

Figure 42: Test bed group pier layout for (a) single pier and unit cell, (b) group of two and four piers, and (c) group of five and six piers (profiles views)

www.manaraa.com

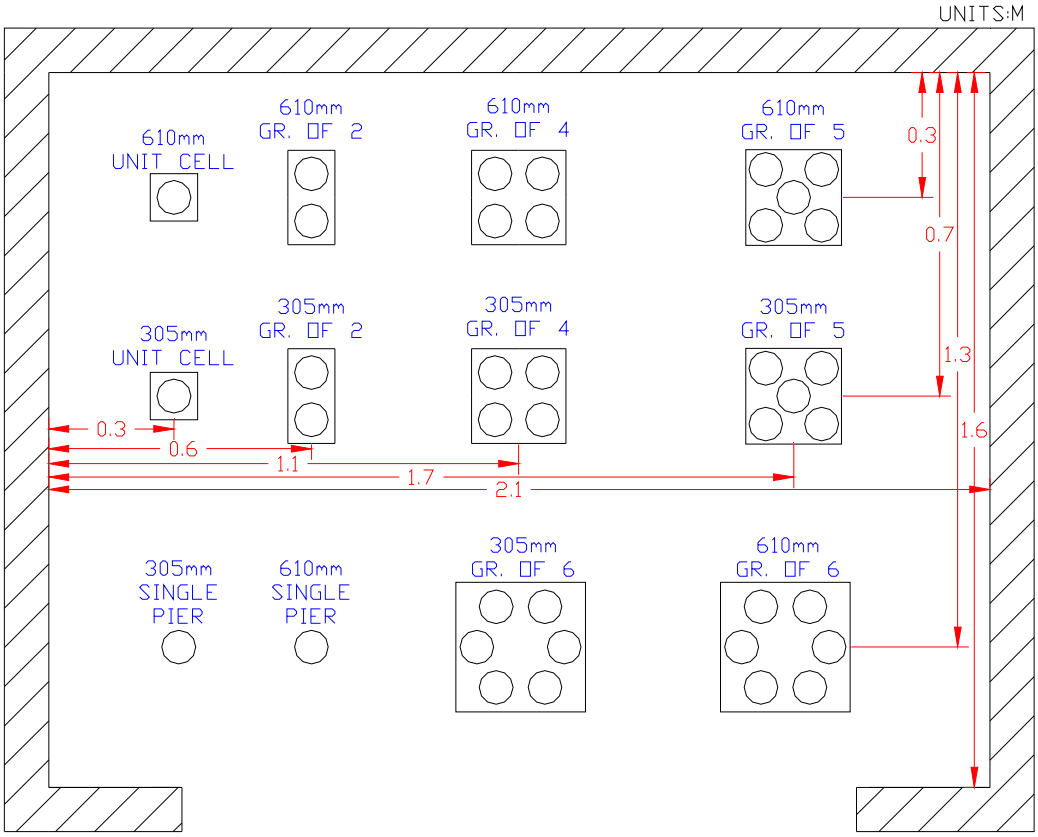

Figure 43: Test bed group pier schematic layout (top view)

Figure 44: Test bed group pier photographic layout (top view)

www.manaraa.com

CHAPTER 4: MATERIALS

The materials that were implemented in this research can be separated into two main categories: matrix loess soil and pier composition mixture materials.

Loess Material

When performing characterization of material being utilized in this research, the first and foremost consideration had to be given to the material used as pier matrix soil. While it is not uncommon to place full-scale aggregate piers in silty clay, peat and other weak deposits with excessive amount of moisture, unit weight of 10 kN/m^3, compression index 0.27 and initial void ratio of 10 (Lien et.al. 2002), the moisture content of the soil to be used for model pier placement was targeted at 30% and the undrained shear strength to range between 30-80 kPa.

In order to be able to identify target moisture content and predict the level of compaction, a Standard Proctor compaction test was performed as outlined by ASTM D698-00. The Standard Proctor curve was developed at 13, 15, 17, 19 and 21 percent moisture content levels (See Figure 45). The maximum dry unit weight of 1,700 kg/m^3 and optimum moisture content of 19 percent were obtained for the loess material.

The value for specific gravity of Western Iowa Loess was obtained by Mark Thompson and was estimated at 2.72. As a result the Zero Air Void Curve was constructed as well. Since the test bed had to be prepared four times for different single and groups of pier tests, the unit weight and moisture content data varied as it can be seen in Figure 46.

Another laboratory test that was performed on loess material was the particle size distribution test. Sometimes referred as gradation test, the examination was given to the level of loess fineness through performing a sieve and hydrometer analysis. The procedure was completed on a representative soil sample and according with the guidelines outlined by ASTM D422-63 (Figure 46).

www.manaraa.com

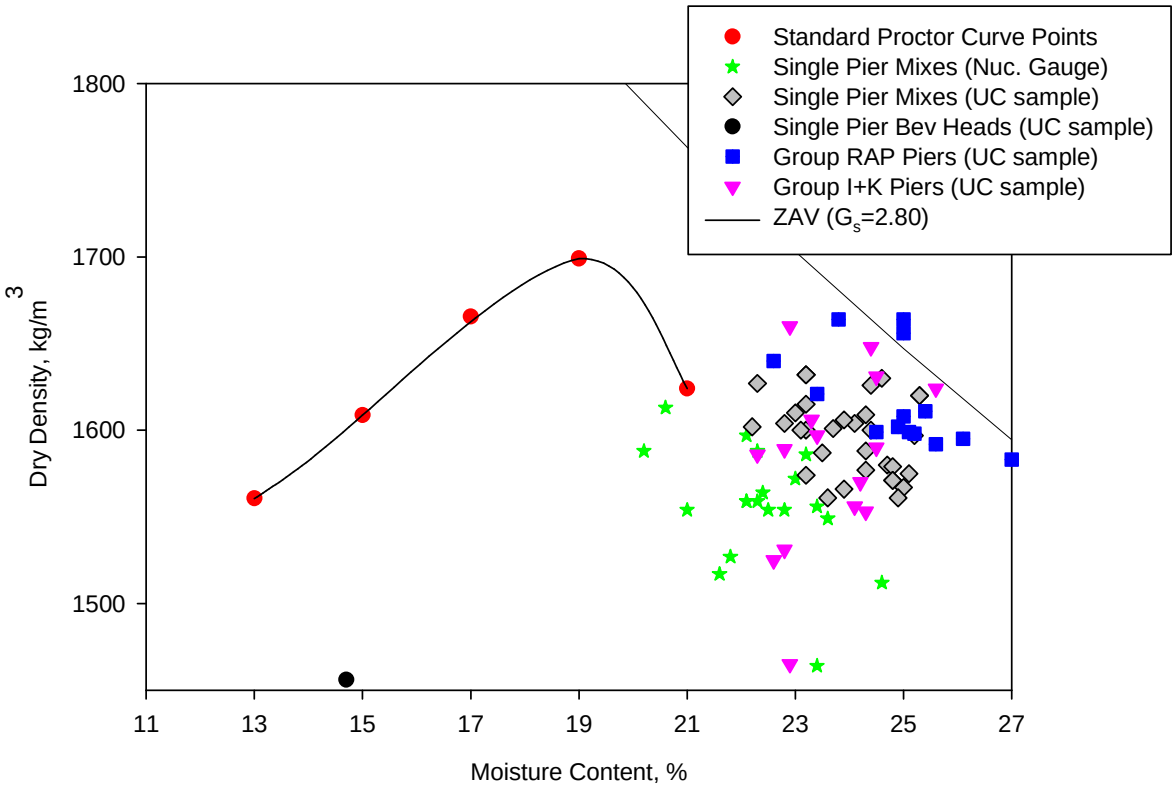

Figure 45: Standard Proctor compaction curve

As it can be observed from the Figure 46, the loess material was found to be 98 percent passing #200 sieve and was, therefore, classifies as ML (silt). Atterberg limits test was another example of a laboratory test that was of great importance and have shown liquid limit of the loess soil to be 31 percent and plasticity index was of 7 percent.

While using the Standard Proctor curve information as a guideline for preparing the test bed, the process of moisture conditioning and compaction had to inevitably go through the process of trial and error. The first set of piers, where various beveled heads were to be utilized for the purpose of pier compaction, was installed in a comparatively stiff soil environment. The moisture content of the initially prepared test bed loess material was estimated at 14.7 percent. This value was lower than the optimum moisture content and, therefore, the compaction was performed on the dry side of optimum. Moreover, the compaction process was performed in the loose 50 mm thickness lifts and by utilizing a vibratory plate compactor, resulting in dry density of 1,456 kg/m^3.

www.manaraa.com

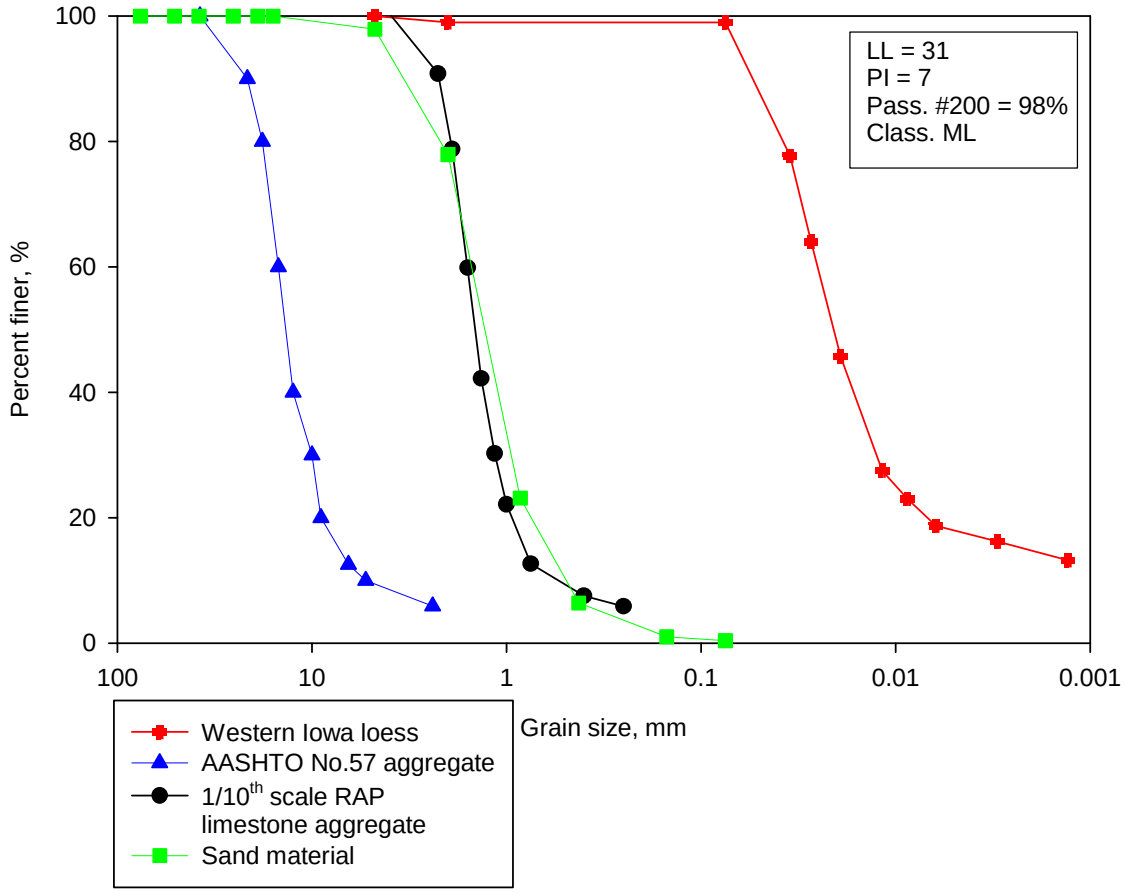

Figure 46: Particle size distribution for loess, full and 1/10th scale AASHTO No. 57, and sand materials

As a consequence, a much higher level of energy, mechanical energy and compaction was delivered to the soil in the test bed at the moisture content significantly lower than the optimum, which resulted in reduced level of compaction and lower density. As it can be seen in Figure 44, the corresponding point plotted for the initial test soil conditions appeared below the Standard Proctor Curve. Moreover, the results of Unconfined Compression (UC) test confirmed the undrained shear strength to be 120 kPa (Table 18). Knowing the typical soil conditions where full-scale aggregate piers are of best performance, the undrained shear strength values were expected to be closer to 30 kPa which was considerably lower than the produced 120 kPa.

www.manaraa.com

Table 18: Average C_u, w% and γ_{dry} for 305 mm and 610 mm loess samples

Pier type	Various Bev. Head Pier Tests	Single Pier Mix Tests	Aggregate Pier Groups Pier Tests	C(I) + C(K) Groups Pier Tests
$\gamma_{dry\ top}$ (kg/m^3)	1,456	1,572	1,610	1,568
$w\%_{top}$ (%)	14.7	23.3	25.5	23.2
$\gamma_{dry\ bottom}$ (kg/m^3)	N/A	1,600	1,626	1,605
$w\%_{bottom}$(%)	N/A	23.4	24.6	24.6
$C_{u\ top}$ (kPa)	120	40	33	32
$C_{u\ bottom}$ (kPa)	N/A	37	35	41

Another effect of having dry and stiff soil conditions, is that there was limited amount of pier bulging. Knowing that the strength of the aggregate pier has a great dependence on the lateral stress developed between the pier aggregate and the matrix soil (Handy, 2001) had lead to a conclusion of the initial test bed soil conditions being undesirable for the model pier testing,

After the first pier placement phase was completed, the new test bed was prepared at targeted moisture content of 30 percent and undrained shear strength in the range of 30 kPa. The test bed at this stage was to be used for the placement and testing of single 305 mm and 610 mm long piers of various compound mixes as outlined in Figure 41. Two density and moisture content evaluation methods were performed where nuclear gauge device and UC samples were used. The average value for density, moisture content and undrained shear strength parameters in the upper 305 mm pier layer of soil were evaluated to be 1,572 kg/m^3, 23.3 percent, and 40 kPa respectively (Table 18). These values were significantly different from the values obtained in the first phase of testing and much closer to the soil conditions where full-scale aggregate piers are of the best performance. On the other hand, the deeper layer of soil to which the 610 mm piers were extended to, featured slightly higher density and comparatively unchanged moisture content and undrained shear strength.

Afterwards, the tests for the short and long groups of aggregate pier and cement type I and K composition piers were conducted in the soil conditions very similar to the once produced at

www.manaraa.com

the second stage of testing. Moisture content was maintained within 23 and 25 percent margin, unit weight 1,600 kg/m^3 and undrained shear strength close to 40 kPa.

Pier Composition Materials

Piers constructed at the first stage of testing were built using 1/10th scaled AASHTO No.57 crushed limestone. The second stage of testing involved constructions of piers of various composition mixes as outlined in Table 19. The groups of aggregate piers at third testing stage were mainly built using manufactured sand and at the last stage cement type I and K composition groups of piers were cast in place according to proportions stated in Table 19.

Table 19: Pier mix proportions, compressive strengths, and pier construction details

Pier type	Length (mm)	Proportions of mixture components (%)							Total number of lifts	Mass per lift (g)	$\sigma_{28\ day}$ (kPa)
		Limestone Aggregate	Fibers	Cement Type I, C(1)	Cement Type K, C(K)	NS7	Sand	Loess Soil			
Aggregate Pier	310	√	—	—	—	—	—	—	11	280	—
	610	√	—	—	—	—	—	—	21	280	
Aggregate Pier w/cem. bulb	310	√	—	20	—	—	—	—	14	320	9,530
	610	√	—	20	—	—	—	—	23	320	
Aggregate Pier w/cem. top 0.1	310	√	—	18	—	—	—	—	13	310	9,530
	610	√	—	18	—	—	—	—	21	310	
Loess + fiber	310	—	1	—	—	—	—	√	15	190	900
	610	—	1	—	—	—	—	√	28	190	
Loess + cement	310	—	—	7	—	—	—	√	14	250	1,990
	610	—	—	7	—	—	—	√	23	250	
Loess + fiber + cement	310	—	1	7	—	—	—	√	13	190	1,990
	610	—	1	7	—	—	—	√	27	190	
C(1) + C(K)	310	—	—	85	15	—	—	—	CIP		29,700
	610	—	—	85	15	—	—	—	CIP		
C(1) + C(K) + NS7	310	—	—	83	14	3	—	—	CIP		7,610
	610	—	—	83	14	3	—	—	CIP		
C(1) + NS7	310	—	—	99	—	1	—	—	CIP		17,660
	610	—	—	99	—	1	—	—	CIP		
Sand	310	—	—	—	—	—	√	—	15	280	—
	610	—	—	—	—	—	√	—	30	280	

Legend:
$\sigma_{28\ day}$ - average 28 day compression strength of 76 mm x 152 mm samples (kPa)
Aggregate pier w/cem. bulb - pier with bulb portion of the pier containing 20% of cement Type I
Aggregate Pier w/cem. top 0.1m - pier with top 100mm of the pier containing 18% of cement Type I
Fiber - polypropylene fibers (19 mm in length), CIP - cast-in-place

www.manaraa.com

Scaled Aggregate Piers – AASHTO No. 57

As the process of 1/10th scale pier testing was being developed, the use of full-scale size aggregate was deemed to be inappropriate for aggregate pier construction. While aggregate pier elements are typically built using well graded aggregate, recycled concrete and often AASHTO No. 57 crushed limestone aggregate (Fox and Cowell, 1998), the gradation of the full-scale material had to be altered by the order of 10 for the method of scaling to be valid. Due to local availability and being relatively inexpensive, AASHTO No. 57 aggregate was first selected and utilized for the purpose of 1/10th scale aggregate pier construction. Knowing the particle size distribution curve for the full size AASHTO No. 57 aggregate, the prototype aggregate mix was developed as outlined in Table 20 and Figure 46 as outlined above (Wisconsin DOT, 2003).

Table 20: Full-scale and 1/10th scale aggregate pier dimensions

	Full-scale size aggregate Pier*	**1/10th scale size aggregate pier**
Total height, m	3.70	0.370
Diameter, m	0.76	0.08
Volume, m^3	1.7	0.0017
Initial void ratio	0.33	0.34
Initial ρ_{dry}, kg/m^3	2,100	2,015
Loose lift thickness, m	0.914	0.09
Compacted lift thickness, m	0.305	0.03
Total mass of aggregate/pier, kg	3,523	3.4
Total number of lifts	12	12
Total mass of aggregate/lift, kg	294	0.282

** Values obtained from Pham and White, 2007*

***Values for prototype aggregate piers are not exactly 1/10thscale due to a difference in density*

While having a typical full-scale compacted aggregate pier to be 0.305 m thick, 0.76 m in diameter and have compacted aggregate density of 2,100 kg/m^3 (White et.al., 2007), the amount of aggregate to be used for each scaled lift was estimated at 280 g by weight.

www.manaraa.com

Knowing the gradation characteristics corresponding to 1/10th scale aggregate, a convenient aggregate proportion table was developed to ease process of mixing aggregate for model piers (Table 21).

Table 21: 1/10th scale aggregate pier mix proportions

Sieve #	Sieve opening	Percent	Amount
#10	2	9	294
#16	1.2	49	1601
#20	0.9	20	653
#30	0.6	9	294
#40	0.5	3	98
Pan	< 0.5	10	327
		Total	3,267

The mix, outlined above, constitutes a certain amount of aggregate retained on each of the specified sieves for the total amount of 3,267 g of mixed material and is suitable for construction of one 305 mm aggregate pier at total number of 12 lifts.

As previously discussed, whenever creating a scaled model aggregate pier it was critical to ensure proper scaling of the composition material being used. The relative dimensions of the aggregate particles present in the sample play important role. Having 76 mm diameter scaled aggregate piers to be used for load testing, the outcome results were to be representative as long as the diameter of the aggregate pier is greater than six times the size of the largest particle present within a sample (Marachi et.al. that 1972). Having 2 mm particle diameter to be the limiting aggregate particle size of the prototype aggregate pier, it is obvious that the diameter/particle size ratio was not affected.

The process of scaling limestone aggregate served the purpose of creating mix for scaled aggregate piers, however, the approach had to inevitably lead to an increased portion of fines which had a potential to impact the overall properties of mixed material (Hanlong, 2008). This could potentially lead to deviation in vital aggregate properties like void ratio, density and shear strength. Therefore, when creating a prototype scale pier it was first important to compact aggregate to the same relative density in order for the particle interlock strength and void ratio parameters to be reproduced (Lim et.al., 2004). It has been observed for the full-

www.manaraa.com

scale aggregate piers to feature a void ratio value of 0.33 and dry unit weight of 2,100 kg/m^3 (Pham and White, 2007). Thus, knowing the target parameters, a direct shear test was performed on the scaled aggregate mix sample where density and void ratio values were determined. As the direct shear test was performed according with ASTM D3080-04 guidelines, the sample was tested at 35, 70 and 100 kPa and an average value for void ratio of 0.32 and dry density of 2,015 kg/m^3 was obtained (Table 22).

Table 22: Direct shear test initial density and void ratio of scaled aggregate pier material

	34.5 kPa	69 kPa	103 kPa	Average
Diameter, cm	6.33	6.33	6.33	-
Area, cm^2	31.46	31.46	31.46	-
Initial height, cm	1.90	2.38	2.16	-
Initial Volume, m^3	5.98E-05	7.49E-05	6.80E-05	-
Mass sample, mold+2p+2s, g	2,176.90	2,176.90	2,176.80	-
Mass mold+2p+2s, g	2,044.20	2,044.20	2,044.20	-
Initial Weight of sample, kg	0.12	0.15	0.14	-
Dry unit weight, kN/m^3	19.86	19.39	20.06	19.77
Dry density, kg/m^3	2,024	1,977	2,045	2,015
Initial void ratio	0.31	0.34	0.30	0.32
Initial Dry Density, kg/m^3	2,024	1,976	2,045	-

The image of the tested scaled limestone direct shear sample is provided in Figure 47.

(a) **(b)**

Figure 47: (a) Direct shear machine and (b) scaled aggregate sample after shearing

www.manaraa.com

More importantly, the performed direct shear test also yielded the angle of aggregate friction to be 44 degrees (Figure 48). Friction angle and void ratio values obtained for prototype aggregate pier material via direct shear test came out to be very consistent with the parameters of full size aggregate pier material and were deemed to be acceptable.

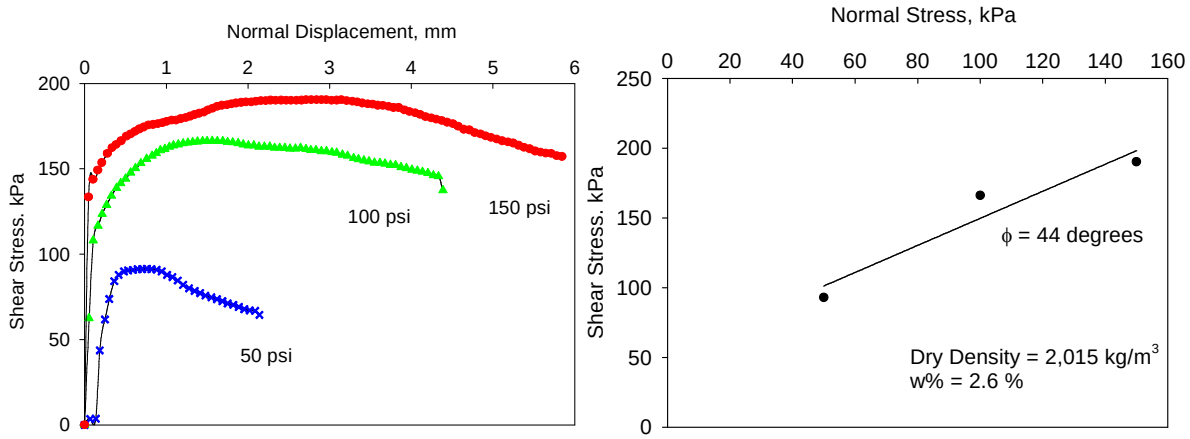

(a) **(b)**

Figure 48: Direct shear (a) test results, failure envelope and (b) plotted friction angle for crushed limestone aggregate

Scaled Aggregate Piers – Manufactured Sand

While the overall process of scaling AASHTO No. 57 aggregate was proven to be successful, the process resulted in a great amount of coarse material retained above #10 sieve to go to waste. Moreover, only limited amount full-scale AASHTO No. 57 limestone aggregate was available and, therefore, additional sources of material had to be identified. The local availability of manufactured sand material had solved the problem of aggregate deficiency and the research was continued to carry on. Manufactured sand typically contains considerably lower amount of material greater than 2 mm in diameter. Thus, the issue of excessive generation of coarse aggregate waste product was resolved as well.

The adopted process used to produce manufactured sands is typically through crushing aggregate to a finer level of gradation (<2.36 mm). Having the manufactured sand mix proportions to be reproduced exactly to the proportions specified in Table 21, the values for

www.manaraa.com

friction angle, void ratio and dry unit weight were assumed to be the same as for the once obtained for scaled limestone aggregate. The justification to such conclusion can be argued from a friction angle point of view, where the research preformed on manufactured sand had confirmed the friction angle to be 45.2 degrees (Park and Lee, 2002). Therefore, the manufactured sand material was deemed to be suitable as a substitute for scaled limestone aggregate and use in scaled aggregate pier application.

Grout Piers - Type 1

Type I cement, obtained from Holcim, Mason City, Iowa, was primarily implemented in this research as a component for the grout type piers, utilized for partially grouting aggregate piers, as a cementing material in loess based piers, and also used for pouring pier load distributing caps. Type I cement was selected due to its non-expansive nature and widespread application.

Typically, the application of cement type I is extended to general use where no special site conditions are implied. Type I cement is known for high early compressive strength and is typically applied in the environments not effected by drastic changes in temperature, presence of sulfate rich soils, and abrasive environments (FHWA, 1999). Even though typical applications of this cement are not extended to retaining walls or abutments, the mixture is very popular in reinforced concrete, masonry units and pre-cast concrete construction.

The type I cement material itself is typically stored in a form of dry paste and is diluted with water when ready for application. The image of the cement type I compound is outlined in Figure 49.

www.manaraa.com

Figure 49: Cement type I compound

By partially grouting aggregate piers, the effect of grout mixtures was evaluated on the amount of reinforcement provided to the piers and overall pier modulus results. The image of the aggregate pier mixed with cement Type I is provided in Figure 50.

Figure 50: 1/10th scaled aggregate pier material mixed with cement type I

Grout Piers - Type K

Type K cement is known for its expansive nature where it has been found to be four times more expansive than type I cement (Pittman, 2009). The application of the material is very

www.manaraa.com

useful when corrosion is of a great concern. Moreover the use of the compound has been proven to reduce the wear of the concrete surface by 30 to 40 percent (Flax, 2005). The type K cement material for this research was obtained from CTS KSC company and the image of the dry compound is provided in Figure 51.

Figure 51: Cement type K compound

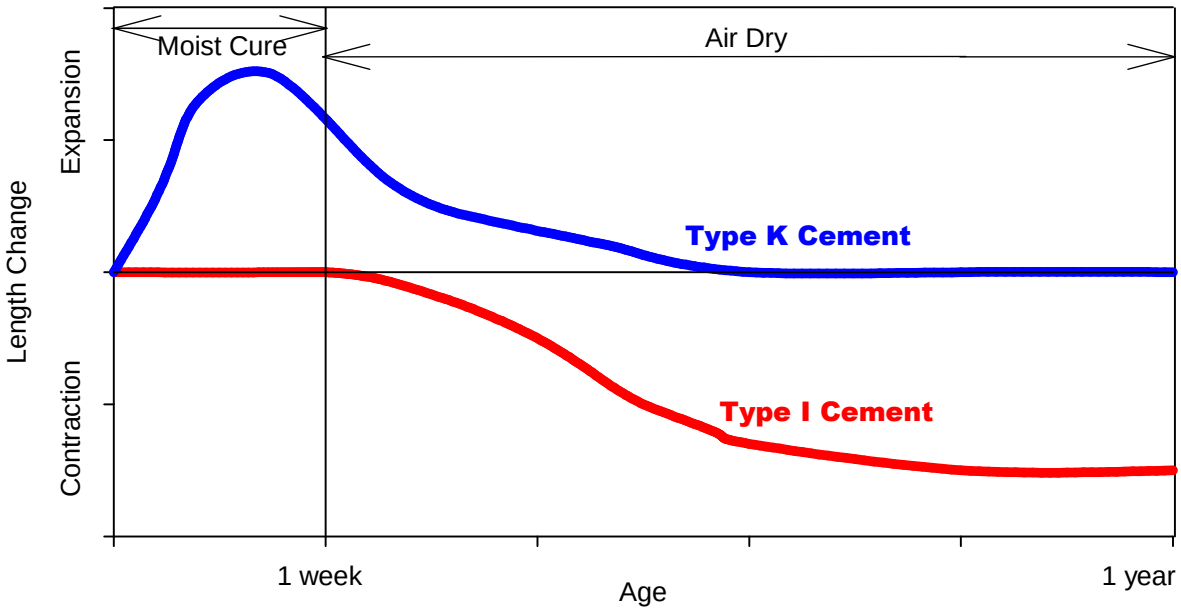

Figure 52: Volumetric changes of type I and type K cements (reproduced per Mehta and Monteiro, 2006).

www.manaraa.com

As the expansive and contractive nature of cement type K mixed with cement type I has been extensively studied by different researchers a good graphical depiction of the behavior of two materials is outlined in Figure 52 (Mehta and Monteiro, 2006).

Grout Piers - NS7

NS7 component was obtained from Fritz-Pak, Anderson Superior Products, Yankton, South Dakota (Figure 53). According to the manufacturer's specification the product is used for the increasing compressive and shear strength, and enhancing workability. Reduced shrinkage for the cement mixes with NS7 is another benefit of the compound.

Figure 53: NS7 admixture compound

It is important to emphasize the expansive nature of NS7 compound in this research. When poring the mixtures in cavities and allowing the grout to cure, the benefit of expansive nature of the material can be outlined where the grout would tend to fill all the voids and maximize skin friction of the column or pier to a better extent. The cement type I, K, NS7 and cement type I, NS7 mixtures expanded significantly within the first few minutes after the mix was poured inside the cavity. It was also observed for the cement type I, K, NS7 mixtures to expand to a much greater degree due to presence of both expansive cement type I and NS7 components. The observations are consistent with the ones obtained in a grout study research performed at Iowa State University (ISU) by White et.al., 2009.

www.manaraa.com

The 76 mm by 152 mm cylinders subjected to 28 day strength evaluation were also noticed to bleed once the grout was poured and the cylinders were capped (Figure 54).

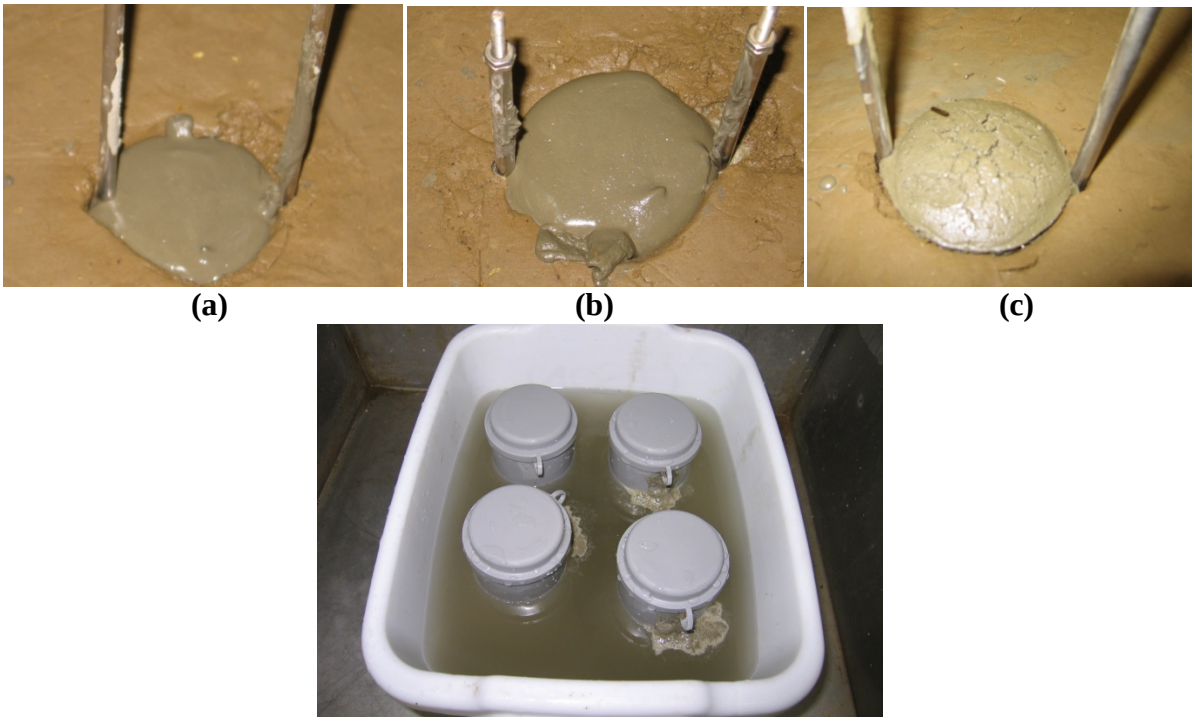

(a) **(b)** **(c)**

(d)

Figure 54: Expansive C(I) + C(K) + NS7 and C(I) + NS7 mixtures (a), (b), (c) shown within the cavity in matrix soil and (d) placed in cylinders for curing and 28 day strength evaluation

Loess Piers – Fibers

Another component that was used in this research was the 19 mm polypropylene fibers. Capable of high tensile strength and ductility, presence of fibers can be very important for the overall strength performance of the mixtures. For the purpose of this research fibers were obtained from PSI company and utilized in loess and grout based mixes.

Previous research has shown the fibrous materials to be successfully implemented in concrete construction applications such as hollow concrete piers (Yeh and Mo, 2005). See Figure 55 for the image provided for the fibers.

www.manaraa.com

Figure 55: 19 mm polypropylene fibers

When utilizing fibers in this research, the moisture content level of the mixture had to be sufficient to achieve appropriate level of curing of cement based piers and binding between soil particles and fibers in case with loess based piers. The level of moisture content of loess was adjusted to the optimum level of 19 percent in the loess and fiber pier applications. However, additional water was used when mixing loess and cement composition piers to achieve water/cement ratio of 0.5. Mix composition of fibers, loess, and cement can be seen in Figure 56.

Figure 56: Loess + C(I) + fiber mix during sample preparation

www.manaraa.com

Other Piers - Sand

Additional to aggregate pier, loess and cement composition piers, the construction of sand piers was also performed. Coincidentally, the particle size distribution curve for sand material appeared to have a very similar with the gradation curve for $1/10^{th}$ scale aggregate pier aggregate (Figure 46). However in spite of similarities in gradation, the friction angle for a typical sand material like Ottawa standard sand is known to vary between 28 and 35 degrees (Holtz and Kovacs, 1981), and, therefore, the modulus of the sand pier was anticipated to be lower than for aggregate pier.

www.manaraa.com

CHAPTER 5: TEST RESULTS AND ANALYSIS

The following section presents plotted and tabulated stress-settlement, bearing capacity and group efficiency results obtained for single and groups of piers tested in this research study.

The stress-settlement results were generated for all tested single piers and groups of piers. The results were plotted and grouped by length for each type of the pier. A supplemental photographic image of the pier profile is provided for the single piers and top view image for the groups of piers.

All the obtained results were quantified and grouped in tables, where pier stiffness and top and bottom pier displacement values were summarized. Two different loading conditions were considered when tabulating the collected results: service load conditions and ultimate or failure load conditions. Bearing capacity parameter was also estimated for single and groups of piers where calculations were distinguished based on bulging and plunging mechanisms of failure. The evaluation of individual pier performance in comparison with the efficiency of a single pier within the group was also completed through group efficiency calculations.

Single Aggregate Piers Compacted via Different Shape Tamper Heads

Stress-Settlement

The preliminary stress-settlement modulus results were obtained for the piers compacted using cone, truncated cone, flat and wedge tamper heads. The plotted curves in Figure 58 outline the behavior of the piers constructed at 305 mm and 610 mm length, as well as, the stress-settlement results for the unreinforced matrix soil (Figure 57). No tell-tale sensors were implemented at this stage of testing.

www.manaraa.com

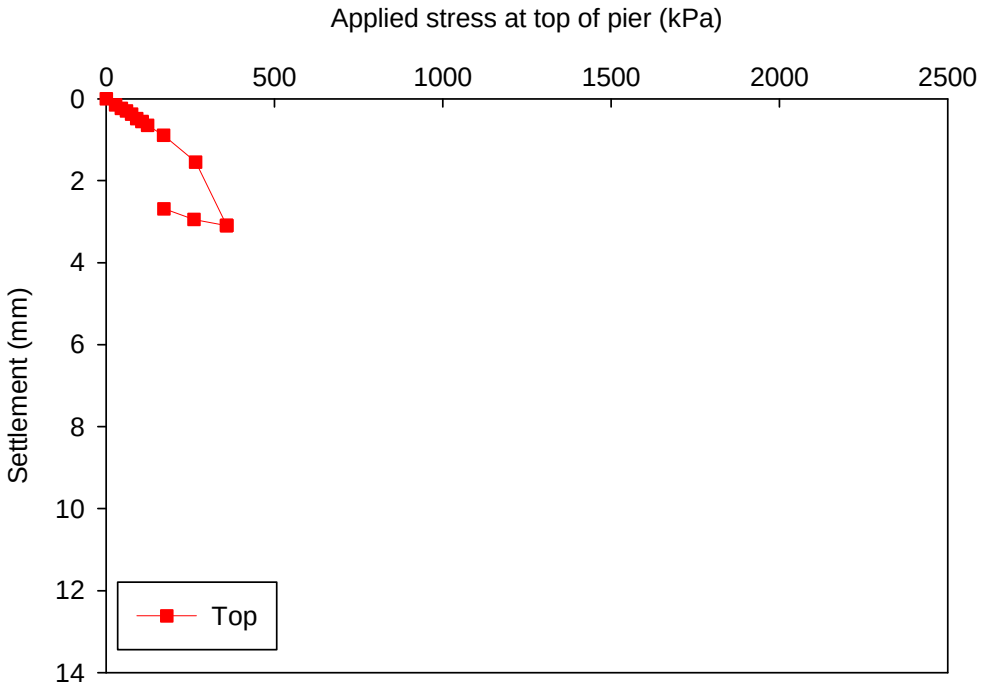

Figure 57: Stress-settlement test results for matrix soil used for placement of piers compacted via different shape tamper heads

The stress-settlement tests performed on the piers at this stage were not carried to the full extent of 12 mm displacement like it was in the later testing stages. Moreover, some piers at this stage were loaded to a greater extent than others and, thus, the only stiffness comparison made was on basis of 2 mm top of the pier displacement (Table 23).

Table 23: Stress and stiffness comparison measurements for simulated aggregate piers constructed via different shape tamper heads

Pier type[1]	Length (mm)	k at δ_{top} = 2 mm (kPa/mm)	σ at δ_{top} = 2 mm (kPa)
Aggregate Pier – Cone	305	188	375
	610	295	590
Aggregate Pier - Truncated Cone	305	150	299
	610	285	548
Aggregate Pier – Flat	305	132	263
	610	274	570
Aggregate Pier – Wedge	305	195	390
	610	197	393
Loess	—	146	291

Legend:
[1]piers were compacted using different beveled heads (cone, truncated cone, flat and wedge)
k - stiffness modulus (kPa/mm)
δ_{top} - deflection at the top of the pier (mm)
σ – stress at top of the pier (kPa)

Conversions:
1 m = 3.3 ft
1 mm = 0.0394 in
1 kPa = 0.145 psi
1 kg/m^3 = 0.0624 pcf

www.manaraa.com

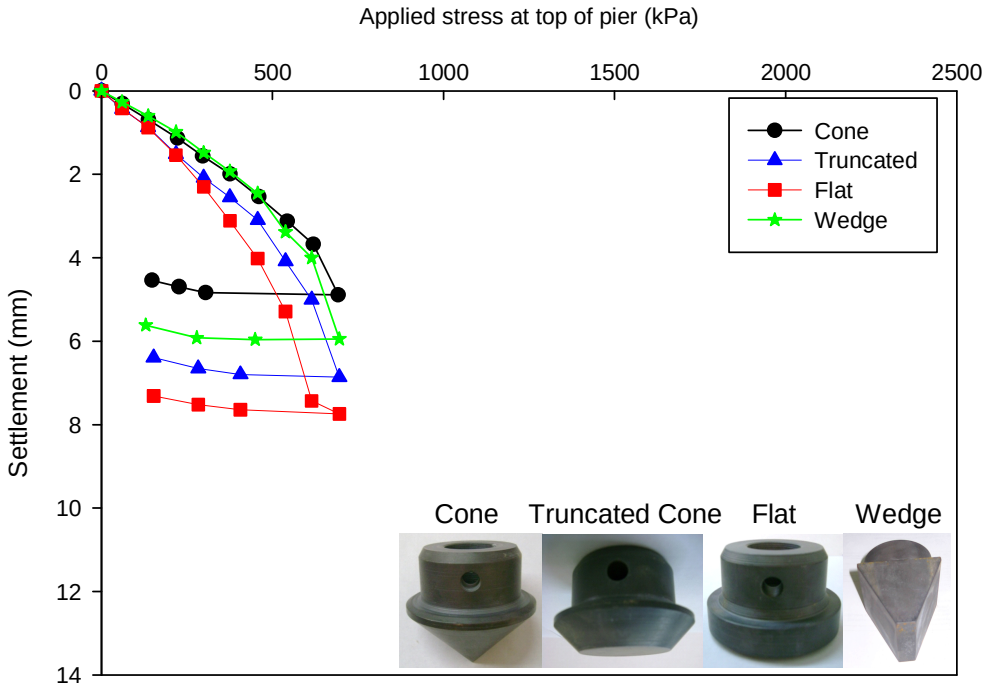

(a)

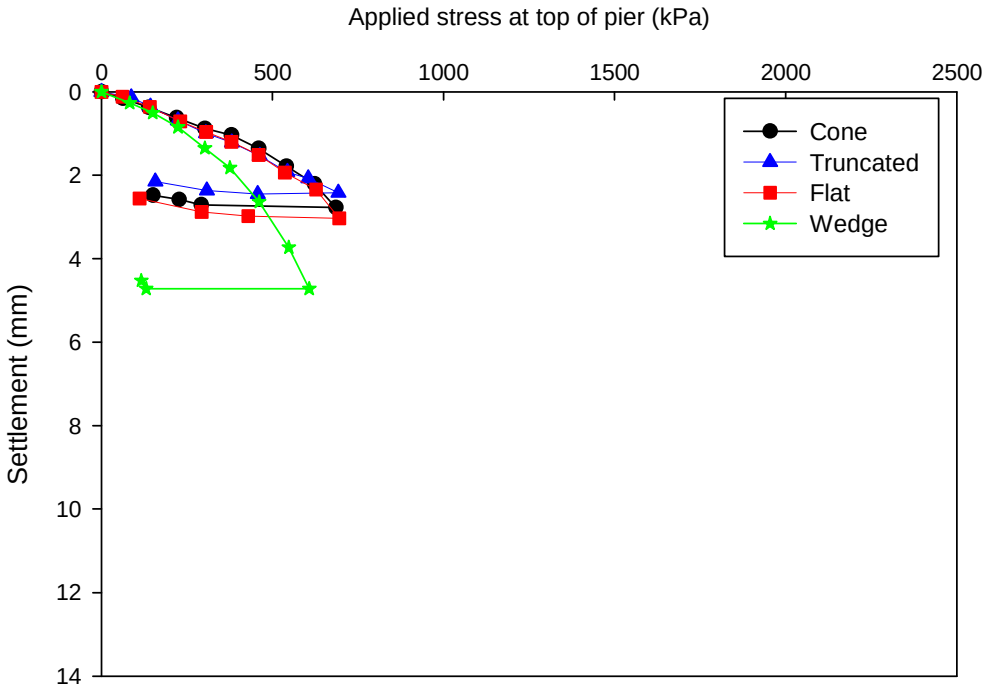

(b)

Figure 58: Stress-settlement test results (a) for 305 mm and (b) for 610 mm long piers compacted using cone, truncated cone, flat and wedge tamper heads

www.manaraa.com

Single Piers of Various Composition

Stress-Settlement

Single piers tested at this stage were constructed of cement, loess and aggregate pier materials as a main component, as well as, other mixture constituents as outlined in Table 19. Stress-settlement results were plotted and grouped by length and the tell-tale information was collected as well. The results were supplemented with pier profile images and are provided in Figure 59 through Figure 70.

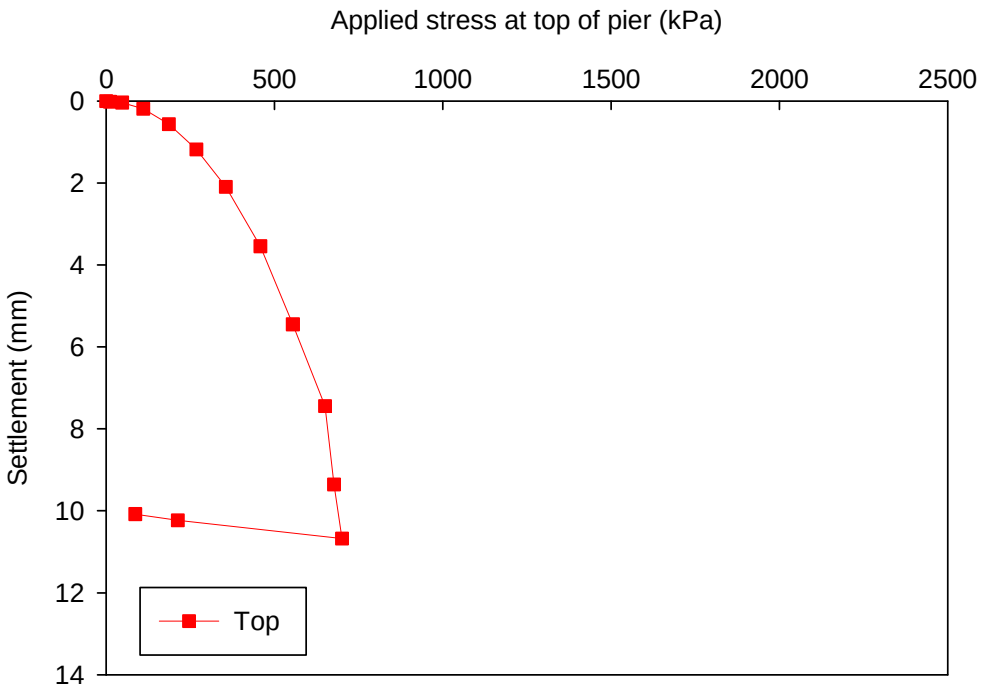

Figure 59: Stress-settlement test results for matrix soil used for placement of single piers of various composition

www.manaraa.com

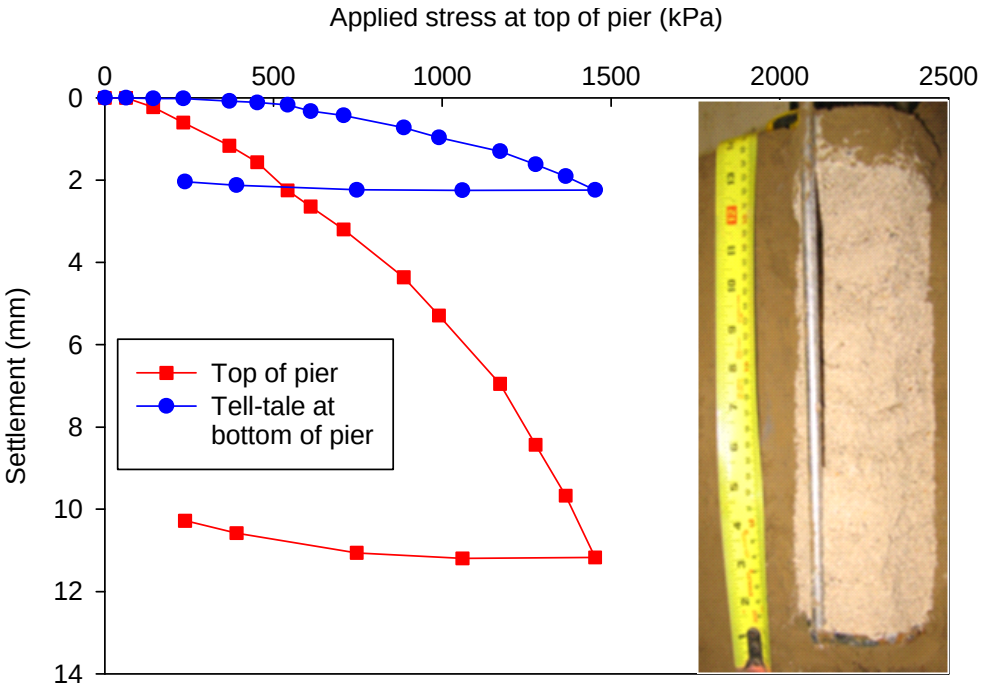

(a)

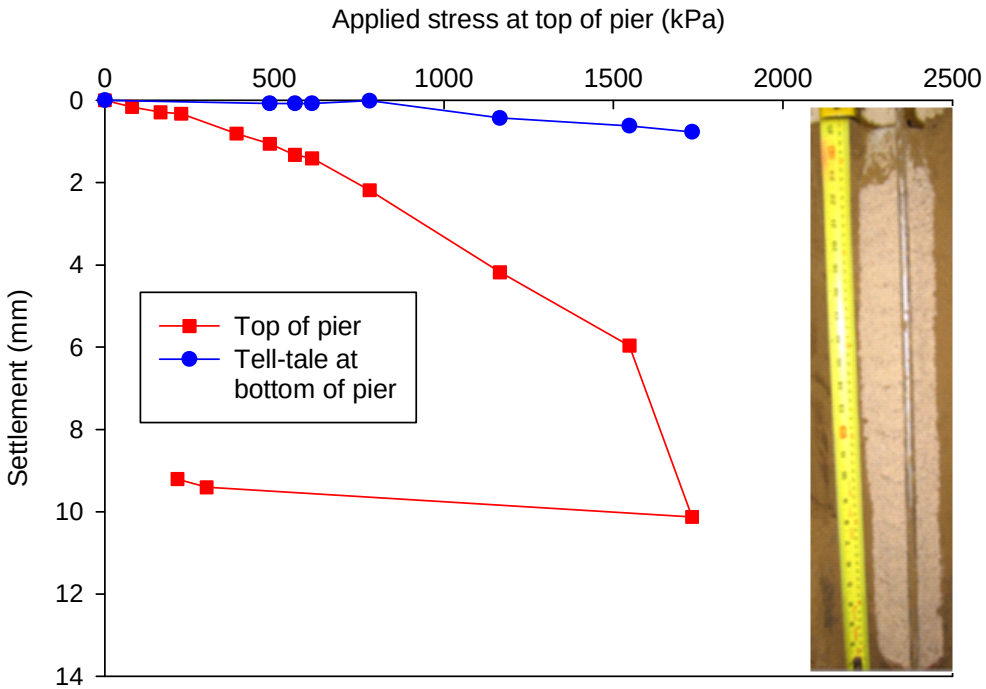

(b)

Figure 60: Stress-settlement test results (a) for 305 mm long aggregate piers and (b) for 610 mm long aggregate piers

www.manaraa.com

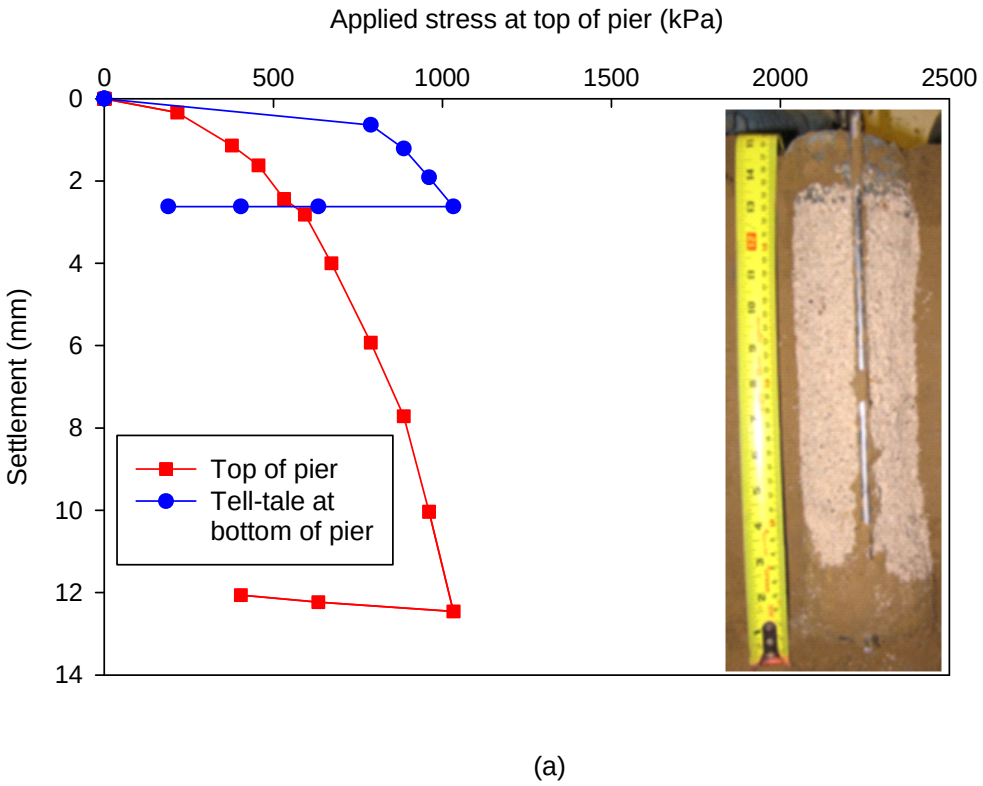

(a)

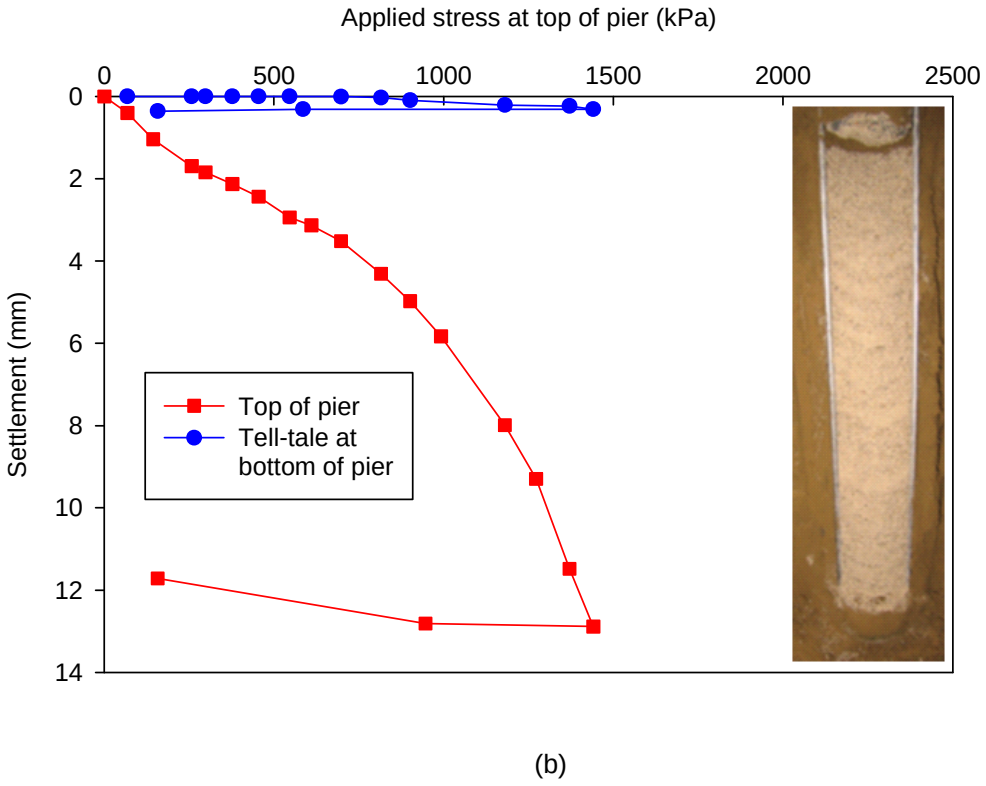

(b)

Figure 61: Stress-settlement test results (a) for 305 mm and (b) for 610 mm long aggregate piers with cemented bulb

www.manaraa.com

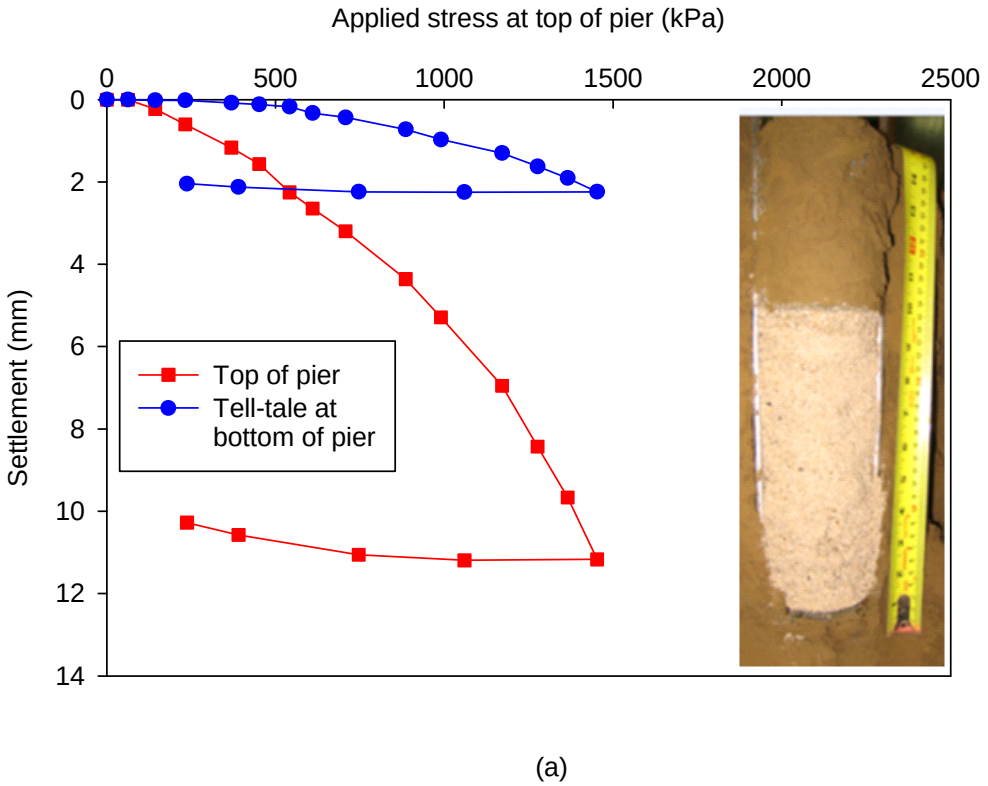

(a)

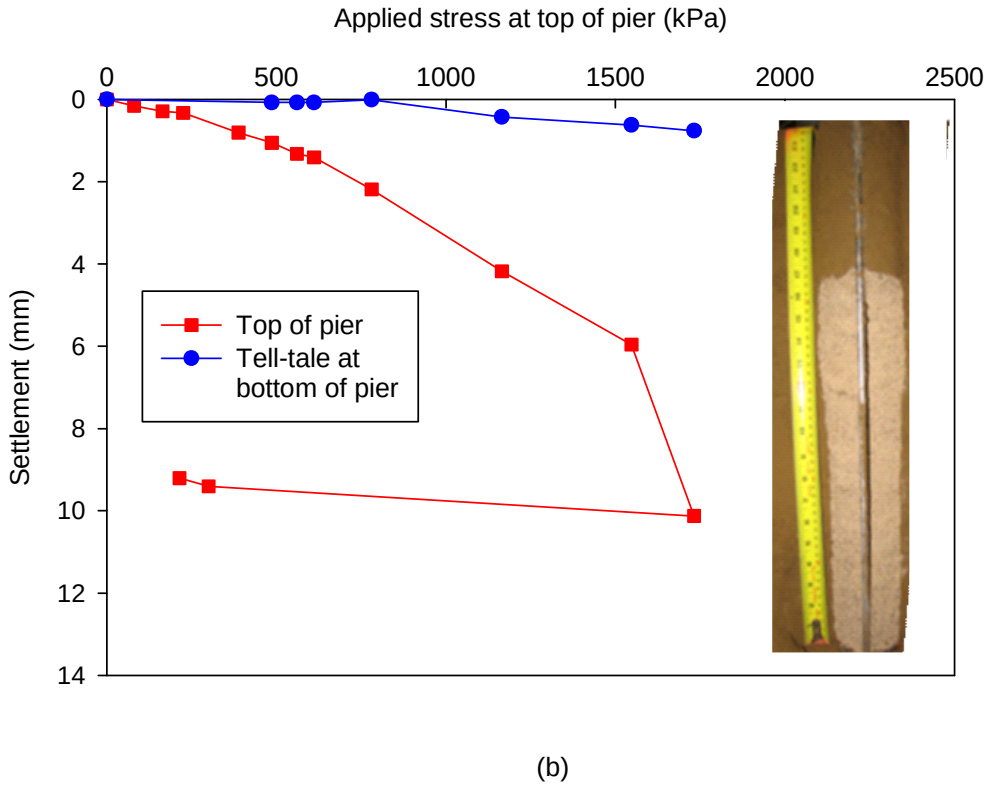

(b)

Figure 62: Stress-settlement test results (a) for 305 mm and (b) for 610 mm long aggregate piers with cemented top 100 mm.

www.manaraa.com

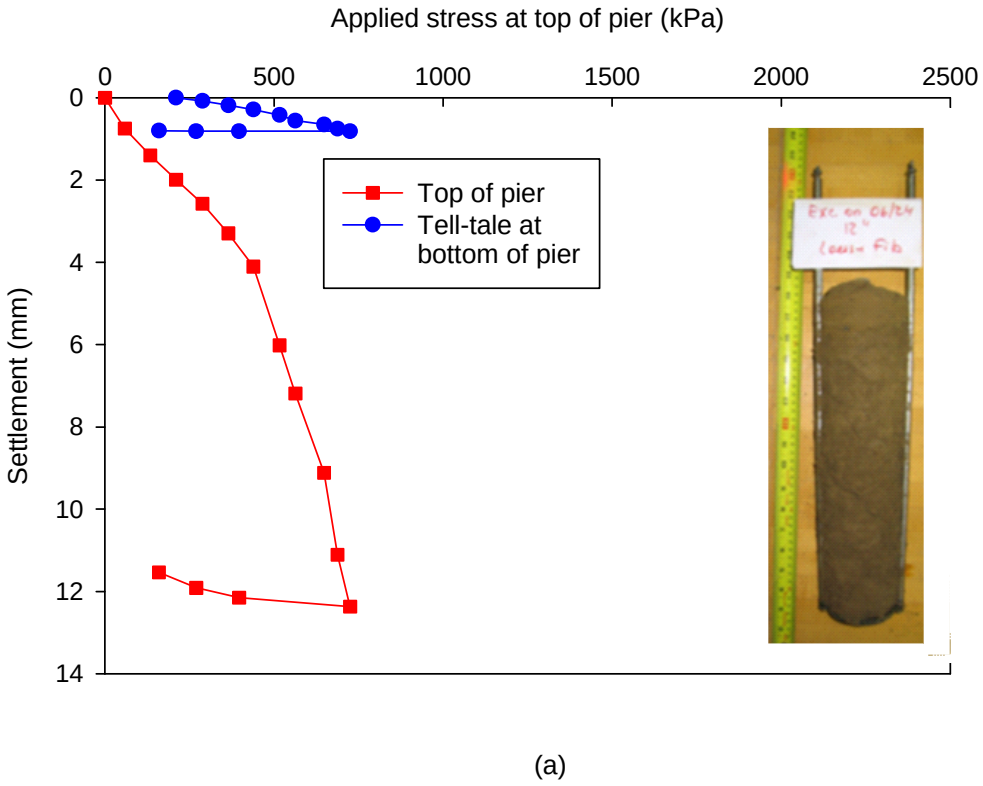

(a)

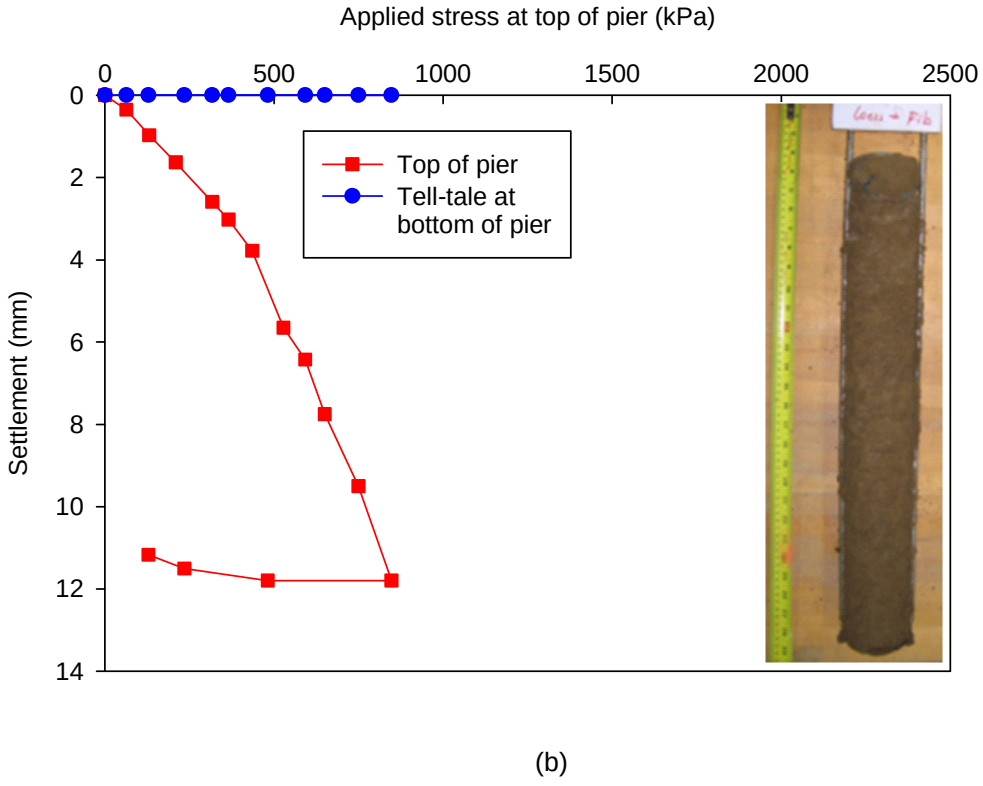

(b)

Figure 63: Stress-settlement test results (a) for 305 mm and (b) for 610 mm long piers composed of loess and fibers

www.manaraa.com

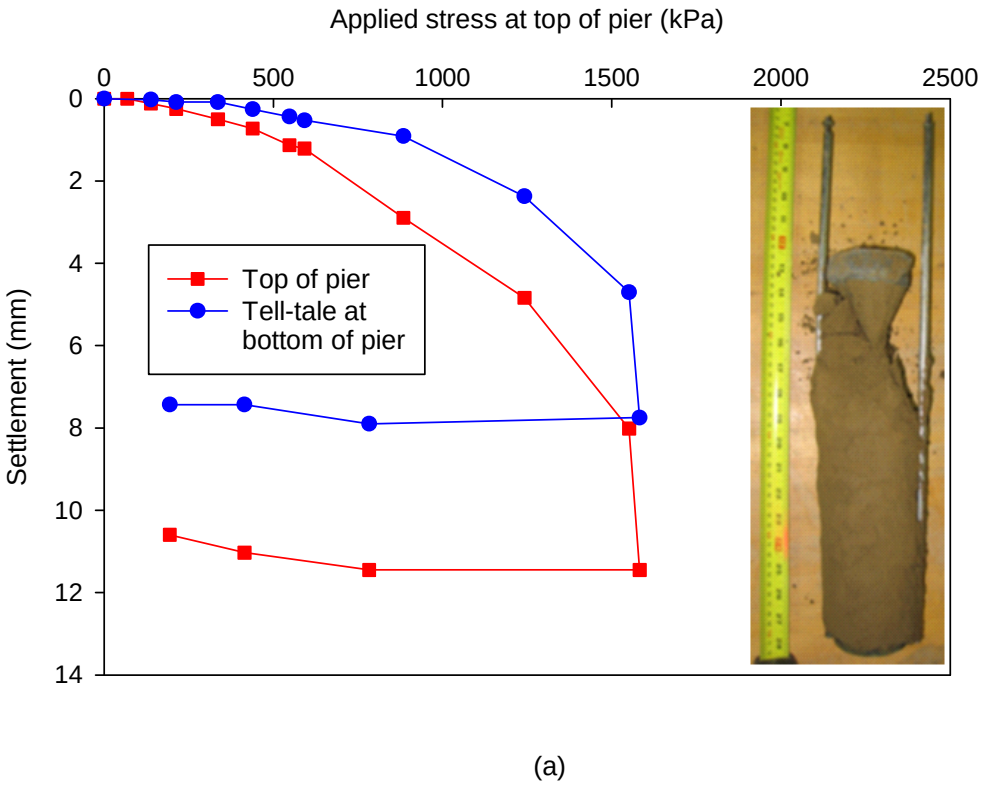

(a)

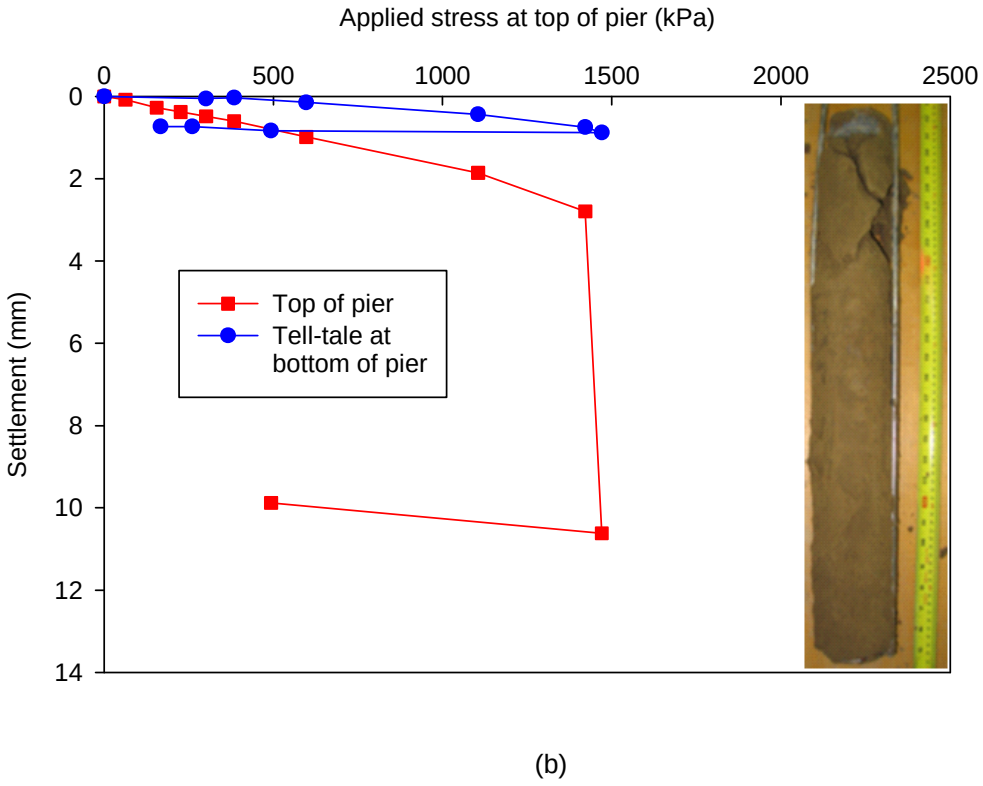

(b)

Figure 64: Stress-settlement test results (a) for 305 mm and (b) for 610 mm long piers composed of loess and cement

www.manaraa.com

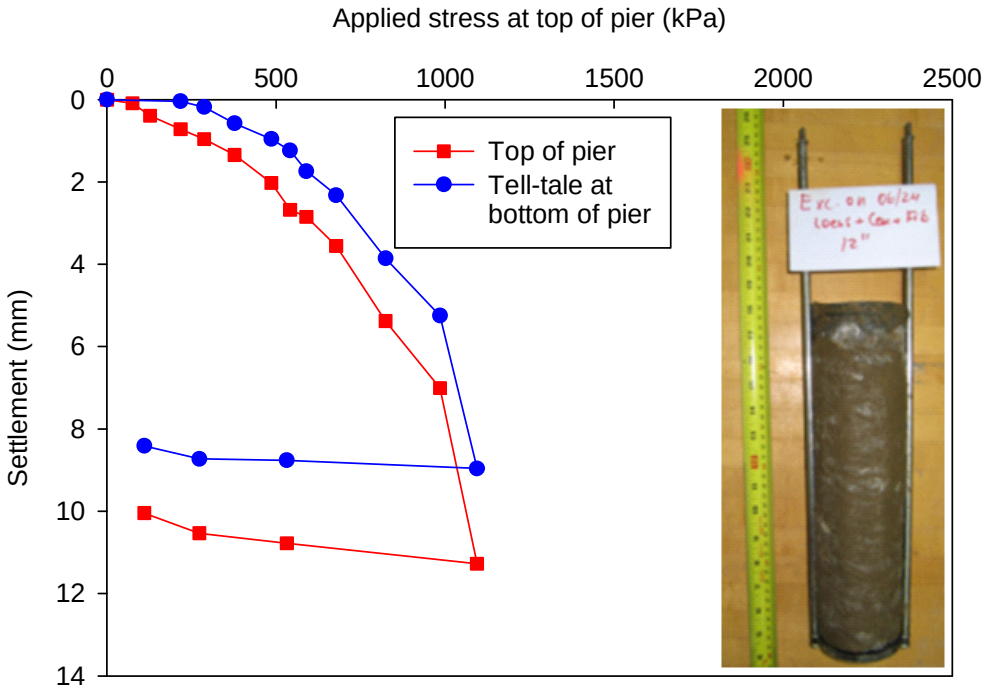

(a)

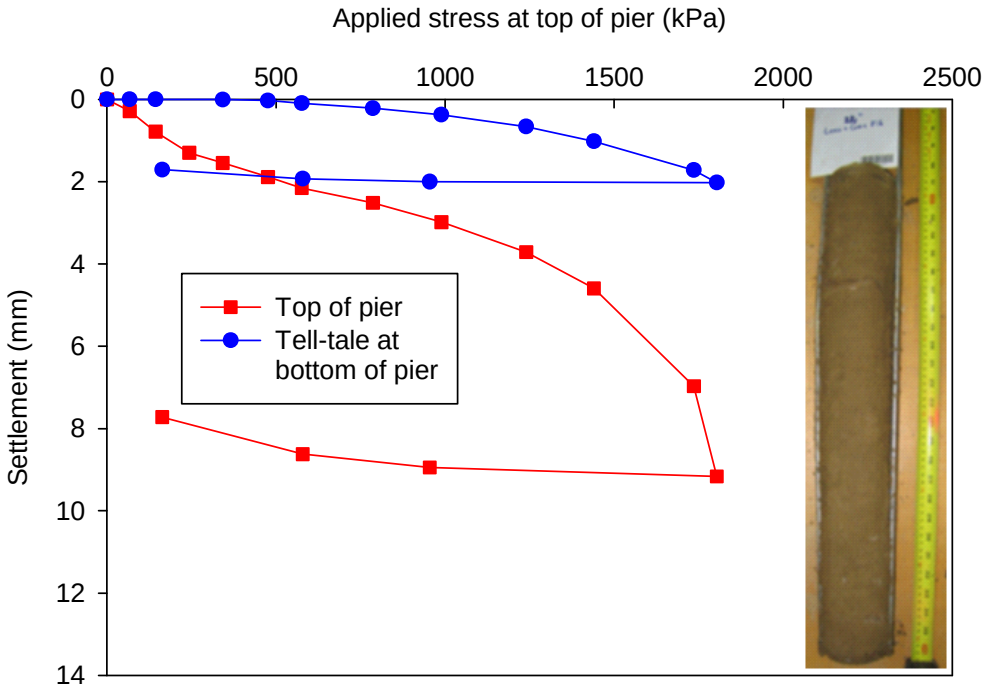

(b)

Figure 65: Stress-settlement test results (a) for 305 mm and (b) for 610 mm long piers composed of loess, cement and fibers

www.manaraa.com

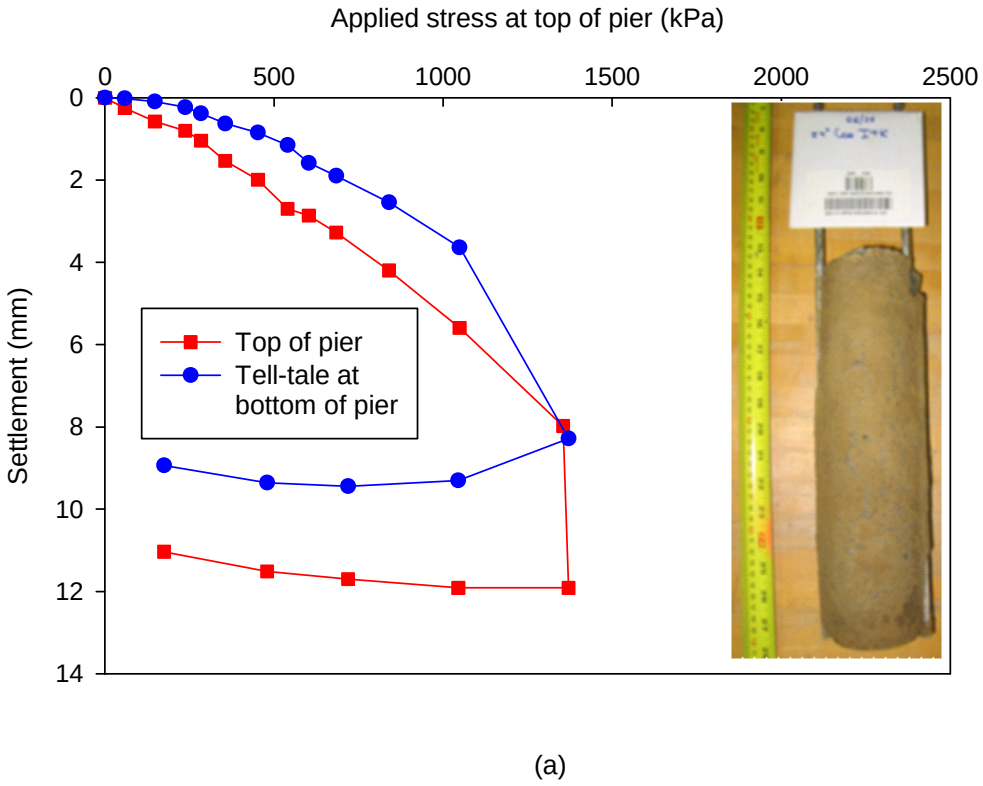

(a)

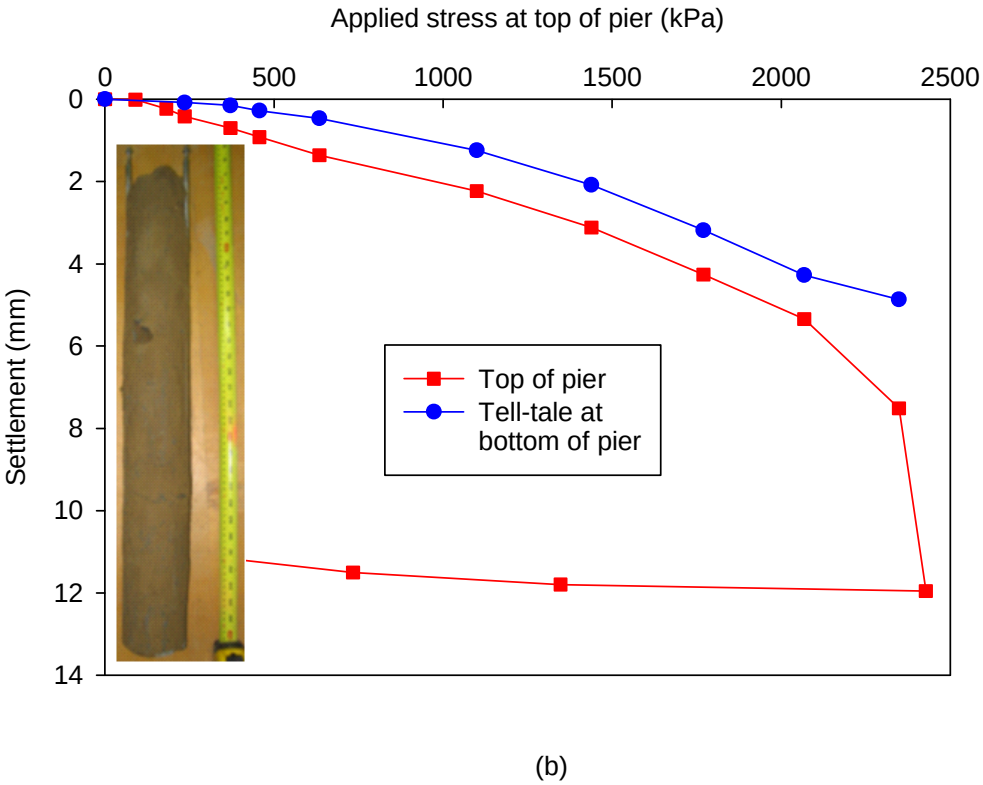

(b)

Figure 66: Stress-settlement test results (a) for 305 mm and (b) for 610 mm long piers composed of cement type I and K

www.manaraa.com

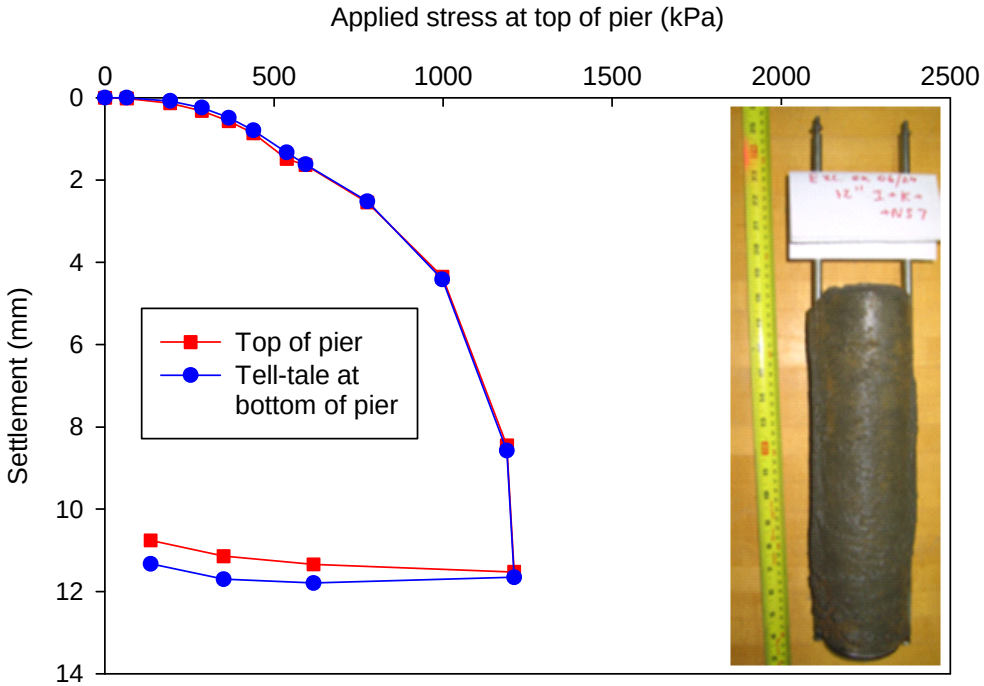

(a)

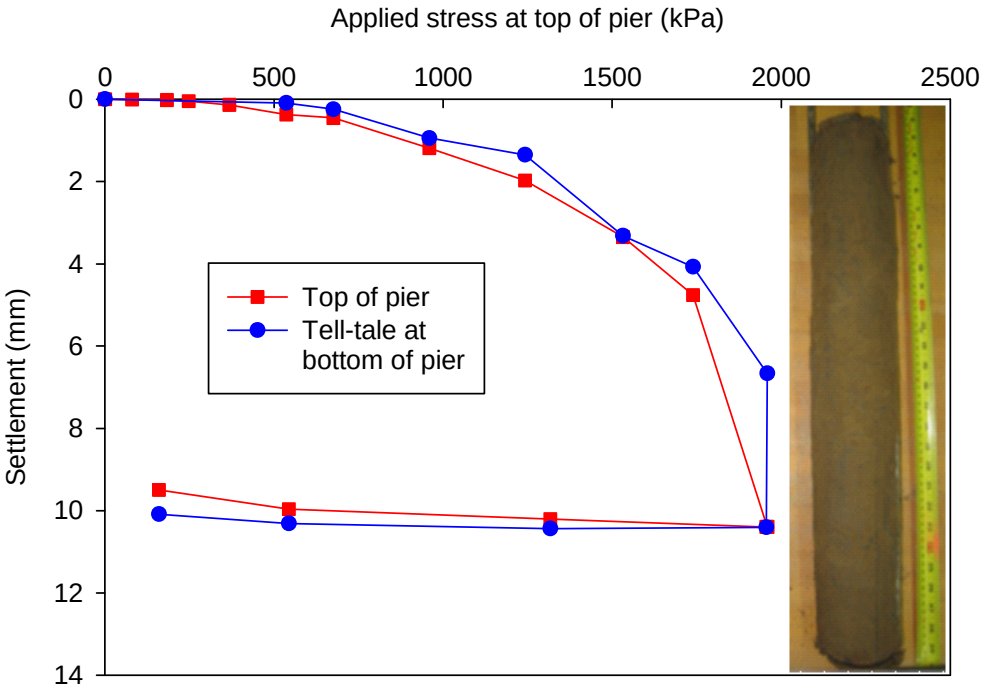

(b)

Figure 67: Stress-settlement test results (a) for 305 mm and (b) for 610 mm long piers composed of cement type I, K and NS7

www.manaraa.com

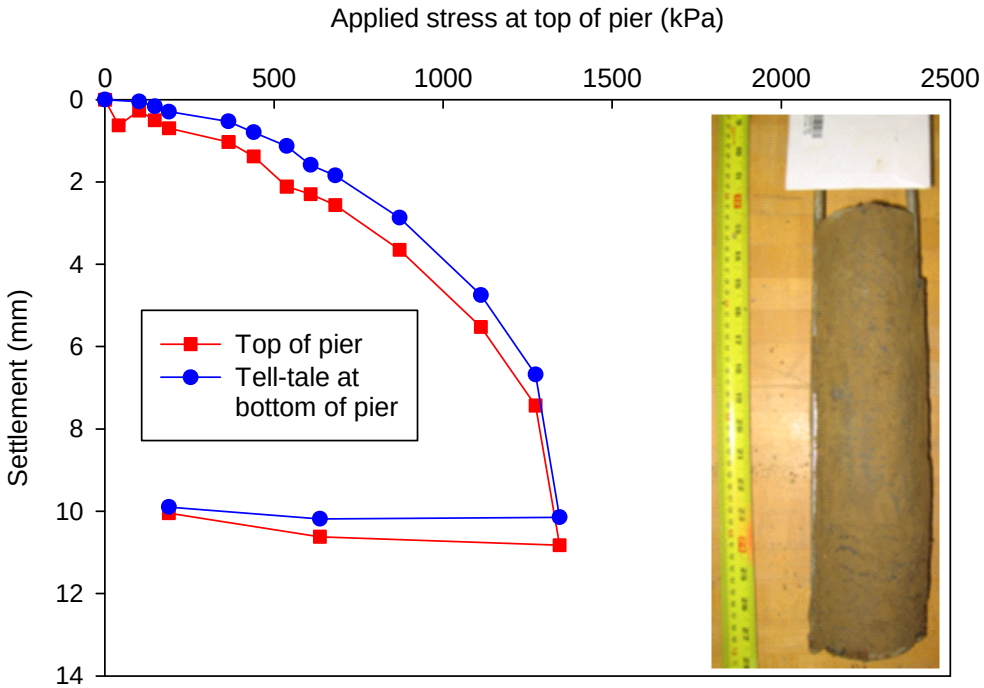

(a)

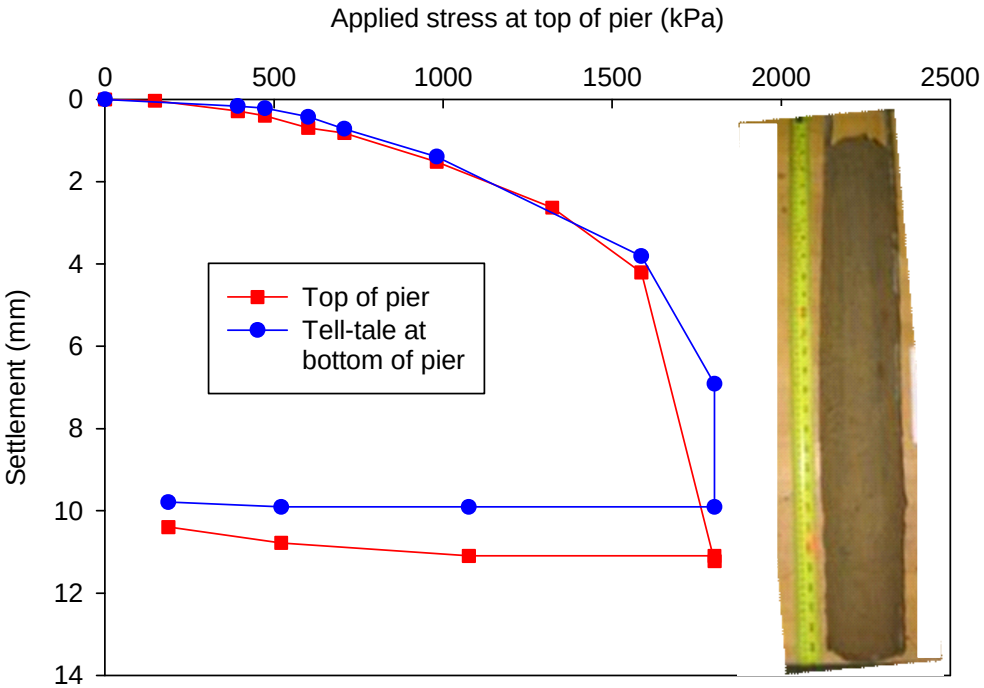

(b)

Figure 68: Stress-settlement test results (a) for 305 mm and (b) for 610 mm long piers composed of cement type I and NS7

www.manaraa.com

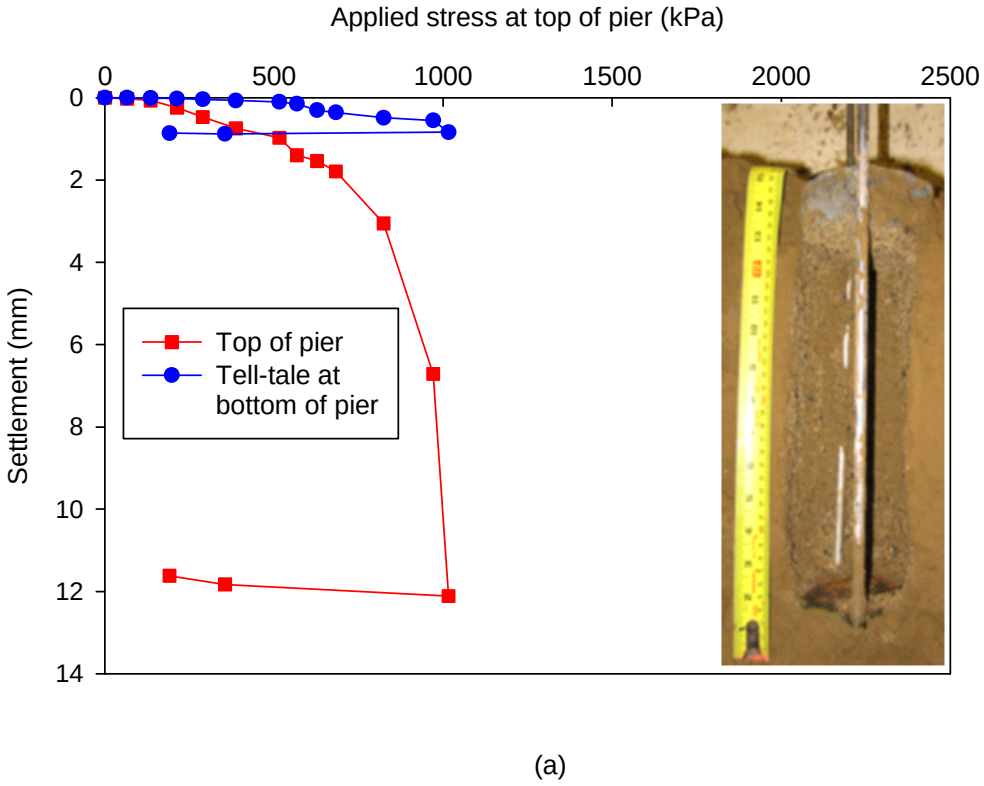

(a)

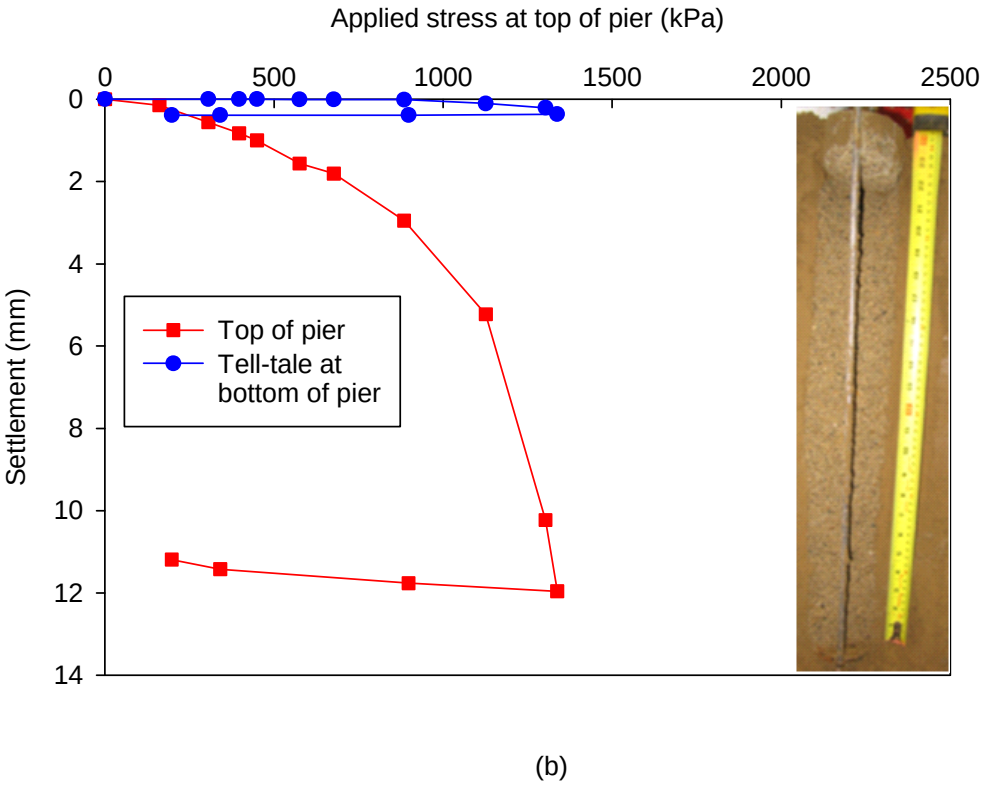

(b)

Figure 69: Stress-settlement test results (a) for 305 mm and (b) for 610 mm long piers composed of sand

www.manaraa.com

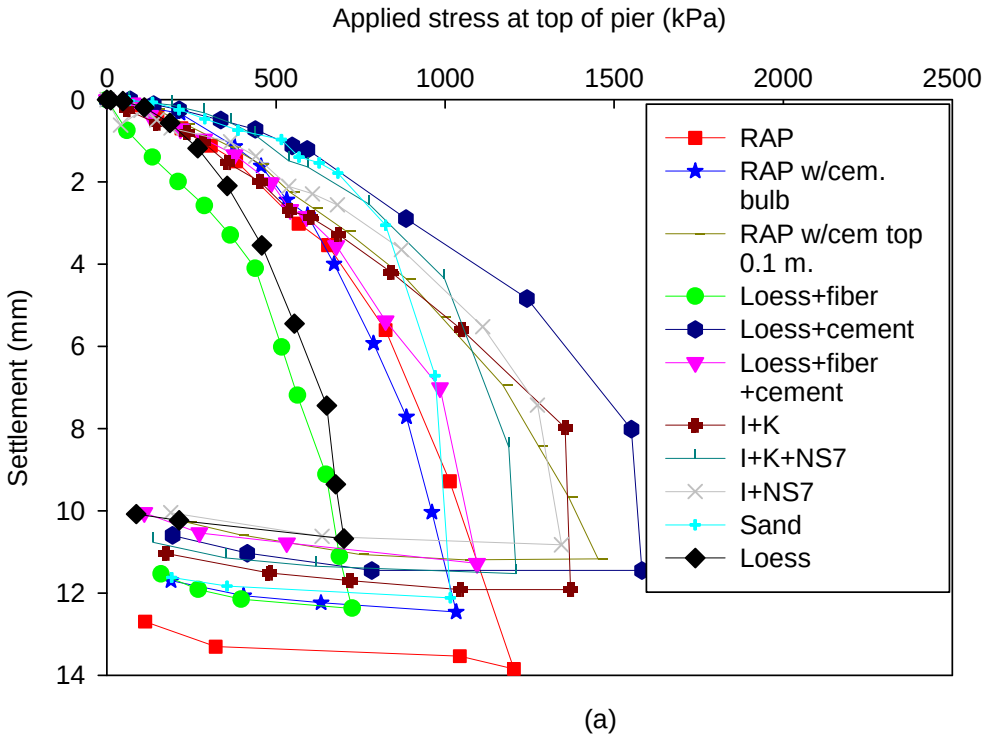

(a)

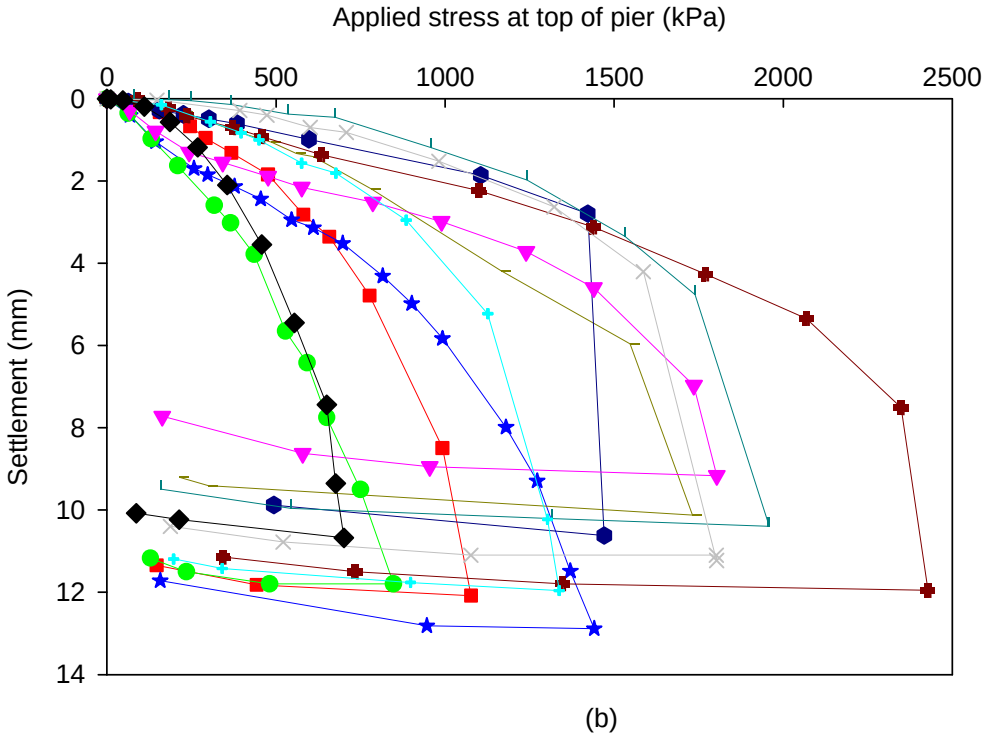

(b)

Figure 70: Overall stress-settlement test results for all (a) 305 mm and (b) 610 mm long single piers of various composition

www.manaraa.com

The stress-settlement plots constructed in Figure 59 through Figure 70 were used to obtain pier stiffness, stiffness and top and bottom displacement information provided in Table 24.

Table 24: Stress, stiffness and deflection comparison measurements for load test results for single piers of various mixes

Pier type[2]	Length (mm)	*k* at δ_{top} = 2 mm (kPa/mm)	σ at δ_{top} = 2 mm (kPa)	σ at δ_{top} = 5 mm (kPa)	σ at δ_{top} = 10 mm (kPa)	$\delta_{tell\text{-}tale}$ at δ_{top} = 10 mm (mm)	Ratio $\delta_{tell\text{-}tale}$ / δ_{top} at δ_{top} = 10 mm
Aggregate Pier Truncated Cone	305	222	443	774	1,044	0.75	0.08
	610	247	494	789	1,028	0.08	0.01
Aggregate Pier w/cem. bulb	305	246	491	732	960	0.22	0.02
	610	170	341	904	1,304	1.90	0.19
Aggregate Pier w/ cem. top	305	254	509	958	1,385	2.00	0.20
	610	370	740	1,341	1,726	0.76	0.08
Loess + fiber	305	105	211	475	667	0.70	0.07
	610	125	251	496	771	0.00	0.00
Loess + cement	305	364	729	1,258	1,570	6.46	0.65
	610	576	1,153	1,436	1,467	0.74	0.07
Loess + fiber + cement	305	241	483	794	1,062	7.85	0.79
	610	259	518	1,491	1,804	2.03[1]	0.20
C(1) + C(K)	305	227	453	960	1,363	6.03	0.60
	610	488	975	1,974	2,393	4.61	0.46
C(1) + C(K) + NS7	305	333	667	1,028	1,200	10.13	1.01
	610	624	1,247	1,749	1,944	6.49	0.65
C(1) + NS7	305	261	523	1,044	1,327	9.31	0.93
	610	565	1,130	1,611	1,765	6.38	0.64
Sand	305	353	707	902	998	0.73	0.07
	610	356	712	1,103	1,295	0.20	0.02
Loess	—	173	347	521	689	—	—

Legend:
[1]no 10 mm reading, maximum top of pier deflection 9.13 mm
[2]all scaled piers were constructed using truncated cone beveled tamper head
k - stiffness modulus (kPa/mm)
δ_{top} - deflection at the top of the pier (mm)
$\delta_{tell\text{-}tale}$ - deflection at the bottom of the pier (mm)
σ – stiffness of the pier (kPa)
Ratio δ_{top} / $\delta_{tell\text{-}tale}$ = 10mm / $\delta_{tell\text{-}tale}$

Conversions:
1 m = 3.3 ft
1 mm = 0.0394 in
1 kPa = 0.145 psi
1 kg/m^3 = 0.0624 pcf

Evaluation of the information collected from the stress-settlement plots was performed on the basis of service and ultimate load conditions. The displacement at the top of the pier at 2 mm and 5 mm was assumed to represent the service load conditions, while 10 mm displacement was treated as a maximum or ultimate amount of settlement. The piers that were not loaded

www.manaraa.com

to the maximum displacement of 12 mm due to testing limitations were still included in Table 24, however, the ultimate amount of settlement was substituted with settlement obtained at maximum point of stress-settlement curve.

The pier stiffness modulus was calculated for each tested pier and obtained only at 2 mm top of the pier displacement. The modulus was evaluated by taking a ratio between the applied stress and corresponding 2 mm displacement:

Equation 18: Stiffness modulus

$$k = \Delta\sigma / \Delta\delta_{top} \qquad \textit{(Equation 18)}$$

The ratio $\delta_{tell\text{-}tale} / \delta_{top}$ between top and bottom of the pier settlement values was calculated in order to interpret the amount of bulging that occurred within the tested pier. The evaluation was made at the point of failure or at ultimate load, therefore, the top of the pier deflection δ_{top} was taken at 10 mm:

Equation 19: Top of the pier tell-tale deflection ratio

$$Ratio = \delta_{tell\text{-}tale} / \delta_{top} = \delta_{tell\text{-}tale} / 10mm \qquad \textit{(Equation 19)}$$

Bearing Capacity

Supplemental bearing capacity calculations were also performed for the piers of different composition. Two different bearing capacity calculation approaches were taken where failure by bulging (Table 25) and failure by plunging (Table 26) mechanisms were applied.

The piers that were deemed to fail by bulging were limited to long 610 mm aggregate pier and sand pier. Due to the pier length and having the bulb portion of all 610 mm piers to be placed against a stiffer layer of soil, the plunging mechanism of failure for the non-cementitious piers was limited and the failure through shearing of the material was induced. Having the failure of long aggregate pier and sand piers to occur through shearing of the

www.manaraa.com

aggregate, the friction angle was of the essence. Aggregate pier friction angle of 44 degree was evaluated from the direct shear test as outlined in Materials Section. For the friction angle of sand material the value was assumed to be 35 degree as per Holtz and Kovacs, 1981, where the dense state of Ottawa sand friction angle was used as a reference. Densification of sand was inevitable in the process of ramming material in even size lifts inside the cavity and, therefore, the dense state of sand friction angle was selected to be used to perform calculations (details are provided in the appendix).

Table 25: Ultimate bearing capacity due to bulging failure for single piers

Pier type	H_{shaft} (mm)	$\gamma_{dry\ loess}$ (kg/m^3)	C_u (kPa)	σ_v' (kPa)	$\sigma_{r,lim}$ (kPa)	q_{ult} (kPa)
Aggregate Pier - Truncated	610	1,556	33	1.5	175	970
Aggregate Pier w/cem. bulb	COMPLICATED MECHANISM OF FAILURE					
Aggregate Pier w/cem. top 100mm.						
Loess + fiber	FAILURE BY BULGING, HOWEVER FRICTION ANGLE OF LOESS AND FIBER COMPOSITION IS UNKNOWN					
Loess + cement	BRITTLE FAILURE BY SHEARING AT TOP PORTION OF THE PIER					
Loess + fiber + cement	FAILURE BY PLUNGING					
C(I) + C(K)						
C(I) + C(K) + NS7						
C(I) + NS7						
Sand	305	1,561	35	1.5	185	683
	610	1,559	39	1.5	206	760

Legend:
$\varphi_{p\ AGGREGATE\ PIER}$ = 44°
$\varphi_{p\ sand}$ = 35°
H_{shaft} - length of the pier (mm)
$\gamma_{dry\ loess}$ - dry unit weight of matrix soil (kg/m^3)
C_u - undrained shear strength (kPa)
σ'_v - overburden stress at the bottom of the pier (kPa)
$\sigma_{r\ lim}$ - limiting radial stress (kPa)
q_{ult} - ultimate bearing capacity due to pier bulging (kPa)

Conversions:
1 m = 3.3 ft
1 mm = 0.0394 in
1 kPa = 0.145 psi
1 kg/m^3 = 0.0624 pcf

www.manaraa.com

The failure mechanism of other piers composed of cement as a main component was projected to develop through plunging, where little to no material deformation was to be observed and, therefore, no bulging deformation was to occur (Table 26). Short 305 mm aggregate pier was also subjected to failure through plunging.

Table 26: Ultimate bearing capacity due to plunging failure for single piers

Pier type	H_{shaft} (mm)	$\gamma_{dry\ loess}$ (kg/m^3)	d_{shaft} (mm)	$d_{nominal}$ (mm)	N_c	N_γ	N_q	d_f (mm)	f_s (kg/m^2)	$C_{u\ top}$ (kPa)	σ_v' (kPa)	q_{shaft} (kPa)	q_{tip} (kPa)	q_{ult} (kPa)
Aggregate Pier - Truncated	305	1,588	84	76	37	19	22	25	489	40	5	85	1,606	1,690
Aggregate Pier w/cem. bulb	305	COMPLICATED MECHANISM OF FAILURE												
Aggregate Pier w/cem. top 100mm.	305													
Loess + fiber	305	FAILURE BY BULGING, HOWEVER FRICTION ANGLE OF LOESS AND FIBER COMPOSITION IS UNKNOWN												
Loess + cement	305	BRITTLE FAILURE BY SHEARING AT TOP PORTION OF THE PIER												
Loess + fiber + cement	305 610	1,517 1,554	84 84	76 76	37 37	19 19	22 22	25 25	467 889	31 37	5 9	81 307	1,266 1,596	1,347 1,903
C(I) + C(K)	305 610	1,559 1,554	76 76	76 76	37 37	19 19	22 22	25 25	480 889	41 41	5 9	75 279	1,639 1,744	1,715 2,023
C(I) + C(K) + NS7	305 610	1,512 1,572	76 76	76 76	37 37	19 19	22 22	25 25	466 900	35 44	5 9	73 273	1,413 1,858	1,486 2,140
C(I) + NS7	305 610	1,564 1,613	78 76	76 76	37 37	19 19	22 22	25 25	482 923	44 43	5 10	76 290	1,751 1,826	1,827 2,116
Sand	305	FAILURE BY BULGING												
Loess	—	1,550	—	—	37	19	22	—	—	—	—	—	—	1,460

Legend:
$\varphi_{p\ loess}$ = 30°
H_{shaft} - length of the pier (mm)
$\gamma_{dry\ loess}$ - dry unit weight (kg/m^3)
d_{shaft} - diameter of the pier * 1.1 due to bulging (mm)
$d_{nominal}$ - diameter of the pier cavity (mm)
d_f - footing depth (mm)
N_c, N_q, N_γ - Terzaghi's Bering Capacity Factors
f_s - unit friction along pier shaft
$C_{u\ top}$ - undrained shear strength (kPa)

σ'_v - overburden stress at the elevation of the pier tip (kPa)
q_{shaft} - bearing capacity due to shaft friction (kPa)
q_{tip} - bearing capacity due to tip end bearing (kPa)
q_{ult} - ultimate bearing capacity due to pier plunging (kPa)

Conversions:
1 m = 3.3 ft
1 mm = 0.0394 in
1 kPa = 0.145 psi
1 kg/m^3 = 0.0624 pcf

www.manaraa.com

Figure 71 and Figure 72 outline the tabulated data in graphical format, where Figure 71 shows the relationship between eh calculated design bearing capacity values and the bearing capacity obtained during the actual testing. The calculated design to actual bearing capacity ratio was also computed and displayed in the figure. Figure 72 shows the linear relationship between design (calculated) and actual bearing capacity values.

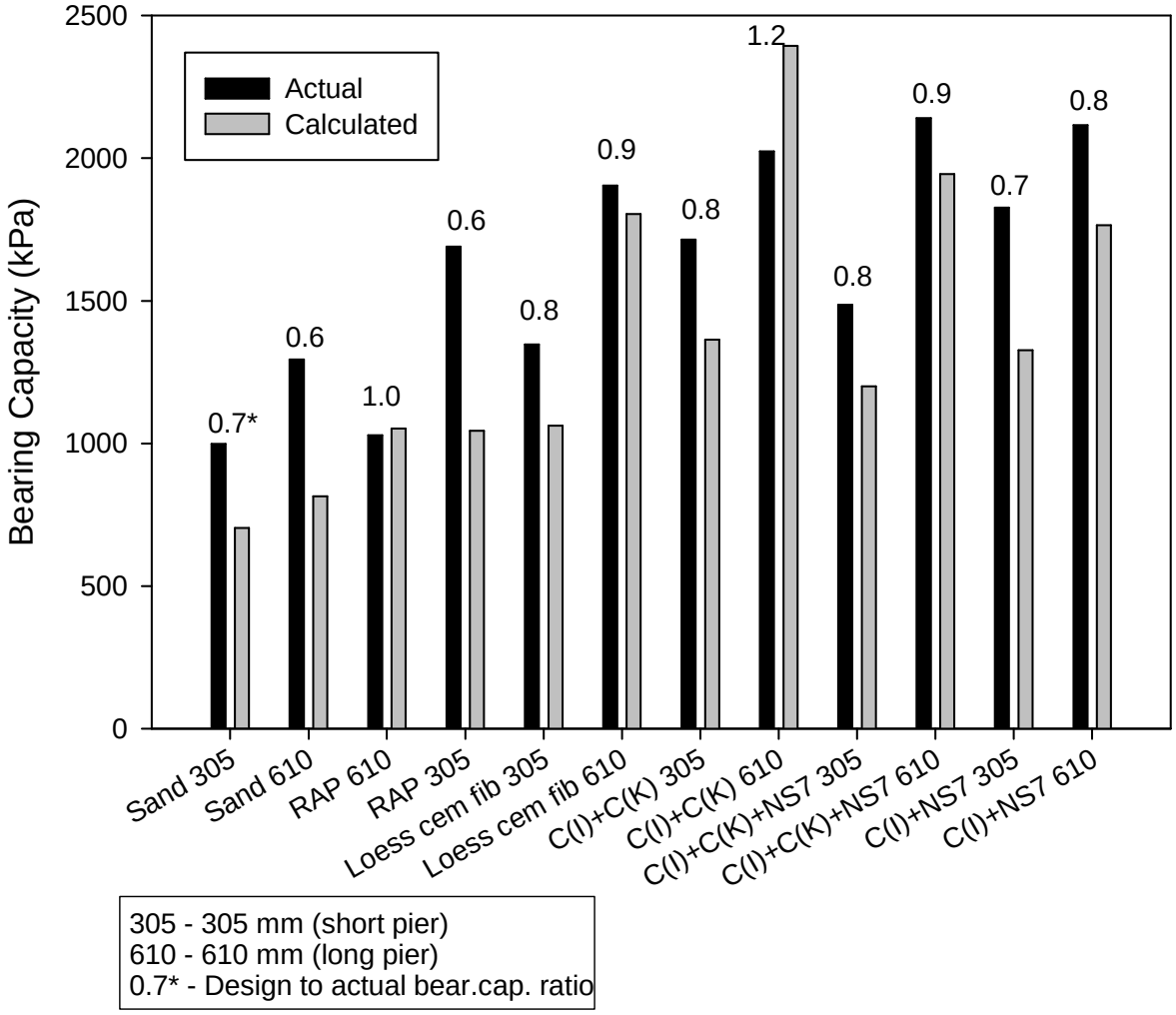

Figure 71: Calculated design versus actual bearing capacity values for single piers of various composition (bar chart)

www.manaraa.com

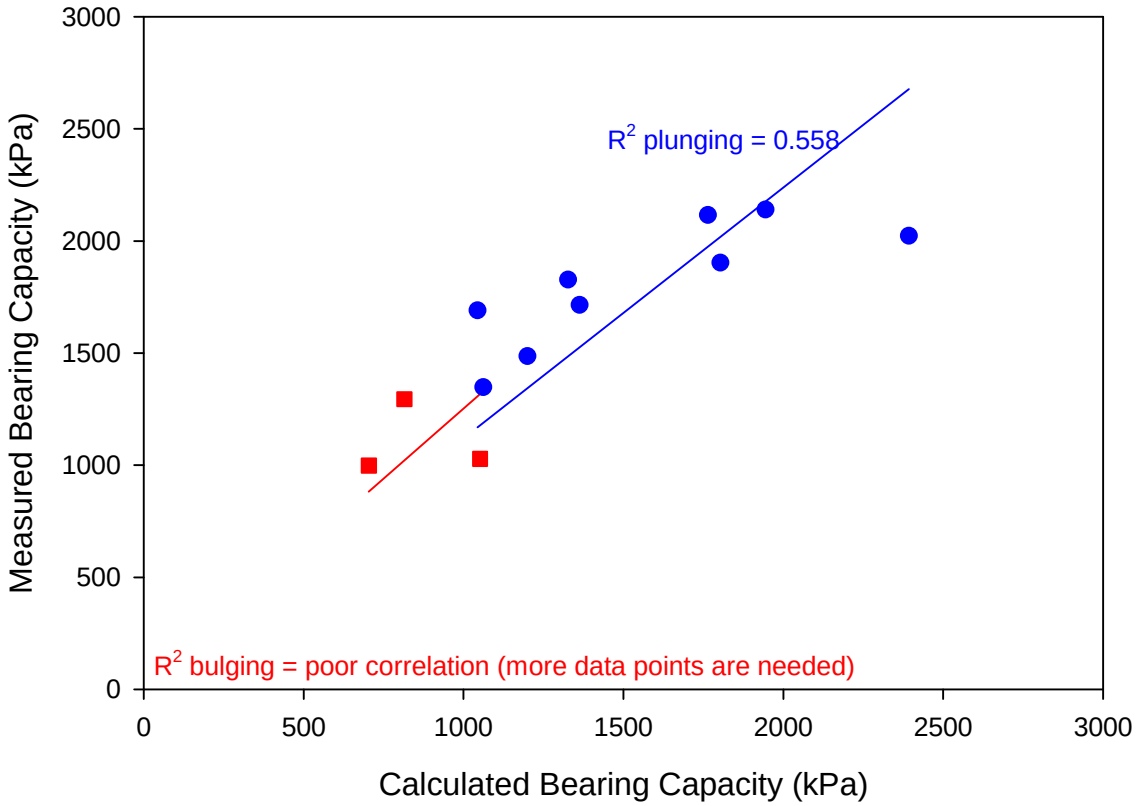

Figure 72: Calculated design versus actual bearing capacity for single piers of various composition (scatter chart)

The brittle failure of the loess and cement composition piers in the top portion of the pier induced complications to the failure mechanism that could neither be described through pure plunging or pure bulging processes. An even more complicated pier failure mechanism was also anticipated for the piers where partial cementing was performed. The bulb and top portions of the aggregate piers that were partially cemented had a unique impact on failure mechanisms by shifting the zone of bulging and, therefore, no bearing capacity evaluation was performed for these piers.

Finally, the 610 mm loess and fiber composition piers were expected to fail similarly to 610 mm aggregate pier and sand piers, i.e. through bulging, however, bearing capacity calculations were limited due to the unknown friction angle of the loess and fiber composition. Further testing could be performed through direct shear testing on a sample specimen of loess and fiber composition in order to obtain the value for the friction angle.

www.manaraa.com

Groups of Piers

Aggregate Piers - Stress-Settlement

Groups of aggregate piers were further constructed and tested in order for the group efficiency of unit cell, and groups of two, four, five and six piers to be evaluated. The stress-settlement results are provided in Figure 73 through Figure 80. The results are grouped by pier length and the summary of all stress-settlement plots is outlined in Figure 80. The stress-displacement testing was performed in a similar manner as the tests completed for single piers of different composition. However, in order to evenly distribute the load from hydraulic jack to every pier in the group several steel cover plates of various dimensions were designed and built. Unreinforced matrix soil was also loaded up to 12 mm of displacement for all the plates and an additional "Loess" curve is provided in figures. A single tell-tale plate was installed for each group of piers and the obtained amount of tip movement was considered to be representative for the entire pier group being tested.

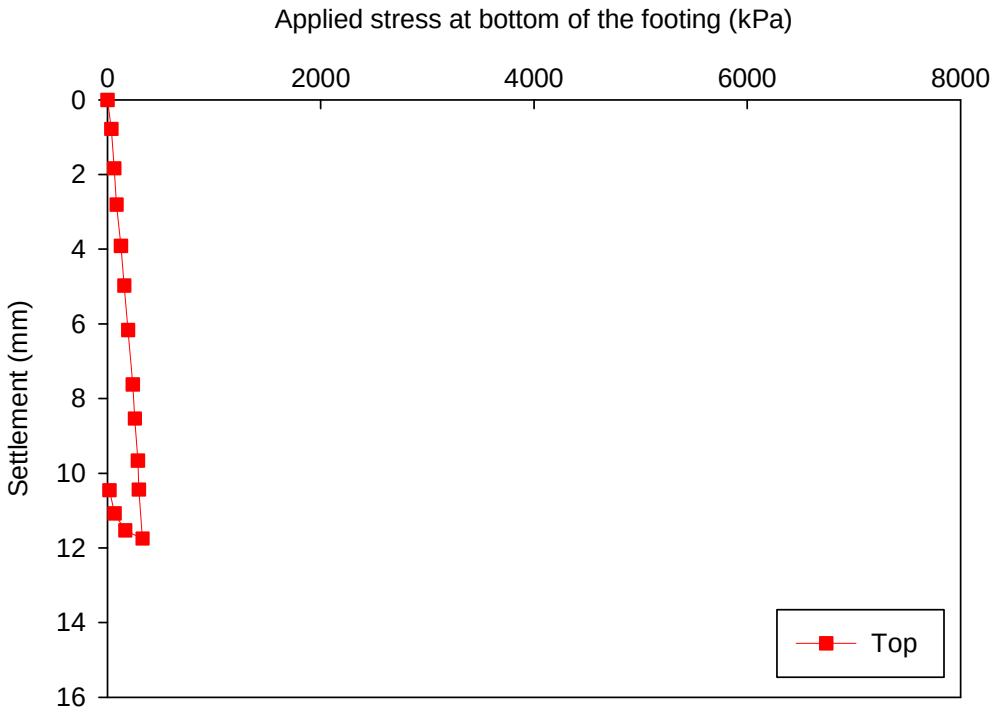

Figure 73: Stress-settlement test results for matrix soil used for placement of aggregate pier groups

www.manaraa.com

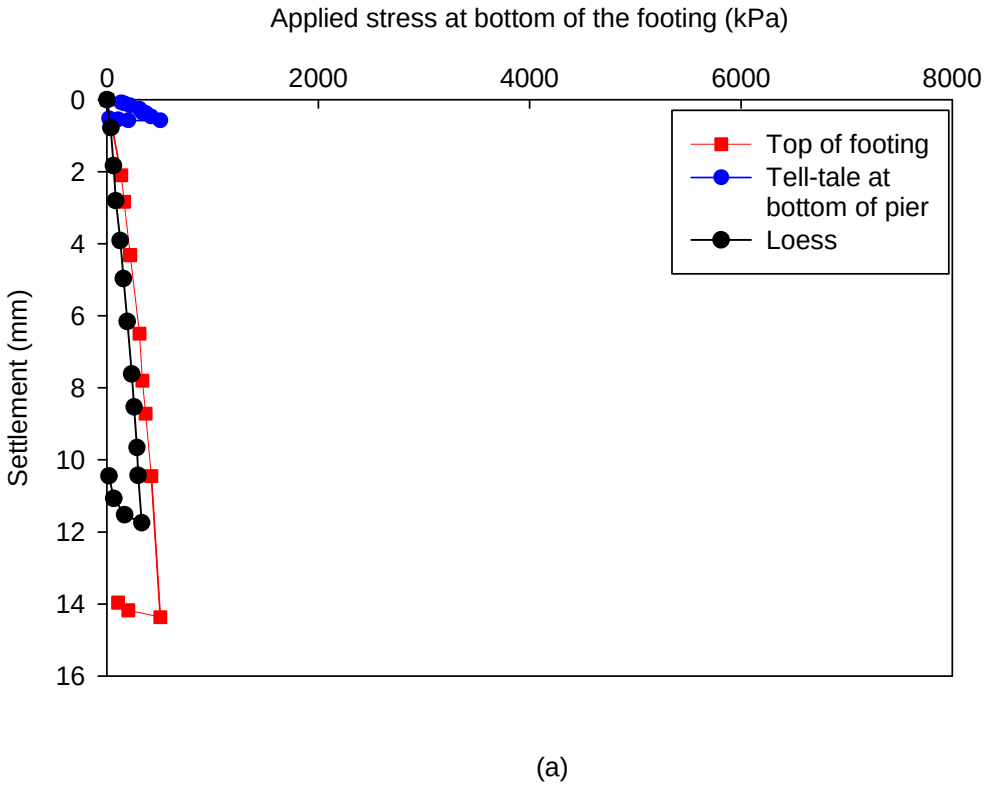

(a)

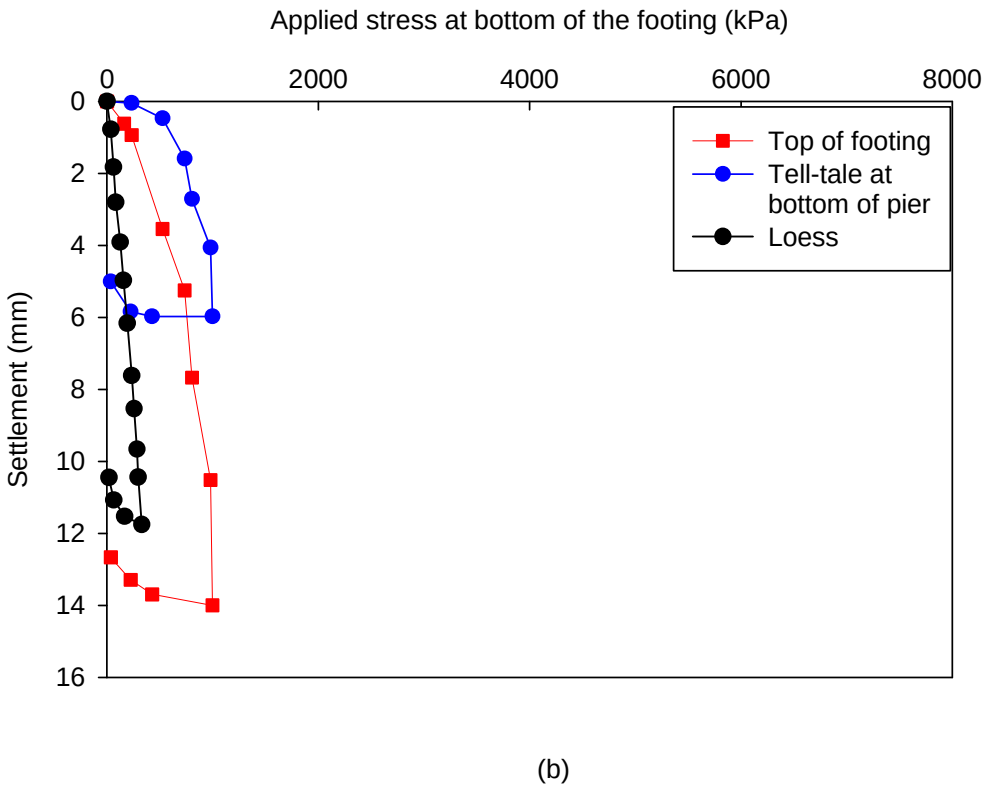

(b)

Figure 74: Stress-settlement test results (a) for 305 mm and (b) for 610 mm long single aggregate piers

www.manaraa.com

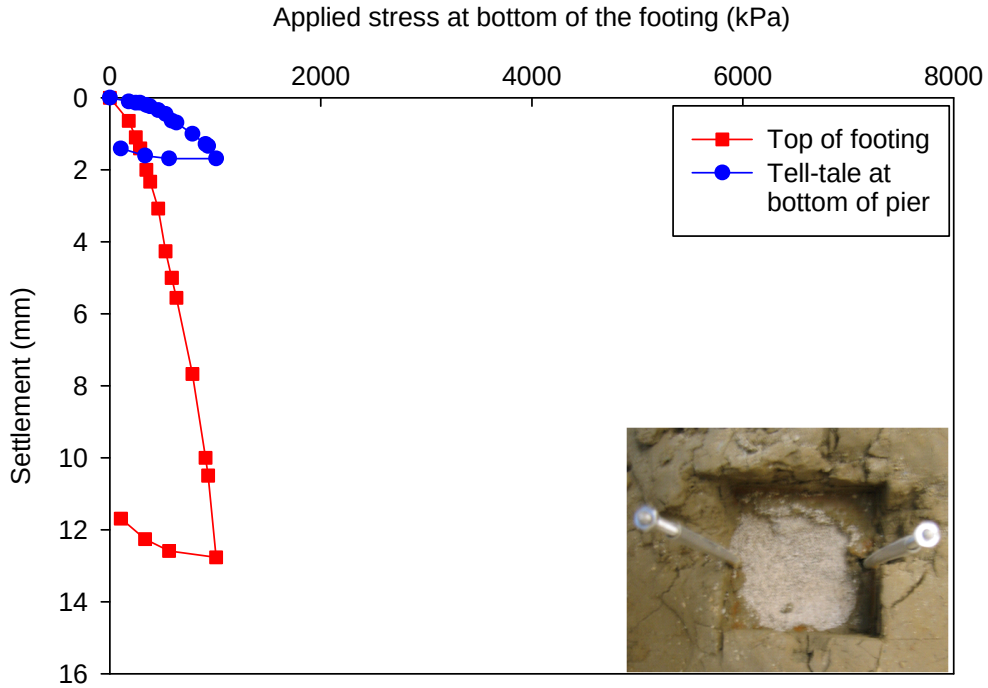

(a)

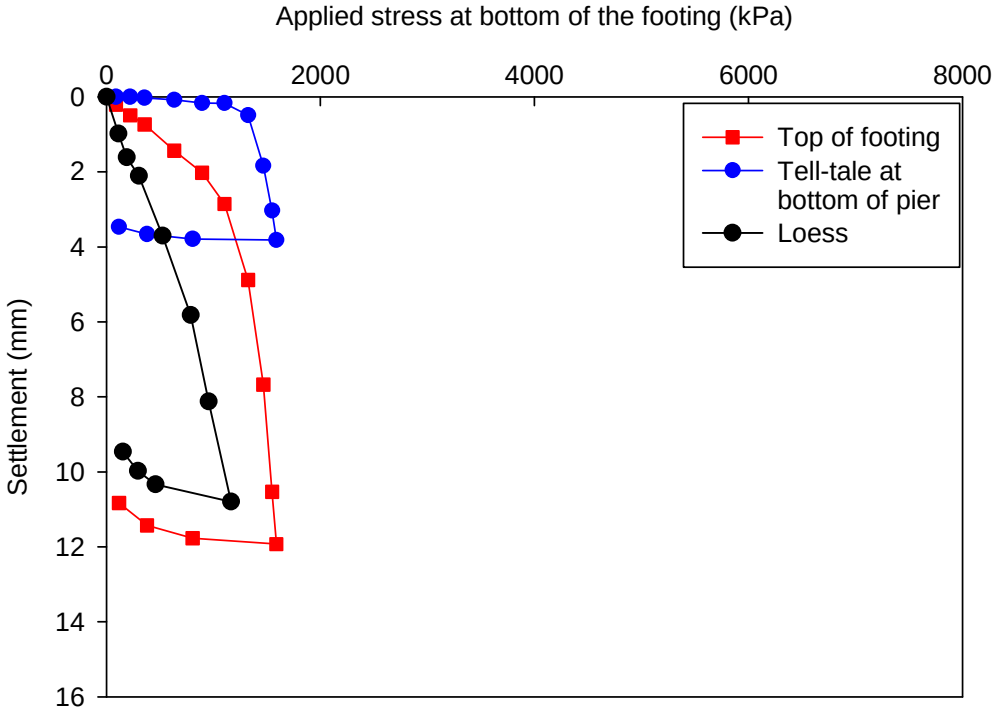

(b)

Figure 75: Stress-settlement test results (a) for 305 mm and (b) for 610 mm long aggregate piers unit cell

www.manaraa.com

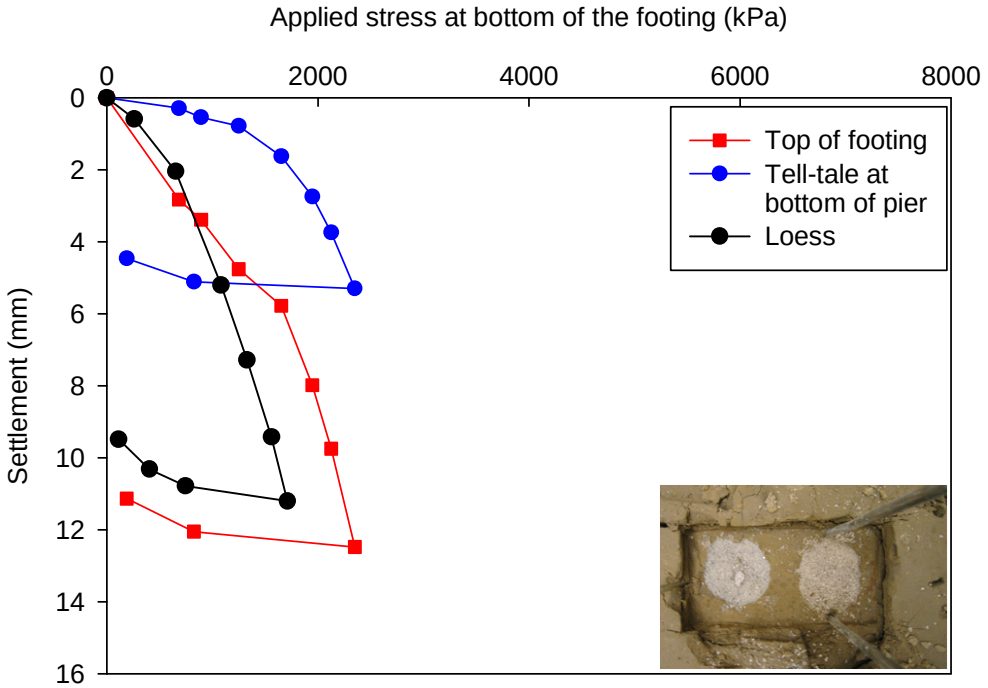

(a)

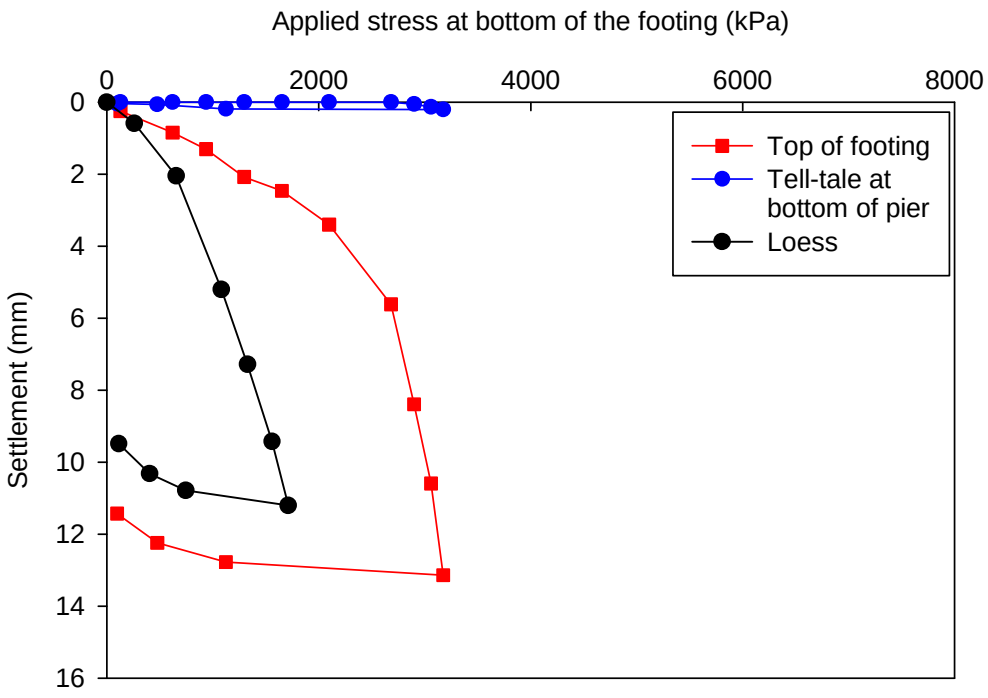

(b)

Figure 76: Stress-settlement test results(a) for 305 mm and (b) for 610 mm long groups of two aggregate piers

www.manaraa.com

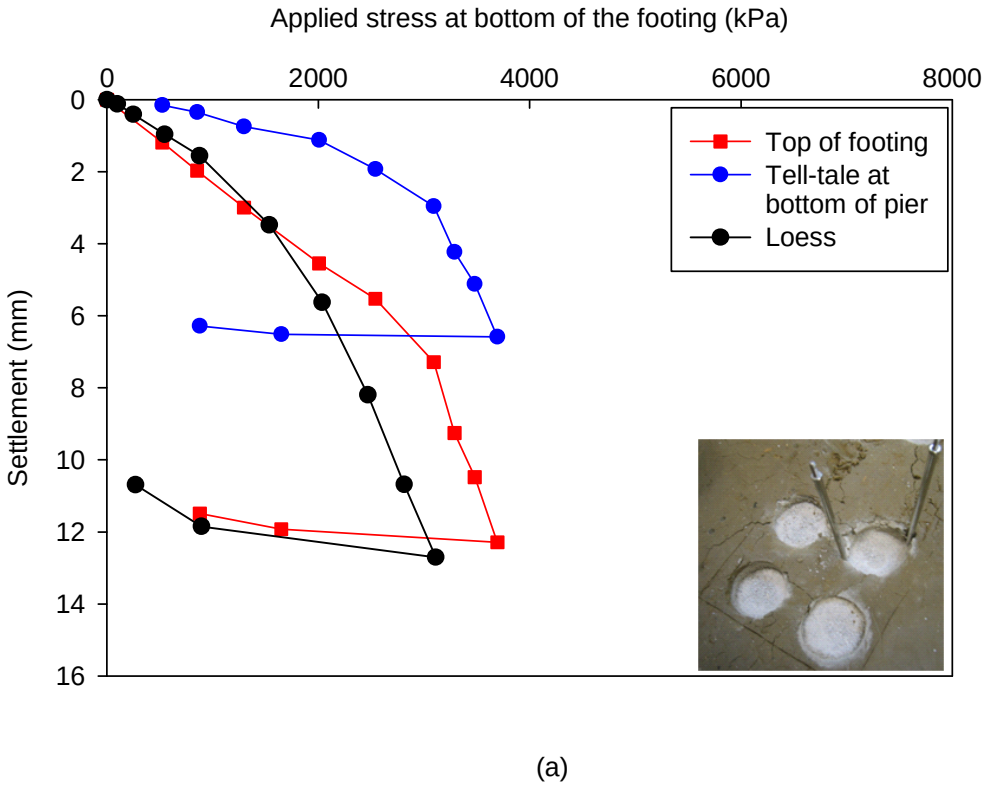

(a)

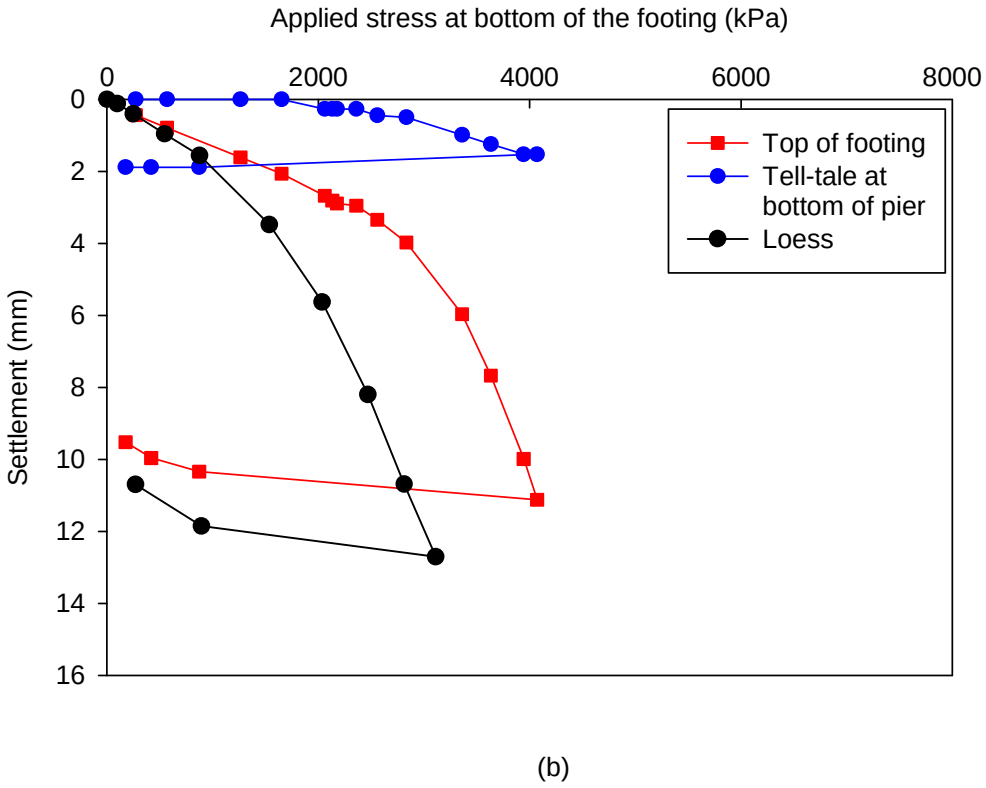

(b)

Figure 77: Stress-settlement test results (a) for 305 mm and (b) for 610 mm long groups of four aggregate piers

www.manaraa.com

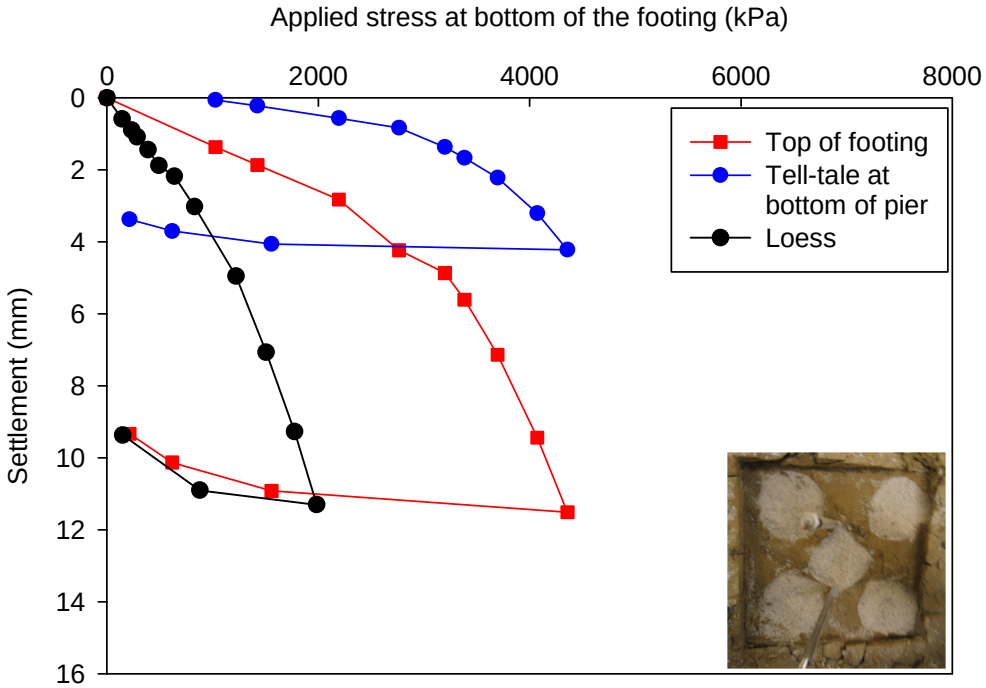

(a)

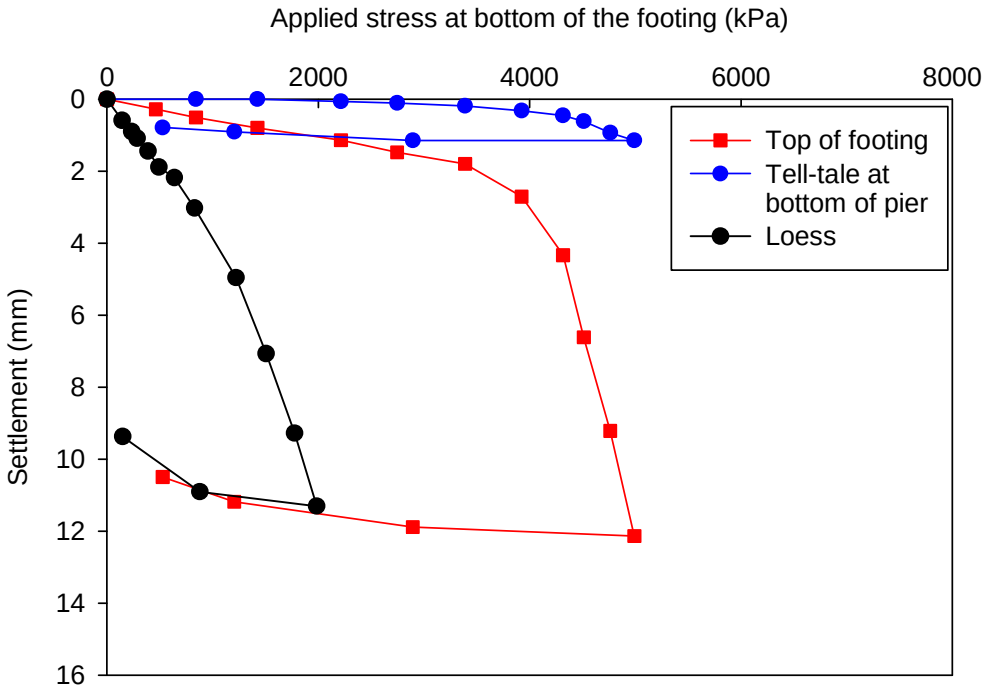

(b)

Figure 78: Stress-settlement test results (a) for 305 mm and (b) for 610 mm long groups of five aggregate piers

www.manaraa.com

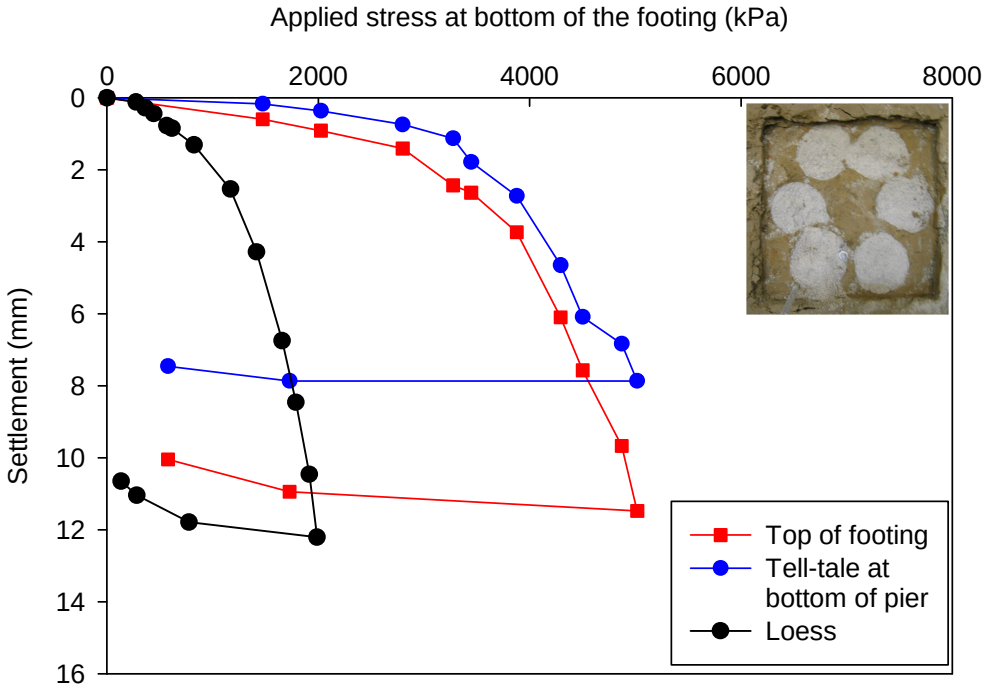

(a)

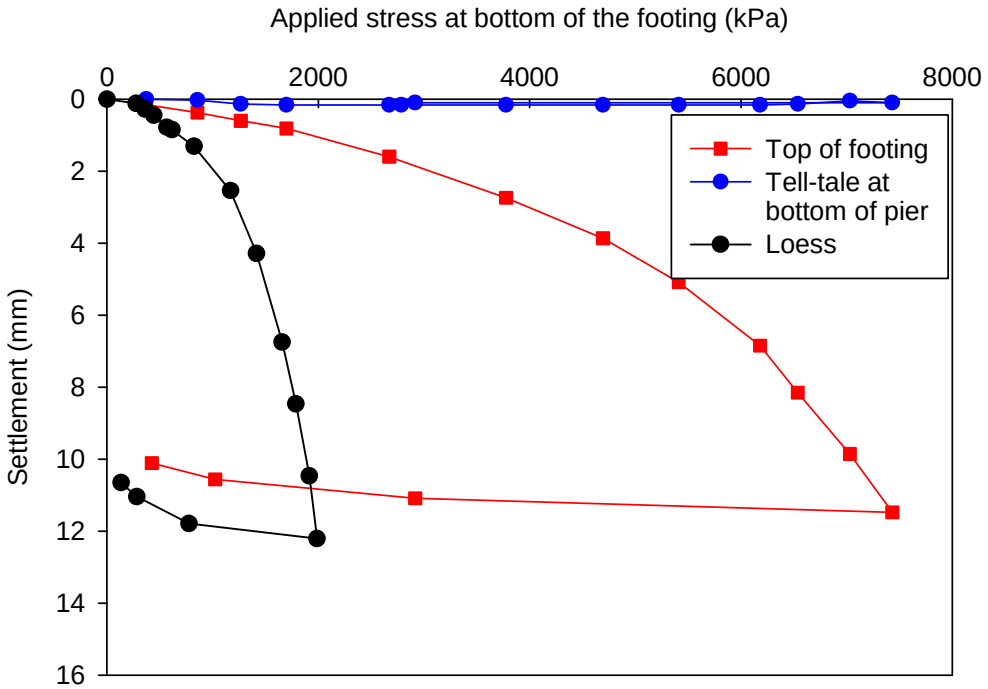

(b)

Figure 79: Stress-settlement test results (a) for 305 mm and (b) for 610 mm long groups of six aggregate piers

www.manaraa.com

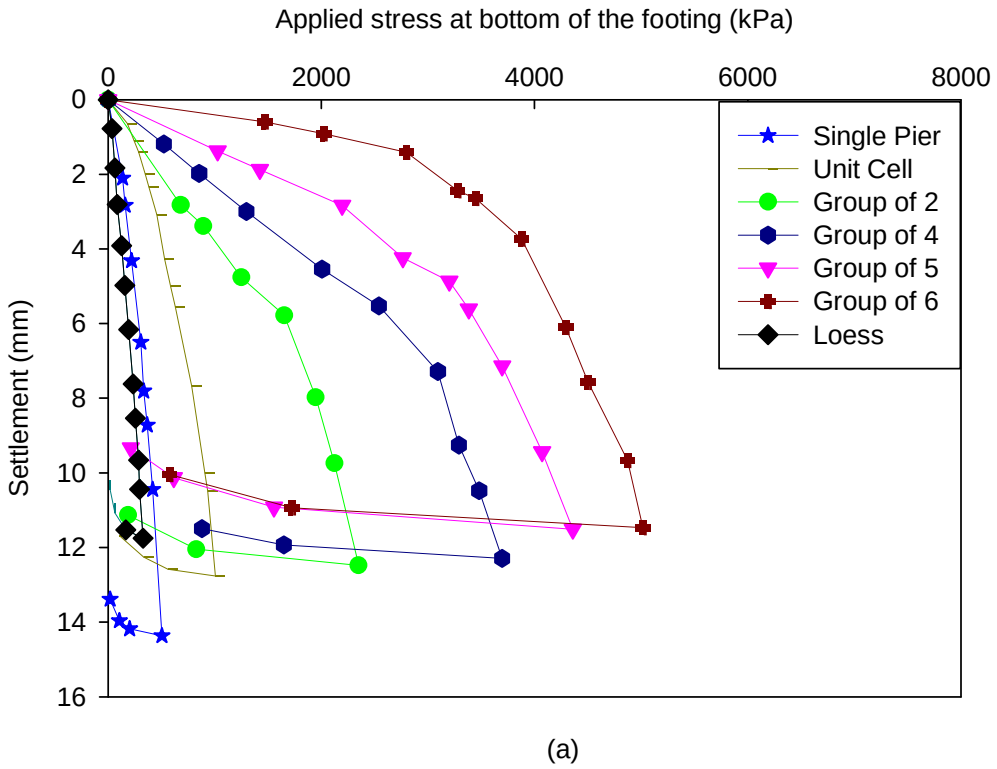

(a)

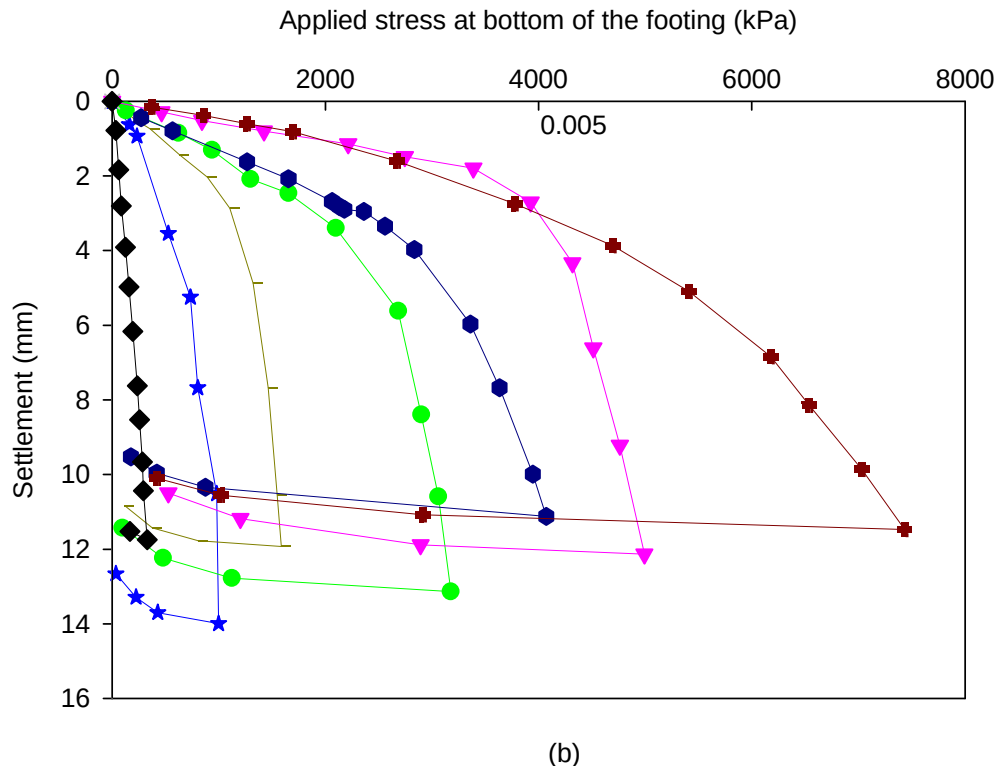

(b)

Figure 80: Overall stress-settlement test results for all (a) 305 mm and (b) 610 mm long aggregate piers

www.manaraa.com

Aggregate Piers - Group Efficiency

The group efficiency parameter was calculated for all the groups of aggregate piers and the comparison between stiffness values of a single pier and multiple piers was made. The stress, stiffness and settlement results were summarized in Table 27 and calculated per Equation 15. Sample calculations can be found in the appendix. Table 27 shows group efficiency values in terms of a single pier and Table 29 in terms of unit cell.

Table 27: Stress, stiffness and deflection comparison measurements for aggregate pier group load test results and group efficiency in comparison to a single pier

								Service load		Ultimate
Pier type[1]	Length (mm)	k at δ_{top} = 2 mm (kPa/mm)	σ at δ_{top} = 2 mm (kPa)	σ at δ_{top} = 5 mm (kPa)	σ at δ_{top} = 10 mm (kPa)	$\delta_{tell\text{-}tale}$ at δ_{top} = 10 mm (mm)	Ratio $\delta_{tell\text{-}tale}$ / δ_{top} at δ_{top} = 10 (mm)	Group Efficiency at 2mm	Group Efficiency at 5mm	Group Efficiency at 10mm
Aggregate Pier	305	64	129	247	406	0.44	0.04	1.0	1.0	1.0
Single Pier	610	176	352	704	949	3.80	0.4	1.0	1.0	1.0
Loess	-	22	67	158	285	-	-	-	-	-
Aggregate Pier	305	174	348	588	908	1.30	0.13	2.7	2.4	2.2
Unit Cell	610	441	894	1,330	1,533	2.80	0.3	2.5	1.9	1.6
Loess	-	139	278	685	1101	-	-	-	-	-
Aggregate Pier	305	241	483	1,345	2,146	3.90	0.4	1.9	2.7	2.6
Group of 2	610	630	1,260	2,521	3,017	0.40	0.04	1.8	1.8	1.6
Loess	-	321	642	1055	1609	-	-	-	-	-
Aggregate Pier	305	433	867	2,254	3,406	4.80	0.5	1.7	2.3	2.1
Group of 4	610	798	1,596	3,105	3,947	1.5	0.2	1.1	1.1	1.0
Loess	-	514	1028	1891	2719	-	-	-	-	-
Aggregate Pier	305	765	1,529	3,233	4,150	3.50	0.4	2.4	2.6	2.0
Group of 5	610	1,755	3,511	4,375	4,825	1.00	0.1	2.0	1.2	1.0
Loess	-	514	1028	1891	2719	-	-	-	-	-
Aggregate Pier	305	1,537	3,073	4,100	4,898	7.00	0.7	4.0	2.8	2.0
Group of 6	610	1,567	3,134	5,361	7,068	0.10	0.01	1.5	1.3	1.2
Loess	-	509	1018	1486	1886	-	-	-	-	-

Legend:
[1]all scaled piers were constructed using cone beveled tamper head
k – stiffness modulus (kPa/mm)
δ_{top} - deflection at the top of the pier (kPa)
$\delta_{tell\text{-}tale}$ - deflection at the bottom of the pier (mm)
σ – stiffness of the pier (kPa)
Ratio $\delta_{tell\text{-}tale}$ / δ_{top} = $\delta_{tell\text{-}tale}$ /10mm

Conversions:
1 m = 3.3 ft
1 mm = 0.0394 in
1 kPa = 0.145 psi
1 kg/m^3 = 0.0624 pcf

www.manaraa.com

The group efficiency results were calculated at service load level of 2 mm and 5 mm of top of the pier settlement. The level of group efficiency for the ultimate load at 10 mm of settlement was also calculated.

Table 28: Stress, stiffness and deflection comparison measurements for aggregate pier group load test results and group efficiency in comparison to a unit cell pier

								Service load		Ultimate
Pier type[1]	Length (mm)	k at δ_{top} = 2 mm (kPa/mm)	σ at δ_{top} = 2 mm (kPa)	σ at δ_{top} = 5 mm (kPa)	σ at δ_{top} = 10 mm (kPa)	$\delta_{tell\text{-}tale}$ at δ_{top} = 10 mm (mm)	Ratio $\delta_{tell\text{-}tale}$ / δ_{top} at δ_{top} = 10 (mm)	Group Efficiency at 2mm	Group Efficiency at 5mm	Group Efficiency at 10mm
Aggregate Pier Single Pier	305	64	129	247	406	0.44	0.04	0.4	0.4	0.4
	610	176	352	704	949	3.80	0.4	0.4	0.5	0.6
Loess	-	22	67	158	285	-	-	-	-	-
Aggregate Pier Unit Cell	305	174	348	588	908	1.30	0.13	1.0	1.0	1.0
	610	441	894	1,330	1,533	2.80	0.3	1.0	1.0	1.0
Loess	-	139	278	685	1101	-	-	-	-	-
Aggregate Pier Group of 2	305	241	483	1,345	2,146	3.90	0.4	0.7	1.1	1.2
	610	630	1,260	2,521	3,017	0.40	0.04	0.7	0.9	1.0
Loess	-	321	642	1055	1609	-	-	-	-	-
Aggregate Pier Group of 4	305	433	867	2,254	3,406	4.80	0.5	0.6	1.0	0.9
	610	798	1,596	3,105	3,947	1.5	0.2	0.4	0.6	0.6
Loess	-	514	1028	1891	2719	-	-	-	-	-
Aggregate Pier Group of 5	305	765	1,529	3,233	4,150	3.50	0.4	0.9	1.1	0.9
	610	1,755	3,511	4,375	4,825	1.00	0.1	0.8	0.7	0.6
Loess	-	514	1028	1891	2719	-	-	-	-	-
Aggregate Pier Group of 6	305	1,537	3,073	4,100	4,898	7.00	0.7	1.5	1.2	0.9
	610	1,567	3,134	5,361	7,068	0.10	0.01	0.6	0.7	0.8
Loess	-	509	1018	1486	1886	-	-	-	-	-

Legend:
[1]all scaled piers were constructed using cone beveled tamper head
k – stiffness modulus (kPa/mm)
δ_{top} - deflection at the top of the pier (kPa)
$\delta_{tell\text{-}tale}$ - deflection at the bottom of the pier (mm)
σ – stiffness of the pier (kPa)
Ratio $\delta_{tell\text{-}tale}$ / δ_{top} = $\delta_{tell\text{-}tale}$ /10mm

Conversions:
1 m = 3.3 ft
1 mm = 0.0394 in
1 kPa = 0.145 psi
1 kg/m^3 = 0.0624 pcf

Group efficiency values obtained in small-scale testing were also compared to the group efficiency parameters obtained on full-scale piers tested by different researchers and are

www.manaraa.com

presented in Table 29. Similar comparison was made for stiffness modulus parameter between the small-scale and full-scale aggregate pier groups (Table 30Table 1).

Table 29: Group efficiency comparison measurements for small and full-scale aggregate piers

	Group Efficiency			
Pier type	Small-Scale Aggregate Piers	Full-Scale Aggregate Pier	Full-Scale Aggregate Pier at loads < 150kN	Full-Scale Aggregate Pier at loads > 150kN
Group of 2	1.6-2.7			
Group of 3	-			
Group of 4	1.0-2.3	1.0	1.0	4.7
Group of 5	1.0-2.6			
Group of 6	1.2-4.0			
Reference	Present study results	Lawton and Warner, 2004	White et al., 2007	

Table 30: Stiffness modulus for small and full-scale aggregate piers

	Stiffness Modulus (kPa/mm)			
Pier type	Small-Scale Aggregate Piers	Full-Scale Aggregate Piers	Full-Scale Aggregate Piers	Full-Scale Aggregate Piers
Single Pier	176-41	80-35	220-170	
Unit Cell	441-91			
Group of 2	630-215			175-125
Group of 4	795-341	260-140		
Group of 5	1755-415		430-260	
Group of 6	1567-490			
Reference	Present study	White et al., 2007	Wissmann et al., 2007	Fox et al., 1998

Aggregate Piers - Group Bearing Capacity

Ultimate bearing capacity was measured and supplemented with additional information and calculations for pier and matrix soil areas under the footing:

www.manaraa.com

Table 31: Measured ultimate bearing capacity

Pier type	Length (mm)	A_g (m^2)	A (m^2)	R_a	q or σ at δtop = 10 mm (kPa)	σ_{loess} at δtop = 10 mm (kPa)	R_s	$q_{g\ total}$ (kPa)
Aggregate Pier Unit Cell	305	0.0046	0.0781	0.058	1,147	1,101	1.0	1,192
	610	0.0046	0.0781	0.058	1,460		1.3	1,900
Aggregate Pier Group of 2	305	0.0091	0.1490	0.061	2,400	1,609	1.5	3,475
	610	0.0091	0.1490	0.061	2,869		1.8	4,882
Aggregate Pier Group of 4	305	0.0182	0.2845	0.064	3,609	2,719	1.3	4,692
	610	0.0182	0.2845	0.064	N/A		N/A	N/A
A Aggregate Pier Group of 5	305	0.0228	0.3413	0.067	4,225	2,719	1.6	6,331
	610	0.0228	0.3413	0.067	4,630		1.7	7,531
Aggregate Pier Group of 6	305	0.0274	0.5426	0.050	4,096	1,886	2.2	8,399
	610	0.0274	0.5426	0.050	5,672		3.0	15,490

Legend:
A_g - cross sectional area of all aggregate pier elements (m^2)
A_g - area of matrix soil beneath the footing (m^2)
R_s - ratio of A_g to gross footprint area of the footing A
R_s - ratio of pier and matrix soil modulus values at δ_{top} = 10mm
q - average contact pressure at the footing bottom (kPa)

Conversions:
1 m = 3.3 ft
1 mm = 0.0394 in
1 kPa = 0.145 psi
1 kg/m^3 = 0.0624 pcf

Figure 81 shows the bearing capacity results obtained for 305 mm and 610 mm groups of four, five and single piers. The figure also outlines the bearing capacity results of full-scale groups of piers tested by other researches. The full-scale piers length is outlined in the figure.

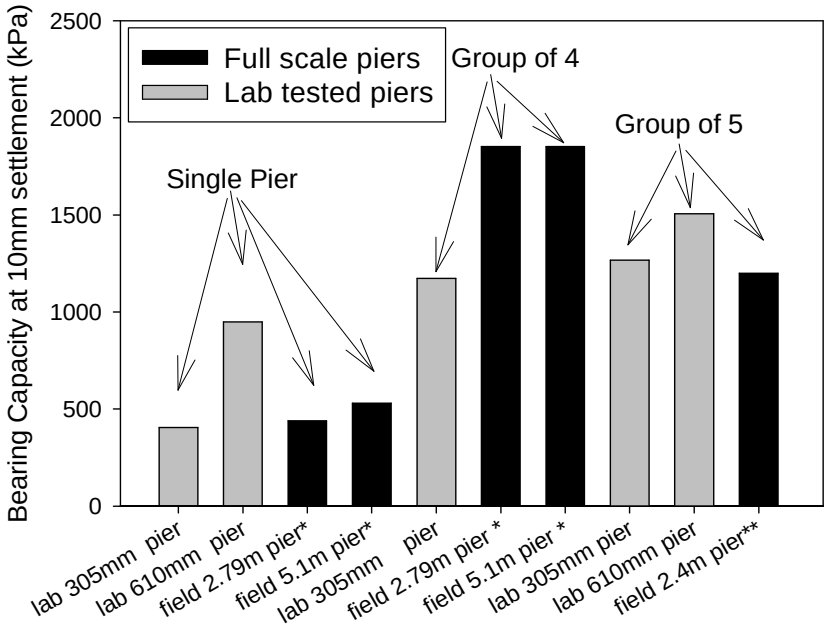

Figure 81: Bearing capacity values compared between laboratory and field tested footings (single pier, group of four and group of five footings)

www.manaraa.com

C(I) + C(K) - Stress-Settlement

Stress-settlement results for groups of cement type I and type K piers are plotted in Figure 82 through Figure 89. The testing was performed similarly tot eh testing of groups of aggregate piers.

The groups of two, four, five and six piers were tested, as well as unit cell and a single pier. All the groups of piers were constructed and tested at 305 mm and 610 mm length except for the 610 mm group of four piers, where the test was omitted and replication of the test resulted in no particular success. The replication of similar matrix soil conditions was complicated by inability to recreate same level of matrix soil compaction and moisture content.

A single tell-tale plate was installed for each group of piers. A great amount of pier movement was anticipated due to a plunging mechanism of failure. Piers were loaded to a level of 12 mm of total top of the pier displacement.

The same steel cover plates were utilized for the purpose of loading and uniform distribution of applied load. Similar to groups of aggregate piers tested in the previous stage, the plates were placed in a neatly excavated footing area and a concrete cap was poured between the plate and the piers to provide a uniform load distribution.

No load tests were performed on plates supported with unreinforced matrix soil at this stage of testing. Only single pier type of load test was performed on the unreinforced matrix soil and, therefore, no results are shown for the unreinforced unit cell, group of two, four, five and six plate stress-settlement tests on the unreinforced matrix soil.

www.manaraa.com

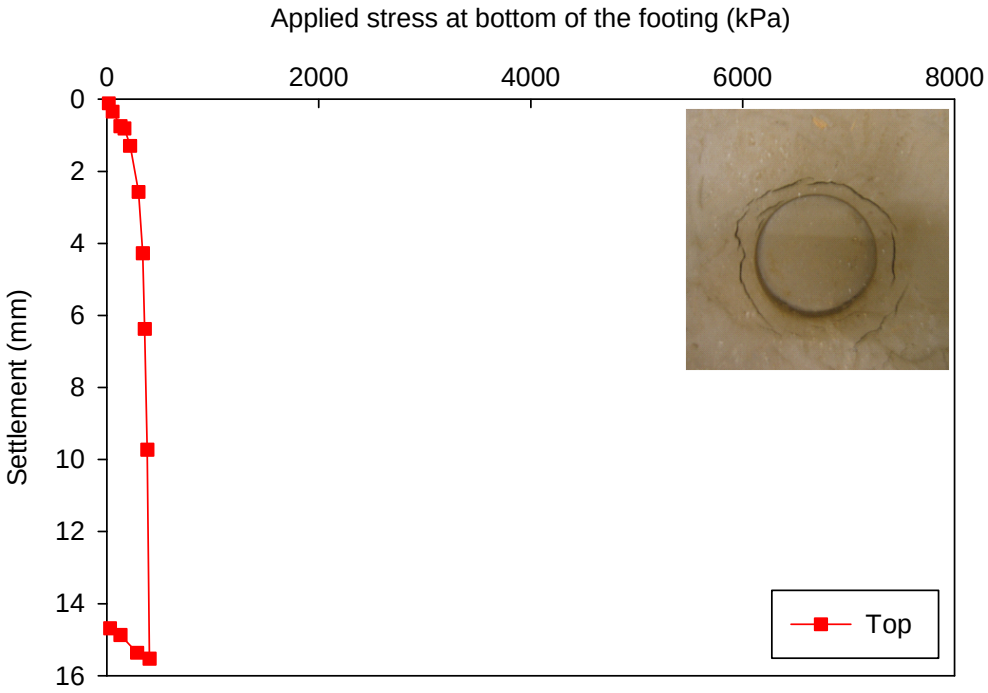

Figure 82: Stress-settlement test results for matrix soil used for placement of C(I) + C(K) groups of piers

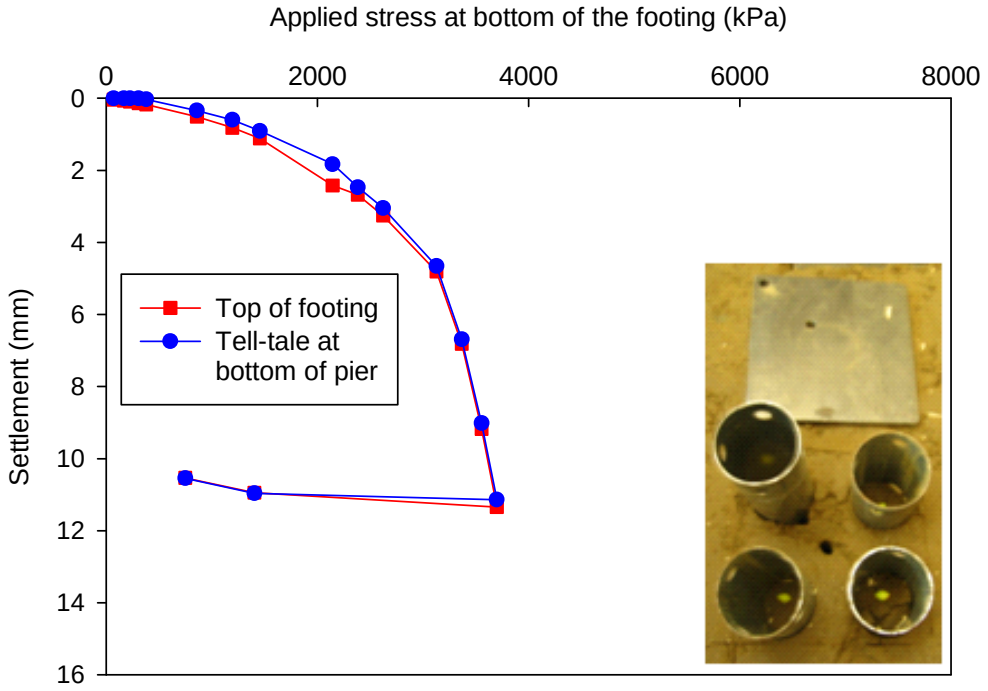

Figure 83: Stress-settlement test results for 305 mm and (610 mm group of four was not tested due to technical difficulties)

www.manaraa.com

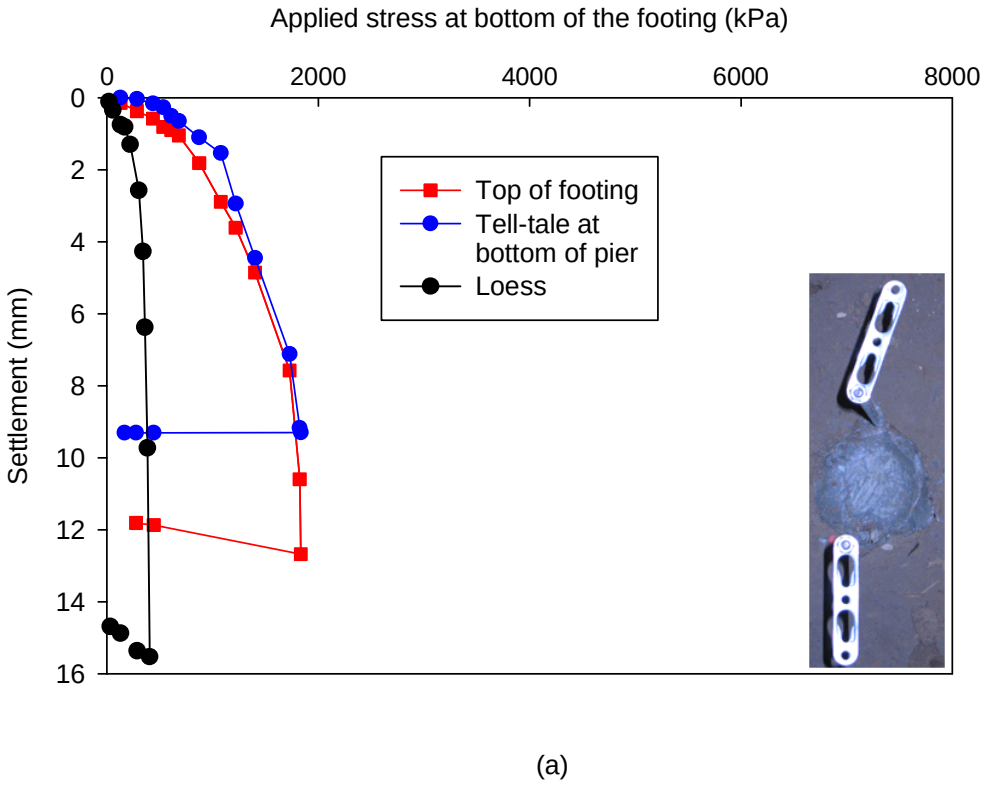

(a)

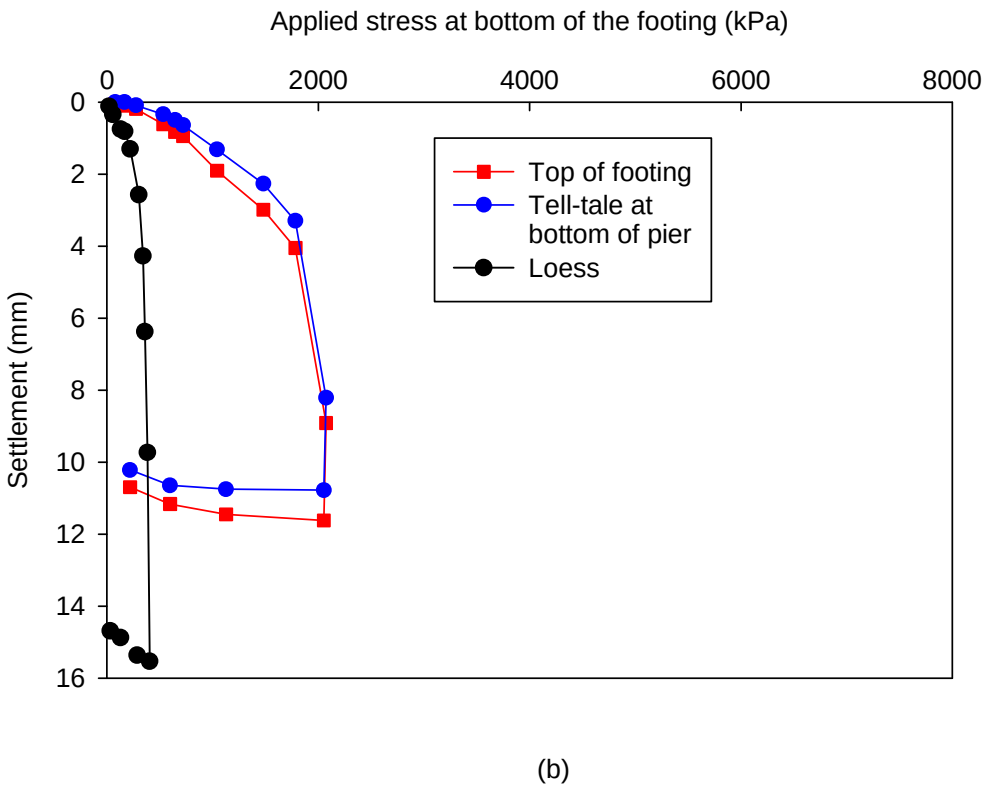

(b)

Figure 84: Stress-settlement test results (a) for 305 mm and (b) for 610 mm long single C(I) + C(K) piers

www.manaraa.com

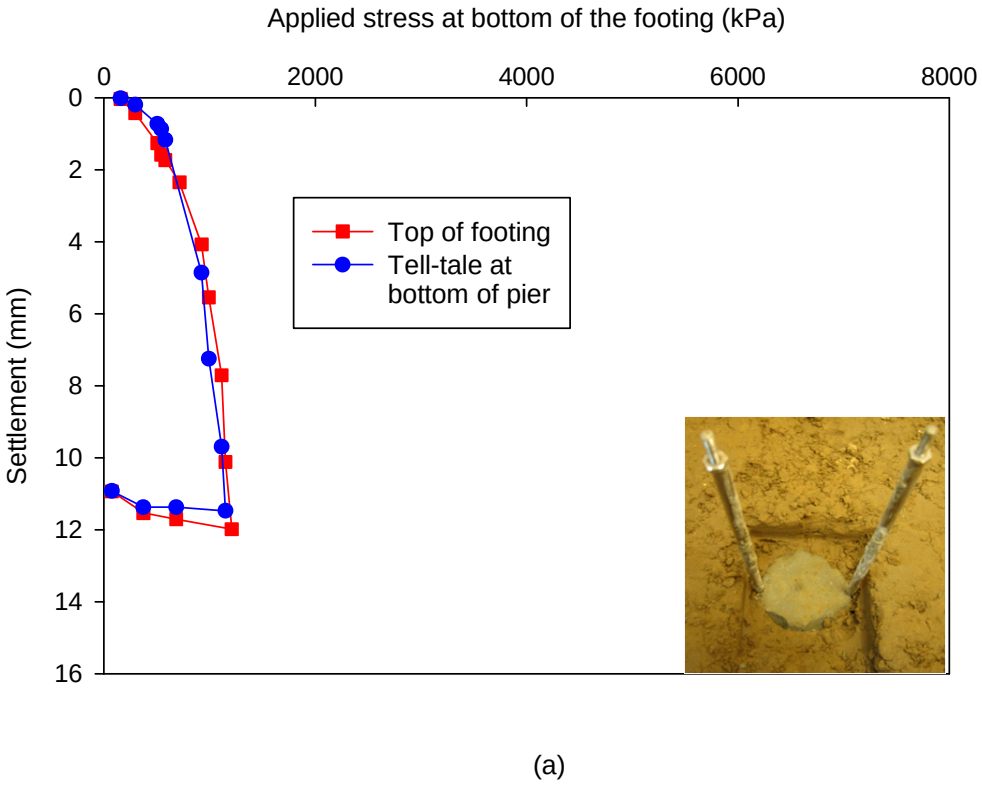

(a)

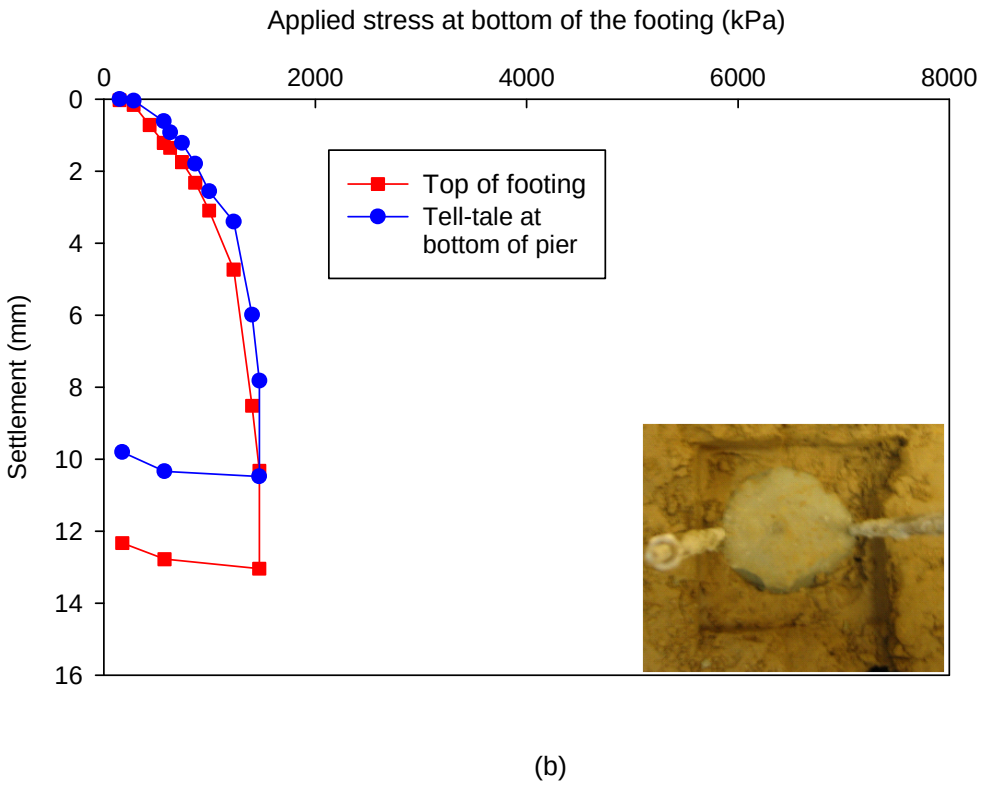

(b)

Figure 85: Stress-settlement test results (a) for 305 mm and (b) for 610 mm long C(I) + C(K) unit cell piers

www.manaraa.com

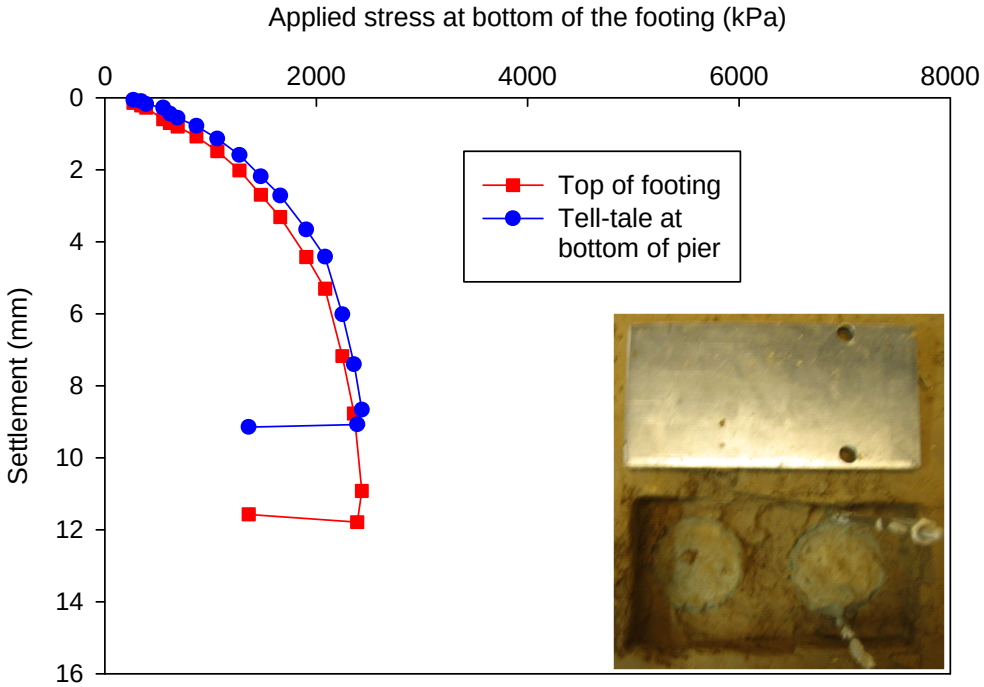

(a)

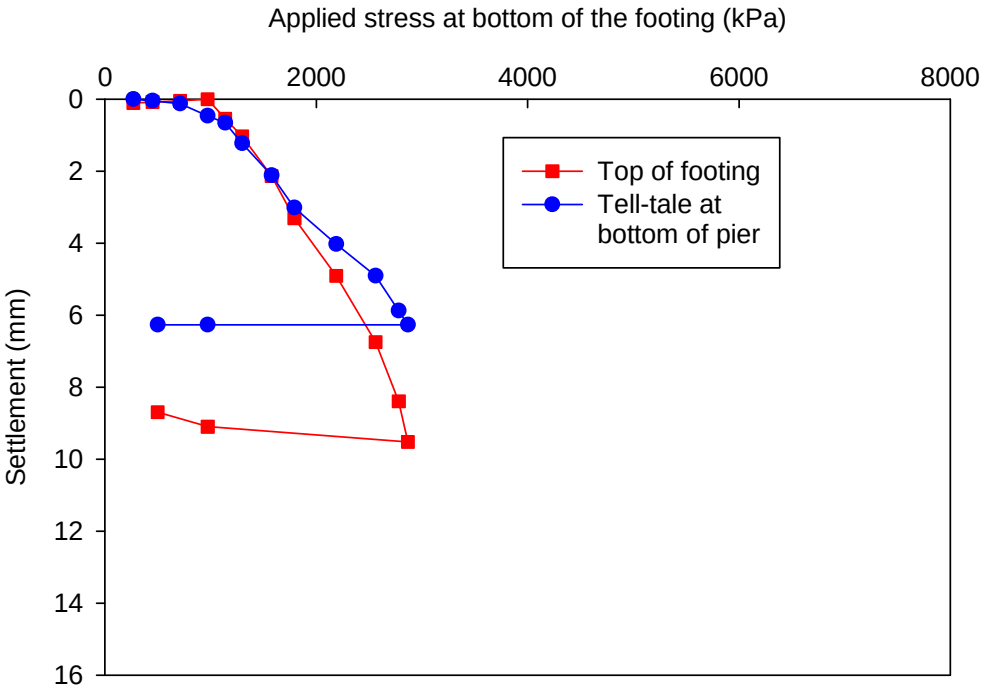

(b)

Figure 86: Stress-settlement test results (a) for 305 mm and (b) for 610 mm long group of two C(I) + C(K) piers

www.manaraa.com

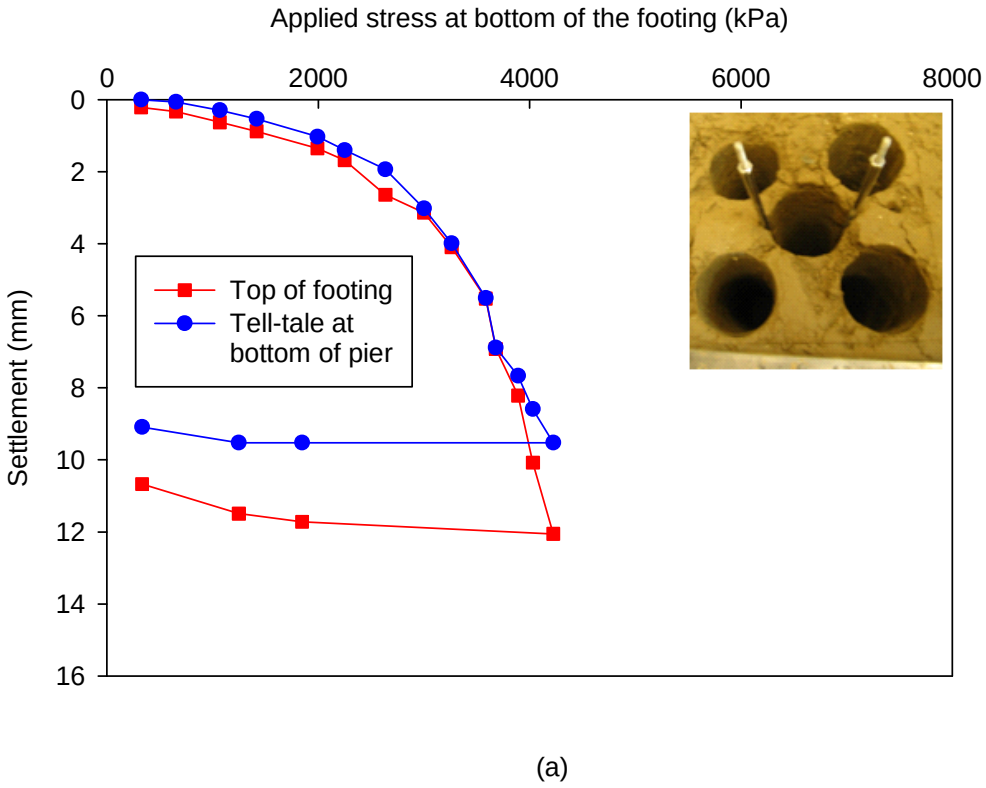

(a)

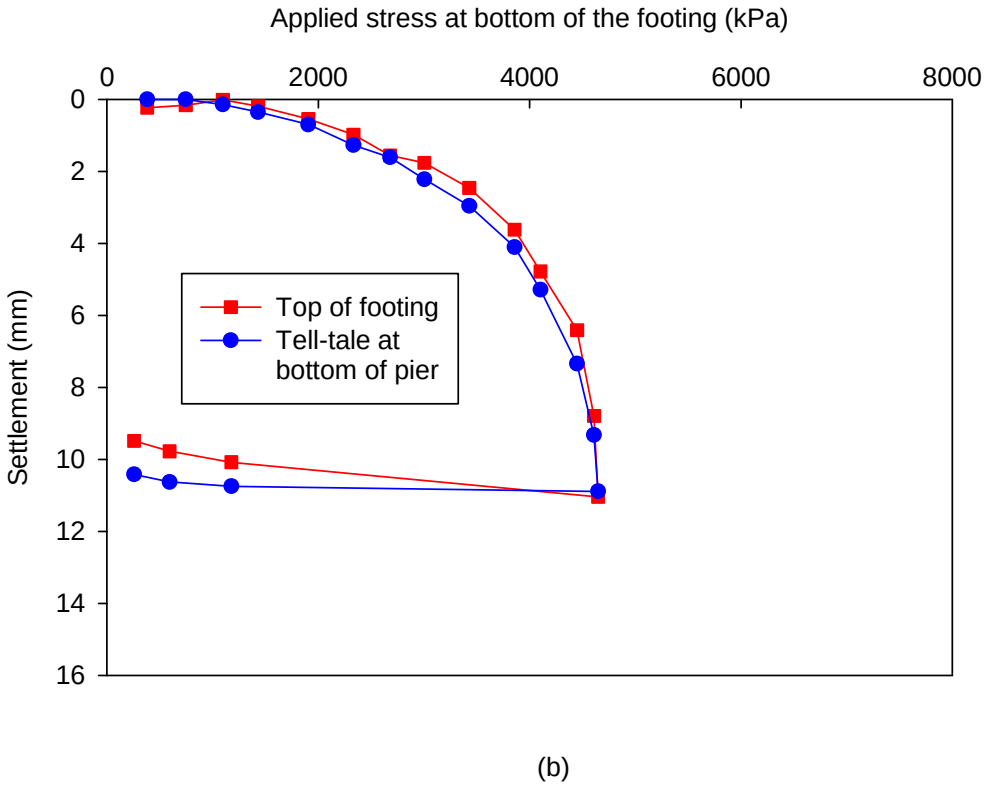

(b)

Figure 87: Stress-settlement test results (a) for 305 mm and (b) for 610 mm long group of five C(I) + C(K) piers

www.manaraa.com

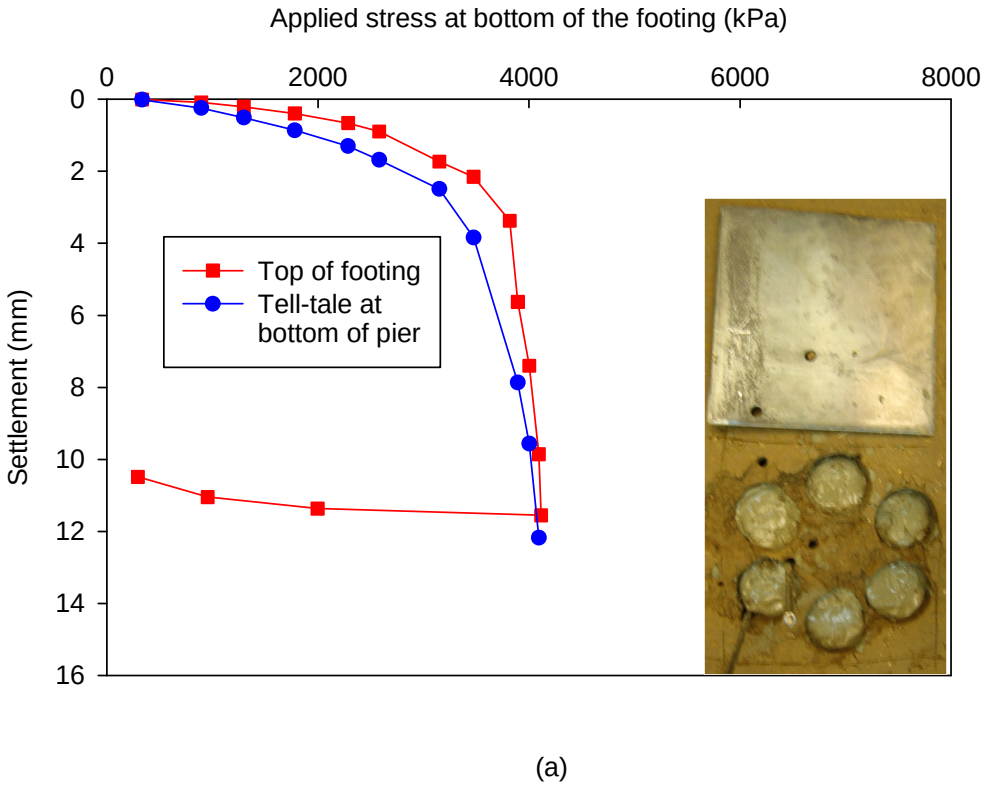

(a)

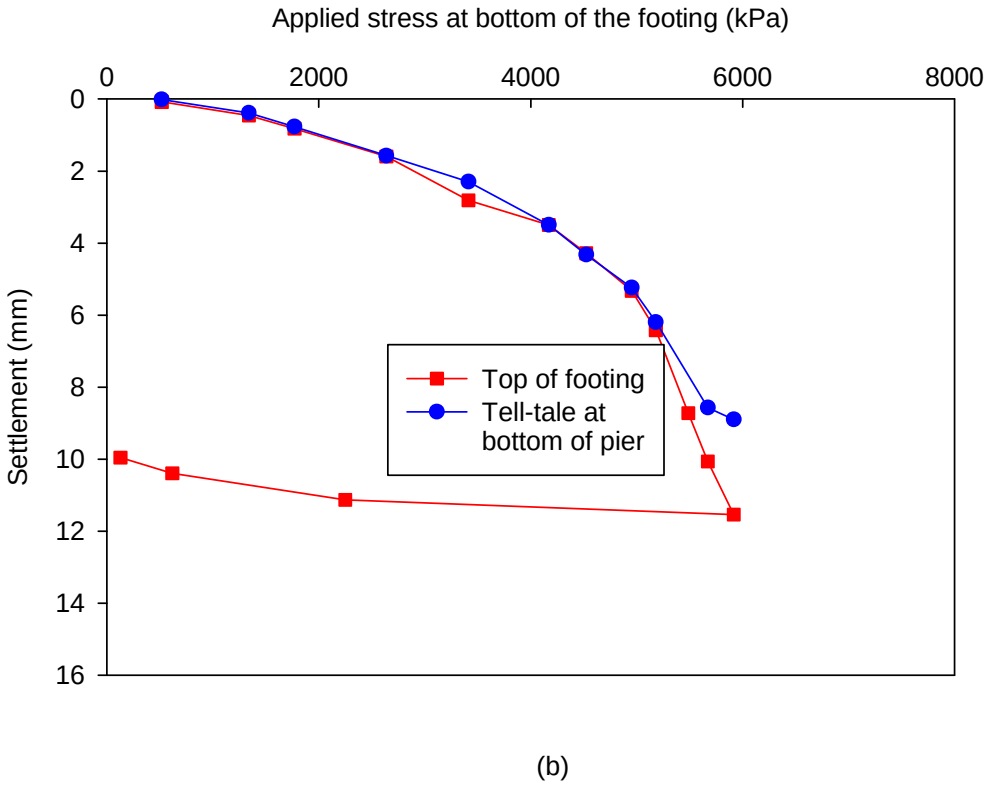

(b)

Figure 88: Stress-settlement test results (a) for 305 mm and (b) for 610 mm long group of six C(I) + C(K) piers

www.manaraa.com

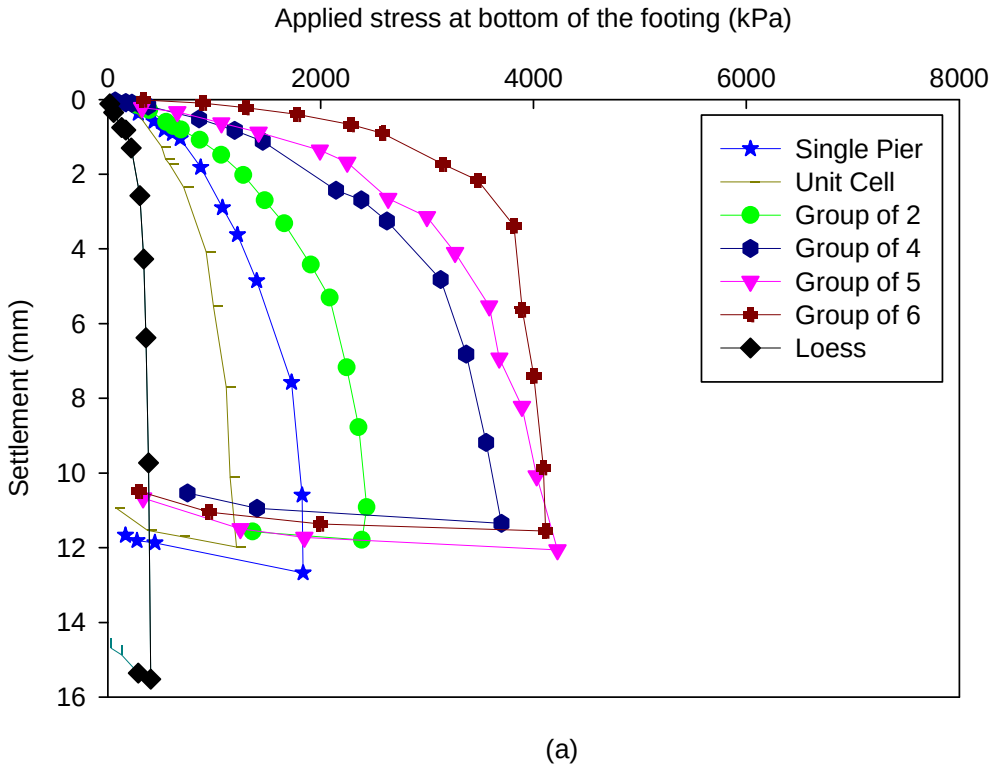

(a)

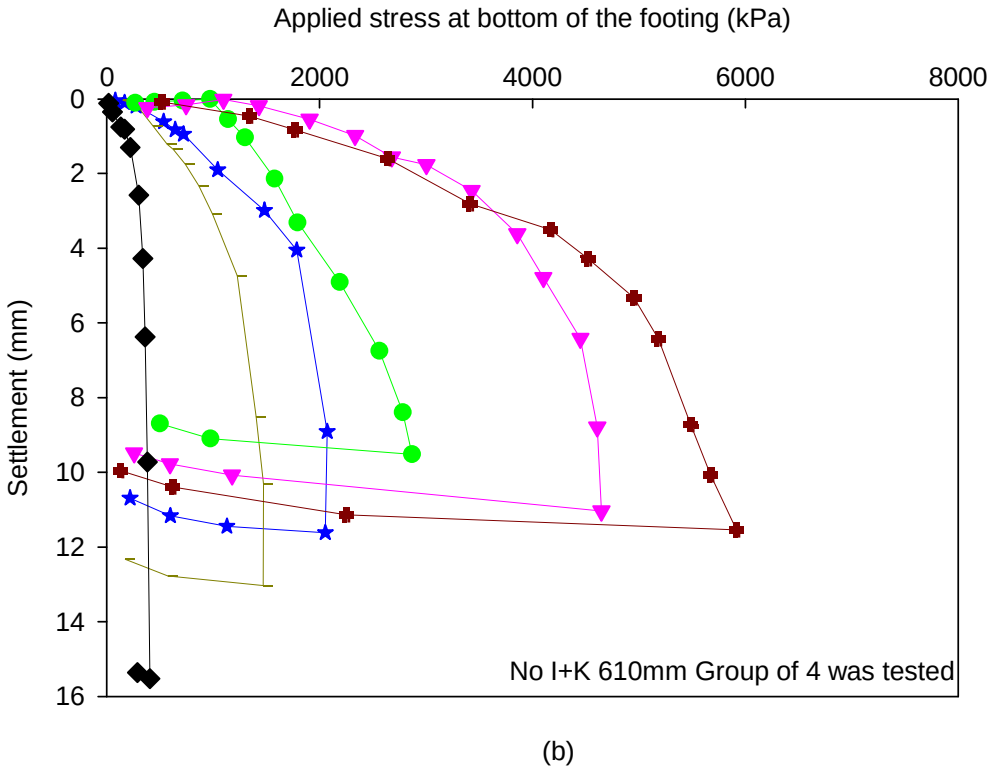

(b)

Figure 89: Overall stress-settlement test results for all (a) for 305 mm and (b) for 610 mm long C(I) + C(K) groups of piers

www.manaraa.com

C(I) + C(K) – Group Efficiency

The group efficiency was calculated for all the cement type I and type K composition groups of piers where the comparison between stiffness of single pier and multiple piers was made. The stiffness, modulus and settlement results were obtained from the stress-settlement curves and summarized in Table 32.

The group efficiency results were calculated at service load or at 2 mm and 5 mm level of displacement. The level of group efficiency for the ultimate load at 10 mm of settlement was also calculated.

Table 32: Stress, stiffness and deflection comparison measurements for C(I) + C(K) group load test results

								Service load		Ultimate
Pier type	Length (mm)	k at δ_{top} = 2 mm (kPa/mm)	σ at δ_{top} = 2 mm (kPa)	σ at δ_{top} = 5 mm (kPa)	σ at δ_{top} = 10 mm (kPa)	$\delta_{tell\text{-}tale}$ at δ_{top} = 10 mm (mm)	Ratio $\delta_{tell\text{-}tale}$ / δ_{top} at δ_{top} = 10 (mm)	Group Efficiency at 2mm	Group Efficiency at 5mm	Group Efficiency at 10mm
C(I) + C(K)	305	454	908	1,418	1,806	8.8	0.9	1.0	1.0	1.0
Single Pier	610	542	1,083	1,841	2,065	9.2	0.9	1.0	1.0	1.0
C(I) + C(K)	305	320	640	968	1,147	11.4	1.1	0.7	0.7	0.6
Unit Cell	610	397	794	1,241	1,460	7.5	0.8	0.9	0.7	0.7
C(I) + C(K)	305	633	1,266	2,023	2,400	8.1	0.8	0.7	0.7	0.7
Group of 2	610	771	1,542	2,209	2,869	6.3	0.6	0.7	0.6	0.7
C(I) + C(K)	305	961	1,921	3,151	3,609	9.8	1.0	0.5	0.6	0.5
Group of 4	610	N/A	N/A	N/A	N/A	N/A	N/A	N/A	N/A	N/A
C(I) + C(K)	305	1,188	2,377	3,647	4,225	9.5	1.0	0.5	0.5	0.5
Group of 5	610	1,574	3,148	4,148	4,630	10.2	1.0	0.6	0.5	0.4
C(I) + C(K)	305	1,677	3,355	3,820	4,096	12.3	1.2	0.6	0.4	0.4
Group of 6	610	1,448	2,896	4,818	5,672	8.6	0.9	0.4	0.4	0.5

Legend:
k – stiffness modulus (kPa/mm)
δ_{top} - deflection at the top of the pier (kPa)
$\delta_{tell\text{-}tale}$ - deflection at the bottom of the pier (mm)
σ – stiffness of the pier (kPa)
Ratio $\delta_{tell\text{-}tale}$ / δ_{top} = $\delta_{tell\text{-}tale}$ /10mm

Conversions:
1 m = 3.3 ft
1 mm = 0.0394 in
1 kPa = 0.145 psi
1 kg/m^3 = 0.0624 pcf

Obtained group efficiency values were also compared to the ones obtained on full-scale piles tested by different researchers and are presented in Table 33.

www.manaraa.com

Table 33: Group efficiency comparison measurements for small and full-scale piles

	Group Efficiency					
Pier type	Small-Scale C(I) + C(K) Piers	Small-Scale Piles in Clay	Full-Scale Steel Piles in Cohesive Soils	Full-Scale Piles in Cohesive Soils	Full-Scale Piles in Cohesive Soils	Full-Scale Piles in Dense Sand
Group of 2	0.6-0.7				0.8-0.9	
Group of 3	-	0.75-0.88		0.59-0.95		0.66-0.80
Group of 4	0.5-0.6	0.68-0.87	0.42-0.63			
Group of 5	0.4-0.6					
Group of 6	0.4-0.6	0.57-0.85				
Reference	Present study	Ilyas et al., 2004	Rollins, 1997	Cox et al., 1984	Sowers, 1986	Sarsby, 1985

C(I) + C(K) – Group Bearing Capacity

The bearing capacity was calculated for the groups of cement type I and K composition piers and are summarized in Table 34.

Table 34: Ultimate bearing capacity for a single pier within C(I) + C(K) group

Pier type	Length (mm)	A_g (m^2)	A (m^2)	R_a	q or σ at δ_{top} = 10 mm	σ_{loess} at δ_{top} = 10 mm	R_s	$q_{g\ total}$ (kPa)
C(I) + C(K) Unit Cell	305	0.0046	0.0781	0.058	1,529	1,101	1.4	2,076
	610	0.0046	0.0781	0.058	1,533		1.4	2,087
C(I) + C(K) Group of 2	305	0.0091	0.1490	0.061	2,146	1,609	1.3	2,805
	610	0.0091	0.1490	0.061	3,017		1.9	5,370
C(I) + C(K) Group of 4	305	0.0182	0.2845	0.064	3,406	2,719	1.3	4,199
	610	0.0182	0.2845	0.064	3,947		1.5	4,866
C(I) + C(K) Group of 5	305	0.0228	0.3413	0.067	4,150	2,719	1.5	6,119
	610	0.0228	0.3413	0.067	4,825		1.8	8,141
C(I) + C(K) Group of 6	305	0.0274	0.5426	0.050	4,868	1,886	2.6	11,637
	610	0.0274	0.5426	0.050	7,068		3.7	23,265

Legend:
A_g - cross sectional area of all aggregate pier elements (m^2)
A_g - area of matrix soil beneath the footing (m^2)
R_s - ratio of A_g to gross footprint area of the footing A
R_s - ratio of pier and matrix soil modulus values at δ_{top} = 10mm
q - average contact pressure at the footing bottom (kPa)

Conversions:
1 m = 3.3 ft
1 mm = 0.0394 in
1 kPa = 0.145 psi
1 kg/m^3 = 0.0624 pcf

www.manaraa.com

CHAPTER 6: DISCUSSION

This section presents the discussion of the analyzed results by means of conclusions, observations and trends based on the graphed and tabulated data provided in the previous chapter. Additional tables were constructed as necessary for better interpretation of the results. Several different criteria were considered when drawing the conclusions such as material composition of the pier, relative pier length, performance of different shape tamping beveled heads and comparison of the results on basis of service and ultimate load conditions.

Aggregate Piers Compacted via Different Shape Tamper Heads

This section will present the evaluation of results obtained for the aggregate piers compacted via different shape tamper heads, performance of which will be analyzed with respect to stiffness and load-bearing capacity of the piers.

Stress-Settlement

As it can be recalled, the piers constructed at the initial stage of the research study were compacted using various beveled tamper heads and were placed in stiff soil conditions. The compaction of the test bed material was performed on the dry side of optimum moisture content, and therefore, little to no bulging was observed. As a consequence no significant lateral stress was developed between the pier and matrix soil materials.

To evaluate the performance of each beveled head, the preliminary stress-settlement modulus results were plotted in Figure 57 and Figure 58. The composed charts outlined the behavior of the piers compacted via cone, truncated cone, flat and wedge heads constructed at 305 mm and 610 mm lengths, as well as, supplemented with the stress-settlement results for the unreinforced matrix soil. No tell-tale sensors were implemented at this stage of testing and, therefore, no bulging or plunging mechanisms of failure were evaluated.

www.manaraa.com

Having a limited amount of experience at this stage of the testing, the process of collecting stress-settlement data had to inevitably undergo trial and error. Therefore, the piers that were subjected to stress-settlement evaluation were tested and loaded to a different top of the pier levels of displacement. As a consequence, the comparison between stiffness values of the piers compacted via different tamper heads could only be made at the level of 2 mm of displacement.

As it can be observed from Figure 57, some of the tamper heads did not show consistency in amount of relative aggregate pier stiffening for short 305 mm and long 610 mm piers, as in the case with cone beveled head. Other beveled heads such as flat shape tamper have shown more consistent results, where the least amount of aggregate stiffening was produced. Moreover, the flat head compacted aggregate piers were observed to have reduction in stiffness below the undisturbed stiffness level of unreinforced matrix soil. This effect can be attributed to the loose state of the last compacted aggregate pier lift that had a tendency to undergo additional amount of compression under imposed loading. For the consecutive test stages the loose portion of the last aggregate lift was cleaned out and the concrete cap was poured to provide full contact load transfer to the top of the pier.

Overall, the obtained results were discovered to have a relatively small variation, however by observing higher stiffness for the short 305 mm aggregate pier compacted via cone tamper head a slight sign for a potential for better performance was noted. Moreover, the conventional aggregate pier truncated cone tamper head has also indicated ability to better stiffen the piers. Therefore, additional testing was required to confirm the hypothesis, where softer soil conditions were to be utilized in order to favor aggregate pier bulging. As a consequence, construction of aggregate piers during the latter stages of testing was partially targeted towards evaluation of relative amount of stiffness provided by cone and truncated cone tamper heads.

As it can be recalled, the aggregate piers constructed during the phase where single piers of various compositions were utilized, the installation was performed using the truncated cone

www.manaraa.com

tamper head. On the other hand, the groups of aggregate piers also featured construction of a single aggregate pier, however compaction of which was completed via cone tamper head. Therefore, neglecting the effect of small deviations in properties of matrix soil between different test beds, and having the same pier construction methods to be utilized, the obtained stiffness results for aggregate piers compacted via cone and truncated cone tampers were compared in Table 35.

Table 35: Comparison measurements for single aggregate piers at different testing stages compacted via cone and truncated cone beveled heads

Stg. #	Test Stage	Pier type	Length (mm)	σ at δ_{top} = 2 mm (kPa)	σ at δ_{top} = 5 mm (kPa)	σ at δ_{top} = 10 mm (kPa)
1	Various Beveled Head Tests	Aggregate Pier – Truncated Cone	305	299	N/A	N/A
			610	548	N/A	N/A
		Aggregate Pier - Cone	305	375	N/A	N/A
			610	590	N/A	N/A
2	Various Pier Mix Tests	Aggregate Pier – Truncated Cone	305	443	774	1,044
			610	494	789	1,028
3	Group Tests	Aggregate Pier - Cone	305	908	1,418	1,806
			610	1,083	1,841	2,065
	Stiffness ratio for truncated vs. cone between aggregate piers at stages 2 and 3		305	51	45	42
			610	54	57	50

Legend:
k - stiffness modulus (kPa/mm)
δ_{top} - deflection at the top of the pier (mm)
$\delta_{tell\text{-}tale}$ - deflection at the bottom of the pier (mm)
σ – stiffness of the pier (kPa)

Conversions:
1 m = 3.3 ft
1 mm = 0.0394 in
1 kPa = 0.145 psi
1 kg/m^3 = 0.0624 pcf

The obtained results for the aggregate pier stiffness parameters for the cone and truncated cone constructed piers at stages two and three respectively were further analyzed where comparison between stiffness results was expressed through percent difference calculation:

Equation 20: Stiffness ratio for cone and truncated cone compacted aggregate piers

$$stiffness\ ratio = \sigma_{truncated\ cone} / \sigma_{cone} \qquad (Equation\ 20)$$

www.manaraa.com

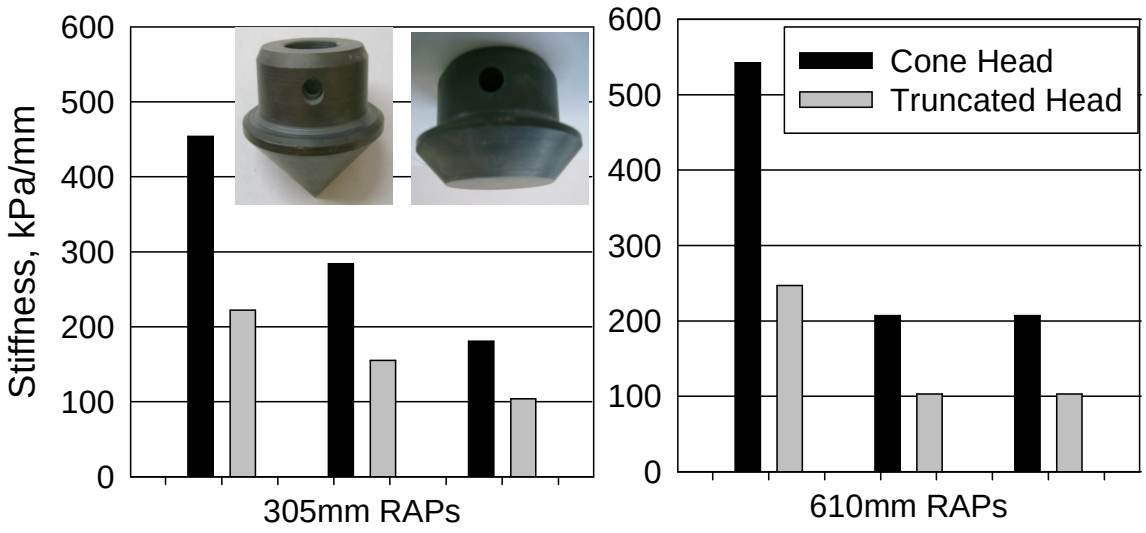

Figure 90: Stiffness comparison at 10mm of settlement for aggregate piers compacted via cone and truncated cone heads

The amount of difference in stress imposed on aggregate pier compacted via cone and truncated cone beveled heads was evaluated at 2 mm, 5 mm and 10 mm of top of the pier displacements, and was observed to be on the order of 50 percent on average. The results were found to be consistent for both short and long piers, where longer piers had a tendency to develop a slightly higher level of stiffness and load resistance. Therefore, one of the major conclusions was made, where the cone head was capable of delivering twice the amount of energy than the truncated cone head and, thus, was of a greater benefit for stiffening the piers.

Single Piers of Various Mixes

Stress-Settlement

The stress-settlement data collected for the tested single piers of various compositions was summarized in Figure 70. The results were grouped by length and the stiffness and displacement results were summarized in Table 24. The piers tested at this stage of the research were equipped with the tell-tale plates installed at the tip of the piers and, therefore,

www.manaraa.com

some major conclusion were made regarding plunging, bulging and combination of two mechanisms of pier failures.

As previously outlined, the aggregate pier testing at this phase of the research included partial cementing of the top and bulb portions of the aggregate piers. The obtained results have shown a significant amount of stiffness improvement provided by cementing the top portion of the long 610 mm aggregate pier. The amount of stress imposed on the partially cemented versus non-cemented aggregate pier increased by a factor of almost two at ultimate load condition. The long aggregate pier was expected to have a significant amount of bulging upon failure and, therefore, the collected data has provided evidence for reduction in pier bulging when using partial cementing technique. However, it must be noted that the aggregate pier was still observed to fail by bulging, though in the area beneath the cemented portion.

At the same time by cementing the bulb portion of the pier it was anticipated to have a reduction in the amount of plunging to occur for short 305 mm aggregate pier. However, no additional confinement was observed to develop within the pier and, therefore, no significant improvement was noticed in pier stiffness or load capacity. Therefore, no definitive conclusion can be made in regard to how the process of cementing bulb portion of the pier can benefit the overall loading or stiffness capacities of the short aggregate pier.

Overall, the tell-tale displacement data has shown no great impact when cementing top or bottom potions of the aggregate piers. As per Table 24, the ratio $\delta_{tell\text{-}tale} / \delta_{top}$ was observed to be relatively small for uncemented aggregate piers, short aggregate pier with cemented bulb and long aggregate pier with cemented top of the pier, thus, suggesting the failure mechanism to occur through bulging. In case with long aggregate pier with cemented bulb and short aggregate pier with cemented top 100 mm, a greater amount of plunging was recorded, however could be better described as combination of bulging and plunging.

www.manaraa.com

In case with the piers consisting of loess as a main component, the addition of fibers to the mixture has proven to significantly reduce pier strength at the level of service load. A similar effect was noticed for the piers composed of loess and cement type I, where addition of the fibers has shown reduction in load bearing capacity of the fiber containing pier at both service and ultimate levels of load.

Another set of remarkable observations and findings was obtained for the piers composed of loess and cement. The loess and cement composition 305 mm pier has shown the highest stiffness results at ultimate load conditions among all the piers tested at this stage of study. The long 610 mm pier has shown a tendency to outperform other single piers at the initial portion of the stress-settlement curve, however a steep decline in load support was observed at 2.5 mm level of settlement. After reaching a total displacement of 12 mm and upon excavation of the tested piers, the short and long loess and cement composition piers were discovered cracked at the top portion. The shear planes, as well as, point of failure can be observed from the stress-settlement curves in Figure 64. The figures confirm a very brittle type of failure and support earlier stated observation of steep loss in load bearing.

As one would anticipate, the tell-tale plate movement represented by the $\delta_{tell\text{-}tale} / \delta_{top}$ ratio was observed to be relatively small for 305 mm loess and fiber mix piers, as well as, long loess and cement composition pier (Table 24). This would suggest a bulging type of failure for loess and fiber composition pier, while no tip movement for loess and cement composition pier would support brittle failure and shearing observations. On the other hand, significant movement at the bulb of the short cement, loess and loess, cement, fiber composition piers suggests a plunging type of failure.

Finally, the piers main components of which were cement type I and K were also evaluated on the basis of stress-settlement performance. The compositions have shown improvement in pier stiffness where mixture of cement type I and K was used, whereas addition of NS7 component has shown no consistent results. While having NS7 component to have negative effect on pier stiffness at the level of ultimate load, the opposite effect was noticed at the

www.manaraa.com

level of service load. On the other hand, the addition of cement type K component to the cement type I and NS7 mixture has shown reduction in pier stiffness at the service load and opposite effect at ultimate load.

Tell-tale plate movement has shown a significant amount of pier plunging for all the cement type I and type K composition piers. As one would expect, a greater amount of plunging was observed in case with short 305 mm piers. As per Table 24, the ratio $\delta_{tell\text{-}tale} / \delta_{top}$ was observed to be relatively large for all cement type I, K and NS7 composition piers, where no internal pier deformation was detected and, therefore, resulted in plunging type of settlement.

While most cast-in-place composition piers have shown a greater capacity for stiffness and load bearing, some of the extraordinary behavior of loess and cement composition piers can be attributed to the ramming and curing effects that contributed to bulging and hardening of the piers. Therefore, while much of the findings at this stage of the research have coincided with the expectations, the findings obtained for loess and cement composition piers have shows a lot of potential for the future investigation where if no cracking is achieved, the composition can be beneficial due to potential for greater performance, simplicity, constructability and affordability.

Additionally to the conclusions drawn from stress-settlement curves, as well as tabulated results provided in Table 24, another table was constructed in order to better understand the overall improvement in stress and stiffness provided by the pier elements in comparison to the unreinforced matrix soil. The stiffness ratio, *n* was calculated as per Equation 21. The stiffness ratio was defined as the ratio between the total stress on the pier and the unreinforced footing. The results were summarized in Table 36.

Equation 21: Stiffness ratio for pier supported versus unreinforced footing

$$n = k_{pier} / k_{unreinforced\ footing} \qquad \textit{(Equation 21)}$$

www.manaraa.com

Table 36: Stiffness ratio calculations for single piers of various composition

Pier type	Length (mm)	σ at δ_{top} = 2 mm (kPa)	σ at δ_{top} = 5 mm (kPa)	σ at δ_{top} = 10 mm (kPa)
Aggregate Pier – Truncated	305	443	774	1,044
	610	494	789	1,028
n. stiffness ratio	-	1.3	1.5	1.5
	-	1.4	1.5	1.5
Aggregate Pier w/cem. bulb	305	491	732	960
	610	341	904	1,304
n. stiffness ratio	-	1.4	1.4	1.4
	-	1.0	1.7	1.9
Aggregate Pier w/cem. top 100mm	305	509	958	1,385
	610	740	1,341	1,726
n. stiffness ratio	-	1.5	1.8	2.0
	-	2.1	2.6	2.5
Loess + fiber	305	211	475	667
	610	251	496	771
n. stiffness ratio	-	0.6	0.9	1.0
	-	0.7	1.0	1.1
Loess + cement	305	729	1,258	1,570
	610	1,153	1,436	1,467
n. stiffness ratio	-	2.1	2.4	2.3
	-	3.3	2.8	2.1
Loess	—	347	521	689

Pier type	Length (mm)	σ at δ_{top} = 2 mm (kPa)	σ at δ_{top} = 5 mm (kPa)	σ at δ_{top} = 10 mm (kPa)
Loess + fiber + cement	305	483	794	1,062
	610	518	1,491	1,804
n. stiffness ratio	-	1.4	1.5	1.5
	-	1.5	2.9	2.6
C(I) + C(K)	305	453	960	1,363
	610	975	1,974	2,393
n. stiffness ratio	-	1.3	1.8	2.0
	-	2.8	3.8	3.5
C(I) + C(K) + NS7	305	667	1,028	1,200
	610	1,247	1,749	1,944
n. stiffness ratio	-	1.9	2.0	1.7
	-	3.6	2.0	2.8
C(I) + NS7	305	523	1,044	1,327
	610	1,130	1,611	1,765
n. stiffness ratio	-	1.5	2.0	1.9
	-	3.3	3.1	2.6
Sand	305	707	902	998
	610	712	1,103	1,295
n. stiffness ratio	-	2.0	1.7	1.4
	-	2.1	2.1	1.9
Loess	—	347	521	689

Legend:
δ_{top} - deflection at the top of the pier (kPa)
σ – stress on the pier (kPa)
n –stiffness ratio

Conversions:
1 m = 3.3 ft
1 mm = 0.0394 in
1 kPa = 0.145 psi

www.manaraa.com

Table 36 outlines the amount of improvement in load support provided by unreinforced matrix soil versus load carried by the pier of the same cross section. In general the trend can be outlined that the long 610 mm piers have shown a better performance in load carrying capacity and improvement through stress increase and stiffening of the soil than short 305 mm piers. As an exception, piers composed of loess and fiber demonstrated stiffness behavior results inconsistent with a general trend, where longer 610 mm pier has shown to be less effective in load bearing capacity.

Another conclusion that was drawn from Table 36 has shown that the piers subjected to bulging or internal deformation mechanisms of failure, such as aggregate pier, sand, and loess, fiber composition piers featured a relatively unchanged or declined stiffness ratio as the loads approached critical or ultimate conditions.

Bearing Capacity

While two primary modes of failure were considered where plunging and bulging mechanisms were of a main concern, some of the piers featured a more complicated mechanism of failure through combination of both plunging and bulging processes.

Some of the piers, bearing capacities of which were not evaluated due to a complicated mechanisms of failure, included partially cemented aggregate piers, loess and cement composition piers, as well as, piers composed of loess and fibers.

Having partially cemented aggregate piers to undergo a more complex mechanism of failure was attributed with the shift in zone of pier bulging for the aggregate piers with cemented 100 mm top portion, and unknown impact of cementing of bulb on plunging mechanism of failure. Therefore, partially cemented aggregate piers could not be evaluated through conventional methods of evaluating bearing capacity since no pure bulging or pure plunging was observed.

www.manaraa.com

Some of the loess composition piers were also not investigated for the bearing capacity parameter. Loess and cement composition piers were excluded from the bearing capacity investigation due to the brittle mechanism of failure at the top portion of the piers. The piers composed of loess and fiber, on the other hand, were not included in bearing capacity calculations either, due to the unknown angle of frictional resistance of the composed material in spite of the anticipated mechanism of failure through bulging.

Overall, the bearing capacity results were generated for aggregate piers, sand piers, as well as, loess, cement, fiber and cement type I and K component piers. According to the stress-settlement information gathered for aggregate piers and sand piers, the long 610 mm aggregate pier and both 305 mm and 610 mm sand piers were subjected to bulging failure as confirmed in Figure 61 and Figure 69. Since the bulging failure of the long aggregate pier and short and long sand piers was mainly dependent on the angle of friction of the pier aggregate, the ultimate bearing capacity values were estimated as follows: $1.0x10^3$ kPa, $0.7x10^3$ kPa and $0.8x10^3$ kPa respectively for long aggregate pier, short sand pier and long sand pier.

On the other hand, piers composed of loess, cement, fiber, as well as, cement type I, K and NS7 composition piers were deemed to fail by plunging due to little to no internal material deformation. Therefore, the bearing capacity for short 305 mm cementitious composition piers was estimated at $1.6x10^3$ kPa on average, while the long 610 mm piers had average bearing capacity values at $2.1x10^3$ kPa. The short 305 mm aggregate was also deemed to fail by plunging and, therefore, the bearing capacity was found at $1.7x10^3$ kPa.

Additionally, a reference bearing capacity value for the unreinforced matrix soil was calculated using Terzaghi's bearing capacity coefficients and estimated at 0.7 kPa. Therefore, a conclusion was made that cementitious composition piers had a great improvement in bearing capacity by factor of 2-3. The long sand and aggregate piers were also proven to increase bearing capacity of the matrix soil, however by a much lesser margin – by factor of 1.1-1.4.

www.manaraa.com

When analyzing the obtained bearing capacity results in terms of the calculated or design bearing capacity values, the conclusion can be made that the calculated results had a tendency to underestimate the actual measured values (Figure 71). On average, the ratio between design and calculated bearing capacity values was 80 percent. The correlation between measured and calculated values shown in Figure 72 did not show a particularly good linear agreement between the values. Therefore, the design approach would need to be revised and modified.

Groups of Piers

Aggregate Piers - Stress-Settlement

As outlined in Figure 88, the plotted stress-settlement results were found to behave in a predictable manner, where least performance was attributed with single aggregate pier and the greatest load bearing capacity was obtained for the group of six piers. As a general trend, the shorter 305 mm groups of aggregate piers were observed to support less load than long piers at the same amount of settlement. The calculated stiffness and stiffness ratio results obtained for unreinforced matrix soil and soil reinforced with aggregate piers are summarized in Table 37. Stiffness ratio, *n* between the reinforced and unreinforced matrix soil was calculated on the basis of difference in stress and is outlined in Equation 20.

The collected stress data for reinforced and unreinforced soil conditions have shown very sporadic results (Table 37). While no definitive conclusion can be made regarding the dependence of number of piers within the group and stiffness ratio parameter, the overall results have shown a minimum value of 1.3 for most cases. However a useful observation can be attributed with the length of the pier criteria, where the stiffness ratio provided by the long piers was approximately twice the amount of improvement provided by short piers for most groups.

www.manaraa.com

Table 37: Stress concentration calculations for groups of aggregate piers

Pier type	Length (mm)	σ at δ_{top} = 2 mm (kPa)	σ at δ_{top} = 5 mm (kPa)	σ at δ_{top} = 10 mm (kPa)
Aggregate Pier Single Pier	305	129	247	406
	610	352	704	949
Loess	-	67	158	285
n. stiffness ratio	-	1.9	1.6	1.4
	-	5.3	4.5	3.3
Aggregate Pier Unit Cell	305	348	588	908
	610	894	1,330	1,533
Loess	-	278	685	1,101
n. stiffness ratio	-	1.3	0.9	0.8
	-	3.2	1.9	1.4
Aggregate Pier Group of 2	305	483	1,345	2,146
	610	1,260	2,521	3,017
Loess	-	642	1,055	1,609
n. stiffness ratio	-	0.8	1.3	1.3
	-	2.0	2.4	1.9

Pier type	Length (mm)	σ at δ_{top} = 2 mm (kPa)	σ at δ_{top} = 5 mm (kPa)	σ at δ_{top} = 10 mm (kPa)
Aggregate Pier Group of 4	305	867	2,254	3,406
	610	1596	3,105	3,947
Loess	-	1028	1,891	2,719
n. stiffness ratio	-	0.8	1.2	1.3
	-	1.6	1.6	1.5
Aggregate Pier Group of 5	305	1,529	3,233	4,150
	610	3,511	4,375	4,825
Loess	-	1,028	1,891	2,719
n. stiffness ratio	-	1.5	1.7	1.5
	-	3.4	2.3	1.8
Aggregate Pier Group of 6	305	3,073	4,100	4,898
	610	3,134	5,361	7,068
Loess	-	1,018	1,486	1,886
n. stiffness ratio	-	3.0	2.8	2.6
	-	3.1	3.6	3.7

Legend:
δ_{top} - deflection at the top of the pier (kPa)
σ – stiffness of the pier (kPa)
n –stiffness ratio

Conversions:
1 m = 3.3 ft
1 mm = 0.0394 in
1 kPa = 0.145 psi

Stiffness modulus results for groups of aggregate piers outlined in Table 30 have shown a greater amount of piers stiffening of the lab constructed piers comparing to the field stiffness modulus results. As the number of piers was to increase within the group the difference in stiffness modulus between lab and field had also a trend to increase.

www.manaraa.com

Aggregate Piers – Bearing capacity

Obtained bearing capacity values were found to have a trend to increase in a non-linear fashion with the increasing number of piers within the group (Table 31). Single pier was found to bear 1.1 MPa - 1.9 MPa, while the group of 6 had a load capacity of 8.4 MPa – 15.5 MPa. For most of the obtained results short piers were found to have similar bearing capacity as long piers within the same pier group, where only group of six was found to be an outlier.

When performing comparative analysis between the lab and field bearing capacity results, it was found that the values were to closely correlate. However, no particular trend was noticed. Figure 82 shows comparison between single piers, groups of four and groups of five aggregate piers. Full-scale piers are not necessarily of the same length as the lab 305 mm and 610 mm piers and, therefore, additional field replicating testing would be required to identify the field and lab correlation.

Aggregate Piers - Group Efficiency

Group efficiency calculations were performed at 2 mm, 5 mm and 10 mm top of the pier displacements. The group efficiency results with respect to single pier were summarized in Table 27 and with respect to unit cell were summarized in Table 28. Some of the major conclusions were made based on the pier length, number of piers within the group and magnitude of settlement at service and ultimate load conditions.

Having the piers built at short 305 mm and long 610 mm lengths, the findings have shown that the group efficiency with respect to single pier was consistently greater in magnitude for short piers than for the long ones. In some cases the difference between short and long piers was exceeded by a factor of two leading to a conclusion that some of the shorter groups of aggregate piers were twice as efficient as the groups of piers of greater length.

www.manaraa.com

Another observation was made, where the trend of reduction of the group efficiency with increasing amount of load was noticed (Table 27). Therefore, piers and groups of piers featured greater group efficiency at service load conditions and much lesser efficiency at failure. As a result, it was concluded that the group efficiency became smaller as the load imposed on a group of piers approached critical or ultimate condition.

Group efficiency values obtained for all 305 mm groups of piers at 5 mm and 10 mm levels of settlement were observed to consistently vary within the margin of 2.0-2.8 for group efficiency calculated in terms of single pier. Therefore, short groups of piers at 5 mm and 10 mm levels of settlement had a consistent group efficiency value ranging between two and three independently of the number of piers within the group. Similarly, the long 610 mm groups of piers featured consistent group efficiency values ranging between 1.0 and 1.9 at 5 mm and 10 mm levels of settlement. Thus, the group efficiency for groups of long piers varied between 1 and 2 at the level of 5 mm and 10 mm levels of settlement independently of the number of piers contained within the group.

For the groups efficiency calculated in terms of unit cell, the values were found to be consistently lower than 1.0 for most of the groups of piers. Consistently with Table 27 group efficiency results, the piers within the short groups of piers were found to be more efficiency than in long groups of piers. No particular trend was noticed with respect to group efficiency related to the amount of pier settlement.

C(I) + C(K) - Stress-Settlement

As outlined in Figure 89, the stress-settlement curves were plotted and grouped by length. The relative position of the plotted data points for the groups of piers was observed to behave in the expected manner, where the greatest amount of stress was carried by the group of six piers and the least by the group of two. As one would expect, the groups of shorter 305 mm piers were also observed to support less load than long piers at the same amount of settlement. However an anomaly was notices where the unit cell has shown to outperformed

www.manaraa.com

single pier for both 305 mm and 610 mm long piers. More testing would be required to confirm the trend and identify cause of the unit cell cementitious pier to have higher bearing capacity.

The calculated stiffness ratio results for unreinforced soil and pier supported conditions were calculated per Equation 20 and summarized in Table 38.

Table 38: Stress concentration calculations for groups of C(I) + C(K)

Pier type	Length (mm)	σ at δ_{top} = 2 mm (kPa)	σ at δ_{top} = 5 mm (kPa)	σ at δ_{top} = 10 mm (kPa)
C(I) + C(K) Single Pier	305	908	1,418	1,806
	610	1,083	1,841	2,065
Loess	-	278	685	1,101
n. stiffness ratio	-	3.3	2.1	1.6
	-	3.9	2.7	1.9
C(I) + C(K) Unit Cell	305	640	968	1,147
	610	794	1,241	1,460
Loess	-	278	685	1,101
n. stiffness ratio	-	2.3	1.4	1.0
	-	2.9	1.8	1.3
C(I) + C(K) Group of 2	305	1,266	2,023	2,400
	610	1,542	2,209	2,869
Loess	-	278	685	1,101
n. stiffness ratio	-	4.6	3.0	2.2
	-	5.5	3.2	2.6

Pier type	Length (mm)	σ at δ_{top} = 2 mm (kPa)	σ at δ_{top} = 5 mm (kPa)	σ at δ_{top} = 10 mm (kPa)
C(I) + C(K) Group of 4	305	1,921	3,151	3,609
	610	N/A	N/A	N/A
Loess	-	278	685	1,101
n. stiffness ratio	-	6.9	4.6	3.3
	-	N/A	N/A	N/A
C(I) + C(K) Group of 5	305	2,377	3,647	4,225
	610	3,148	4,148	4,630
Loess	-	278	685	1,101
n. stiffness ratio	-	8.6	5.3	3.8
	-	11.3	6.1	4.2
C(I) + C(K) Group of 6	305	3,355	3,820	4,096
	610	2,896	4,818	5,672
Loess	-	278	685	1,101
n. stiffness ratio	-	12.1	5.6	3.7
	-	10.4	7.0	5.2

Legend:
δ_{top} - deflection at the top of the pier (kPa)
σ – stiffness of the pier (kPa)
n –stiffness ratio

Conversions:
1 m = 3.3 ft
1 mm = 0.0394 in
1 kPa = 0.145 psi

www.manaraa.com

As previously outlined, the stiffness ratio calculations were performed and the results have shown a significant amount of soil improvement as outlined by *n* value increasing proportionally to the number of piers within a group. Another conclusion was made where regardless of the pier length the same group of piers had a relatively the same impact on the amount of soil improvement.

The loess unreinforced matrix soil values were adopted from the plate load tests performed during testing of groups of aggregate piers. No plate load tests were done on the unreinforced soil for test bed conditions prepared specifically for groups of type I and K composition piers. Therefore, some discrepancy may have been induced due to slightly varying test bed soil conditions.

Also, the tell-tale plate deflection information was collected for all the tested groups of piers, however most of the groups had the steel plate cemented to the housing tubes containing tell-tale rods. The binding happened in the process of pouring a grout cap in order to provide even distribution of the load among the piers within the group. Therefore, even though most of the groups of piers experienced the same amount of relative movement between the tip and top of the pier, the tell-tale data must be utilized with caution.

C(I) + C(K) – Bearing Capacity

The obtained bearing capacity results for cementitious composition groups of piers are shown in Table 34. The values were found to increase with the increasing number of piers within the group. No particular trend was noticed between short and long groups of piers, where the difference varied between 1.0 for unit cell and 2.0 for group of six piers.

No comparison between lab and field bearing capacity was performed and can be a subject of investigation in future research.

www.manaraa.com

C(I) + C(K) - Group Efficiency

Group efficiency calculations performed on the groups of piers composed of cement type I and type K are presented in Table 32. The calculations were only performed with respect to single piers and no analysis was done with the respect to unit cell. Similar observations were made in regard with the findings obtained for the previously described groups of aggregate piers that were evaluated in terms of single pier.

The group efficiency results analyzed on the basis of variation in pier length have shown no significant difference in group efficiency between short or long piers. Therefore, the obtained results can lead to a final conclusion that the efficiency of the piers within the group is independent of the length of the pier.

Based on the amount of settlement that the groups of piers had undergone, the efficiency was also compared at levels of 2 mm, 5 mm and 10 mm of settlement. A general conclusion can be made that for the most piers a trend of reduction in group efficiency was observed with increasing amount of settlement. This observation is consistent with the reduction of group efficiency trend observed in case with earlier described groups of aggregate piers.

Finally, by looking at the influence of number of piers within the group on the overall group efficiency results, no definitive conclusion could be made due to a very close margin of variation in the calculated efficiency values. The unit cell was observed to have group efficiency in the vicinity of 0.7, while group of six had the efficiency of 0.4, thus, it can be speculated that there is some evidence for the reduction in efficiency with increasing number of piers within the group. However, in order to confirm the hypothesis more testing would be required.

Having obtained similar test results between tested groups of aggregate pier and cement type I and K composition groups, it must be noted that the group efficiency results calculated for I and K composition groups were found within 0.4 - 0.9 margin, while almost all aggregate

www.manaraa.com

pier group efficiency values were found to be greater than one. Therefore, one main difference observed in the behavior of tested groups can be made that the performance of a single cement type I and K pier within the group of piers could not achieve efficiency of an isolated pier efficiency, while a pier within group of aggregate piers behaved at efficiency significantly exceeding 1.0.

The group efficiency values obtained for cementitious composition groups of piers were also found tot be consistent with field observation and results obtained by other researchers (Table 33).

Aggregate Piers vs. C(I) + C(K) - Load-settlement

Having evaluated information for groups of aggregate piers and cement type I and K composition piers on the individual basis, a side by side comparison can be made between the stiffness values for aggregate piers and cement type I and K. The results are outlined in Table 39 through Table 41.

Table 39: Stiffness comparison at 2 mm displacement between groups of aggregate piers and C(I)+C(K)

Pier type	Length (mm)	$\sigma_{aggregate\ pier}$ at δ_{top} = 2 mm (kPa)	Pier type	σ_{I+K} at δ_{top} = 2 mm (kPa)	n. stiffness ratio
Aggregate Pier Unit Cell	305	348	C(I) + C(K) Unit Cell	640	1.8
	610	894		794	0.9
Aggregate Pier Single Pier	305	129	C(I) + C(K) Single Pier	908	7.0
	610	352		1,083	3.1
Aggregate Pier Group of 2	305	483	C(I) + C(K) Group of 2	1,266	2.6
	610	1,260		1,542	1.2
Aggregate Pier Group of 4	305	867	C(I) + C(K) Group of 4	1,921	2.2
	610	1,596		N/A	N/A
Aggregate Pier Group of 5	305	1,529	C(I) + C(K) Group of 5	2,377	1.6
	610	3,511		3,148	0.9
Aggregate Pier Group of 6	305	3,073	C(I) + C(K) Group of 6	3,355	1.1
	610	3,134		2,896	0.9

www.manaraa.com

Table 40: Stiffness comparison at 5 mm displacement between groups of aggregate piers and C(I)+C(K)

Pier type	Length (mm)	$\sigma_{aggregate\ pier}$ at δ_{top} = 5 mm (kPa)	Pier type	σ_{I+K} at δ_{top} = 5 mm (kPa)	n. stiffness ratio
Aggregate Pier Unit Cell	305	588	C(I) + C(K) Unit Cell	968	1.6
	610	1,330		1,241	0.9
Aggregate Pier Single Pier	305	247	C(I) + C(K) Single Pier	1,418	5.7
	610	704		1,841	2.6
Aggregate Pier Group of 2	305	1,345	C(I) + C(K) Group of 2	2,023	1.5
	610	2,521		2,209	0.9
Aggregate Pier Group of 4	305	2,254	C(I) + C(K) Group of 4	3,151	1.4
	610	3,105		N/A	N/A
Aggregate Pier Group of 5	305	3,233	C(I) + C(K) Group of 5	3,647	1.1
	610	4,375		4,148	0.9
Aggregate Pier Group of 6	305	4,100	C(I) + C(K) Group of 6	3,820	0.9
	610	5,361		4,818	0.9

Legend:
δ_{top} - deflection at the top of the pier (kPa)
σ – stiffness of the pier (kPa)
n –stiffness ratio

Conversions:
1 m = 3.3 ft
1 mm = 0.0394 in
1 kPa = 0.145 psi

Table 41: Stiffness comparison at 10 mm displacement between groups of aggregate piers and C(I)+C(K)

Pier type	Length (mm)	$\sigma_{aggregate\ pier}$ at δ_{top} = 10 mm (kPa)	Pier type	σ_{I+K} at δ_{top} = 10 mm (kPa)	n. stiffness ratio
Aggregate Pier Unit Cell	305	908	C(I) + C(K) Unit Cell	1,147	1.3
	610	1,533		1,460	1.0
Aggregate Pier Single Pier	305	406	C(I) + C(K) Single Pier	1,806	4.4
	610	949		2,065	2.2
Aggregate Pier Group of 2	305	2,146	C(I) + C(K) Group of 2	2,400	1.1
	610	3,017		2,869	1.0
Aggregate Pier Group of 4	305	3,406	C(I) + C(K) Group of 4	3,609	1.1
	610	3,947		N/A	N/A
Aggregate Pier Group of 5	305	4,150	C(I) + C(K) Group of 5	4,225	1.0
	610	4,825		4,630	1.0
Aggregate Pier Group of 6	305	4,898	C(I) + C(K) Group of 6	4,096	0.8
	610	7,068		5,672	0.8

Legend:
δ_{top} - deflection at the top of the pier (kPa)
σ – stiffness of the pier (kPa)
n –stiffness ratio

Conversions:
1 m = 3.3 ft
1 mm = 0.0394 in
1 kPa = 0.145 psi

www.manaraa.com

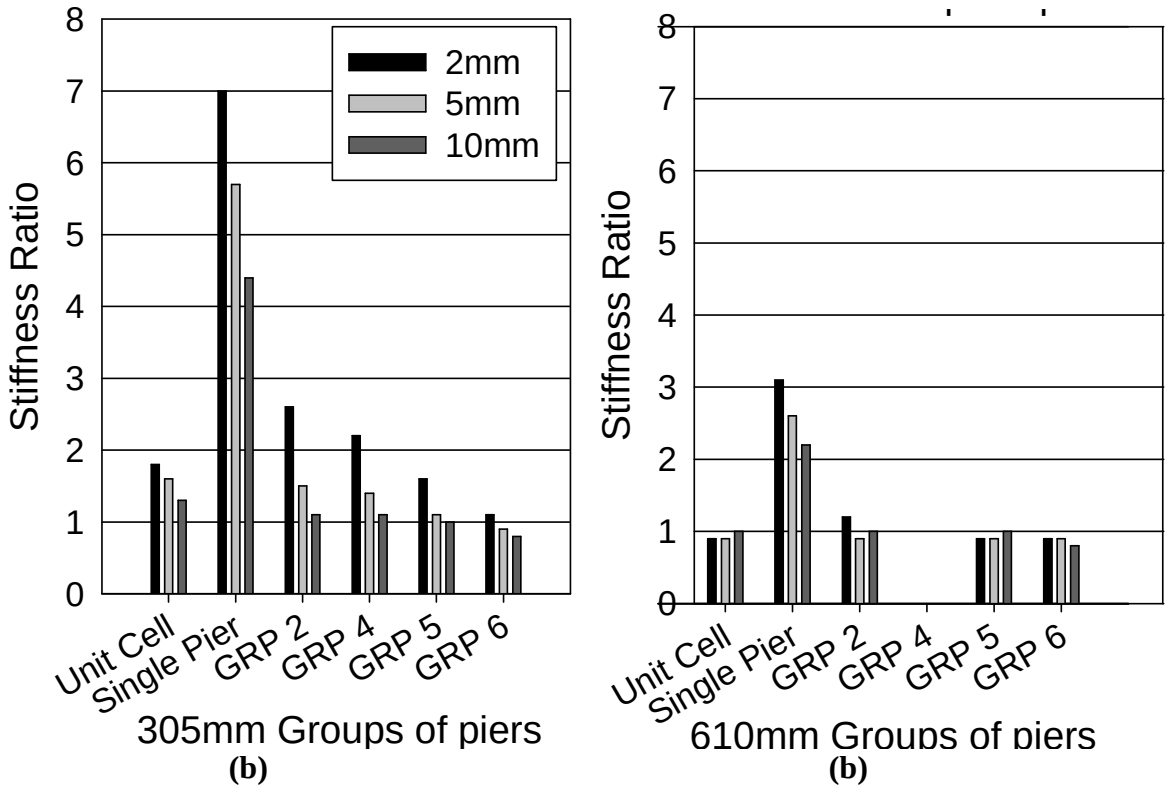

Figure 91: Stiffness ratio comparison between (a) 305 mm and (b) 610 mm long C(I) + C(K) composition piers and aggregate piers

By utilizing information summarized in Table 39 through Table 41 and Figure 91 a conclusion can be made where the difference between the aggregate pier and cement type I and K stiffness values was negligent for most groups of two, four, five and six piers at ultimate load. Therefore, independently of the material being used, the groups of two, four, five and six piers were able to bear the same amount of stress imposed on the piers. Contrarily, a very significant difference in the stiffness behavior of single aggregate pier and cement type I and K composition pier was observed.

Another observation that can be made is the greater stiffness ratio difference between the two types of pier groups for shorter piers. Therefore, speculation can be made that as the dimensions of the piers were to increase the difference in stiffness of aggregate pier and cement type I and K composition piers in general was reduced.

www.manaraa.com

Aggregate Piers vs. C(I) + C(K) - Group Efficiency

In general, efficiency of pier with the group of aggregate piers varied between two and three for short piers and one and two for long piers. On the other hand, the efficiency of cement type I and K pier within the group was observed no to exceed a value of 1.0. Thus, the performance of single pier within the group of aggregate piers is much greater than for the piers composed of cement type I and K.

Another major conclusion applicable for both groups of aggregate piers and cementitious piers can be made where a reduction in the group efficiency was observed with increasing amount of load imposed or settlement that the group had undergone. Thus, the efficiency of a group of piers is the least at the point of failure and is much greater at the level of service load.

www.manaraa.com

CHAPTER 7: SUMMARY AND CONCLUSIONS

The section provides the concluding comments obtained for the 1/10th scale piers of different length, composition, and number within the group. The finding obtained for scaled aggregate piers are somewhat ground breaking in its nature, as very little to no research has been accomplished so far in the area. The discussion will briefly summarize the findings in the areas of best performing tamper heads, effects of material and admixtures, as well as, bearing capacity, group efficiency, and overall scientific and technical application of the obtained results. The concluding remarks are summarized in the following format:

Aggregate Piers

Tamper Heads

By evaluating performance of different beveled tamper heads, the following was concluded:

- flat tamper head was concluded to produce the least degree of aggregate pier stiffening,
- cone tamper head was capable of delivering twice the amount of energy than the truncated cone head.

Therefore, while the obtained results were consistent with expectations, a new correlation between cone and truncated cone tamper head levels of compaction was established.

Partial Grouting

Aiming towards improvement in pier strength performance, the main outcomes of grouting of the aggregate piers are provided as following:

- by cementing top 100 mm portion of the long 610 mm aggregate pier, the capability of aggregate pier to withstand the imposed stress increased by at least 25 percent for

www.manaraa.com

stiffness ratio at ultimate load level and bulging area was shifted beneath the cemented portion of the aggregate pier,

- having the bulb portion of the short 305mm. aggregate pier cemented, resulted in favor of bulging type of failure, however had no significant impact on the overall loading capacity of the pier.

Therefore, the process of cementing top 100 mm of the pier had resulted in pier capability to carry double amount of the load, while cementing of the bulb has provided no practical benefit.

Bearing Capacity

The following bearing capacity outcome results were obtained for aggregate piers:

- aggregate piers compacted in soft loess have shown increase in matrix soil load bearing capacity by a factor of 1.1-1.4,
- lab generated bearing capacity values for groups of aggregate piers were found to closely correlated to full-scale field values, however no particular pattern could be established, thus more testing would be required,
- calculated design bearing capacity values were found to be within 80% of actual bearing capacity values obtained in the lab. The methods of calculations are needed to be modified.

Laboratory generated bearing capacity values were not particularly correlated with full-scale results and thus more testing would be required. Moreover, laboratory generated bearing capacity values were higher than design calculated values, thus, calculation methods have to be modified.

www.manaraa.com

Materials

Loess-Cement

Very intriguing discoveries were produced for the loess and cement composition piers and are outlined below:

- upon the failure, shear planes were developed within the top portion of the piers,
- the piers had undergone a very sudden and brittle type of failure,
- prior to cracking the loess piers were found to develop the highest level of stiffness among all loess, cement and aggregate composition single piers.

Therefore, loess and cement composition piers have shows a lot of potential for the future investigation, where if no cracking is achieved, the composition can be beneficial due to potential for greater performance, simplicity, constructability and affordability.

Admixtures

As the admixture components were utilized in a variety of applications, the impact on overall load and pier stiffness performance was studies and the results are outline below:

- addition of fiber component to the loess and cement composition piers has proven to be ineffective and showed significant reduction in pier strength at the level of service load,
- addition of NS7 component has shown improvement in load bearing in cement composition piers at the level of service load and the opposite effect at the ultimate load,
- addition of cement type K component has shown reduction in pier stiffness at the service load and opposite effect at ultimate load.

www.manaraa.com

As a result, no definitive conclusion can be made regarding successfully utilizing cement type K or NS7 components, while addition of fiber has proven to negatively impact the strength of the pier.

Single Piers

Bulging

As some of the tested piers failed through bulging mechanism, the associated findings are provided below:

- sand, and loess, fiber composition piers failed by internal deformation or shearing,
- short sand, and loess, fiber composition piers have shown no change or reduction in stress concentration as the loads approached critical or ultimate condition,
- long sand pier was proven to increase bearing capacity by a much margin of 1.4.

Piers, failed by bulging, were found to lose their stiffness at increasing amount of imposed load and have shown to increase bearing capacity by a small factor.

Plunging

As some of the tested piers failed through plunging mechanism, the associated findings are provided below:

- the cement type I and K composition single pier was found to provide better load resistance than unit cell,
- cementitious composition piers had a significant improvement in bearing capacity of the matrix soil by a factor of 2-3.

Piers, failed by plunging, have shown a great improvement in bearing capacity, however single pier versus unit cell strength relationship must be verified through additional testing.

www.manaraa.com

Groups of Piers

Group of Aggregate Piers

Several findings were discovered associated with the behavior of the aggregate piers within the group:

- the stress imposed on group of short piers was twice as less as the stress carried by the group of long piers at the same amount of settlement,
- stiffness modulus values obtained in the lab were found to be higher than the once typically obtained in the field,
- short groups of aggregate piers at service load had a consistent group efficiency value ranging between two and three independently of the number of piers within the group,
- long groups of aggregate piers at service load had a consistent group efficiency value ranging between one and two independently of the number of piers within the group,

Major findings for groups of aggregate piers have shown relationship between imposed stress and group efficiency factors in terms of pier lengths. Also, the scaling may have contributed towards the stiffer response of lab piers, thus, methods of scaling must be revisited.

Group of C(I) + C(K) Piers

Several findings were discovered associated with the behavior of the cement type I and K composition piers within the group:

- a single cement type I and K composition pier within the group of piers could not achieve efficiency of an isolated pier efficiency of 1.0,
- group efficiency lab generated values were found to closely correlate to the field group efficiency values,
- at the same amount of settlement short piers were able to resist less load than long piers.

www.manaraa.com

Group of Aggregate Piers versus C(I) + C(K) Piers

Several findings were discovered to be associated with the behavior of both aggregate pier and cement type I and K composition piers within the group:

- trend of reduction of the group efficiency with increasing amount of load was noticed i.e. piers and groups of piers featured greater group efficiency at service load conditions and much lesser efficiency at failure,
- regardless of the pier length, the same type of group of piers (ex. Group of 4) had produced similar amount of stiffness and resistance to the imposed load,
- independently of the material being used, the groups of two, four, five and six piers were able to bear the similar amount of stress imposed on the piers, while the stiffness ratio of single piers was greatly dependent on the pier composition material.

Important findings were discovered for the groups of piers, where the material and length parameters did not necessarily have a significant effect on the group of pier stiffness ratios.

Overall, the obtained results have exceeded any expectation. The variety of material, length, and performance of a single pier within a group discoveries are of a great benefit from the technical and scientific stand points. Moreover, the findings have opened a great variety of opportunities and options for a future and more in-depth research.

www.manaraa.com

CHAPTER 8: FUTURE RESEARCH

The future research will involve continuation of testing of the loess-cement composition piers within a group of piers, as well as, an attempt will be made towards modifying the composition to avoid development of cracking ad shear planes within top portion of the pier.

The test bed and equipment that was designed and constructed can be utilized for load testing in the future. The research can be used in many different applications where specimen is to be confined in soil and loaded in the vertical direction.

Having obtained the stiffer aggregate piers in the lab than in the field suggests that the modification is to be made to the scaling and construction methods.

There is a lot of potential for development of new methods of pier construction. The design of beveled heads is one of them and could be subjected to modification.

Finally, the tendency for matrix soil cracks to propagate radially away from the constructed pier is of a great interest, where if one understands the way matrix soil behaves when failed, the possible improvement can be made and, therefore, enhancement in the soil-pier system can be achieved.

www.manaraa.com

REFERENCES

AISC (2007). "American Institute of Steel Construction Manual of Steel Construction ASD and LRFD." AISC, USA.

Allgood, C., Weppler, L., Lien, B.H., and Fox, N.S. (2003). "GEOPIER Intermediate Foundation Systems – Case Studies for Building Foundations over Soft Soils and Peat." *Nottingham Problematic Soils Conference, Nottingham, United Kingdom.*

ASTM D2166-00. "Standard Test Method for Unconfined Compressive strength of Cohesive Soil." Copyright ASTM International, West Conshohocken, PA.

ASTM D3080-04. "Standard Test Method for Direct Shear Test of Soils Under Consolidated Drained Conditions." Copyright ASTM International, West Conshohocken, PA.

ASTM D422-63. "Standard Test Method for Particle-Size Analysis of Soils." Copyright ASTM International, West Conshohocken, PA.

ASTM D698-00. "Standard Test Methods for Laboratory Compaction Characteristics of Soil Using Standard Effort (12,000 ft-lbf/ft^3 (600 kN-m/m^3))." Copyright ASTM International, West Conshohocken, PA.

ASTM D7013-04. "Standard Guide for Nuclear Surface Moisture and Density Gauge Calibration Facility Setup." Copyright ASTM International, West Conshohocken, PA.

Bachus, R.C., and Barksdale, R.D. (1984). "Vertical and Lateral Behavior of Model Stone Columns." *Proceedings, International Conference of In-situ Soil and Rock,* Paris, p. 99-104.

Balaam, N.P., Poulos, H.G., and Brown, P.T. (1977). "Settlement Analysis of Soft Clays Reinforced with Granular Piles."*5th Southeast Asian Conference on Soil Engineering.* Vol 1, Bangkok, Thailand, p. 81-91.

Barksdale, R.D., and Bachus, R.C. (1983). "Design and Construction of Stone Columns." Report FHWA/RD-83/026, National Technical Information Service, VA.

www.manaraa.com

Black, J.A., Sivakumar, V., Madhav, M.R., and Hanill, G.A. (2007). "Reinforced Stone Columns in Weak Deposits: Laboratory Model Study." *Journal of Geotechnical and Geoenvironmental Engineering.* Vol 133, No. 9, p. 1154-1161.

Black, J., Sivakumar, V., and McKinley, J.D. (2007). "Performance of Clay Samples Reinforced with Vertical Granular Columns." *Canadian Geotechnical Journal.* Vol 44, p. 89-95.

Bowles, J.E. (1978). "Engineering Properties of Soils and their Measurements." *McGraw-Hill, Inc.* USA.

Bucher, S., Bullard, J., and Parra, J.R. (2008). "Comparison of Load results and Performance of the Rammed Geopier System in Undocumented Fill in Urban Areas." *15th Annual Great Lakes geotechnical/Geoenvironmental Conference,* Carmel, IN.

Burnham, T., and Johnson, D. (1993). "In-Situ Foundation Characterization Using the

Dynamic Cone Penetrometer." Final Report MN/RD-93/05, Minnesota Department of Transportation, St. Paul, MN.

Construction of Great Pyramids (2002). "Mystic Places." World Mysteries. http://www.world-mysteries.com/mpl_2_1asok.htm (Oct. 30, 2009)

Cox, W.R., Dixon, D.A., and Murphy, B.S. (1984). "Lateral-load Tests on 25.4mm Diameter Piles in Very Soft Clay in Side-by-side and in-line Groups." *Laterally Loaded Deep Foundations: Analysis and Performance,* ASTM STP 835, p. 122-139.

Das, B.M. (2006). "Principles of Geotechnical Engineering." *McGraw-Hill, Inc.* USA.

Fang, Z., and Yin, H. (2007). "Responses of Excess Pore Water Pressure in Soft Marine Clay around a Soil Cement Column." *International Journal of Geomechanics.* Vol 7, No. 167, 9. 167-175.

www.manaraa.com

FHWA (1999). “Portland Cement.” U.S. Department of Transportation, FHWA. http://www.fhwa.dot.gov/infrastructure/materialsgrp/cement.html (Oct. 15, 2007=9).

Fox, N.S., and Cowell, M.J. (1998). “Geopier Foundation and Soil Reinforcement Manual.” RAP Foundation Manual, RAP Foundation Company, Inc., Scottsdale, AZ.

Fox, N.S., Weppler, L.R., and Scherbeck, R. (2004). “Geopier Soil Reinforcement System – Case Histories of High Bearing Capacity Footing Support and Floor Slab Support.” *Fifth International Conference on Case Histories in Geotechnical Engineering,* New York, NY.

FitzPatrick, B.T., Wissmann, K.J., and White, D.J. (2003). “Settlement Control for Embankment and Transportation – Related Structures using Geopeir Soil Reinforcement.” *Technical Bulletin, No.6,* Geopier Foundation Co., Inc., Scottsdale, AZ.

FitzPatrick, B.T., and Wissmann, K.J. (2002). “Geopier Shear Reinforcement for Global Stability and Slope Stability.” *Technical Bulletin, No.5,* Geopier Foundation Co., Inc., Scottsdale, AZ.

FitzPatrick, B.T., and Wissmann, K.J. (2006). “Vibration and Noise Levels.” *Technical Bulletin, No.9,* GEOPIER Foundation Co., Inc., Scottsdale, AZ.

GFC Newsletter (2000). “The Ice House Hackensack, New Jersey.” News Letter, GEOPIER Foundation Company, Mooresville, NC. http://o.b5z.net/i/u/10034179/i/G-H001_LR.pdf (Oct. 18, 2009).

Handy R.L., and Spangler, M.G. (2007). “Geotechnical Engineering Soil and Foundation Principles and Practice.” *McGraw-Hill, Inc.* USA.

Handy, R.L. (1973). “Collapsible Loess in Iowa.” *Soil Science Society of America Journal,* Vol 37, Ames, IA, p. 281-284.

Handy, R.L. (2001). “Does Lateral Stress Really Influence Settlement?” *ASCE Journal of Geotechnical and Geoenvironmental Engineering.* Vol 127, No. 7, Ames, IA, p. 623-636.

www.manaraa.com

Hanlong, L., An, D., and Yang, S. (2008). "Shear Behavior of Coarse Aggregates for Dam Construction under Varied Stress Paths." *Water Science and Engineering Journal,* Vol 1, No. 1, Nanjing, China, p. 63-77.

Harrison, J.A. (1987). "Correlation between California Bearing Ratio and Dynamic Cone Penetrometer Strength Measurements of Soils". *Proceedings Institution of Civil Engineering,* Part 2, Bandung, Indonesia, p. 833-844.

Holtz, R.D., and Kovacs, W.D. (1981). "An Introduction to Geotechnical Engineering." *Prentice-Hall, Inc.* Englewood Cliffs, NJ.

Hughes, J.M.O., and Withers, N.J. (1974). "Reinforcing of Soft Cohesive Soils with Stone Columns." *Journal of Ground Engineering.* Vol 17, No. 3, London, p. 42-49.

Ilyas, T., Leung, C.F., Chow. Y.K., and Budi, S.S. (2004). "Centrifuge Model Study of Laterally Pile Groups in Clay." *Journal of Geotechnical and Geoenvironmental Engineering,* Vol 130, No. 3, Indonesia, p. 274-283.

Jian, W., and Park, Y. (2007). "Drained Triaxial Compression Test on 21b and No. 57 Gravels." Virginia Polytechnic Institute and State University, Blacksburg, VA.

Kumbhojkar, A.S. (1993). "Numerical Evaluation of Terzaghi's N_y." *Journal of Geotechnical Engineering,* ASCE, Vol 119, No. GT3, p. 598-607.

Kwong, H.K., Fox, N.S., and Lien, B.H. (2002). "Innovative and Alternative Foundation System." *Proceedings of the 2nd INKRAP International Geotechnical Conference (IGEO-2),* Malaysia.

Lawton, E.C. (2000). "Performance of GEOPIER Foundations During Simulated Seismic Tests at South Temple Bridge on Interstate 15, Salt Lake City, UT." Final Report, University of Utah, Salt Lake City, UT.

www.manaraa.com

Lawton, E.C., and Warner, B.J. (2004). "Performance of a Group of Geopier Elements loaded in Compression to Single Geopier." Final Report, University of Utah, Salt Lake City, UT.

Lechner, K.M., and Hanagan, L. (2009). "St. Vincent Mercy Medical Center Heart Pavilion." *Final Thesis Report,* Toledo, OH.

Lien, B.H., Fox, N.S., and Kwong, H.K. (2002) "GEOPIER Floating Foundations – A Solution for Roadway Embankments over Soft Soils in Asia." *Proceedings of the 2nd World Engineering Congress,* Sarawak, Malaysia.

Lim, W.L., McDowell, G.R., and Collop, A.C. (2004). "Quantifying the Relative Strengths of Railways Ballasts." *Proceedings of the Institution of Civil Engineers,* University of Nottingham, UK, p. 107-111.

Lohnes R.A., and Kjartanson B.H. (2007). "Slope Stability of Loess revisited." *Transportation Research Record – Journal of the Transportation Research Board.* No. 1786, TRB, National Research Council, Washigton, D.C., p. 76-81.

Mehta, P.K., and Monteiro, P.J.M. (2006). "Expansive Cements Figure."University of California, Berkley, CA.

Park, D.W., and Lee, H.S. (2002). "Test Methods for Fine Aggregate Angularity Considering Resistance of Rutting." *KSCE Society of Civil Engineering Journal,* Vol 6, No. 4, Texa A&M University, College Station, Texas, p. 421-427.

Pham, H.T.V., and White, D.J. (2007). "Support Mechanism of Rammed Geopiers II: Numerical Analysis." *Journal of Geotechnical and Geoenvironmental Engineering,* Vol 133, No. 12, Ames, IA, p. 1512-1521.

Ping W.V., Yang, Z., and Gao, Z. (2002). "Field and Laboratory Determination of Granular Subgrade Moduli." *Journal of Performance of Constructed Facilities,* Vol 16, No. 4, Tellahassee, FL, p. 149-159.

www.manaraa.com

Randrup T.B., and Lichter, J.M. (2001). "Measuring Soil Compaction on Construction Sites: A Review of Surface Nuclear Gauges and Penetrometers." *Journal of Arboriculture,* Vol 27, No. 3, Savoy, IL, p. 109-117.

Rollins, M.K., and Weaver, T.J. (1997). "Statnamic Lateral Load Testing of a Full-scale Fixed-head Pile group." Report, UDOT, FHWA.

Sarsby, J.H. (1985). "The Behavior of Model Pile Groups Subjected to Lateral Loads." *38th Canadian geotechnical Conference, Theory and Practice Foundation Engineering,* Bolton, England.

Sivakumar, V., McElvey, D., Graham, J., and Hughes, D. (2004). "Triaxial Tests on Model Sand Columns in Clay." *Canadian Geotechnical Journal.* Vol 41, No. 2, p. 299-312.

Sowers, G.F. (1986). "Pile Group Behavior under Long Term Lateral Monotonic and Cyclic Loading." *Proceedings, International Conference on Numerical Methods of Offshore Piling,* Nantes, p. 286-302.

Terzaghi, K. (1943). "Theoretical Soil Mechanics." Wiley, New York.

Webster, S.L., Grau R.H., and Williams, R.P. (1992). "Description and Application of Dual Mass Dynamic Cone Penetrometer." Instruction Report GL-92-3, U.S. Army Engineer Waterways Experiment Station, Vicksburg, MS.

White, D.J., Gieselman, H.H., and Prokudin M.M. (2008). "Freeze/Thaw Investigation for Rammed Aggregate Pier Elements." Technical Report, Iowa State University. Ames, IA.

White, D.J., Gieselman, H.H., Zhao, L., and Vennapusa, P. (2009a). "Laboratory Investigation of Low Modulus, High Modulus, and Expansive Grouts." Technical Report, Iowa State University. Ames, IA.

White, D.J., Pham, H.T.V., and Hoevelkamp, K.K. (2007). "Support Mechanisms of Rammed Aggregate Piers I: Experimental Results." *Journal of Geotechnical and Geoenvironmental Engineering,* Vol 133, No. 12, Ames, IA, p. 1503-1511.

www.manaraa.com

White, D.J., Prokudin, M.M., and Gieselman, H.H. (2009b). "Full-scale Field Hydraulic Conductivity Tests – Impact Rammed Aggregate Pier Installations." Technical Report, Iowa State University, Ames, IA.

White, D.J., and Suleiman, M.T. (2004). "Design of Short Aggregate Piers to Support Highway Embankments." *Transportation Research Record – Journal of the Transportation Research Board.* No. 1868, TRB, National Research Council, Washigton, D.C., p. 103-112.

Wisconsin DOT (2003). "AASHTO No.57 Gradation Specifications." Wisconsin Department of Transportation, Madison, WI. http://training.ce.washington.edu/WSDOT/state_information/03_materials/wsdot_gradations.htm (Oct. 13, 2007).

Wissmann, K.J. (1999). "Bearing Capacity of GEOPIER – Supported Foundation Systems." *Technical Bulletin, No.2,* GEOPIER Foundation Co., Inc., Scottsdale, AZ.

Wissmann, K.J., Caskey J.M., and FitzPatrick, B.T. (2001a). "GEOPIER Uplift Resistance." *Technical Bulletin, No.3,* GEOPIER Foundation Co., Inc., Scottsdale, AZ.

Wissmann, K.J., Lawton, E.C., and Farrell, T.M. (1999). "Behavior of GEOPIER – Supported Foundation Systems During Seismic Events." *Technical Bulletin, No.1*, GEOPIER Foundation Co., Inc., Scottsdale, AZ.

Wissmann, K.J., White, D.J., and Lawton, E. (2007b). "Load Test Comparison for Rammed Aggregate Piers and Pier Groups." *Proceedings of the GeoDenver 2007 congress, geotechnical special publication.* No. 172, American Society of Civil Engineers, Denver, CO.

Wissmann, K.J., Williamson, T., Jean, C., and Ringholz, R. (2001b). "Use of GEOPIER Soil Reinforcing Elements to Support a Large Aboveground Storage Tank facility in Texas." *Independent Liquid Terminals Association 2001 Annual Operating Conference,* Houston, TX.

www.manaraa.com

Yeh, Y.K., and Mo, Y.L. (2005). "Shear Retrofit of Hollow Bridge Piers with Carbon Fiber-Reinforced Polymer Sheets." *ASCE Journal of Composites for Construction*, Vol 9, No. 4, Taipei, Taiwan, p. 327-336.

www.manaraa.com

APPENDIX

Sample Calculations

Ultimate bearing capacity for single pier

Long Aggregate Pier (Table 25)

$\sigma'_v = H_{shaft}\,\gamma_{dry\ loess} = 0.1m \times 1{,}556kg/m^3 \times 9.81m/s^2 / 1000 =$ **1.5kPa**

$\sigma'_{r.lim} = \sigma'_{r.o} + C_u\,(1+In(E/(2C_u(1+\mu)))) = 2\sigma'_v + 5.2C_u = 2 \times 1.5kPa + 5.2 \times 33kPa =$

$=$ **175kPa**

$q_{ult\ AGGREGATE\ PIER} = \sigma'_{r.lim}\ tan^2(45+ \varphi_{p\ AGGREGATE\ PIER}/2) = 175kPa \times tan^2(45+44/2) =$

$=$ **970kPa**

Short Aggregate Pier (Table 26)

$f_s = \sigma'_{v\ avg}\ tan(\varphi_s)k_{p,s} = (d_f+H_{shaft}/2)\gamma tan(\varphi_{p\ loess})tan^2(45+\varphi_{p\ loess}/2) = (25mm+305mm/2) /$

$1{,}000 \times 1{,}588kg/m^3 \times tan(30) \times tan^2(45+30/2) =$ **489kg/m²**

$q_{shaft} = 4f_s d_{shaft}H_{shaft}/d_{nominal}^{\ 2} = 4 \times 489kg/m^2 \times 9.81m/s^2 / 1{,}000 \times 305mm \times 84mm\ /\ 76^2mm^2 =$

85kPa

$q_{tip} = C_u N_c + 0.5 d_{shaft}\gamma N_\gamma + \sigma'_v N_q = 40kPa \times 37 + 0.5 \times 84mm / 1{,}000 \times 9.81m/s^2 \times$

$1{,}588kg/m^3 \times 19 / 1000 + 0.305m \times 1{,}588kg/m^3 \times 9.81m/s^2 / 1{,}000 \times 22.5 = 1{,}480kPa +$

$12.4kPa + 107kPa =$ **1,606kPa**

$q_{ult} = q_{shaft} + q_{tip} = 85kPa + 1{,}606kPa =$ **1,690kPa**

Loess (Table 26)

$q_u = 1.3c'N_c + \sigma'_v N_q + 0.3 d_{steel\ cap}\gamma N_\gamma = 1.3 \times 40kPa \times 37.2 + 1{,}550kg/m^3 \times 0.0254m \times$

$9.81m/s^2 / 1{,}000 + 0.3 \times 76mm / 1{,}000 \times 1{,}550\ kg/m^3 \times 9.81m/s^2 / 1{,}000 \times 19 = 1{,}451kPa +$

$0.4kPa + 6.6kPa =$ **1,460kPa**

www.manaraa.com

Group Efficiency

Aggregate Pier Group of Four 305mm piers at Ultimate Load level (Table 19)

Group Efficiency *= Total Load on the pier Group / (Load on the Isolated Pier x Number of Piers in the Group) = 2,254kPa / (406kPa x 4) =* ***2.1***

Ultimate load for groups of piers

Aggragte Pier Group of Two 305mm piers (Table 20)

$\boldsymbol{q_g}$ *=* $qR_s / (R_sR_a - R_a + 1) = 2{,}400kPa \times 1.5 / (1.5 \times 0.061 - 0.061 + 1) =$ ***3,490kPa***

$\boldsymbol{q_m}$ *=* $q_g / R_s = 3{,}475kPa / 1.5 =$ ***2,316kPa***

$\boldsymbol{Q} = Q_g + Q_m = q_g A_g + q_m A_m = 3{,}490kPa \times 0.0091m^2 + 2{,}316kPa \times 0.1399m^2 =$ $\boldsymbol{355 \times 10^3 kN}$

www.manaraa.com

DCPI Profiles

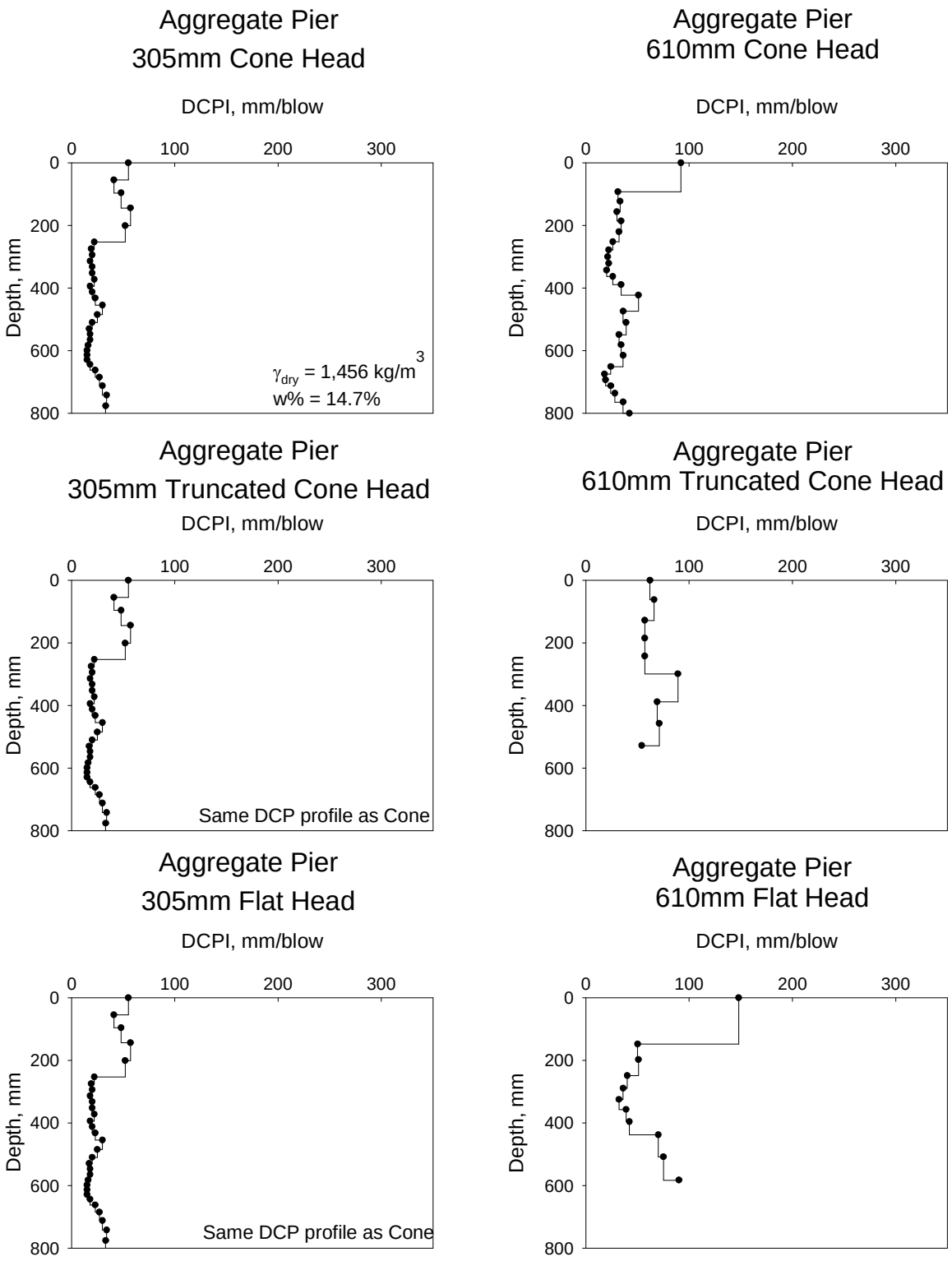

Figure 92: DCPI for single piers compacted via cone, truncated cone, and flat heads

www.manaraa.com

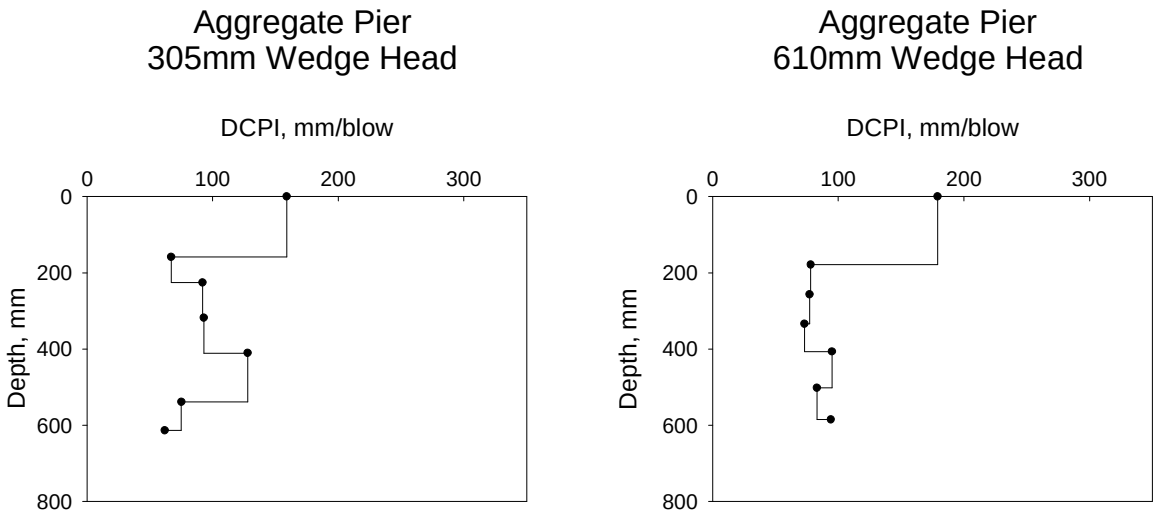

Figure 93: DCPI for single piers compacted via wedge head

www.manaraa.com

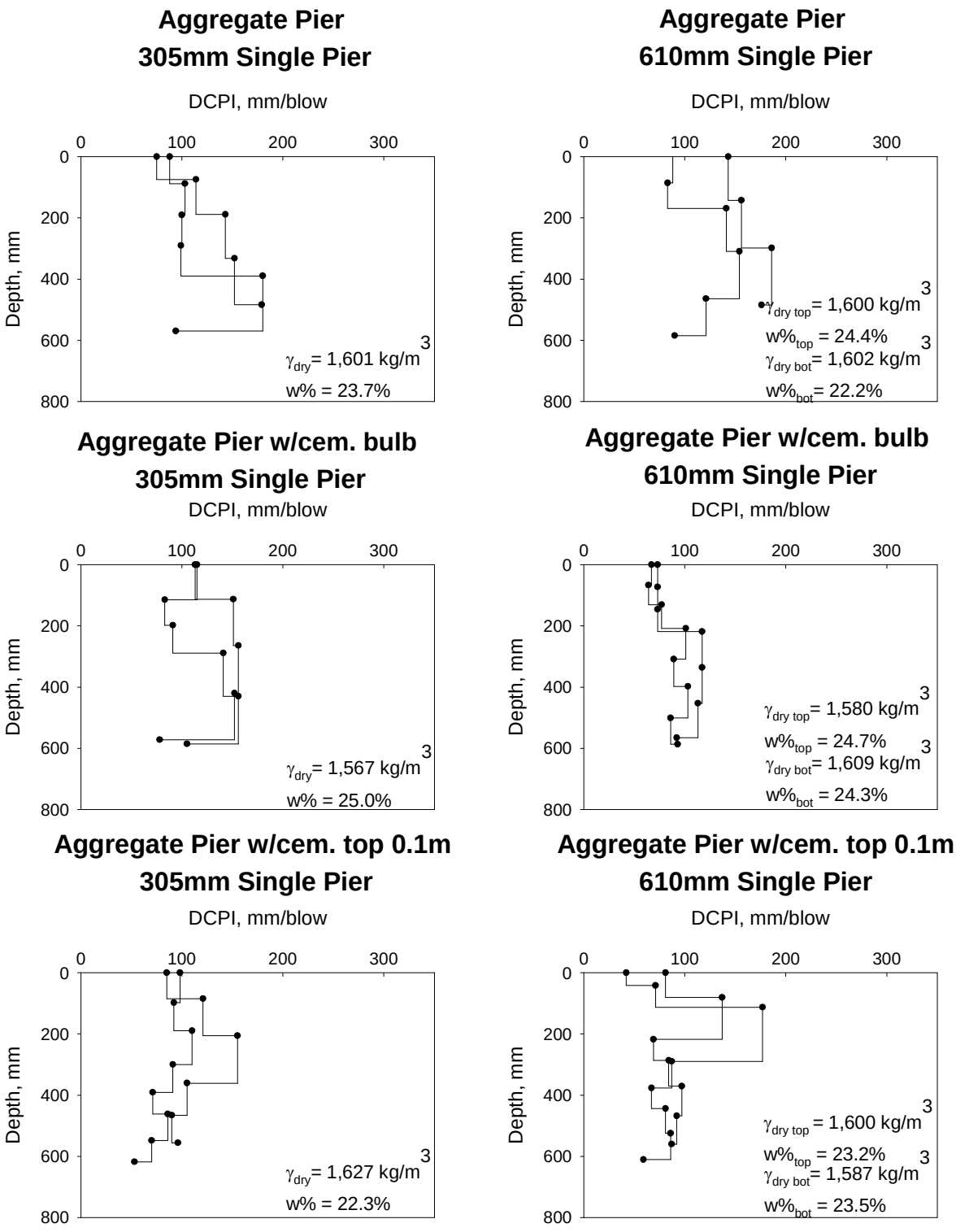

Figure 94: DCPI for single aggregate piers: aggregate pier, aggregate pier w/cem. bulb and aggregate pier w/cem. top 0.1m

www.manaraa.com

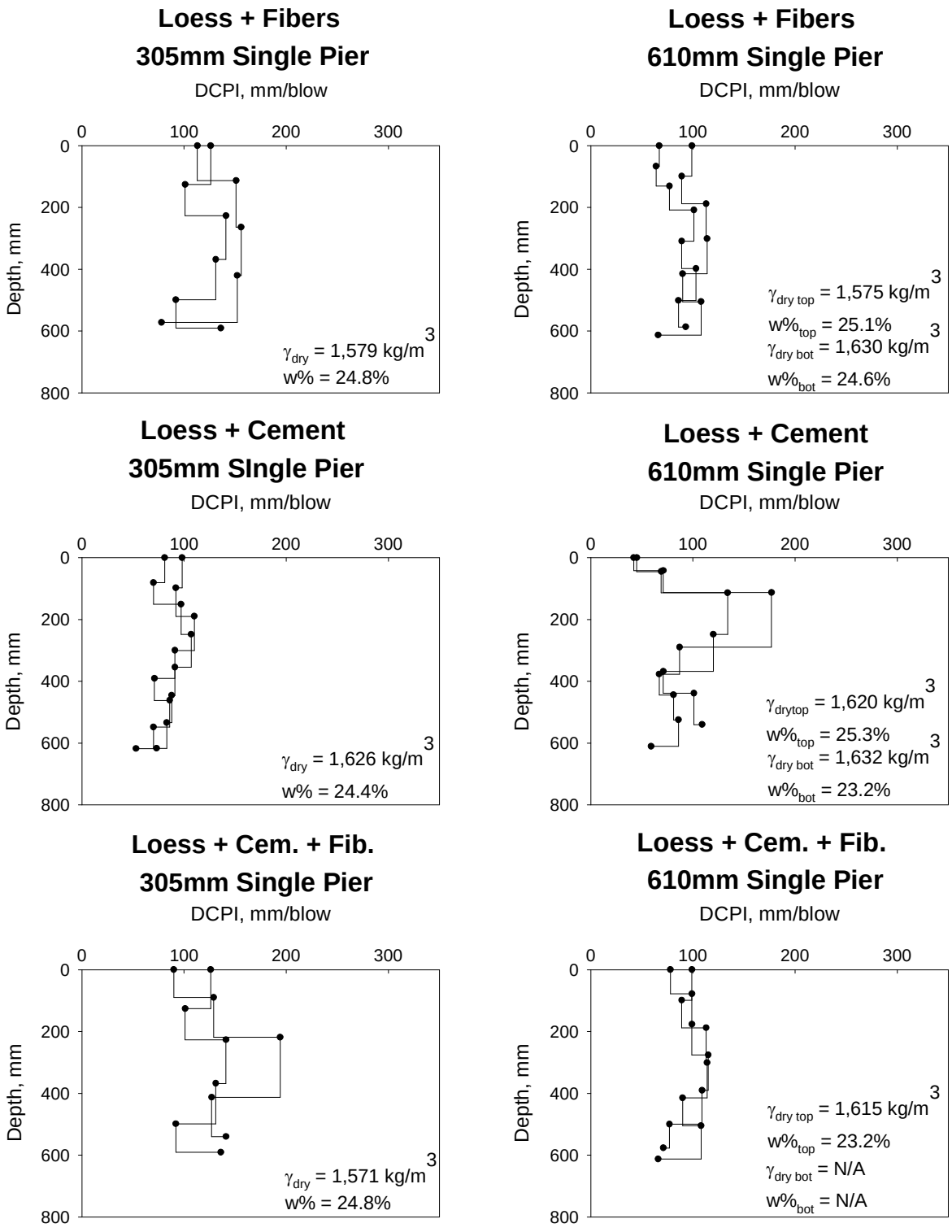

Figure 95: DCPI for single loess piers: loess+fibers, loess+cement, loess+cement+fibers

www.manaraa.com

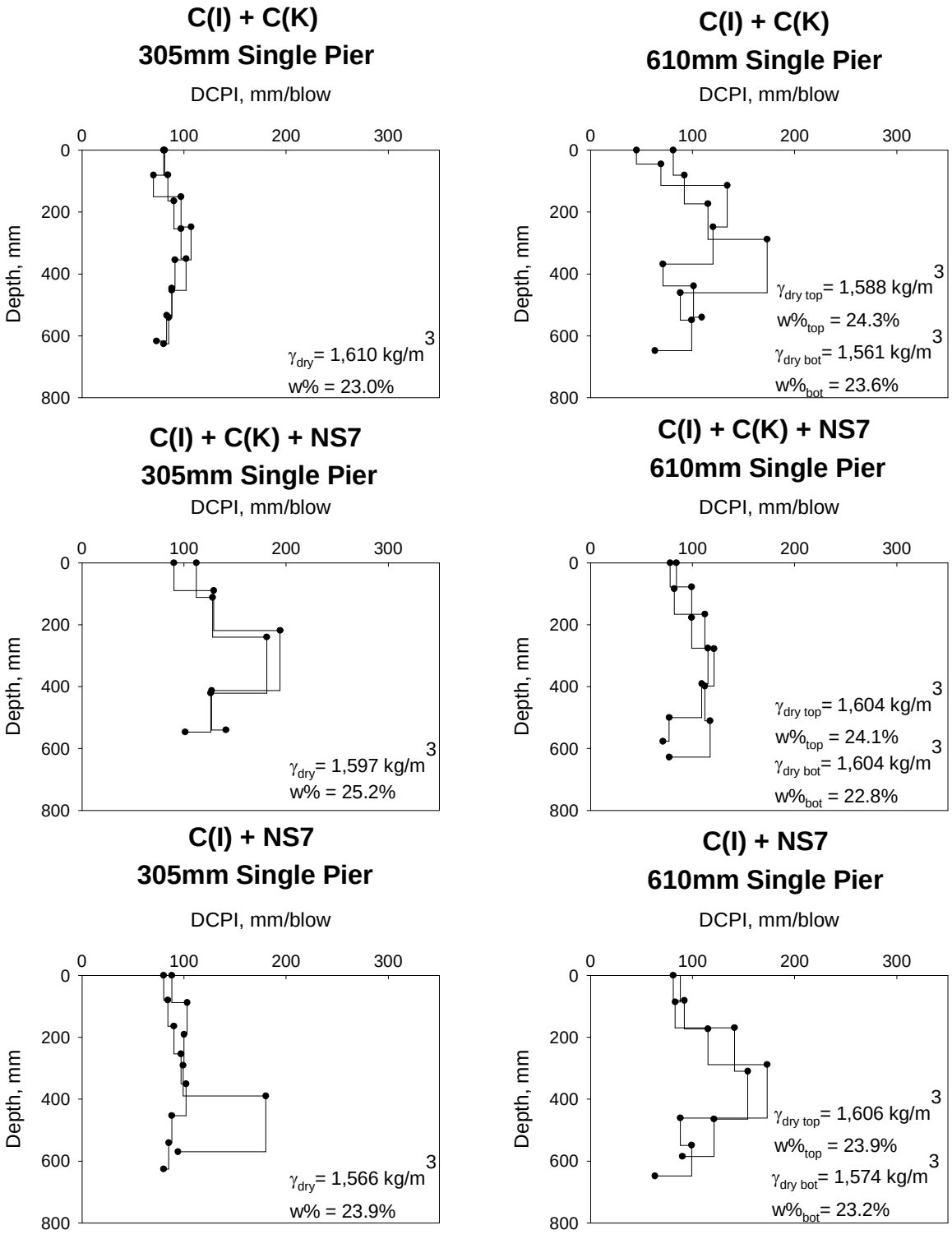

Figure 96: DCPI for single cement piers: C(I) + C(K), C(I) + C(K) + NS7, C(I) + NS7

www.manaraa.com

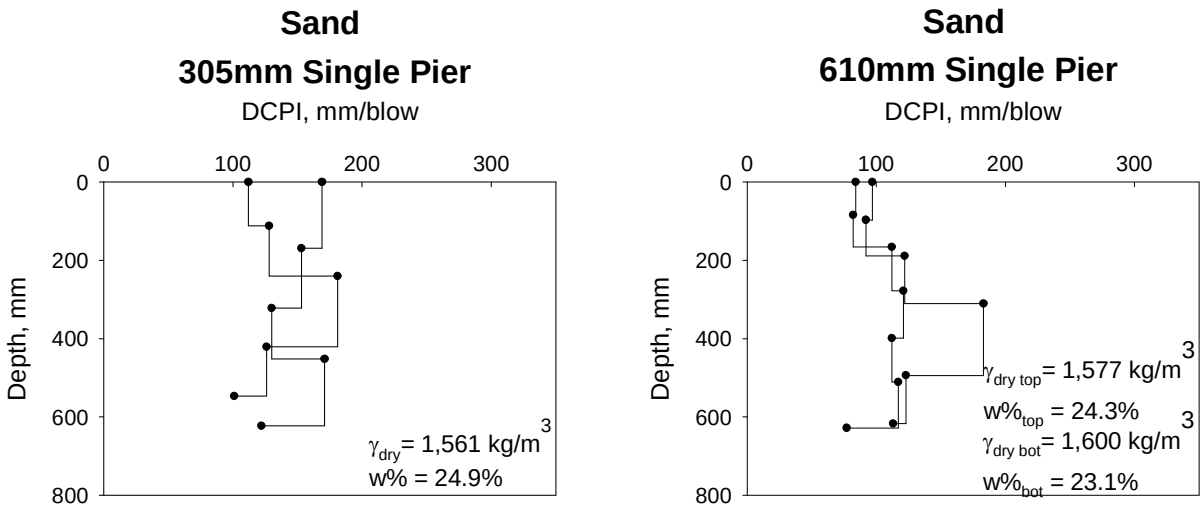

Figure 97: DCPI for single sand piers

www.manaraa.com

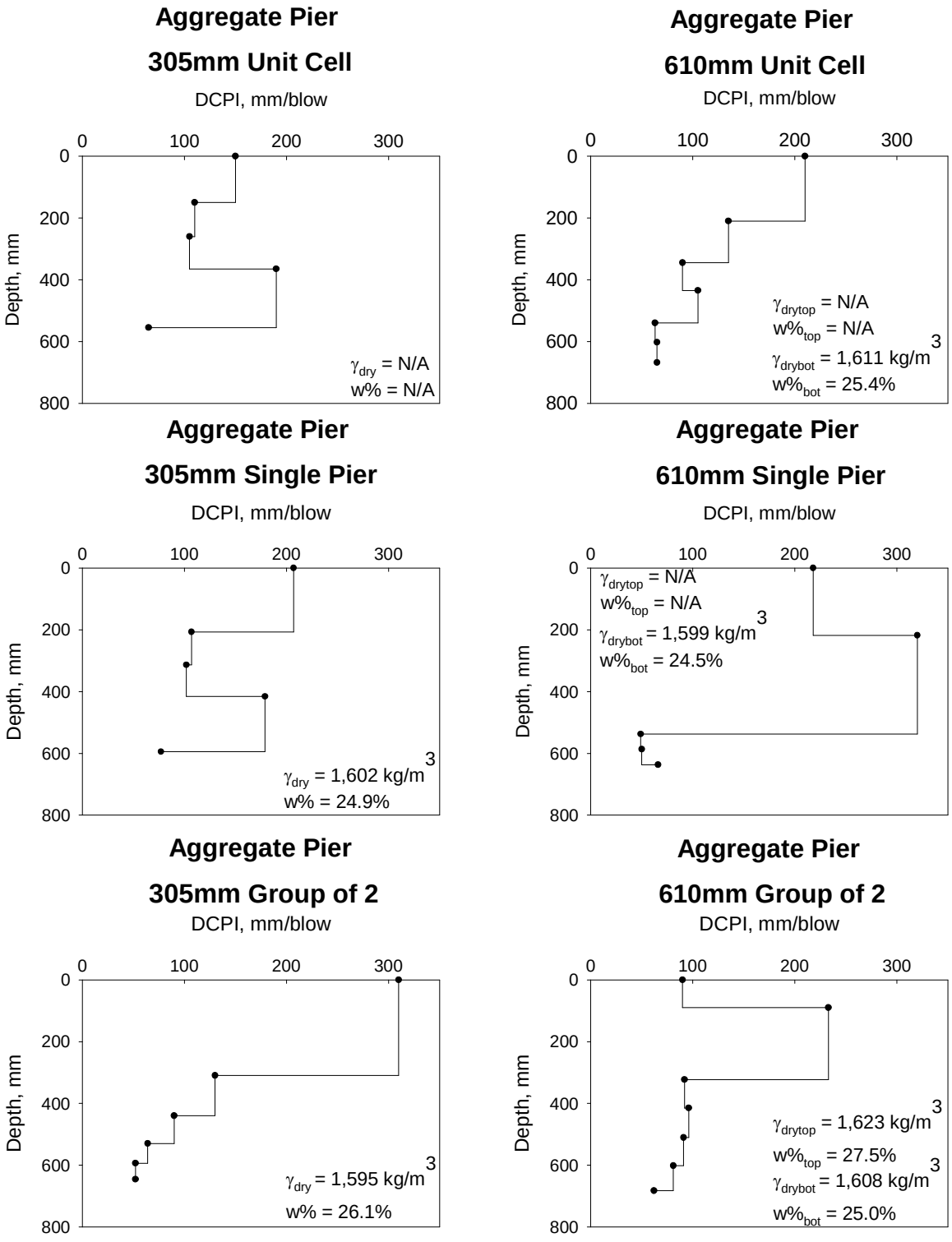

Figure 98: DCPI for group aggregate piers: unit cell, single pier, group of 2

www.manaraa.com

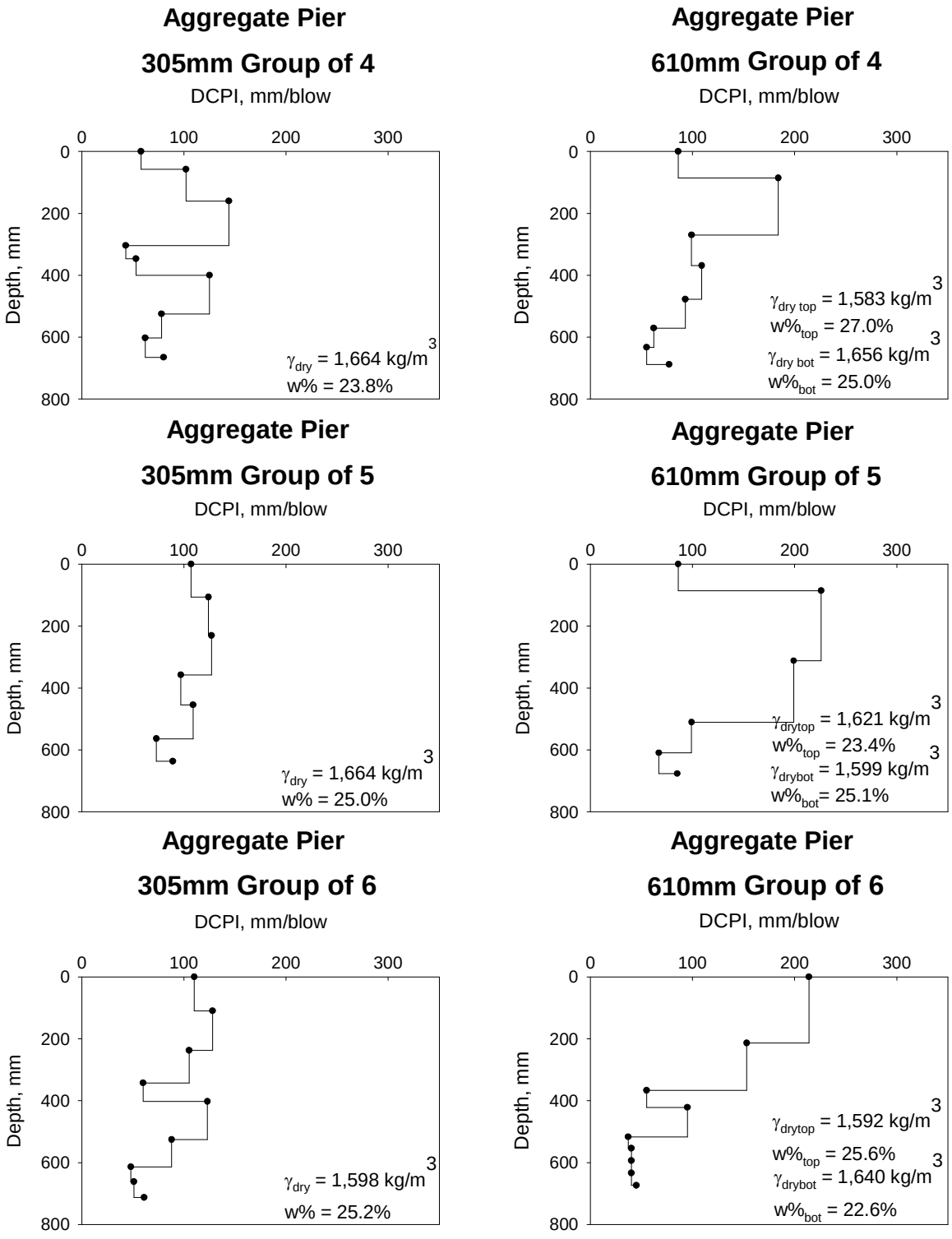

Figure 99: DCPI for group aggregate piers: group of 4, group of 5, group of 6

www.manaraa.com

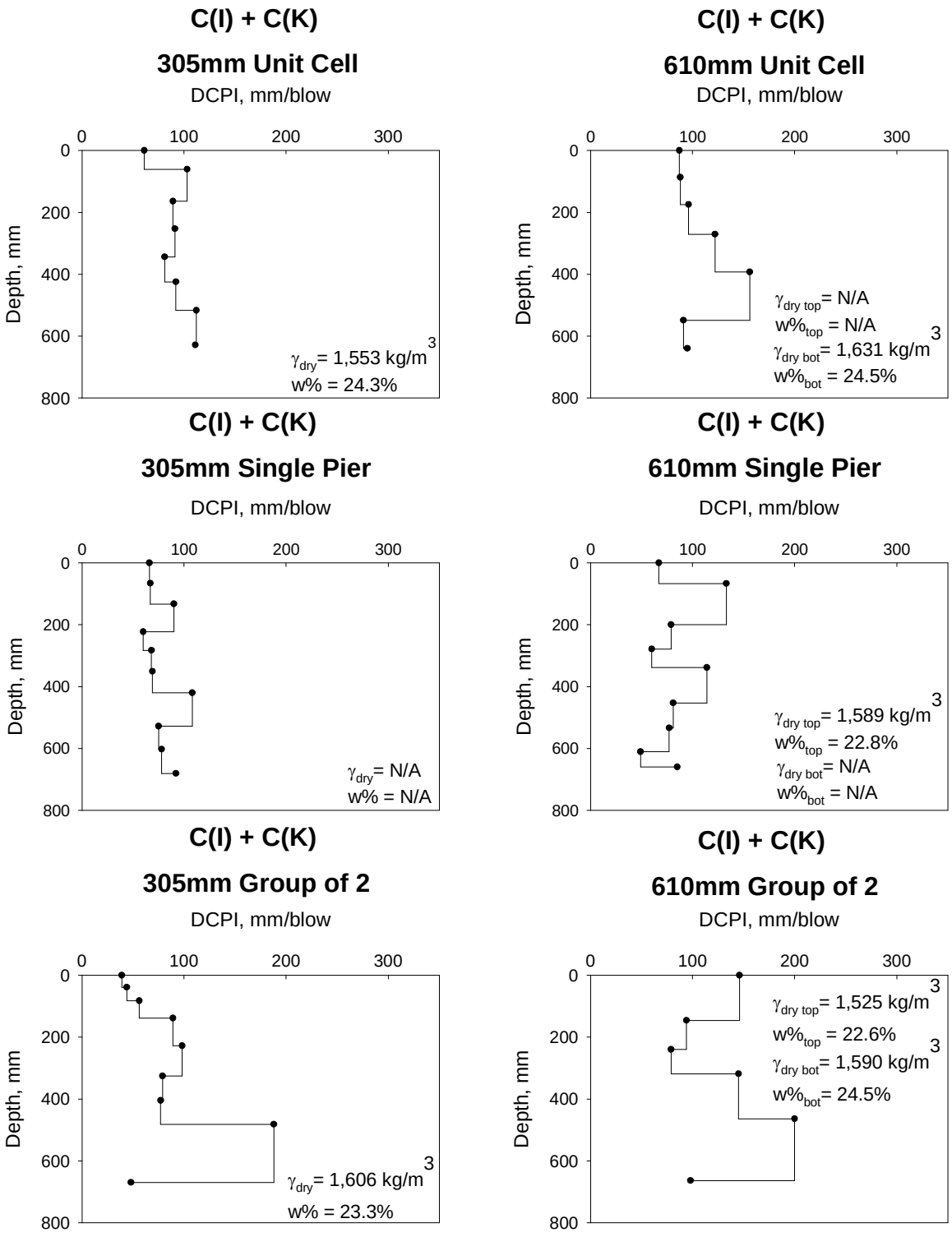

Figure 100: DCPI for group C(I) + C(K) piers: unit cell, single pier, group of 2

www.manaraa.com

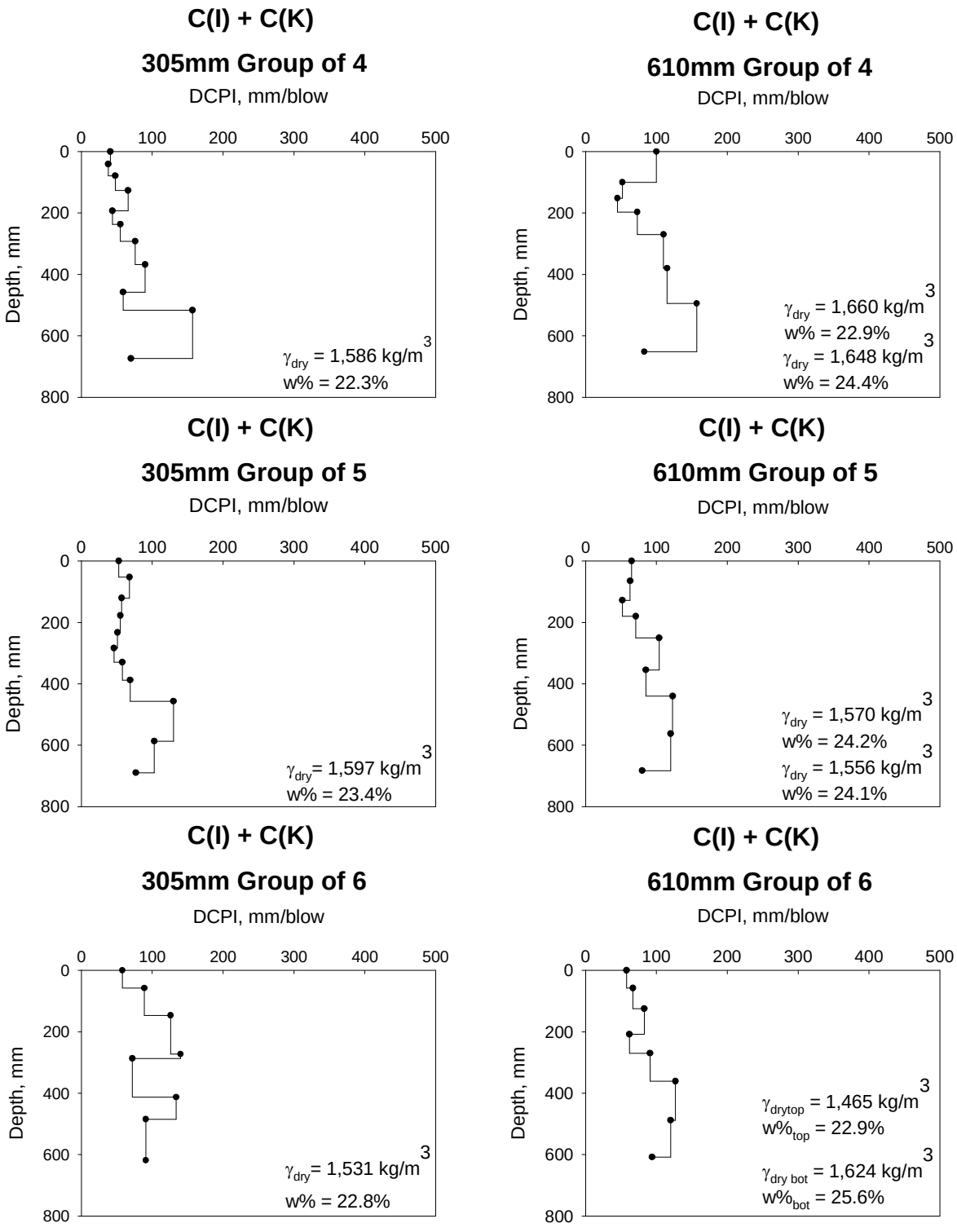

Figure 101: DCPI for group C(I) + C(K) piers: group of 4, group of 5, group of 6

www.manaraa.com

CBR Profiles

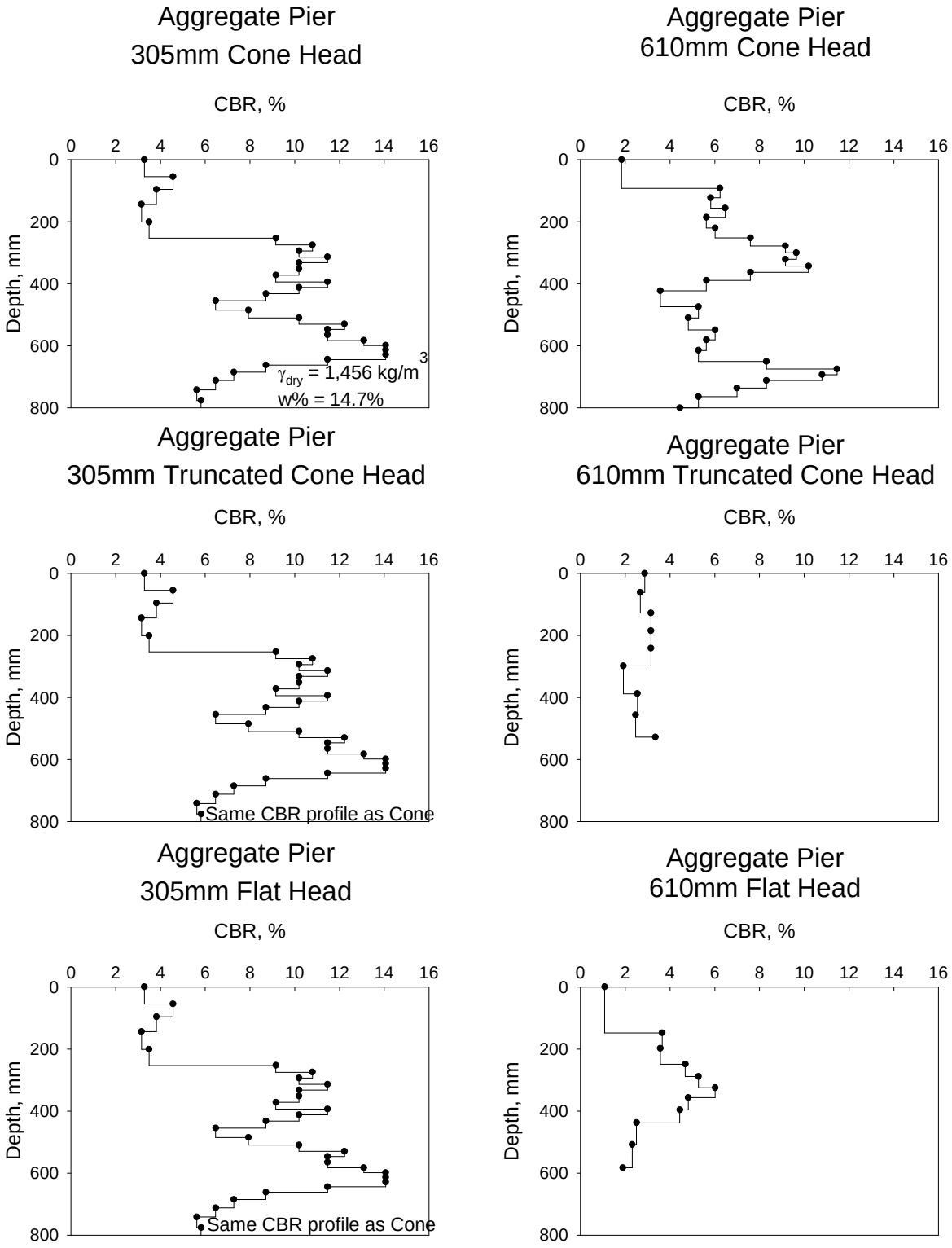

Figure 102: CBR for single piers compacted via cone, truncated cone, and flat heads

www.manaraa.com

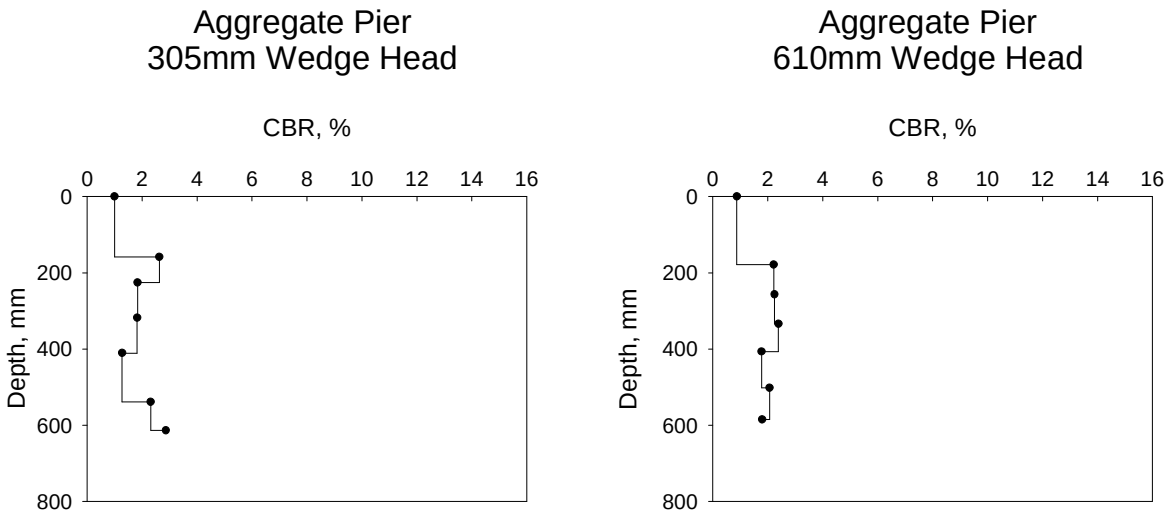

Figure 103: CBR for single piers compacted via wedge head

www.manaraa.com

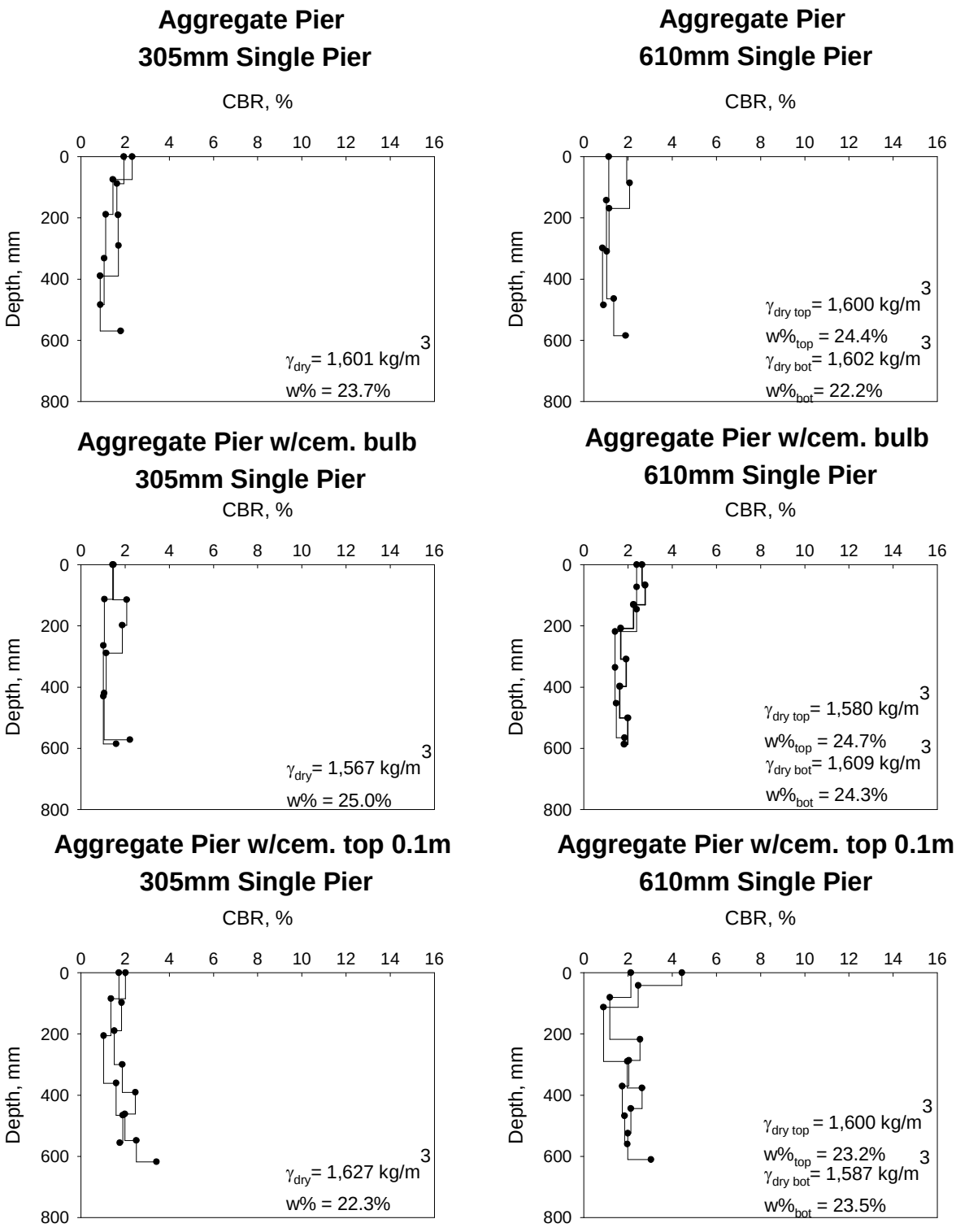

Figure 104: CBR for single aggregate piers: aggregate pier, aggregate pier w/cem. bulb and aggregate pier w/cem. top 0.1m

www.manaraa.com

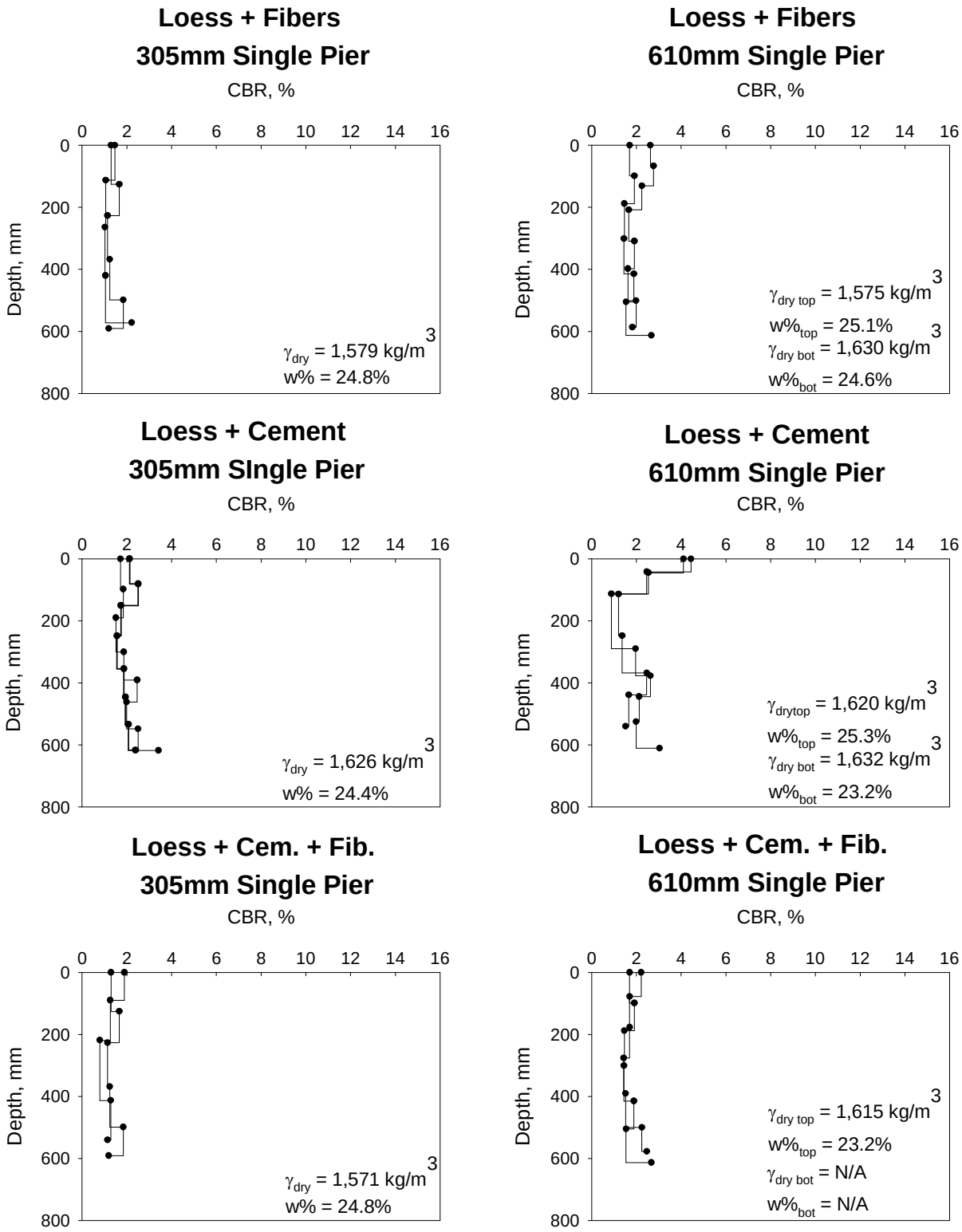

Figure 105: CBR for single loess piers: loess+fibers, loess+cement, loess+cement+fibers

www.manaraa.com

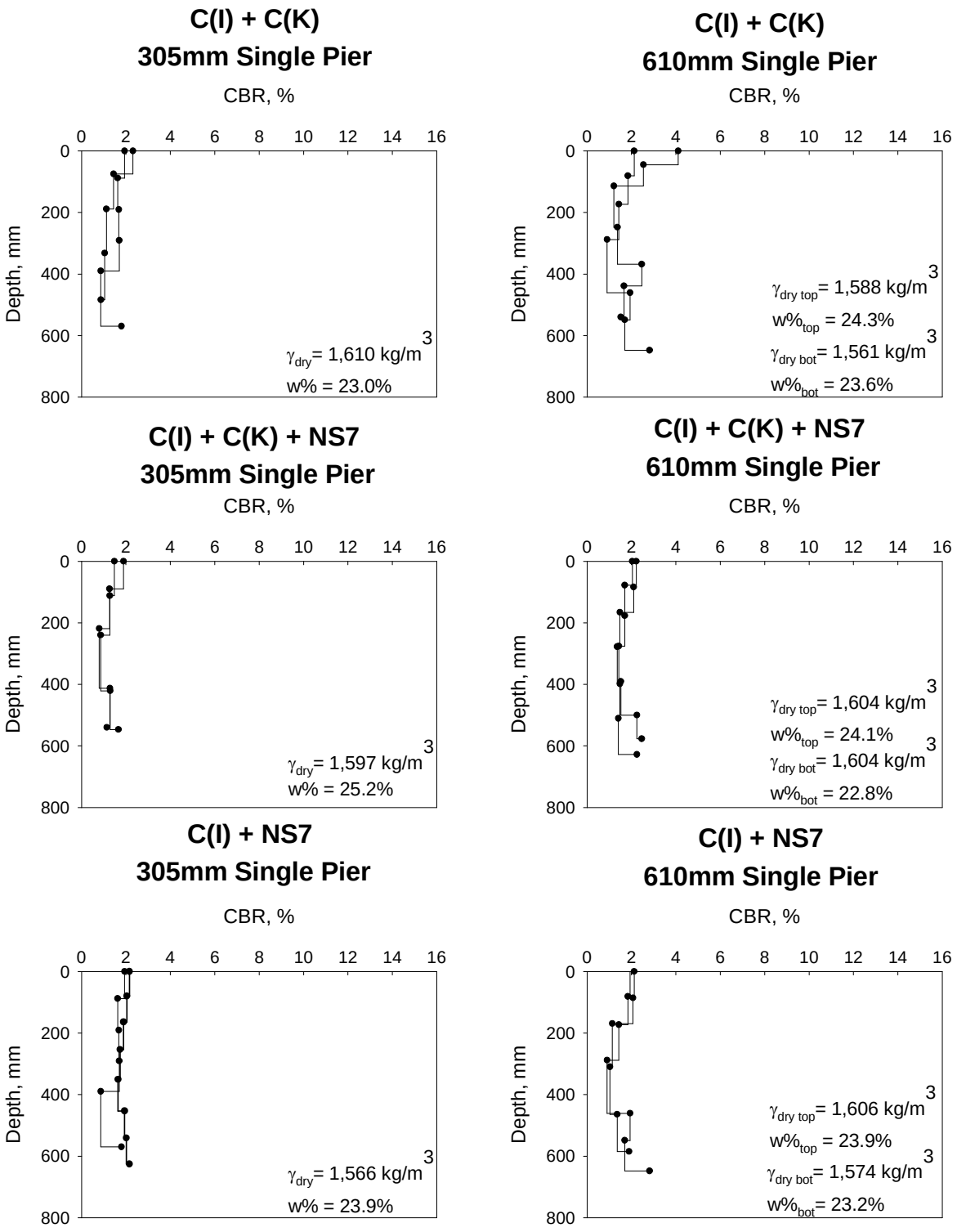

Figure 106: CBR for single cement piers: C(I) + C(K), C(I) + C(K) + NS7, C(I) + NS7

www.manaraa.com

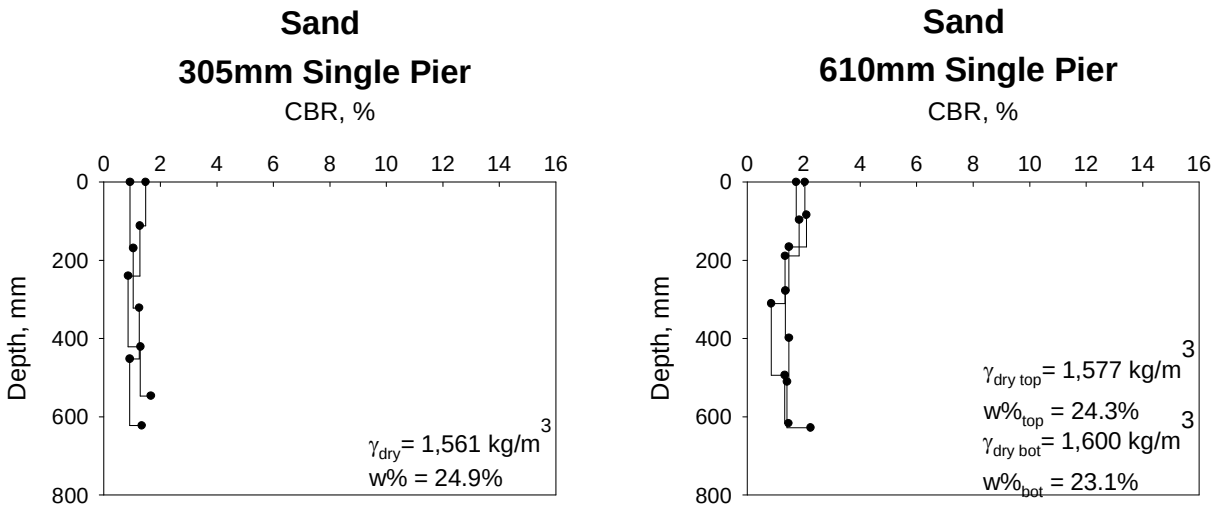

Figure 107: CBR for single sand piers

www.manaraa.com

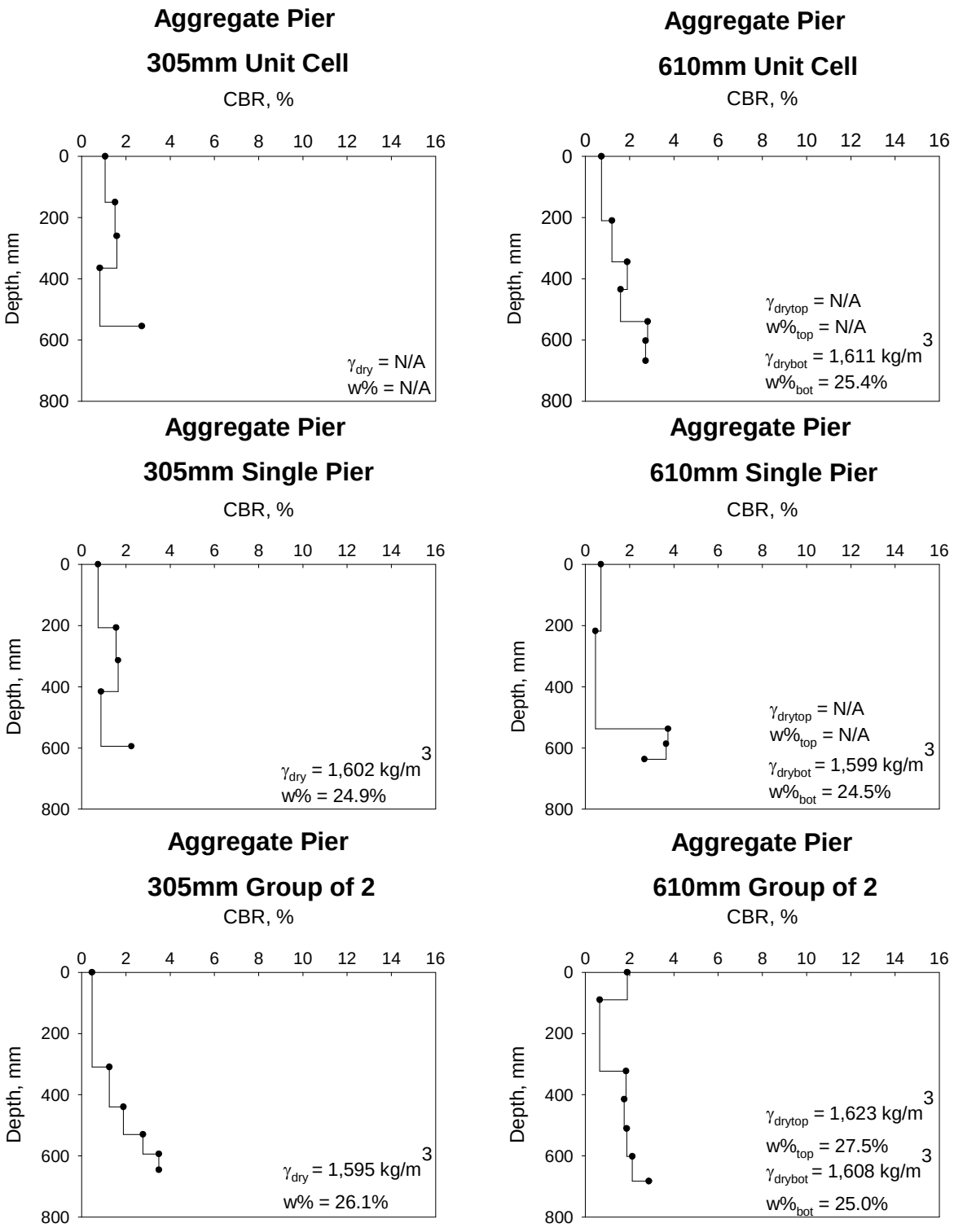

Figure 108: CBR for group aggregate piers: unit cell, single pier, group of 2

www.manaraa.com

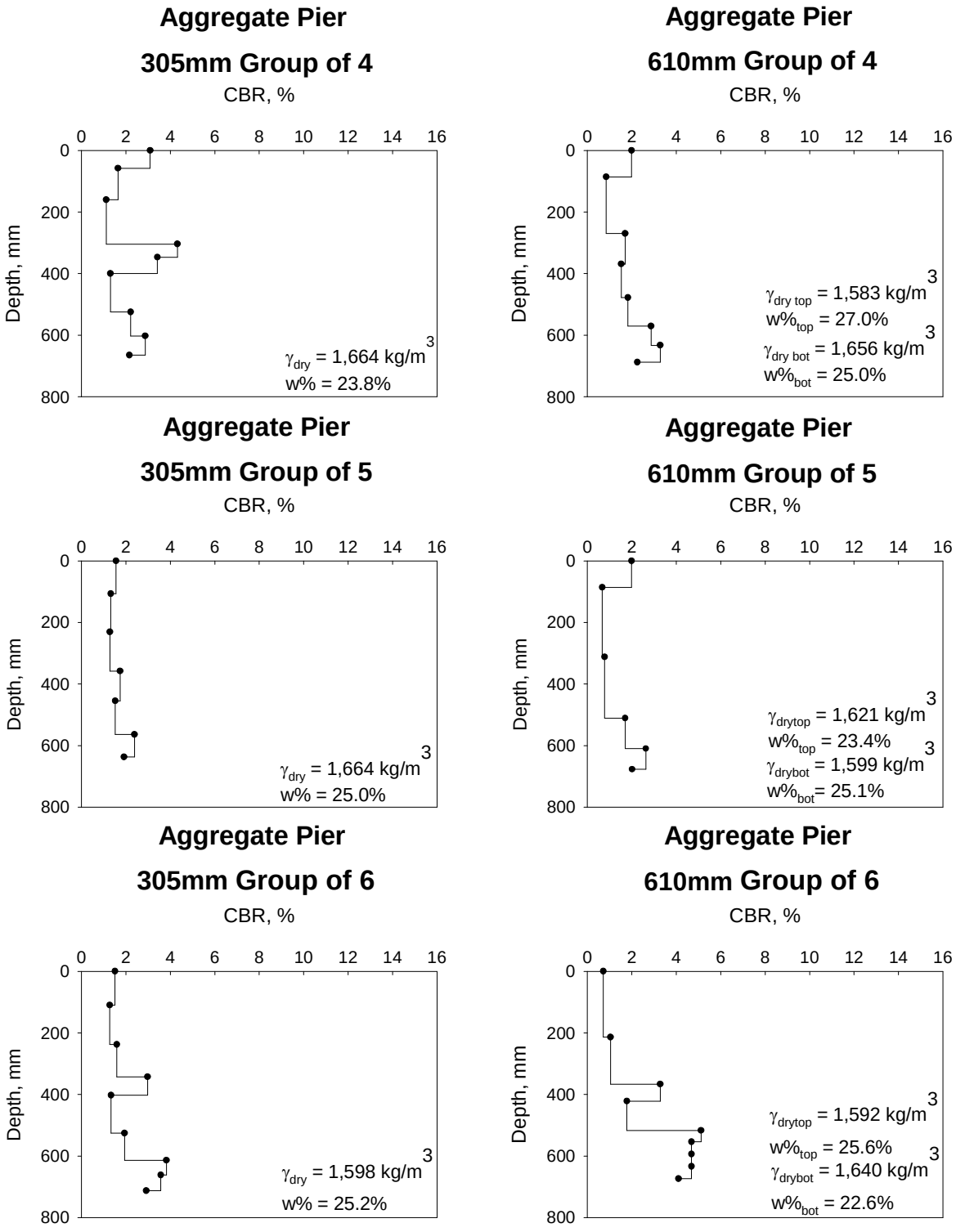

Figure 109: CBR for group aggregate piers: group of 4, group of 5, group of 6

www.manaraa.com

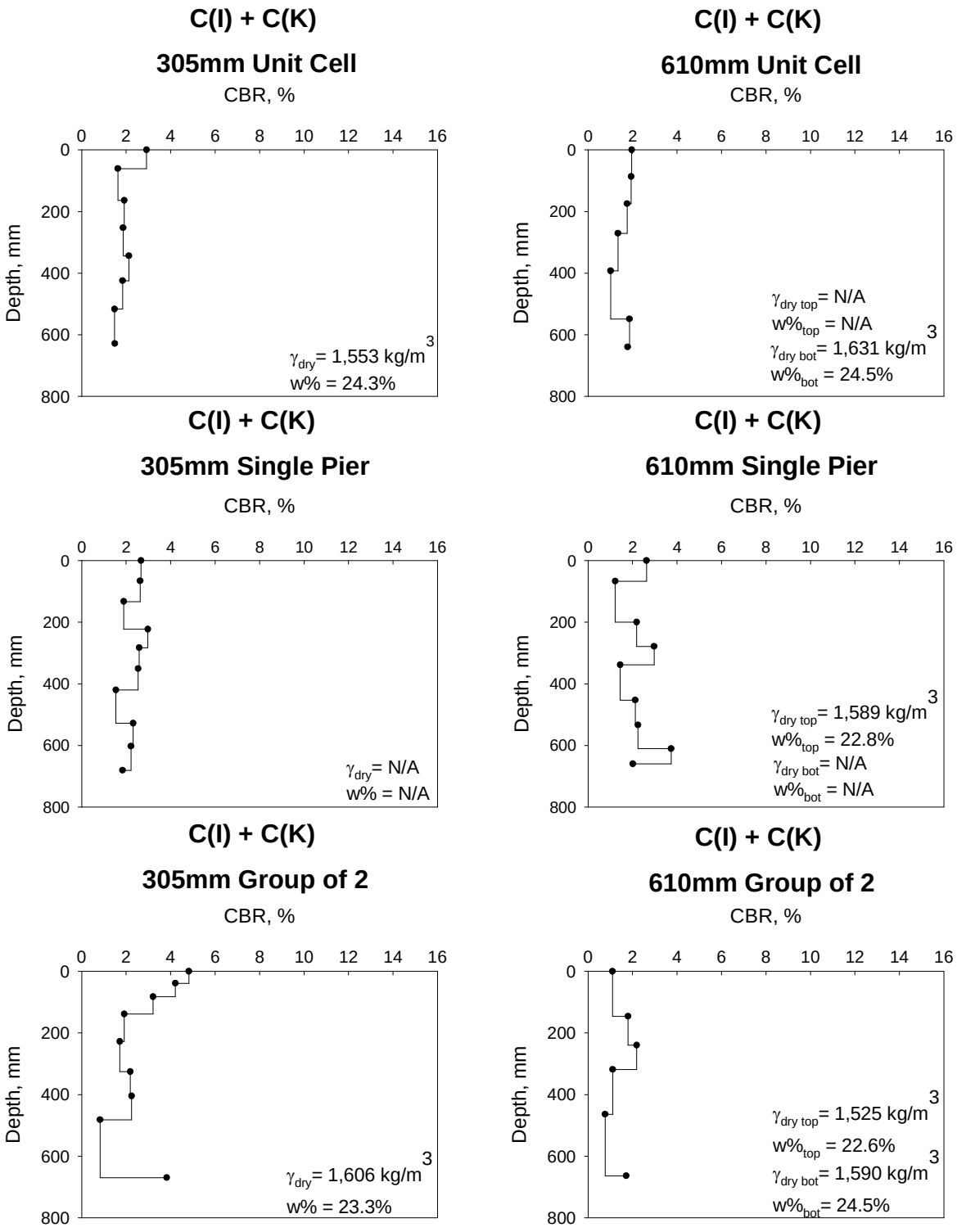

Figure 110: CBR for group C(I) + C(K) piers: unit cell, single pier, group of 2

www.manaraa.com

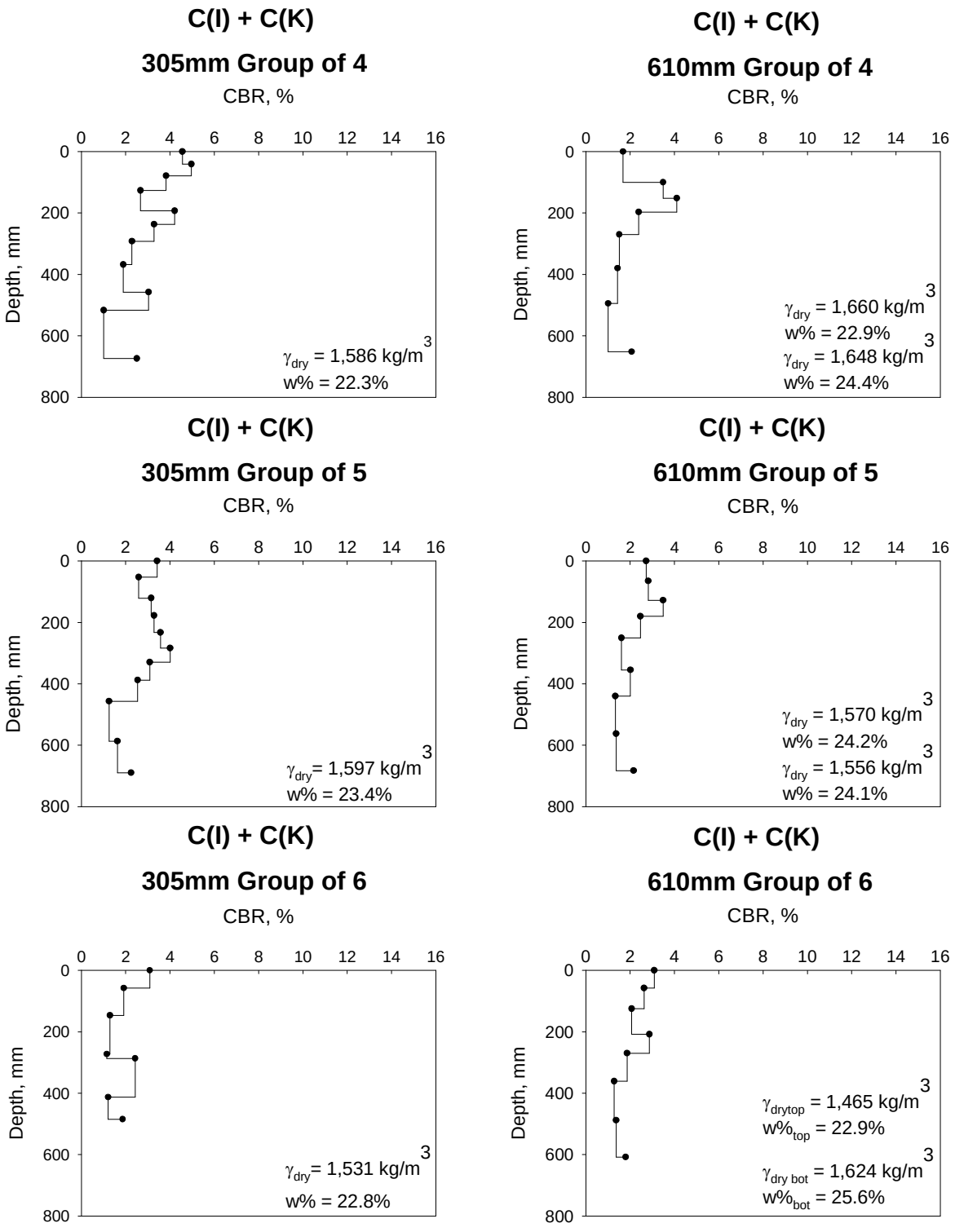

Figure 111: DCPI for group C(I) + C(K) piers: group of 4, group of 5, group of 6

www.manaraa.com

ACKNOWLEDGEMENTS

I would like to express my gratitudes to my major professor, guardian and excellent mentor – Dr. David J. White for his continuous support, word of encouragement and guidance throughout every step of my research.

Moreover, I would like to thank Geopier Foundation Company for being a generous supporter of this research and involvement in innovative research and development with Iowa State University.

Finally, I would like to express my warmest feeling to my friends that walked this path with me and never doubted my capabilities and strength.

www.manaraa.com